11-14-2016

Development of an Anaerobic-Phototrophic Bioreactor System for Wastewater Treatment

Onur Yilmaz Ozcan
University of South Florida, onurzcn@gmail.com

Development of an Anaerobic-Phototrophic Bioreactor System for Wastewater Treatment

by

Onur Y. Ozcan

A dissertation submitted in partial fulfillment
of the requirements for the degree of
Doctor of Philosophy
Department of Civil and Environmental Engineering
College of Engineering
University of South Florida

Major Professor: Daniel Yeh, Ph.D.
Jan Bartacek, Ph.D.
Jeffrey Cunningham, Ph.D.
Piet Lens, Ph.D.
John Love, Ph.D.
Aydin Sunol, Ph.D.

Date of Approval:
November 10, 2016

Keywords: decentralized treatment, anaerobic baffled reactor, membrane bioreactor, algae, nutrient management

Acknowledgements

I would like to thank Dr. Daniel Yeh, my valuable mentor and advisor, for guiding me in this journey, and my advisory committee members, Drs. Bartacek, Cunningham, Lens, Love, and Sunol for taking the time to evaluate my progress. I would also like to thank all of my professors for sharing their accumulated knowledge throughout my years in college and graduate school. Special thanks to Dr. Robert Bair for countless hours of mentoring, support, and friendship, and to all members of the DHY Research Group with whom I have had the pleasure of collaborating. I would especially like to thank Dr. Ana Prieto and Dr. Ivy Drexler for their support and contributions to my development as a young researcher. Special thanks to Jorge Calabria, George Dick, Peter Zydek, and Melanie Pickett for their friendship, and Erkan Uman, Sarah Brownlee, and Herby Jean both for their friendship and for their invaluable help with my work.

And lastly, I would like to thank my family for always being there for me.

Special thanks to the USEPA Center for Reinventing Aging Infrastructure for Nutrient Management (Grant No: 83556901) and National Science Foundation's ICARUS Project (Award No: 1236746) for helping to fund this work.

Disclaimers: "This dissertation was made possible by USEPA grant 83556901. Its contents are solely the responsibility of the grantee and do not necessarily represent the official views of the USEPA. Further, USEPA does not endorse the purchase of any commercial products or services mentioned in the publication."

“Any opinions, findings, and conclusions or recommendations expressed in this material are those of the author(s) and do not necessarily reflect the views of the National Science Foundation.”

Table of Contents

List of Tables

List of Figures

Abstract

For decades, mainstream domestic wastewater treatment has relied on activated sludge processes to remove organic matter, and on biological nutrient removal systems like the A^2/O process to remove nutrients. Recently, membrane filtration was also added to the realm of possible technologies for domestic wastewater treatment, with aerobic membrane bioreactors (MBRs) becoming increasingly popular, especially for decentralized, and small to medium scale applications. However, the aerobic activated sludge and MBR processes, which are often combined with biological nutrient removal processes, have high energy costs associated with supplying oxygen to the process, and end up converting the organic matter into CO_2 and high amounts of microbial biomass, instead of more useful byproducts.

In order to remedy the aforementioned shortcomings of the aerobic processes, anaerobic wastewater treatment has been a focus of research, with anaerobic baffled reactors (ABRs) and anaerobic membrane bioreactors (AnMBRs) having shown promise for achieving acceptable organic matter removal performance, along with potential to be energy neutral or positive through biogas production. In addition, phototrophic technologies, such as algal photobioreactors, have recently been shown to be able to remove nutrients from waste streams, while at the same time having the potential to be used as feedstock to produce biofuels.

In this dissertation, a novel concentrically-baffled reactor (CBR) was designed that has the potential to reduce heat loss by transfering more of the heat between reactor zones than traditional baffled reactor designs, which will increase energy efficiency for heated systems. A prototype CBR was operated abiotically under varying hydraulic retention times (HRTs) from 4

h to 24 h, and achieved over 90% removal of total suspended solids (TSS) for all HRTs tested with feed particle sizes below 1.7 mm.

In parallel with the baffled reactor research, phototrophic membrane bioreactors (PMBRs) were tested with low aeration conditions to decrease their energy demand, which resulted in nitrification-dominated systems. A phototrophic technology was developed for increasing the pH of waste streams to potentially aid pH-sensitive nutrient recovery processes. Phototrophic pH increase from 6.42±0.13 to 8.87±0.06 was achieved using batch reactors, and an increase of pH from 6.73 to 8.61 was recorded during a continuous reactor trial.

Finally, the CBR was combined with a post-CBR membrane filtration process, and two PMBRs treating the effluent and permeate streams from the CBR in order to achieve complete organic matter and nutrient removal. The combined systems were tested both for high strength-high HRT and low strength-low HRT scenarios. Using the combined CBR-PMBR system, over 90% TN and TP removal were possible for 10 d HRT operation at high-strength feed conditions, with post-CBR membrane filtration. COD removal over 90% was possible for both high-strength and low-strength scenarios under all conditions tested.

Chapter 1: Introduction

This dissertation is about the development of two separate wastewater treatment technologies with the goal of developing alternative strategies for recovering resources from wastewater. Ultimately, the purpose of this work is starting a new path for recycling wastewater more effectively than currently existing technologies. To this end, a unique reactor design was developed mainly for the anaerobic treatment of wastewaters, as well as a unique way of processing wastewater using phototrophic processes that may aid in the easier recovery of nutrients. These two technologies are eventually integrated, and the results of this exercise presented.

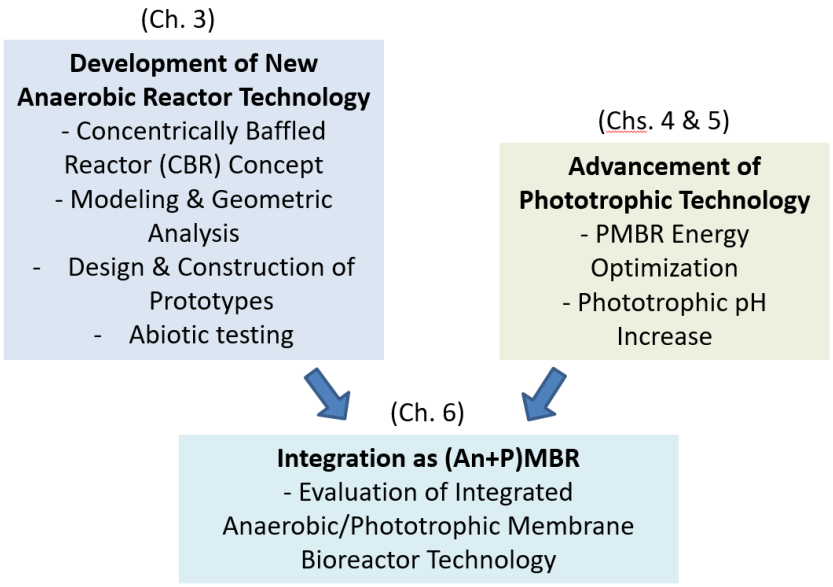

Figure 1.1. How this dissertation is organized after Chapters 1 (Introduction) & 2 (Materials and Methods)

The dissertation is structured so that the two technologies are addressed separately within their own respective chapters, beginning with the new reactor design. After the two technologies are presented, it moves onto addressing the case of the integrated operation (Figure 1.1). The main research question addressed by this body of work is: "Is it possible to develop new ways of treating wastewater and/or recovering resources that have the potential to be alternatives to existing technologies?"

1.1. Aerobic and Anaerobic Wastewater Treatment

For the last half of the past century along with the first decade of this century, the conventional approach to domestic wastewater management has largely been to subject the wastewater to various chemicals and high energy processes in an effort to bring the treated effluent down to the water quality standards established by the contemporary policymaking entities. After treatment, the effluent is typically discharged into a suitable receiving medium, usually a water body such as a river or a lake. Although this approach has prevented a multitude of other scenarios which would have had much worse implications for the environment, it may have run its course to make way for a new paradigm that is emerging. This new paradigm views wastewater as a valuable resource from which energy, water, nutrients, and other commodities can be extracted, and it has been taking root in the scientific community and the professional water sector alike, with the (re)emergence of technology that renders the latter premise not only possible, but also arguably more feasible than the former (McCarty *et al.*, 2011; Porwal *et al.*, 2008).

The conventional approach to domestic wastewater treatment involves settling out any settleable (also called "particulate" or "suspended") solids within the wastewater and treating the

remaining portion using an aerobic consortium of bacteria which is commonly referred to as "activated sludge" (Figure 1.2). This approach is energy intensive due to the aeration requirement of the activated sludge process, which commonly constitutes most of the energy demand of the entire treatment operation, including the total energy demand for pumping (IAWPRC, 1998). In addition, much of the energy embedded in the chemical bonds of the soluble organic material inside the wastewater is lost through biochemical oxidation to CO_2 and other end products within the aeration tank.

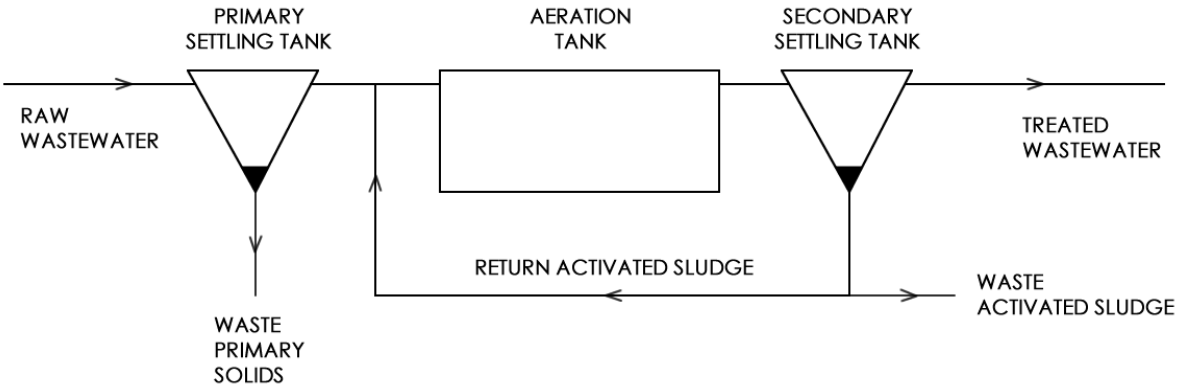

Figure 1.2. Conventional activated sludge process flow diagram

An alternative method to treat organic waste and wastewater is the biochemical conversion of the organic material in the absence of external electron acceptors (such as dissolved free oxygen, nitrate, sulfate, *etc.*), which is facilitated by an anaerobic microbial population. This process is called "anaerobic digestion", and it has been applied for the treatment of human wastes and settleable domestic wastewater solids since the end of the 19th century (van Lier *et al.*, 2001), although it has not been widely adopted as the main process for the treatment of the relatively more dilute municipal wastewaters. The anaerobic digestion process has an inherent economic advantage over the widely adopted activated sludge process, because it does

not require oxygen to be constantly supplied to the system, which considerably lowers the energy demand. In addition, a healthy balance of methanogenic archaea and fermentative microorganisms within the anaerobic digester can yield a significant amount of methane gas which can be used as fuel to generate electricity and heat. Finally, anaerobic digestion has a lower biosolids yield compared to aerobic systems; that is, a much greater fraction of the incoming wastewater organics is converted to gas than to more biomass compared to aerobic systems (Rittmann & McCarty, 2001). This is important, because periodic wasting of the excess biomass and inert particulate solids is required to prevent solids accumulation in biological treatment systems. A lower biosolids yield results in relatively lower biosolids production, and consequently, a decrease in the costs associated with the processing of waste solids for anaerobic treatment systems.

For all its aforementioned intrinsic advantages, numerous researchers and engineers employing anaerobic digestion for the treatment of the relatively low strength domestic wastewaters have largely not been able to observe the higher treatment efficiencies seen with aerobic processes, especially under ambient temperature regimes (Seghezzo *et al.*, 1998). This, in addition to the lower robustness observed with anaerobic digestion due to the sensitivity of methanogenic populations to environmental conditions has largely prevented the wide adoption of the anaerobic digestion technology as an alternative to the activated sludge process for domestic wastewater treatment, although anaerobic digestion has been adopted as a complementary process for the management of waste solids resulting from the main process train in activated sludge systems.

1.2. Membrane Bioreactors

Towards the end of the 20th century, Membrane Bioreactor (MBR) technology became popular thanks to the introduction of the relatively more energy-efficient submerged MBR process (Judd, 2008; Yamamoto *et al.*, 1989) and the advances in materials science – especially in the field of synthetic polymers – and the reduction in cost associated with the manufacturing of artificial membranes, mostly driven by research into seawater desalination and hemodialysis (Strathmann, 2011). By coupling an activated sludge process with a membrane filter, any biomass washout would be prevented, allowing for the decoupling of how long the biomass and other particulate solids remained within the reactor (the solids retention time – SRT) from how long the water and any soluble matter remained within the system (the hydraulic retention time – HRT), enabling slow-growing species to be retained and to contribute to the conversion of organic waste (Melin *et al.*, 2006). In addition, the membrane filter unit would replace the settling tanks used for separation of the biomass from the treated effluent, resulting in a considerable reduction in system footprint. Absolute retention of biomass within the reactor with a membrane filter would also render any design and operational considerations associated with the settling properties of the biomass obsolete, one of the side effects of which is being able to have a much greater biomass concentration within the reactor than was possible with conventional systems. This in turn enabled high rate treatment with smaller reactor volumes, further reducing treatment system footprint and paving the way towards small scale and package treatment plants designed for more stringent water quality requirements and water reuse applications, opening up opportunities for integrated decentralized domestic wastewater treatment and reuse facilities (Wisniewski, 2007).

The main premise behind decentralized treatment and reuse is that it is both more economical and more sustainable to treat wastewater near the source and final reuse locations, rather than investing in the infrastructure required to convey the wastewater and the final product to and from discrete, centralized facilities (Butler and MacCormick, 1996; Gikas and Tchobanoglous, 2009). According to the U.S. Environmental Protection Agency's Clean Water and Drinking Water Infrastructure Gap Analysis Report (2002), EPA is looking at up to an estimated $495 billion gap in operations and maintenance funding by the year 2020, $52 billion of which is attributed to the renewal of aging transmission lines and distribution mains. EPA's funding projections highlight the urgency of adopting solutions that will bridge the gap between available and required funding. In this sense, decentralized treatment and reuse in the form of "satellite treatment" (Gikas & Tchobanoglous, 2009) and/or "sewer mining" (Butler & MacCormick, 1996) has become an attractive solution for lowering some of these infrastructure costs.

Although a strong motivator, economics is not the only compelling reason to adopt decentralized wastewater treatment and reuse facilities. Through the integration of the historically discrete processes of wastewater treatment and water supply and conveyance, sustainable recycling of wastewater for a number of end uses can be achieved, transforming the conventional open-loop treatment infrastructure to a more sustainable, closed-loop recycling system.

Sustainable development has been the focus of attention in policy making since The Brundtland Commission in 1987 (Redclift, 2005), but modern cities continue to be grossly unsustainable ecosystems, especially due to the effects of the industrial revolution starting in the 18th century and the population boom seen in the 20th century. Cities can exceed their ecological

carrying capacity by a factor of 20, relying on their surroundings and beyond for resources required for maintenance and growth, and to dump their waste. The resources are extracted from their respective environment, processed to create commodities, and ultimately end up as waste materials confined within a very linear, open-loop metabolism (Doughty & Hammond, 2004; Girardet, 1996; Rees, 1992). Decentralized wastewater treatment and on-site reuse facilities can help to close the open loop associated with the recycling of water, nutrients and energy within the sprawling cities of the 21st century, where modifying the existing centralized infrastructure to achieve the same goal could be much less feasible or outright impossible.

Anaerobic Membrane Bioreactor (AnMBR) technology has been gaining interest with the increasing popularity of the Aerobic Membrane Bioreactor (AeMBR), owing to the premise of combining the advantages of anaerobic treatment in terms of resource recovery with higher effluent qualities obtained with membrane filtration seen in aerobic systems. To this end, AnMBRs have been suggested as an alternative to existing technologies for recovering water, energy and nutrients from domestic wastewater (McCarty et al., 2011), and transforming the linear metabolism of cities to a more sustainable structure that incorporates closed loops for these resources, instead of relying on their hinterlands to carry the burden of their ecological footprint.

AnMBRs have been shown to achieve high organic matter removal efficiencies treating both simulated (Hu & Stuckey, 2006) and real wastewater (Yoo *et al.*, 2013) with high-rate processes that have achieved hydraulic retention times (HRTs)[1] as low as 3 h and 2.3 h, respectively. For comparison, typical HRTs employed for high rate aerobic MBRs are within the 4 h to 6 h range (Le-Clech, 2010). This indicates AnMBRs may be a viable alternative to AeMBRs in terms of treatment efficiency and system footprint.

[1] Hydraulic retention time is a measure of how long it takes for the water to exit the system from the time that it enters the system, and it is the governing variable for system footprint – the lower the HRT, the smaller the reactor size for a unit volume of wastewater to be treated over unit time.

1.3. Traditional Nutrient Management

Management of nutrients within wastewaters is also of significance when considering alternatives for treatment. Nutrients in treated wastewater effluents discharged into receiving water bodies can cause an off-balance ecosystem state called *eutrophication*, characterized by an increase in primary production facilitated by a bloom in algae populations, resulting in the aquatic ecosystem exceeding its own carrying capacity, and consequently, experiencing highly reduced biodiversity due to competition, depletion of resources, and changes in environmental conditions. In order to prevent this phenomenon, nutrients entering water bodies need to be controlled. Typically state of the art (aerobic) domestic wastewater treatment facilities that incorporate some sort of nutrient management strategy do so by employing biological nutrient removal (BNR) processes. A widely employed combined activated sludge/BNR process train called A^2/O (Anaerobic-Anoxic-Oxic) is depicted in Figure 1.3.

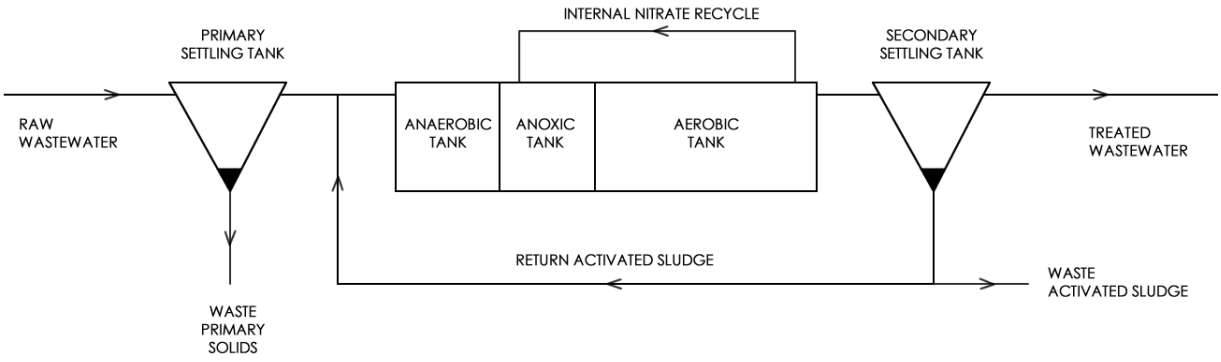

Figure 1.3. A^2/O process flow diagram

Traditional BNR involves the bioconversion of excess nitrogen to nitrogen gas, and the accumulation of excess phosphorus within waste biosolids. For nitrogen removal, the ammoniacal and organic nitrogen species found in raw domestic wastewater is biochemically

converted to nitrite (NO_2^-) and then to nitrate (NO_3^-) in the aerobic tank through a biological process called nitrification, carried out by autotrophic nitrifying bacteria. The resulting nitrate is subsequently converted to nitrogen gas (N_2) through a denitrification process facilitated by heterotrophic denitrifying bacteria within an anoxic environment, which can be pre- or post-aerobic treatment. The phosphorus within the wastewater stream is removed by cultivating phosphate accumulating organisms (PAOs) that can store greater amounts of phosphorus within their cell cytoplasm when subjected to stressful conditions. This process is called enhanced biological phosphorus removal (EBPR), and requires the cycling of biomass between an additional non-aerated tank and the aerated tank to stress the PAOs and induce phosphorus uptake from the medium (Comeau *et al.*, 1986). The phosphorus that is taken up by PAOs is then removed from the system via biosolids wasting.

1.4. Algal & Phototrophic Technologies

An emerging new alternative to employing traditional BNR processes is the use of algal or phototrophic processes in tandem with organic matter removal via anaerobic treatment (Prieto, 2011). Algal processes have been receiving interest in the recent years due to their efficiency as a biological substrate in the creation of renewable fuels and bulk chemicals (Wijffels *et al.*, 2010), as well as pharmaceuticals and dietary supplements, among other products (Subhadra & Grinson-George, 2011). Fat-storing algae can be converted to biofuels and have been cited as an upcoming alternative to water- and energy-intensive biofuel crops from which fuel additives are currently being derived and blended with petroleum based fuels in the United States (Singh & Gu, 2010).

Algae require water, nutrients (mainly N and P), CO_2, sunlight, and trace elements for growth. Since water and nutrients required for algal growth are abundant in wastewater and its treated effluent streams, and wastewater treatment plants tend to produce CO_2 via biological pathways as well as combined heat and power (CHP) processes used to combust biogas for its energy content, the idea of integrating wastewater treatment operations with the concept of algal biorefineries has been suggested (Olguín, 2012). Algal biorefineries-biofactories, or integrated renewable energy parks (IREPs), can potentially fuse wastewater treatment processes into the production of new materials, creating closed loop recycling systems for urban environments (Subhadra & Grinson-George, 2010; Garcia Alba *et al.*, 2011; Adarme-Vega *et al.*, 2012). Indeed, algae can be used to recover and/or remove nutrients within wastewater, helping the wastewater treatment plant meet its water quality requirements, and can help to mitigate gaseous carbon emissions by sequestering any CO_2 produced in the wastewater treatment process train. The algae produced in this manner can then further be processed for the creation of various end products. Depending on selected reuse applications, it may therefore be preferable to combine anaerobic treatment (with or without a membrane unit) with algae processes. Further polishing of the effluent can be achieved by selecting an appropriate membrane filtration operation with or without additional polishing steps after the algal process. Thus, an end product stream of water can be created with the desired quality based on the selected end use, including direct potable reuse. The proposed alternative domestic wastewater treatment process train is given in Figure 1.4.

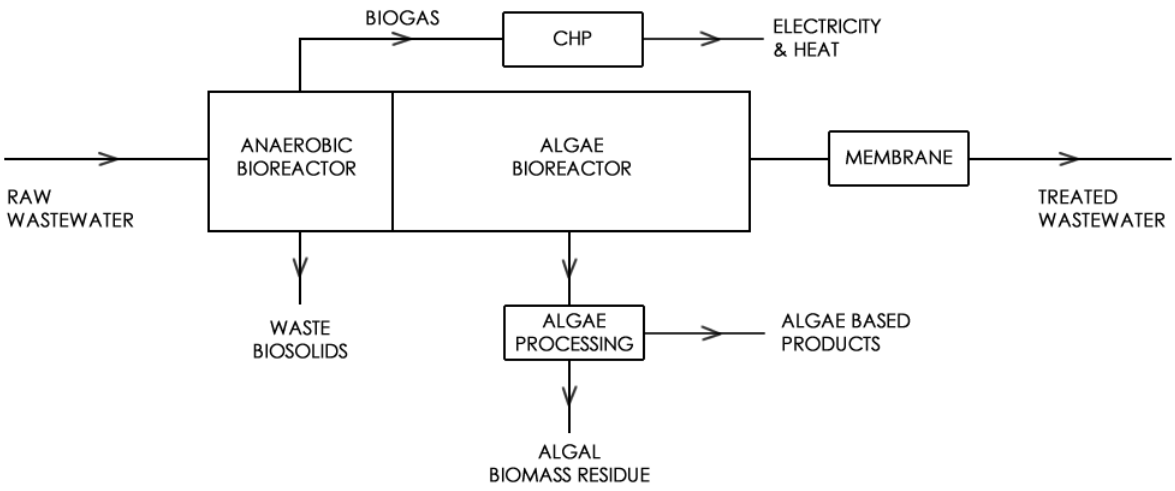

Figure 1.4. Alternative domestic wastewater treatment process flow diagram based on anaerobic and algal technologies

Anaerobic membrane bioreactor technology offers an opportunity for sustainably realizing integrated domestic wastewater treatment and reuse at smaller scales for end uses ranging from direct fertigation (Hagin & Lowengart, 1995) of agricultural lands to the reclamation of high-quality drinking water depending on the selected polishing steps. Recovery and recycling of water, energy, and nutrients from domestic wastewater using small-scale integrated facilities ensures the transition from the linear, parasitic metabolism of cities to a sustainable, closed loop homeostasis while accomplishing the replacement of the aging water and wastewater infrastructure with a model that holds promise from both economic and logistical standpoints. Finally, the synergies that exist between wastewater treatment and algal biorefineries create opportunities for developing systems that have been configured to close even more loops for industries that make use of the products and by-products of this integration.

There is, however, an important problem associated with the concept of marrying algal material production facilities with wastewater treatment – footprint and capital cost

requirements. Especially with the rise of membrane bioreactor systems, current wastewater treatment facilities are mainly geared towards high-rate nutrient removal processes and have comparatively lower processing rates than processes that seek to incorporate algae production into main stream municipal wastewater treatment. One way to alleviate this problem and bridge the gap between the current technological trend in municipal wastewater treatment and the concept of algal material production facilities is to seek out high-rate algal processes that will be attractive alternatives to current biological nutrient removal technologies.

Much of the recent literature on the cultivation of algal species using wastewater streams is focused on the synergy between the production of algal products and wastewater treatment, which can reduce the cost of cultivating algae for biofuels and other products (Pittman *et al*., 2011). Furthermore, the use of algal processes for wastewater treatment in its own right – especially for nutrient management – is also of interest. To this end, a number of algae-based treatment technologies are being developed, such as high rate algal ponds (Park *et al*., 2011), algal membrane bioreactors (Kumar *et al*., 2010), rotating algal biofilm reactors (Christenson & Sims, 2012), air-lift algal bioreactors (Vunjak-Novakovic *et al*., 2005), and various immobilization techniques (Mallick, 2002). These technologies mainly rely on the nutrient uptake mechanism of algae to manage nitrogen and phosphorus concentrations in wastewater. The O_2 supplied by algae to their environment may in some cases also facilitate the growth of O_2-utilizing heterotrophic species for Chemical Oxygen Demand (COD) removal, as well as nitrifying species for additional nitrogen removal.

Under conditions explained further below, algal species have the ability to increase the pH of their environment. Even though a correlation between increased primary production, decreased inorganic carbon concentrations, and increased pH levels has previously been

observed (Middelboe & Hansen, 2007; Lopez-Archilla *et al*., 2004; Talling, 1976; O'Brien & DeNoyelles, 1972), there is a gap in current environmental engineering and science literature with regard to the biochemical foundations of this phenomenon, and no attempts in using it for engineering novel wastewater treatment processes.

Phototrophic species can potentially increase the pH of their environment if their rate of $CO_{2(g)}$ uptake for photosynthesis exceeds the rate of $CO_{2(g)}$ mass transfer into the environment (for instance, from the atmosphere). Net removal of $CO_{2(g)}$ from the environment can push the carbonic acid – carbon dioxide equilibrium towards carbon dioxide, resulting in more alkaline conditions. In addition, a study of plant sciences literature reveals a unique cellular mechanism to be another likely candidate for the observed pH increase, namely the CO_2-Concentrating Mechanism (CCM), which evolved to enable phototrophic species to increase the intracellular concentration of $CO_{2(g)}$ to be used in photosynthesis by taking up and converting the inorganic carbon species available in the environment (Kaplan & Reinhold, 1999). This increase in pH can potentially be used for nutrient removal or aid pH-dependent recovery technologies.

1.5. Current Gaps in the Literature

In order to be able to replace their aerobic counterparts for the treatment of domestic wastewaters, anaerobic membrane bioreactors need to be able to demonstrate high treatment efficiency, low system footprint, high energy efficiency, and increased process robustness under hydraulic and organic perturbations. As described subsequently, there is currently no AnMBR system within published scientific literature that has decisively shown capability to fulfill all four of the listed criteria. Design and operating parameters that are associated with and can be used to evaluate these four criteria are given in Table 1.1.

Table 1.1. Design and operating parameters for the evaluation of given criteria

Criterion	Parameter
Treatment Efficiency	Chemical Oxygen Demand (COD)[2] Removal Efficiency
System Footprint	Hydraulic Retention Time (HRT)
Energy Efficiency	System Energy Demand
	Methane Production Rate
Robustness	Hydraulic & Organic Shock Response
	Fats, Oil & Grease (FOG) Loading

All of these parameters need to be considered together as they are interrelated. For example, COD removal efficiency is a function of HRT, because HRT affects how much contact time the microbial consortia within the bioreactor have to degrade the dissolved solids within the aqueous phase. COD removal efficiency is also a function of system energy demand, as COD removal can be enhanced by using energy intensive processes. HRT and system energy demand also affect system shock response, which is evaluated using COD removal efficiency and the time it takes for the system to recover from shocks.

COD removal efficiencies of high-rate AnMBR processes are commonly around 90% (Hu & Stuckey, 2006: Yoo *et al.*, 2013), unless the feed being treated is a readily biodegradable substance like acetate or glucose, in which case efficiencies can increase up to 99% (Kim *et al*., 2011). What is meant by "high-rate" is that the feed is treated in a short amount of time (up to 6 hours for systems treating only the soluble fraction of the waste), usually denoted by the operational HRT. Studies incorporating systems with very long HRTs are not practical because they simply take up too much space for the same treatment efficiency, resulting in increased capital cost and system footprint, especially when high-rate aerobic processes can produce the same result without the additional footprint. It is also important to distinguish between studies

[2] Chemical Oxygen Demand (COD) is a measure of the amount of organic matter within the wastewater, used for denoting its strength (*i.e.* how polluted the wastewater is).

that explore the treatment of only the soluble fraction of domestic wastewater or synthetic feed versus the complete, raw sewage or synthetic feed, with both its particulate and soluble fractions. This is especially important when lower temperature (*i.e. psychrophilic*) operation is required, because hydrolysis of the particulate and the complex fraction of the wastewater becomes the rate-limiting step under these conditions, although lower temperature operation is usually more energy efficient (Lettinga, 2001). One gap in the literature is whether high-rate treatment can be achieved with an AnMBR treating both the particulate and the soluble fractions of domestic wastewater simultaneously. Another gap is the establishment of the nature of the relationship between energy efficiency, system footprint and treatment efficiency.

Although there has been research on the effects of temperature shocks on AnMBR performance (Gao *et al*., 2011), there are no current studies evaluating the effects of hydraulic and organic loading shocks on treatment efficiency in AnMBRs treating domestic wastewater. This is important because wastewater characteristics can change significantly throughout the day (Butler *et al*., 1995), especially for small-scale systems that cannot field equalization tanks due to space restrictions or capital cost considerations. In addition, incoming wastewater volume can be enhanced by storm events for combined collection systems or leaky sanitary sewer systems, increasing hydraulic loading. Therefore, it is imperative to demonstrate the ability of biological systems to handle these shocks, especially where anaerobic processes are employed, due to the inherent sensitivity of anaerobic equilibrium state to environmental perturbations.

There are two large gaps in the current literature regarding the use of algae in conjunction with AnMBRs. The first gap is the demonstration of algae-pH-alkalinity interaction and nutrient removal at higher pH levels with AnMBR effluents. The second gap is related to the direct comparison of nutrient removal and/or recovery efficiencies of algae photobioreactors treating

filtered AnMBR effluent versus unfiltered anaerobic digester (AD) effluent. An AnMBR fielding a membrane unit with a small enough nominal pore size will retain almost all of its microbial population within the digester, allowing the algae full reign within their photobioreactor. However, the unfiltered AD effluent will most likely be more turbid and contain other microorganisms that may compete with the algae for the nutrients, changing the growth conditions for algal species and acting as selection pressure. It is unclear what will come of this competition, and whether similar results will be obtained with the two configurations.

Even though numerous different configurations are possible for anaerobic digesters, most AnMBRs studied within the literature have been designed and operated as completely stirred type reactors (CSTRs) or upflow anaerobic sludge blankets (UASBs) (Ozgun *et al.*, 2013). Although these configurations can achieve high treatment efficiencies when combined with a membrane unit, novel configurations that can demonstrate higher robustness are required for widespread adoption. In addition, since it is less feasible to separate out incoming particulates and treat them in a separate anaerobic digestion unit, a complete solution that addresses both the particulate and the soluble fractions within wastewater will have an advantage over systems that only address specific fractions of the wastewater.

An alternative configuration is the Anaerobic Baffled Reactor (ABR) (Bachmann *et al*., 1985), which incorporates baffles to improve treatment efficiencies and robustness in plug-flow anaerobic reactor designs. ABR can retain biomass within each zone created by the baffles using gravity and can subsequently lead to the cultivation of distinct populations on the travel path of the incoming wastewater. This gives the ABR design the versatility and robustness of the two-phase anaerobic digesters, where fermentation and methanogenesis processes occur in different

reactors, increasing stability. ABR has also been shown to perform exceptionally well under psychrophilic conditions (Nachaiyasit & Stuckey, 1997).

Although ABR is effective, hybrid designs combining ABR and Anaerobic Filters (AF) have been shown to yield better treatment performances and greater robustness against the suspension or flotation of biomass (Barber & Stuckey, 1999). AFs can retain biomass by incorporating high-surface-area media within the reactor on which microorganisms can attach themselves and grow, creating layers of biofilm. This enables the biomass to be retained within the reactor, and perhaps more importantly (for AnMBRs), within their respective zones under high hydraulic loading rates, preventing washout from each zone. If floating media are used in conjunction with a baffled design, any biomass that floats can be captured and retained by the floating media, increasing solids retention within each specific zone. Floating media can also help with the degradation of any fats, oil & grease (FOG) that will tend to float to the surface, by increasing the amount of biomass in contact with the FOG layer.

Another design consideration, especially for treatment at lower temperatures, is the hydrolysis of particulates within the wastewater, as mentioned earlier. Hydrolysis can be enhanced, among other techniques, by subjecting the incoming feed to higher temperatures and applying thermophilic digestion for a relatively short amount of time. This lead to the invention of the Temperature Phased Anaerobic Digestion (TPAD) process (Han & Dague, 1997), which incorporates a smaller volume thermophilic stage designed to quickly hydrolyze the feed, followed by a mesophilic stage which continues the digestion process for a longer period of time. This process has been shown to increase the solubility of the feed and enhance volatile solids destruction via enhanced hydrolysis (Ge *et al*., 2011), although its feasibility needs to be evaluated from an energy efficiency perspective.

A novel hybrid reactor design that can combine the strengths of these systems may effectively be able to overcome the shortcomings of anaerobic reactors for domestic wastewater treatment, and potentially offer a complete, high performance, robust, and energy efficient solution to the problem. Furthermore, combining this anaerobic reactor configuration with a phototrophic process can, in theory, result in both adequate organic matter and nutrient removal from wastewater streams.

1.6. Hypotheses Tested

The specific hypotheses tested with the experimental trails conducted throughout this doctoral work are presented below. The findings pertaining to these hypthoses and whether the results were true or false can be found in the last chapter of this dissertation.

- It is possible to lower the energy requirements of phototrophic membrane bioreactors (PMBRs) by lowering their aeration rates, while retaining acceptable (>80%) nutrient removal rates.
- It is possible to raise the pH of phototrophic systems using batch- and continuously-fed reactors.
- It is possible to induce distinct temperature and solids profiles within the Concentrically Baffled Reactor (CBR), where over 90% of the influent suspended solids are captured within the reactor.
- It is possible to achieve over 90% COD removal with the CBR alone.
- It is possible to achieve over 95% COD removal with the combined CBR-PMBR system.
- It is possible to achieve over 90% TN and TP removal with the combined CBR-PMBR system.

Chapter 2: Materials and Methods

2.1. Sampling, Wasting & Stock Reactor Maintanence

Reactor samples were taken directly from each reactor using appropriate sampling ports. To ensure the representativeness of samples taken, reactor contents were mixed before each sampling event. Feed samples were taken directly from reactor feed tanks after mixing. Membrane permeate samples were taken directly from the permeate lines attached to the membrane modules using pre-installed sampling ports. In case of reactor effluent sampling, samples were taken directly from sampling ports pre-installed on reactor effluent lines. All samples were kept in 50 mL Corning Falcon conical clarified polypropylene tubes at 4°C and were analyzed at most one week after being taken. Sample containers were washed with tap water, triple rinsed with deionized water and dried prior to sample collection. Sampling was done at weekly (1/week) or bi-weekly (2/week) intervals, depending on the experimental run. Reactor wasting was done using wasting ports installed at the bottom of the reactors. Amount of reactor contents varied depending on the chosen theoretical average Solids Retention Time (SRT). Wasting was done bi-weekly (2/week).

A 5 L mixed-culture, cylindrical, clear acrylic stock photobioreactor was maintained throughout the experimental studies, and the batch- and continuously-operated photobioreactors used throughout this body of work were initially seeded from cultures taken from this stock reactor. The initial mixed phototrophic culture for the stock reactor was bioprospected from primary and secondary clarifiers at Howard F. Curren Advanced Wastewater Treatment Plant (Tampa, FL, USA). The reasoning for the use of mixed phototrophic cultures bioprospected from

a wastewater treatment plant was their existing adaptation towards raw domestic wastewater and wastewater treatment plant effluents. The stock reactor itself was wasted and fed once a week, where a quarter of reactor contents were wasted and then the volume was brought back up to 5 L using tap water. The reactor was fed using 2.5 g MaxiGro fertilizer afterwards. The nutrient content of the fertilizer used is given in Chapter 5, Table 5.2.

2.2. Water Quality Parameters & Analytical Methods

Chemical Oxygen Demand (COD) is a parameter used for measuring the aggregate amount of organic matter in a given sample, with respect to the amount of O_2 required to oxidize the organic material. This makes the COD parameter dependent upon the oxidation state of the organic matter being measured in addition to its weight – i.e. the more reduced the organic matter is, the greater the amount of O_2 required to completely oxidize it to CO_2, H_2O, and other final end products. Organic matter is an important water quality parameter in the environmental engineering field, both because it can include potentially toxic compounds, and because it can lead to the depletion of O_2 in receiving water bodies, leading to septic or near septic conditions. In its Directive 91/271/EEC on Urban Waste Water Treatment, European Commission set a COD limit of 125 mg/L and a minimum percentage reduction of 75% for wastewater treatment plant effluents discharging to receiving water bodies. In the United States, the 5-day Biochemical Oxygen Demand (BOD_5) parameter is still favored over COD for quantifying (the biodegradable fraction of) organic material in wastewater streams.

Total Nitrogen (TN) and Total Phosphorus (TP) indicate the total amount of nitrogen and phosphorus species within a sample that is being analyzed. Nitrogen and phosphorus are of special interest for water quality purposes, because these nutrients are commonly the limiting

nutrients for primary productivity in receiving water bodies, and their discharge can lead to excess primary productivity, resulting in algal blooms and eutrophication. The Total Nitrogen parameter includes all inorganic nitrogen species, which can include ammonium nitrogen and nitrate nitrogen, among other species, as well as all organic nitrogen species. Similarly, the Total Phosphorus parameter includes all inorganic phosphorus species, such as orthophosphate, and all organic species. In its Directive 98/15/EEC amending Directive 91/271/EEC, European Commission set a TN limit of 10 mg/L to 15 mg/L and a minimum percentage reduction of 70% to 80% for wastewater treatment plant effluents being discharged to receiving water bodies. In the same directive, TP discharge limit was set to 1 mg/L to 2 mg/L and a minimum percentage reduction of 80% was required. Ammonium Nitrogen (NH_4-N) and Nitrate Nitrogen (NO_3-N) can also be measured separately from TN, using their respective analytical methods.

Total Solids (TS) is a parameter quantifying the total amount of solids within a given sample – this includes all soluble solids, such as salts and soluble organic compounds, and all particulate solids. Total Suspended Solids (TSS) measures only the particulate fraction of Total Solids. In the field of water quality, the word "particulate" has a varying definition based on the pore size of the filter being used to separate soluble and particulate fractions, which can be anywhere between 0.45 μm to 2 μm. Therefore, there is still a general need for better standardization for this parameter. Fortunately, with its Directive 91/271/EEC on Urban Waste Water Treatment, European Commission sets a TSS limit of 35 mg/L to 60 mg/L and a minimum percentage reduction of 70% to 90% for wastewater treatment plant effluents discharging to receiving water bodies, while specifying the pore size on which the suspended solids are to be retained: 0.45 μm.

Optical Density (OD) uses a set wavelength of light that passes through a sample which is then detected using a light detector. The loss of light intensity yields information on the light absorbance of the sample being measured. OD can be used to measure the color and turbidity of samples, as well as the (loosely correlated) amount of molecules such as *chlorophyll a*, which absorb light better at certain wavelengths than others.

In this dissertation, COD, TN, TP, NH_4-N, and NO_3-N analyses were done in accordance with spectrophotometric Hach Methods 8000, 10072, 10127, 10031, and 10206, respectively, using a Hach DR 4000 UV/VIS Spectrophotometer and respective commercial Test 'N Tube reagent sets (Hach Company, Loveland, CO, USA). TS and TSS measurements were done according to Standard Methods 21st Ed., Method 2540 (APHA *et al*., 2005). For the testing of soluble fractions, samples were centrifuged at 5000 Relative Centrifugal Force (RCF) for 10 min, and the resulting supernatant was filtered through 0.45 μm filters before being analyzed. Optical Density (OD) of the cultures was monitored using a Hach DR 4000 UV/VIS Spectrophotometer at a wavelength of 680 nm.

2.3. Experimental Systems & Equipment

Phototrophic trials were conducted using two identical 2 L borosilicate glass photobioreactor columns fitted with external 8-mm diameter tubular polyvinylidene fluoride (PVDF) ultrafiltration (UF) membranes with a nominal pore size of 0.03 μm and a membrane area of 0.025 m^2 per module (Pentair X-Flow, Enschede, The Netherlands). The photobioreactors were fed using two small, 12 VDC, 0.30 Ampere microdiaphragm pumps with no speed control and adequate power supplied by a 12 VDC 5 Ampere power supply. The pumps were connected to the power supply in parallel. The timing of the feeding was determined by level sensors in the

form of magnetic float switches installed in the reactors. As the level of the reactors decreased by permeate withdrawal from the systems, the float switches would trip and activate the feed pumps. A level change of approximately 1 cm would be enough to trip the float switches in this manner. The external membrane modules were fed with the reactor contents using two larger and more powerful 12 VDC, 5 Ampere microdiaphragm pumps with two separate 12 VDC, 5 Ampere power supplies so that required crossflow velocities could be reached within the membrane tubes. Generic 12 VDC, 5 Ampere motor control circuits were connected to the pumps and the power supplies to enable speed control. The concentrate stream from the membrane modules is fed back into the reactor in this configuration. A Masterflex L/S Digital Drive, 600 RPM, 115/230 VAC 07522-20 peristaltic pump (Cole-Parmer, IL, USA) was used for permeate collection from the membrane module. Collected permeate was stored in two separate 500 mL Erlenmeyer flasks with discharge ports at the top from which excess permeate overflowed into a drain. A Masterflex peristaltic pump with two pumpheads was used to direct produced permeate from the permeate storage tanks back into the membrane tube for the purposes of periodically back-flushing the membrane. This was an automated procedure for which a digital or analog timer can be used. In this specific case, an Arduino UNO was programmed and connected to the pump to time backwash sequences.

Abiotic Concentrically Baffled Reactor (CBR) trials were conducted using a 15 L, 5-zone CBR made of acrylic, fed from the center. The 5-zone CBR had a diameter of 0.45 m. Effluent from the reactor was directed to a drain using an overflow port at the outermost zone of the reactor. The reactor was fed from a 50 L, continuously-stirred feeding tank at a set speed based on the selected Hydraulic Retention Time (HRT) using a Masterflex peristaltic pump (Cole-Parmer, IL, USA). For reactor heating, flexible, 1/4” internal diameter, 3/8” outer diameter vinyl

tubing was formed into a heat-exchanger-like coil pattern and submerged into the center of the reactor. DI water heated by a water bath was pumped using another Masterflex peristaltic pump (Cole-Parmer, IL, USA) into the heating coil and returned to the water bath.

Biotic (anaerobic) trials were conducted using a 7-zone CBR unit with an effective liquid volume of 32 L. A 50-L continuously-stirred feed tank was connected to a 12 VDC, 1.7 A, 35 PSI, 1.2 GPM microdiaphragm pump, which fed the reactor from the center based on input from magnetic float switches that tripped based on reactor level decreases as the reactor effluent was removed from the outermost zone. A DC speed control board was connected to the microdiaphragm pump to adjust the flow rate with which the reactor was fed. A Masterflex L/S Digital Drive, 600 RPM, 115/230 VAC 07522-20 peristaltic pump (Cole-Parmer, IL, USA) was used to remove effluent from the reactor at a specified rate to obtain the desired HRT based on the specific experimental trial. The effluent was then pumped into an effluent storage tank, which had an overflow to a drain to remove excess effluent. Another 12 VDC, 1.7 A, 35 PSI, 1.2 GPM microdiaphragm pump was used to circulate the effluent storage tank contents through the external membrane module fitted with external tubular polyvinylidene fluoride (PVDF) ultrafiltration (UF) membranes with a nominal pore size of 0.03 μm (Pentair X-Flow, Enschede, The Netherlands). The diameter of tubular membranes used and the effective filtration area varied between experimental trials. Another Masterflex L/S Digital Drive, 600 RPM, 115/230 VAC 07522-20 peristaltic pump (Cole-Parmer, IL, USA) was used to produce permeate from the membrane module. The permeate removed from the reactor effluent was stored in a permeate storage tank, and was periodically pumped back into the membrane for back-flushing using another Masterflex peristaltic pump (Cole-Parmer, IL, USA).

Temperature was monitored by manual sampling using digital thermometers. The transmembrane pressure of the membrane modules was monitored using –14.7 to 15 psig ±0.25%-Accuracy Compound Transmitters (Cole-Parmer Instrument Company, IL, USA) connected to U30 Data Loggers (Onset Computer Corporation, MA, USA). The signal from the pressure transducers was recorded as voltage levels, which were converted to pressure readings using calibration curves. In order to calibrate the pressure transducers, an assembly featuring manual pressure gauges and a syringe was used. The syringe was pushed in or pulled out to produce a certain pressure (or vacuum) level within the assembly, which was logged electronically, and the corresponding voltage was recorded to generate data points for the calibration curve.

Permeate was measured both manually and using hand-made permeate measuring equipment which used float switches installed within a small volume (20 mL) metering chamber. As the chamber was filled, the pulse from the float switch was counted using an Onset data logger as a pulse input. The number of pulses within a given time period were then converted to the total liquid volume that passed through the chamber. Manual permeate measurements were done using graduated cylinders and a timing device to determine the flow rate of the permeate being produced.

2.4. Membrane Module Construction, Chemical Cleaning & Clean Water Tests

The single-tubing membrane modules were hand-built using 1/2” clear PVC pipe and appropriate 1/2” fittings adhered together using Oatey PVC Purple Primer and Oatey Regular Clear PVC Cement (Oatey SCS, OH, USA). The membrane tube itself and the clear PVC were cut to approximately 1 meter length. A tee fitting was installed close to one end of the PVC pipe

assembly to allow for a permeate line. Two small holes were drilled into the clear PVC pipe at both ends. After a membrane tube of either 5.2 mm or 8 mm diameter was inserted into the clear PVC pipe, the bottom end was plugged using Oatey Plumber's Putty (Oatey SCS, OH, USA) or similar non-adhering, doughy material. This was done to ensure the adhesive used to set the membrane tube in place within the PVC pipe does not leak from the bottom and stays in place until it sets. Epoxy was used as the adhesive for setting the membrane tube in place within the PVC pipe. Once the putty was in place at the bottom of the PVC pipe and the membrane tube snugly in place, the epoxy was injected to the very bottom part of the PVC pipe throught the small injection holes previously drilled into the pipe. After an adequate amount of epoxy was injected into the pipe, the hole was sealed using more putty and duct tape. The module was left for the adhesive to set overnight, and the same procedure was applied to the other end of the PVC pipe the next day.

Chemical cleaning was performed in-between different experimental trials and whenever the transmembrane pressure (TMP) of the systems exceeded 50 kPa. The cleaning procedure included cleaning with a NaClO solution to remove organic fouling, followed by acid cleaning to remove inorganic fouling. 500 ppm (0.05% w/w) NaClO solution was used to control organic fouling. During chemical cleaning, membrane backwash was set to happen every 5 min for 30 s. NaClO cleaning and acid cleaning was performed for 30 min each. For acid cleaning, an HCl solution was prepared with a pH of 2.5. Before, after, and inbetween different types of chemical cleaning, the membranes were rinsed multiple times with tap water until the membrane concentrate was clear, and the permeate lines were free of cleaning chemicals.

Clean water tests were performed with virgin membrane modules to make sure there were no defects with the membranes themselves. The manufacturer lists clean water fluxes

expected of virgin membrane tubes in respective specification documents corresponding to each type of membrane. If the clean water fluxes are not adequate, the membrane is discarded and a new membrane unit is built. For their 5.2 mm tubular ultrafiltration membranes, Pentair X-Flow lists a clean water flux above 1000 L/m^2/h/bar, whereas for 8 mm membranes, the expected clean water flux is above 750 L/m^2/h/bar. In order to test clean water flux, new membrane modules are operated under varying transmembrane pressures from 20 kPa to 80 kPa. The permeate flow rate is measured, either manually or using a permeate meter, and converted into a flux value using the total membrane filtration area. This flux value is later divided by the transmembrane pressure to obtain a flux value specific to the pressure being applied to the membrane, and compared to the listed specification by the manufacturer.

2.5. Calculation of Transmembrane Pressure, Membrane Flux & Specific Flux

The mixed-phase pressure within feed, concentrate, and permeate lines connected to membrane modules were monitored and recorded separately using Onset data loggers, and were read out using HOBOware software from the same company (Onset Computer Corporation, MA, USA). These three pressure readings were then used to calculate the transmembrane pressure (TMP) of the membrane unit as shown in *Eq. 1*:

$$P = \frac{P_f + P_c}{2} - P_p \qquad (1)$$

Here, P stands for transmembrane pressure, and P_f, P_c, and P_p stand for feed-side pressure, concentrate-side pressure, and permeate-side pressure, respectively. However, note that this equation is only true if the permeate-side pressure is lower than the feed/concentrate-side

pressure. TMP should always be calculated by subtracting the lower-pressure side of the membrane from the higher-pressure side.

Membrane flux is a standardized parameter that includes the filtration performance of membrane filters by including the membrane area used for the filtration in the flow rate that can be acquired from the filtration operation. The equation used for calculating membrane flux is given below:

$$J = \frac{Q}{A} \qquad (2)$$

In the above equation, *J* stands for membrane flux, measured in standardized units of $L/m^2/h$, commonly denoted as LMH. *Q* and *A* stand for flow rate (L/h) and effective membrane filtration area (m^2), respectively.

Another parameter of note, which is useful in clean water tests, is the specific membrane flux. This parameter adds another level of dependency to the flow rate being measured besides the membrane area used to acquire it: namely the transmembrane pressure under which the flow rate was obtained. This is important for comparing the performance of membrane filtration operations, because even though a type of filter may look like it is performing well by generating an adequate amount of permeate with the membrane area utilized, if it is performing well because it is highly pressurized (and therefore drawing higher amounts of energy), this would not lead to a fair comparison between it and other membrane units performing similarly under lower pressures. The equation for calculating specific flux is given in *Eq. 3*.

$$J_s = \frac{J}{P} \tag{3}$$

In this equation, J_s represents the specific flux, J represents the membrane flux, and P represents the transmembrane pressure.

Chapter 3: Development of a Concentrically Baffled Reactor

Baffles are used in a number of industries, usually for the fundamental functions of directing fluid flow, reducing short-circuiting, or facilitating mixing (Gupta *et al*., 1995; Tasnim & Collins, 2004). Specifically, baffles have been used to create eddies to help with non-turbulent flow kinetics in plug flow reactors used in chemical engineering, as is with the case of oscillating baffle reactors (Ni *et al*., 2003). Baffles have also been used in the fields of water and wastewater treatment, to enhance settling efficiencies in clarifiers (Zhou *et al*., 1992), and to improve the performance of biological reactors (Barber & Stuckey, 1999).

One major biological process where baffles have historically been studied is anaerobic digestion for the treatment of domestic wastewater streams. Currently anaerobic digesters are most commonly employed to stabilize primary and secondary solids from conventional domestic wastewater treatment systems that use activated sludge as their core technology. Anaerobic reactors for the direct treatment of mainstream domestic wastewaters have historically had problems achieving high treatment efficiencies due to the generally lower reaction kinetics of anaerobic digestion combined with lower substrate concentrations in domestic wastewater. On the other hand, recent advances in membrane technology and the declining cost of membrane filters have enabled anaerobic membrane bioreactors (AnMBRs) to be an acceptable candidate for the direct treatment of mainstream domestic wastewater (Ozgun *et al*., 2013).

There are two approaches to anaerobically treating domestic wastewater. The first approach assumes preliminary separation of particulate material from the main wastewater stream (Yoo *et al*., 2012), and utilizes two distinct anaerobic reactors for treating the two

streams. This configuration would have a primary clarifier before the mainstream AnMBR process, and the AnMBR would receive considerably reduced organic matter loading as a result. The settled solids would be anaerobically digested in a separate reactor. The main advantage of this approach is that it considerably decreases the processing time for the treatment of the main wastewater stream by enabling two different hydraulic retention times (HRTs) for the solid and liquid fractions of domestic wastewater. The second approach assumes complete treatment of all incoming wastewater within a single AnMBR unit (Prieto *et al*., 2013). The main advantage of this approach is increased kinetics within the reactor owing to higher substrate concentrations, decreased overall treatment system complexity, and possibly decreased footprint depending on feed characteristics, the chosen HRT and organic loading rate (OLR). Although AnMBRs have been demonstrated to be able to achieve acceptable treatment efficiencies and energy use profiles for mainstream domestic wastewater treatment, novel configurations that can demonstrate higher performance and robustness may be desirable for widespread adoption of anaerobic reactors for the direct and complete treatment of domestic wastewater, especially where decentralized treatment with higher volatility in feed characteristics is of concern. In addition, since separating out incoming particulates using an additional gravity settling unit and treating them in a separate anaerobic digester increases system complexity, and in some cases overall footprint, a complete solution that addresses both the particulate and the soluble fractions within wastewater may have an advantage over systems that only address specific fractions of the wastewater.

An alternative configuration to traditional reactor designs is the Anaerobic Baffled Reactor (ABR) (Bachmann *et al*., 1985), which incorporates baffles to improve treatment efficiencies and robustness in plug-flow anaerobic reactor designs. ABR can retain biomass within each zone created by the baffles using gravity and subsequently lead to the cultivation of

distinct populations on the travel path of the incoming wastewater. This gives the ABR design the versatility and robustness of the two-phase anaerobic digesters, where fermentation and methanogenesis processes occur in different reactors, increasing stability. ABR has also been shown to perform exceptionally well under psychrophilic conditions (Nachaiyasit & Stuckey, 1997).

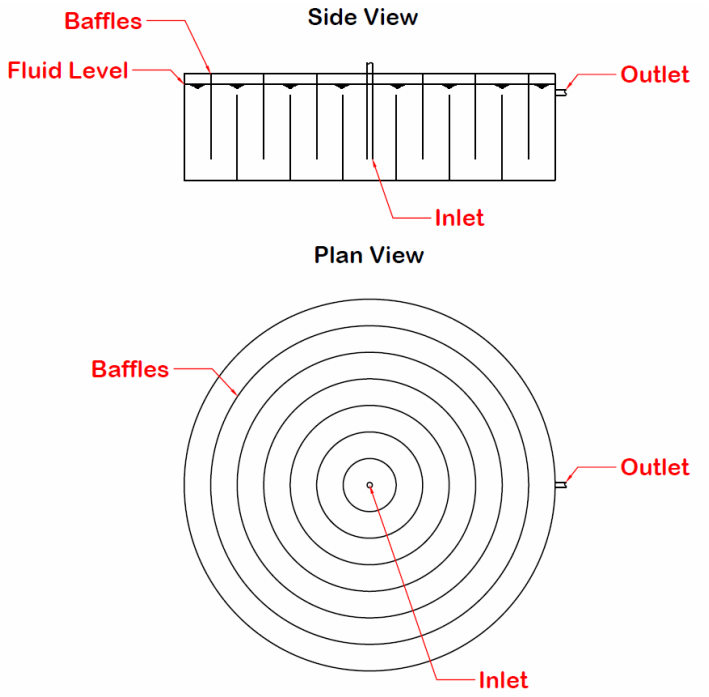

Figure 3.1. Concentrically Baffled Reactor (CBR) side and plan views

This section introduces a reactor design that consists of concentrically arranged baffle rings wherein the inlet of the reactor is in the center and the fluid flow occurs from the center outwards, traveling through zones that are separated by these concentric baffles, flowing vertically up and down through each zone, and consequently and cumulatively along a horizontal path along the diameter of the reactor (Figure 3.1). The design is primarily aimed towards water and wastewater treatment applications; providing a compact, high performance alternative

combining the traditionally separate unit operations of gravity settling and biological treatment, but the design can be used for any other desired application outside this field where the unique advantages and geometry will favor process conditions.

Through the use of baffles, different process conditions can be maintained through discrete reaction volumes, while the flow of reactants and products from one reaction volume to the next is carried out completely passively. The use of baffled reactors has three main advantages over using individual units for an industrial process: firstly, the complexity of actively transferring the flow from one reactor to the next, and any potential points of failure associated with the equipment utilized to carry out the active transfer, are avoided; secondly, any equipment costs and energy inefficiencies due to the use of individual pumps to keep the flow going between the reactors are also avoided; and finally, a baffled reactor will have a much tighter footprint than a process train with discrete units, which can save on capital costs and enable deployment in situations where space is a constraint. In addition, through the use of baffles, a gradient of conditions (temperature, particle size, solids concentration, pH, redox potential, microbial populations, and others) can be maintained within a single continuous reactor volume.

3.1. Implications of CBR Geometry

One of the main advantages of concentric baffling is seen when the central chamber is heated and a thermal gradient in the horizontal direction is established in order to enhance reaction performance (Figure 3.2). Concentric baffling enables more of the heat to be retained within the system, since the zones themselves become insulators for each subsequent inner zone, reducing heat loss when compared with traditional baffled reactor designs. This has direct

implications for anaerobic treatment of wastewater streams, which is commonly done at mesophilic (35°C) and thermophilic (55°C) temperatures.

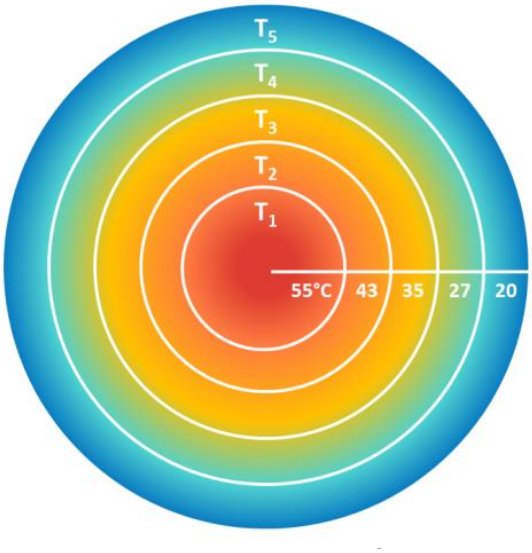

Figure 3.2. CBR temperature gradient (plan view)

Temperature phasing from thermophilic down to mesophilic and psychrophilic temperatures has the advantage of pathogen destruction within the thermophilic zone, as well as the rapid hydrolysis and acidification of particulates and complex molecules to be used as substrates in the subsequent zones. This increases the stability of the process by separating the acidogenesis stage of anaerobic digestion from subsequent processes. The concentrically baffled design, combined with temperature phasing, is able to create a gradient of profiles for temperature, solids concentrations, water quality, and microbial populations along the treatment path. This change in profiles will enable the waste to be subjected to different treatment conditions, and may enhance overall degradation due to a potentially broader range of enzymatic

reactions involved in the process (Russell, 2000). To illustrate, theoretical gradients along the reactor radius from the center to the outer wall are shown in Figure 3.3.

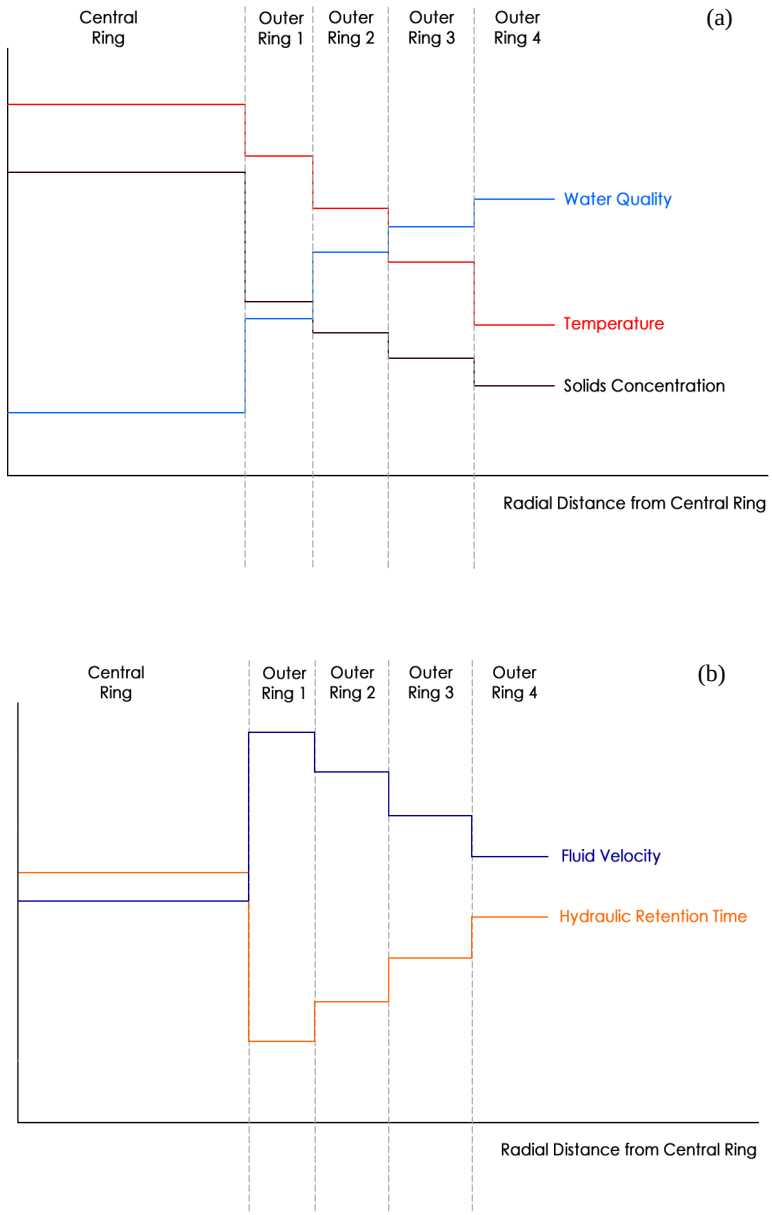

Figure 3.3. Theoretical gradient for (a) temperature, solids and water quality, and (b) fluid velocity and hydraulic retention time along the reactor radius from the center to the outer wall

One way to model the Concentrically Baffled Reactor is as a series of CSTRs (rings) of increasing volumes and HRTs. If the baffle spacing is kept at a constant value, the volume of each subsequent ring increases as the liquid travels from the center of the reactor outwards (Figure 3.4). By adjusting the baffle spacing and the number of baffles, discrete zones with desired HRTs can be created for a specific purpose.

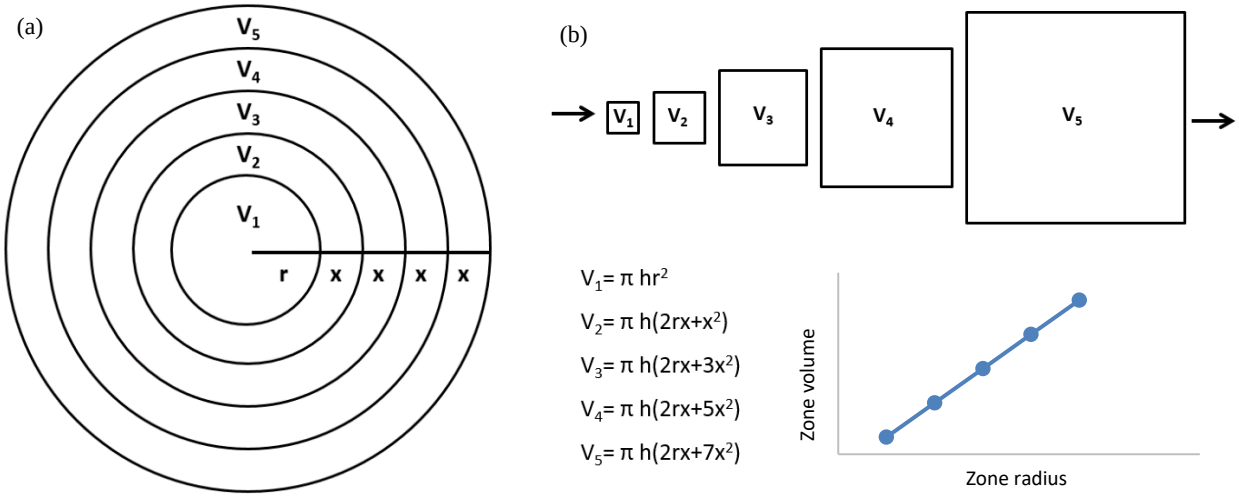

Figure 3.4. (a) Plan view of CBR with evenly spaced baffling (b) a model showing the increase in volumes of each subsequent ring as the liquid travels from the center to the outermost ring

A well-mixed CBR can also perform much better than a Completely Stirred Tank Reactor (CSTR), depending on reaction kinetics and required residence times. This is due to the fact that CSTRs-in-series approach ideal plug flow conditions as the number of discrete reaction volumes increases. A theoretical comparison of equal volume CSTR and CBR systems are given in Figure 3.5. The comparison assumes enough zoning with CSTRs-in-series where plug flow regime can be achieved in the CBR system, which may or may not be the case for real life applications.

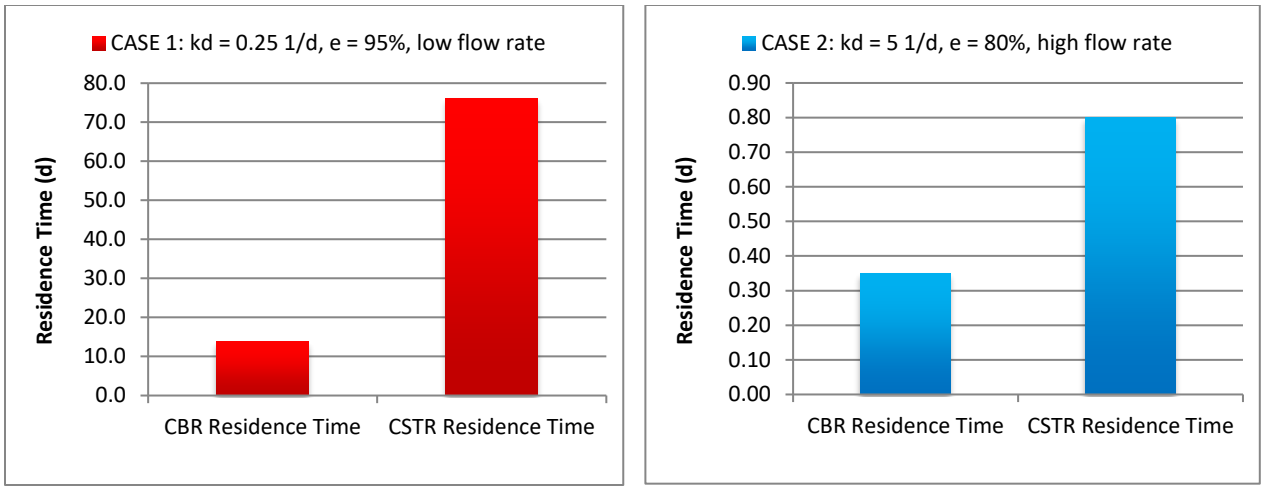

Figure 3.5. Comparison of required hydraulic residence times for CBR and CSTR under two different kinetic and hydraulic conditions (kd: decay constant, e: reaction efficiency, first order decay is assumed for both cases)

Assuming a first-order reaction, the effluent concentration of a single reactant can be expressed as given in *Eq. 4*:

$$C = \frac{C_0}{1 + k_d t} \tag{4}$$

In the above equation, C stands for remaining reactant concentration, C_0 for starting reactant concentration, k_d for decay constant, and t stands for residence time. As the number of reactors increases for a given finite volume, the equation will be as follows:

$$C = \frac{C_0}{(1 + k_d \frac{t}{n})^n} \tag{5}$$

In *Eq. 5*, *n* represents the number of equal volume reactors. As *n* approaches infinity, the efficiency of the reactions increases, approaching the efficiency of an ideal plug flow system, the first-order reaction kinetics of which is represented by *Eq. 6* given below:

$$C = C_0 e^{-k_d t} \tag{6}$$

3.2. CBR Configurations

Concentrically Baffled Reactor can be designed and operated using various alternative configurations for wastewater treatment (Figure 3.6). Each configuration is briefly discussed in this section to give the reader an idea of how CBR can readily be utilized within this field. The list of configurations is by no means complete, and it is given as a reference for potential applications of the technology for wastewater treatment.

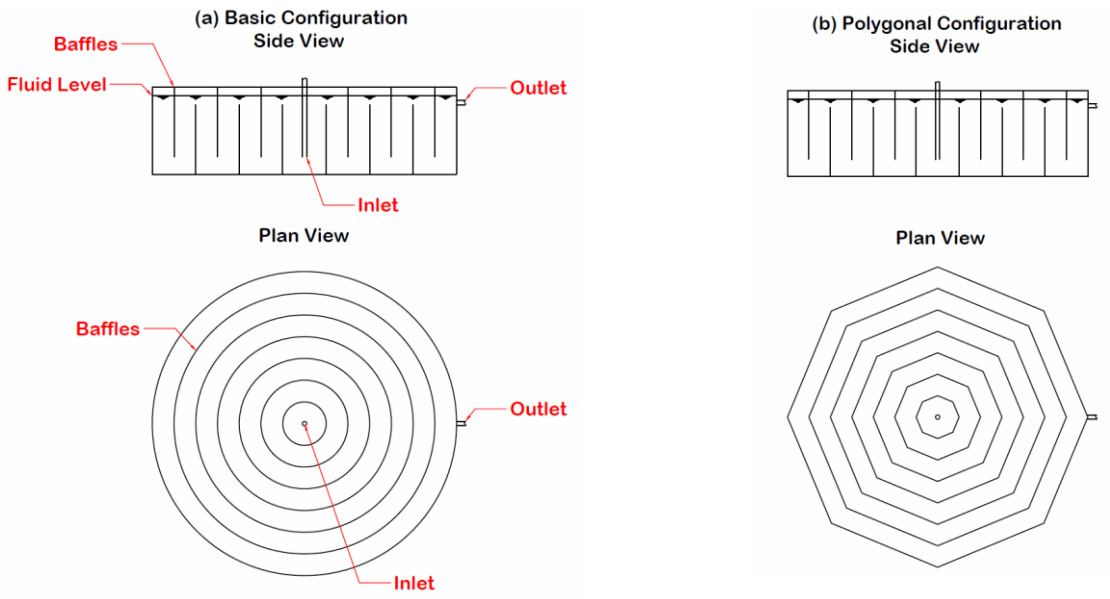

Figure 3.6. CBR Configurations

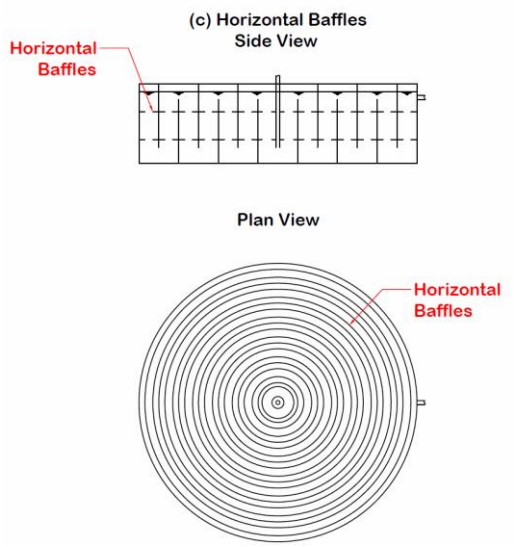

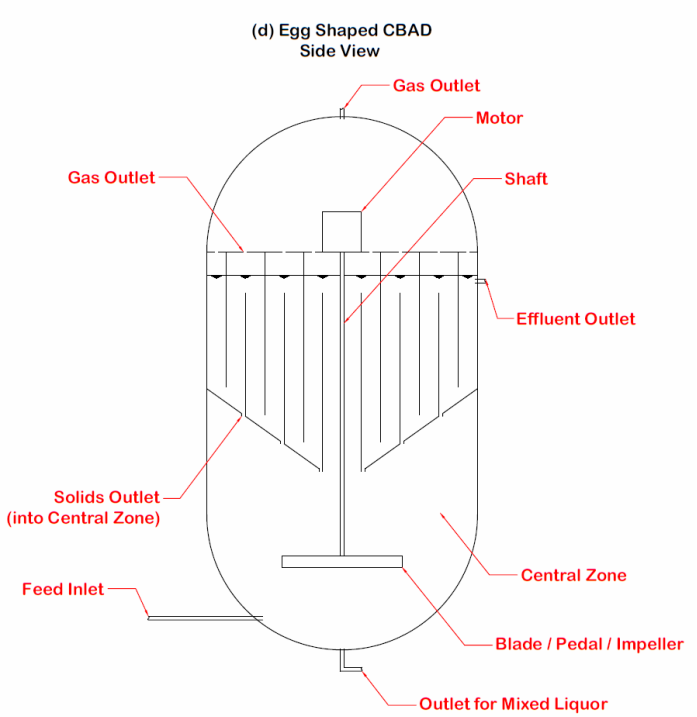

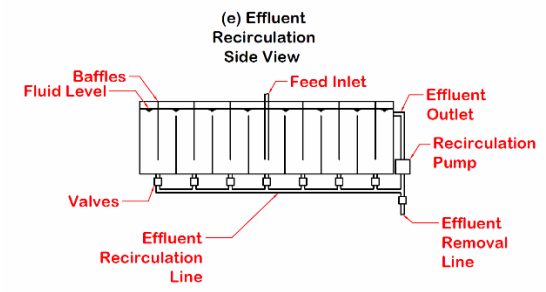

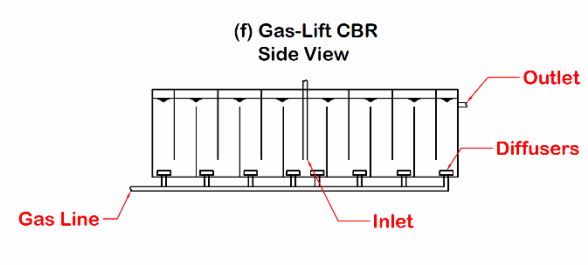

Figure 3.6. (Continued)

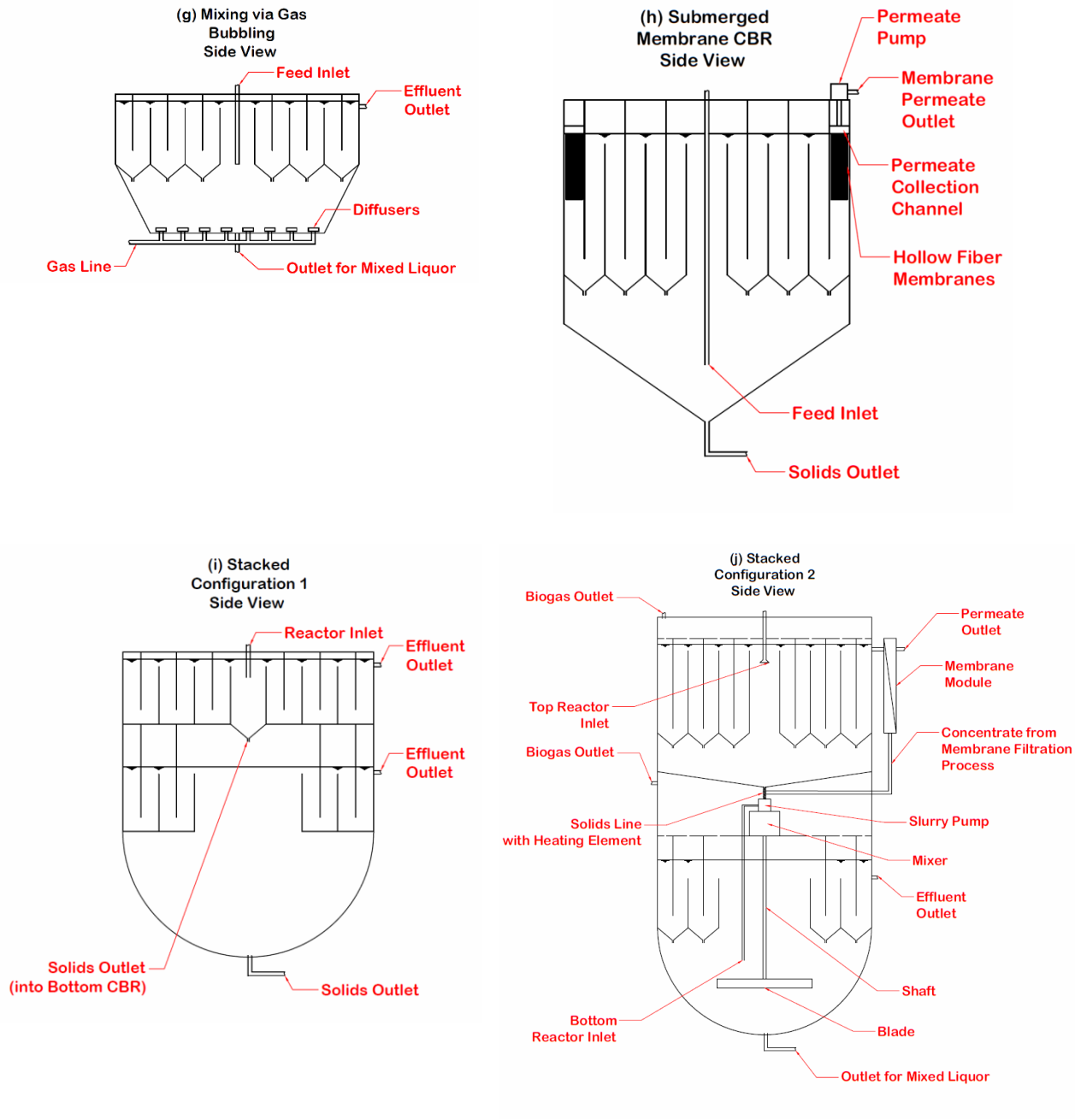

Figure 3.6. (Continued)

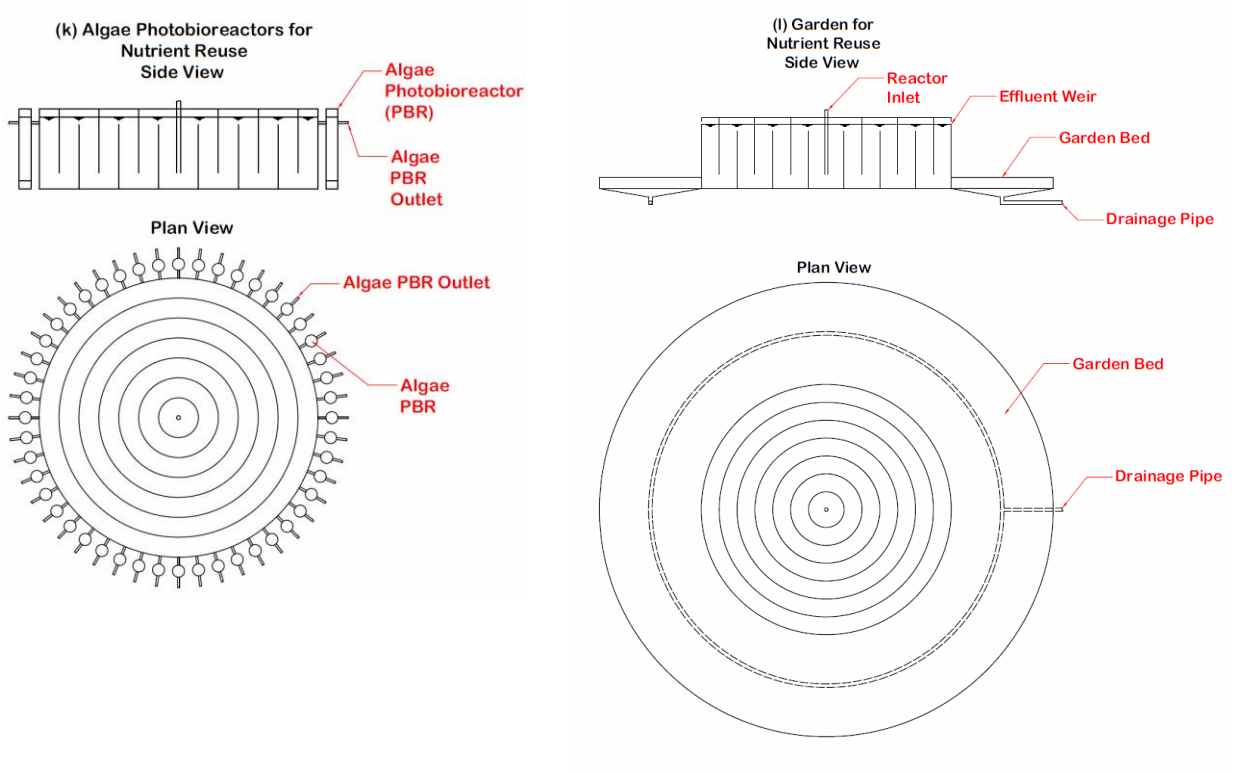

Figure 3.6. (Continued)

(a) Base Configuration

This is the fundamental form of the Concentrically Baffled Reactor. It is cylindrical, with concentric, cylindrical baffles to guide the fluid flow. The inlet is in the middle of the reactor, and the outlet is connected to the outermost ring. The fluid flow is from the center to the outer ring. The wastewater enters the system from the top, making the CBR an ideal candidate for replacing or retrofitting existing septic tank systems.

(b) Polygonal Configuration

The reactor is a polygon instead of a cylinder. This is recommended when it will be easier or less costly to build or manufacture the reactor using flat panels.

(c) Horizontal Baffles

Additional horizontal baffling is used in addition to vertical. Horizontal baffles are attached to vertical baffles at a right angle. The fluid moves sideways as well as going up and down as a result. Horizontal baffles create eddies that help with mixing under laminar flow conditions.

(d) Egg Shaped Concentrically Baffled Anaerobic Digestion (CBAD)

Egg-shaped anaerobic digesters have been shown to provide more efficient mixing than cylindrical digesters (Wu, 2010), and have been widely adopted for the digestion of primary and secondary solids originating from the treatment of domestic wastewaters. This CBR configuration features the installation of concentric rings along the flow path, redirecting the effluent into a series of concentric zones before it exits the system. Existing egg-shaped digesters can be retrofitted with concentric baffles to create distinctive reaction zones along the flow path, leading to higher removal efficiencies. The mixing system can be designed to extend into each concentric ring to create completely mixed conditions in all reaction zones.

(e) Effluent Recirculation

The effluent from the CBR process can be returned to any individual zone within the reactor to increase HRT and mixing within the reactor. This may be required if greater contact time or better homogenization is needed for the wastewater constituents to be degraded.

(f) Gas-lift CBR

In this configuration, the diffusers in the upflow zones help to mix and move reactor contents into subsequent zones. Liquid motion is achieved via the upward motion of the bubbles. Gas supplied to the CBR can be air, biogas, or any other gas depending on the process.

(g) Mixing via gas bubbling

This configuration features a larger central zone which is reserved for slower reactions (like hydrolysis) to take place before the contents move into subsequent zones. The mixing is facilitated through the use of diffusers at the bottom of the central zone. Alternatively, mixing in the central zone can be provided with the use of a mechanical impeller or similar mechanism.

(h) Submerged Membrane CBR (SM-CBR)

A circular submerged membrane unit is placed into the outermost zone of the CBR for membrane filtration. Hollow fiber micro- or ultra-filtration membranes are recommended for most wastewater applications. Membrane fouling can be controlled by installing diffusers to the bottom of the outermost ring.

(i) Stacked configuration 1 (passive)

In this configuration, two CBRs are stacked on top of one another, with the CBR on top (CBR_T) treating incoming wastewater at a high rate, while the CBR at the bottom (CBR_B) treats the solids that settle down during the high rate CBR_T process. In this passive configuration, the solids originating from CBR_T move into CBR_B passively via an opening at the bottom of the central zone of CBR_T. In alternative configurations, CBR_T can be made much larger to

accommodate particulate-rich feed streams, and any or all subsequent zones can be connected to CBR_B passively. CBR_B central zone can be mixed to facilitate contact between wastewater and biomass in wastewater treatment processes.

(j) Stacked configuration 2 (active)

This is another version of the stacked configuration, where the solids from CBR_T are pumped into CBR_B actively via a slurry pump. CBR_T has an external membrane module installed at the outlet, and the contents of CBR_B central zone are mixed using an impeller. Another membrane module can be used at CBR_B outlet or as a submerged unit at the outermost zone, converting both CBRs into Concentrically Baffled AnMBRs (CB-AnMBR).

(k) CBR + Algae cultivation

Nutrient rich CBR or CB-AnMBR effluent can be used to cultivate algae for simultaneous nutrient uptake and the potential production of biofuels and other commodities from algal cultures, as described elsewhere (Chen *et al*., 2011). In this depiction, cylindrical photobioreactors are placed around the outside wall of the outermost ring. Alternative designs may include having CBR effluent flow passively into an open pond that circles the perimeter of the CBR, or using various other vertical and horizontal placement schemes for the photobioreactors (Carvalho *et al*., 2006). Natural daylight can be utilized for the purpose of cultivating algal cultures, as well as artificial lighting.

(l) CBR + Garden bed

In a similar manner to (k), nutrients coming out of a CBR wastewater treatment process can be used to grow industrial or food crops on a circular garden bed surrounding the perimeter of the reactor. In addition to the management of nutrients and potential additional revenue stream from the crops, the garden bed also has the potential to enhance the aesthetics in the wastewater treatment site, prevent any potential malodors, and regulate the temperature of the treatment unit with respect to ambient temperatures.

The CBR can also be operated as a temperature-phased anaerobic reactor. In this case the reactor is termed the Anaerobic, Concentrically-Baffled, Temperature-phased Bioreactor (ACT-Bioreactor). The ACT-Bioreactor can further be combined with a membrane to function as a membrane bioreactor (MBR), thereby become the ACT-MBR (Figure 3.7). The system is expected to be robust and highly efficient, and able to handle shock loadings.

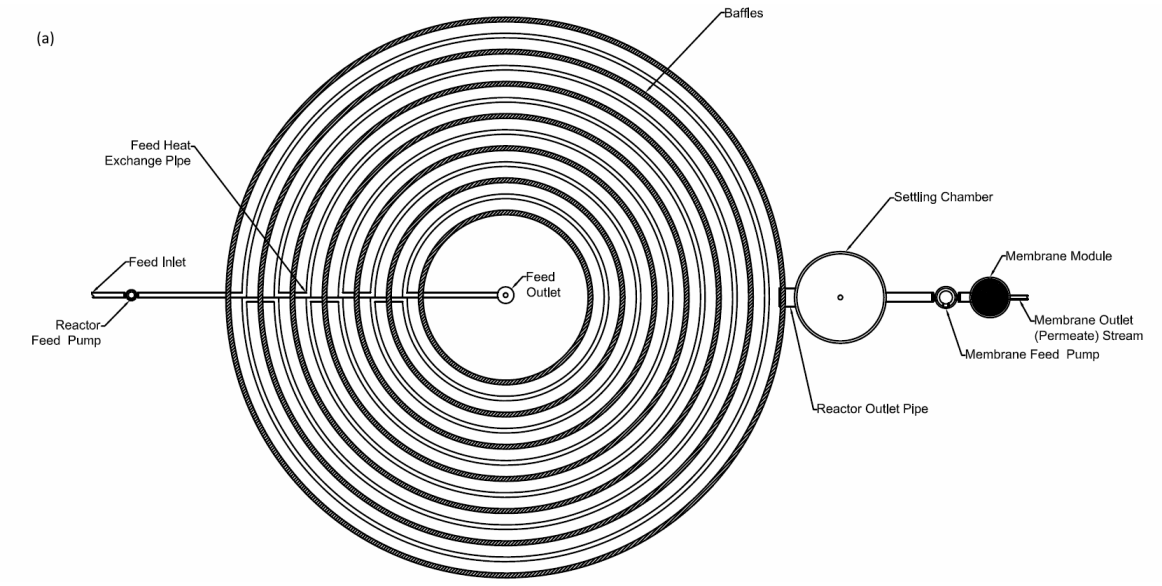

Figure 3.7. ACT-MBR (a) plan and (b) side views

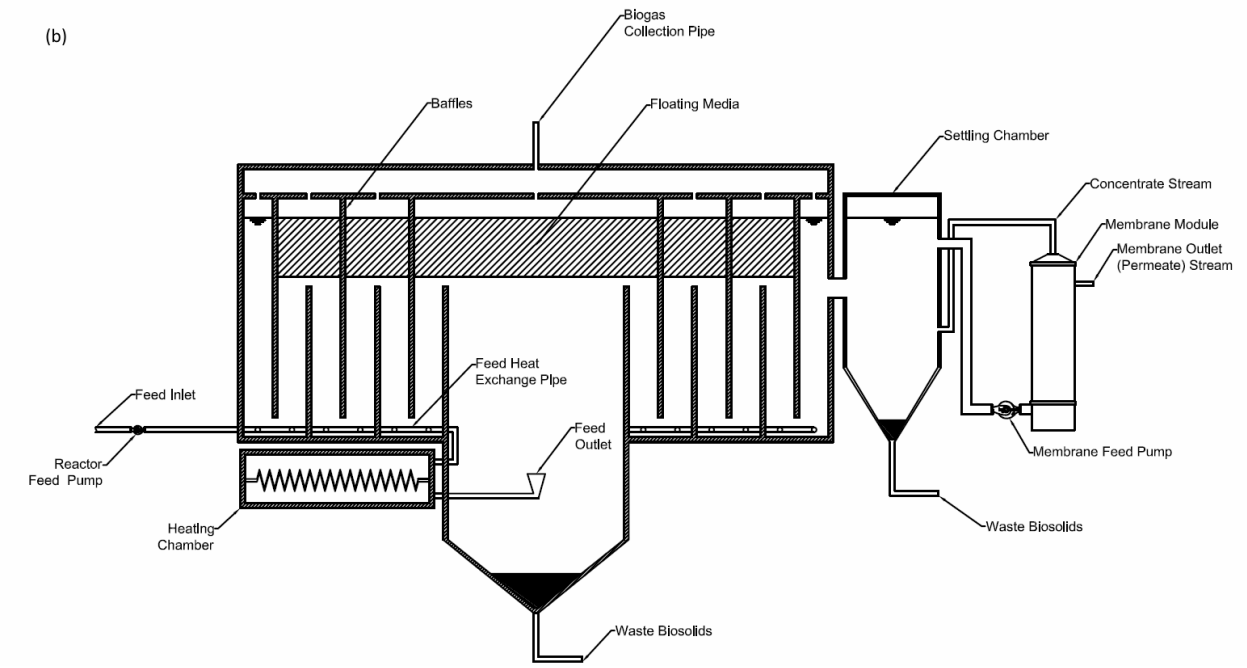

Figure 3.7. (Continued)

In the ACT-MBR configuration, the feed pipe goes through the reactor in a concentric fashion, exchanging heat with the contents of the reactor to create a temperature gradient within the system and to transfer energy to the feed stream in the process. After reaching the central ring, the feed is heated in an external preheating unit up to 60°C depending on the feed preheating regime and supplied to the central ring of the bioreactor, which was designed as a hybrid settling/digestion zone to promote the hydrolysis of the incoming organic particulates. As the particulate fraction of the organic matter hydrolyzes within the central ring, it travels with the water and the soluble fraction of organics to subsequent rings, where further breakdown takes place. Treated liquid is then drawn from the outermost zone through a pipe or an overflow mechanism to an external settling chamber or an additional CSTR zone, depending on the configuration. Supernatant or mixed liquor drawn from this zone is then fed to an external membrane filtration unit, where further separation takes place. The concentrate from the

membrane unit is returned to the settling chamber. Biosolids that accumulate within the central ring and the settling chamber are collected from the bottom through drainage pipes.

This design marries concentric baffling with temperature phasing and heat exchange with the medium. Concentric baffling limits heat loss compared to linear rectangular designs, because the liquid moving through the reactor has considerably less contact with surfaces that can act as heat sinks to the ambient environment. Combination of a heat exchanger with temperature phasing is feasible from both reactor design and energy efficiency perspectives, because the formation of a temperature gradient is achieved by transferring some of the heat within each concentric ring to the incoming feed, decreasing the energy required to heat the feed up to desired temperatures. Baffling itself has been shown to make anaerobic systems more resistant to hydraulic, organic, toxic shock loads than single column PFRs such as UASBs (Barber & Stuckey, 1999), which increases system robustness. Baffling has also been shown to reduce membrane fouling in AnMBRs, which can be attributed to reduced solids concentrations and extracellular polymeric substance (EPS) production in the later zones of the baffled reactor (Pillay *et al.*, 2008). The most important aspect of baffling is perhaps the prevention of biomass washout to subsequent zones, enabling the cultivation of different microbial populations along the treatment path. In addition, the floating attached growth media enable a more homogeneous spatial distribution of biomass along the reactor gradient and the flow path, regardless of the velocity of the moving liquid. It is also hypothesized that the floating media will keep any floating or suspended biomass within each reactor ring from being washed out to subsequent rings. Another advantage may be in treating organic matter that floats, such as in the case of fats, oil and grease (FOG), enabling a greater number of microorganisms to come in contact with the substrate and speeding up its degradation.

3.3. Modeling and Analysis

Before moving onto designing and manufacturing the first CBR prototype, it was necessary to predict how the system would perform under different design and operational conditions. To this end, a steady-state mass balance model of the system was created, initially using Microsoft Excel, and later on using the Python programming language. The model was then incorporated into a geometric analysis algorithm, which was used to predict system response using 10 variables with 2 value levels (a low and a high value) for 9 different possible feed compositions. This gave an idea of how to size the reactor, what height-to-diameter ratio to use, what number of baffles to incorporate, how much to space out the baffles from one another, *etc*. under different HRTs, SRTs, decay rates, and for different feed compositions. Lastly, a sensitivity analysis was conducted where a feed composition that was predicted to be close to real raw domestic wastewater was selected, and the sensitivity of the system response to design parameters was predicted with respect to a baseline scenario. The geometric and sensitivity analyses were essential to gather generalized guidelines about the unique geometry of the CBR, and to ultimately be able to make more informed design decisions for the first prototype.

3.3.1. Model

The model is a non-dynamic steady-state mass balance model incorporating 3 processes: (1) Settling of particulate solids, (2) disintegration of particulate solids into soluble fractions, and (3) the decay of soluble solids. Disintegration and decay processes follow first order kinetics. It was a priority to keep the model simple and add only those processes and parameters that were absolutely necessary to obtain meaningful results, but not more, since the model was going to inform the design of the first prototype and therefore could never be calibrated. Table 3.1 shows

the processes incorporated into the model, along with their governing equations. The Python source code for the model can be found in Appendix A.

Table 3.1. Model processes and governing equations

Process	Equation
Settling	$u_s = \frac{g(\rho_p - \rho)d_p^2}{18\mu}$
Disintegration	$-\frac{dC_p}{dt} = k_{dis}C_p$
Decay	$-\frac{dC_s}{dt} = k_{dec}C_s$

In the above equations, u_s stands for settling velocity (m/s), g stands for gravitational acceleration (m/s^2), ρ stands for density of water (g/m^3), ρ_p stands for mean density of affected particles (kg/m^3), d_p stands for mean diameter of affected particles (m), μ stands for dynamic viscosity of water (kg/m/s), C_p stands for concentration of particulate solids (g/m^3), k_{dis} stands for disintegration rate constant (1/d), C_s stands for concentration of soluble solids (g/m^3), and k_{dec} stands for decay rate constant (1/d). Disintegration and decay processes rely on first order kinetics, whereas settling is represented by Stokes' law. Disintegration process produces soluble solids, which are subject to the decay process. Laminar flow was determined to be the dominant regime for all hydraulic retention times tested. For Stokes' settling, all particles were assumed to be spherical. Influent temperature was assumed to be 20°C for the purposes of determining dynamic viscosity and density of water for all model runs.

Since the model uses Stokes law for settling, a Reynolds number check is required to make sure Stokes law can be applied. To this end, the model was run with the input parameters relating to settling as shown in Table 3.2.

Table 3.2. Model inputs used for the Reynolds number check

Parameter	Value	Unit
Reactor Volume	0.032	m^3
Flow Rate (10d HRT)	3.7E-08	m^3/s
Flow Rate (0.01d HRT)	3.7E-05	m^3/s
Mean particle diameter	2.00E-04	m
Kinematic viscosity	1.00E-06	m^2/s
Dynamic viscosity	1.00E-03	kg/m/s
Mean particle density	1250	kg/m^3
Density of water	1000	kg/m^3
Gravitational acceleration	9.81	m/s^2
Stokes Settling Velocity	5.44E-03	m/s

For Stokes law to be applicable Reynolds number needs to be less than 1. Reynolds number was calculated for high HRT (10 d) and low HRT (0.01 d) scenarios. The results are given in Table 3.3.

Table 3.3. Reynolds number check results

		Zones			
Parameter	**Unit**	**Z1**	**Z3**	**Z5**	**Z7**
Inner Dia	m	0.00	0.20	0.35	0.50
Outer Dia	m	0.15	0.30	0.45	0.60
Inner Surface Area	m^2	0.00	0.03	0.10	0.20
Outer Surface Area	m^2	0.02	0.07	0.16	0.28
Surface Area	m^2	0.02	0.04	0.06	0.09
Upflow Velocity (10d HRT)	m/s	2.1E-06	9.4E-07	5.9E-07	4.3E-07

Table 3.3. (Continued)

		Zones			
Parameter	**Unit**	**Z1**	**Z3**	**Z5**	**Z7**
Upflow Velocity (0.01d HRT)	m/s	2.1E-03	9.4E-04	5.9E-04	4.3E-04
Mean Particle Velocity (10 d HRT)	m/s	5.4E-03	5.4E-03	5.4E-03	5.4E-03
Mean Particle Velocity (0.01 d HRT)	m/s	3.3E-03	4.5E-03	4.9E-03	5.0E-03
Reynolds Number for Particles (10 d HRT)	-	1.09	1.09	1.09	1.09
Reynolds Number for Particles (0.01d HRT)	-	0.67	0.90	0.97	1.00

The results are slightly above 1 for high HRT and less than or equal to 1 for low HRT. The slight exceedance of the Reynolds number criterion for the high HRT scenario was ignored in this case, because the number is very close to the criterion, and due to the simplicity that Stokes equation provides for modeling settling. Model inputs are listed in Table 3.4.

Table 3.4. Model inputs and their descriptions

Input	**Definition**	**Unit**
i_f_Xi	Influent fraction, particulate inert	-
i_f_Xr	Influent fraction, particulate reactive	-
i_f_Si	Influent fraction, soluble inert	-
i_f_Sr	Influent fraction, soluble reactive	-
i_V_r	Total reactor volume	m^3
i_SRT	Total particulate solids retention time	d
i_k_dis	Disintegration rate constant for particulate solids	1/d
i_k_dec	Decay rate constant for soluble solids	1/d
i_MPD	Mean particle diameter for particulate solids	µm
i_f_std_PSD	Standard deviation fraction of the particle size distribution curve	-
i_rho	Mean particle density of particulate solids	kg/m^3
i_HRT	Total hydraulic retention time	d
i_f_dC0	Fraction of central zone diameter with respect to reactor diameter	-
i_n_z	Number of zones	-
i_HDR	Reactor height-to-diameter ratio	-

The model calculates solids removal through settling, disintegration and decay processes for each zone, the number of which is defined using the *i_n_z* (number of zones) model input. Influent fractions *i_f_Xi* and *i_f_Xr* are particulate fractions, and are therefore subject to settling, whereas *i_f_Si* and *i_f_Sr* are soluble fractions, and therefore are not subject to settling. The inert fractions of the influent, *i_f_Xi* and *i_f_Si*, are not subject to disintegration or decay, whereas the particulate reactive fraction *i_f_Xr* is subject to disintegration, and the soluble reactive fraction *i_f_Sr* is subject to decay. The decay process uses only the Hydraulic retention time *i_HRT* for its rate equation, whereas the disintegration process uses Particulate solids retention time *i_SRT*. Mean particle diameter for particulate solids *i_MPD*, and Standard deviation fraction of the particle size distribution curve *i_f_std_PSD* are used as inputs in a normal probability distribution function to create a particle size distribution curve, which is used to determine the percentage of particulate solids that are settlable. For each upflow reactor zone, the overflow rate (or upflow velocity) is calculated by dividing the flow rate by the surface are of the zone. The overflow rate is then used in Stokes equation to determine the particle diameter cut-off for settlable particles. Fraction of central zone diameter with respect to reactor diameter *i_f_dC0*, number of zones *i_n_z*, reactor height-to-diameter ratio *i_HDR* are the main variables informing the optimal geometric shape for the reactor given the influent characterization and the operational conditions.

3.3.2. Geometric Analysis

A geometric analysis would yield more general information and guidelines to direct the design of the prototype. To this end, for two levels (a high and a low level) of the ten parameters selected, the model was run 2^{10} = 1,024 times for 9 different possible feed compositions, yielding

9,216 responses to analyze. The main focus for this analysis was to reach generalized conclusions about the optimal geometry of the design under different feeding regimes and operational conditions. The Python code used for the geometric analysis can be found in Appendix B. The list of the ten input variables used for the analysis are given in Table 3.5.

Table 3.5. Input parameters used for the geometric analysis with their high and low levels

Input	Definition	Unit	Low	High
i_HRT	Hydraulic retention time	d	1	5
i_SRT	Solids retention time	d	10	50
i_k_dis	Disintegration rate constant for particulate solids	1/d	0.01	0.05
i_k_dec	Decay rate constant for soluble solids	1/d	0.1	0.5
i_f_dC0	Fraction of central zone diameter with respect to reactor diameter	-	0.2	0.8
i_n_z	Number of zones	-	3	9
i_HDR	Reactor height-to-diameter ratio	-	0.2	5
i_MPD	Mean particle diameter for particulate solids	μm	50	200
i_f_std_PSD	Standard deviation fraction of the particle size distribution curve	-	0.2	0.8
i_rho	Mean particle density of particulate solids	kg/m^3	1050	1825

The low and high values for the input parameters entered into the geometric analysis model were chosen to reflect a broad spectrum of environmental and operational conditions in order to gather the greatest amount of information on the behavior of the reactor with respect to these parameters and its geometry. The variables fraction of central zone diameter with respect to reactor diameter *i_f_dC0*, number of zones *i_n_z*, and reactor height-to-diameter ratio *i_HDR* were the geometric inputs, whereas the rest of the variables defined environmental and operational inputs. Reaction rate related inputs *i_HRT*, *i_SRT*, *i_k_dis*, and *i_k_dec* were selected so as to result in a maximum of 95% removal in the "all reactive" influent composition scenario described below, with *i_HRT* and *i_SRT* selected to reflect common operational values used in

anaerobic treatment of wastewaters. The values selected are in the lower range for *i_HRT* owing to consideration of anaerobic membrane bioreactors, which are typically operated with lower HRTs than traditional anaerobic reactors.

Table 3.6. Feed compositions used as inputs for the geometric analysis

#	Desc	i_f_Xi	i_f_Xr	i_f_Si	i_f_Sr
1	All equal	25%	25%	25%	25%
2	All particulate inert	100%	0%	0%	0%
3	All particulate reactive	0%	100%	0%	0%
4	All soluble inert	0%	0%	100%	0%
5	All soluble reactive	0%	0%	0%	100%
6	All particulate	50%	50%	0%	0%
7	All soluble	0%	0%	50%	50%
8	All inert	50%	0%	50%	0%
9	All reactive	0%	50%	0%	50%

The feed compositions tested for the geometric analysis involved testing for the balanced composition which contains equal parts of all four fractions (particulate inert, particulate reactive, soluble inert and soluble reactive), and testing for the extremes where one or more of the fractions dominate the composition. The testing of the extremes was done to gather as much relatively accurate information about the behavior of the system as possible by preventing any noise that could interfere with the analysis by the use of more complex combinations of the feed constituents. The 9 different compositions used for the analysis are given in Table 3.6.

Outputs of the model consisted of effluent concentrations and removal percentages for each individual fraction of influent solids, as well as aggregations of the fractions to yield total solids removal data. The analysis focused on the total solids removal parameter to rank the 1,024 responses for each feed composition. The input parameter combinations that yielded the best

total solids removal percentages were then interpreted to reach generalized conclusions about the behavior of the system. Output parameters are presented in Table 3.7.

Table 3.7. Output parameters of the geometric analysis model

Output	Definition	Unit
o_Xi	Effluent X_i concentration	g/m^3
o_Xr	Effluent X_r concentration	g/m^3
o_Si	Effluent S_i concentration	g/m^3
o_Sr	Effluent S_r concentration	g/m^3
o_rem_Xi	X_i removal	%
o_rem_Xr	X_r removal	%
o_rem_Si	S_i removal	%
o_rem_Sr	S_r removal	%
o_rem_X	Total particulate solids removal	%
o_rem_S	Total soluble solids removal	%
o_rem_i	Total inert solids removal	%
o_rem_r	Total reactive solids removal	%
o_rem_tot	Total solids removal	%

The results of the analysis featuring the top 10% responses (out of 1,024) ranked by total solids removal for each feed composition are listed in Appendix D. A breakdown of the how many times the high and low values for each parameter appear in the top 10%, 5%, and 1% of the results for each feed composition analyzed are given in Appendix E. The percentages indicate the frequency of appearance with respect to number of responses within the respective percentile (a total of 102 responses analyzed out of 1,024 for the top 10%, 51 responses for the top 5%, and 10 responses for the 1%). Note that the (4) “all soluble inert” scenario was not analyzed in this manner, because, as expected, there was no solids removal and therefore no way to rank the results.

There were a few distinct patterns with respect to the results, which became clear after the analysis. Some of these findings were expected, while others offered further insight into the design of the CBR prototype:

- High decay rate and high HRT result in better solids removal performance for feed streams that contain high amounts of soluble reactive solids, which is expected.
- High particle density and size, and high reactor HRT, result in better settling performance for particulate solids.
- High disintegration rate and high SRT result in greater particulate reactive solids destruction, but where total solids removal (and not destruction) is concerned, low disintegration rates with low SRT result in better removal. This is because the solids that settle are wasted to achieve the desired SRT and are considered to be removed from the system regardless of whether they are disintegrated. A high disintegration rate can yield more soluble solids in the reactor effluent, decreasing overall solids removal rates. Whether this is a desired effect for real life wastewater treatment applications depends on the specific needs of the treatment operation.
- For settling-dominated removal scenarios, larger diameter is favored for the central zone, along with lower total number of zones and low height-to-diameter ratio. This is because settling works best with one single, large, and uninterrupted overflow surface in the upflow direction for cylindrical column reactors.

3.3.3. Sensitivity Analysis

In order to gauge how much each parameter would affect the removal performance for the first CBR prototype, a sensitivity analysis was conducted, where the analyzed variables were

HRT (*i_HRT*), reactor height-to-diameter ratio (*i_HDR*), number of reactor zones (*i_n_z*), and the fraction of central zone diameter with respect to reactor diameter (*i_f_dC0*). All other input parameters were held constant. A list of constant input parameters is presented in Table 3.8.

Table 3.8. List of constant inputs used in the sensitivity analysis

Constant	Definition	Unit	Value
i_SRT	Solids retention time	d	100
i_k_dis	Disintegration rate constant for particulate solids	1/d	0.1
i_k_dec	Decay rate constant for soluble solids	1/d	3
i_MPD	Mean particle diameter for particulate solids	µm	100
i_f_std_PSD	Standard deviation fraction of the particle size distribution curve	-	0.3
i_rho	Mean particle density of particulate solids	kg/m^3	1250

The constants were chosen so as to make sure the system is not dominated by removal via settling, but organic solids destruction. To this end, relatively higher *i_SRT*, *i_k_dis*, and *i_k_dec* values, and relatively lower *i_MPD*, *i_f_std_PSD*, and *i_rho* values were selected for the analysis. Whether these values reflect real life conditions will depend on the specific feed composition and the operational/environmental factors affecting the treatment operation. For this analysis, it is assumed that the reactor is able to handle the incoming organic loading as far as solids destruction is concerned. The particle size distribution parameters *i_MPD* and *i_f_std_PSD* are loosely based on the study by Levine *et al*. (1991).

The feed composition, as presented in Table 3.9, was selected so as to loosely reflect an average domestic wastewater feed composition, based on the study by Orhon *et al*. (1997).

Table 3.9. Feed composition used in the sensitivity analysis

Input (Constant)	Definition	Unit	Value
i_f_Xi	Influent fraction, particulate inert	-	0.1
i_f_Xr	Influent fraction, particulate reactive	-	0.5
i_f_Si	Influent fraction, soluble inert	-	0.05
i_f_Sr	Influent fraction, soluble reactive	-	0.35

For the analysis, a baseline scenario was selected wherein the variables were set to the baseline values of 0.5 d, 0.4, 6, and 1 for *i_HRT*, *i_f_dC0*, *i_n_z*, and *i_HDR*, respectively. These parameters were then varied 50% in both the positive and negative directions to yield different total solids removal rates. The differences in solids removal with respect to the baseline scenario were recorded for each parameter varied. The results are given in Table 3.10.

Table 3.10. Scenarios tested for the sensitivity analysis and analysis results

	i_HRT (d)	i_f_dC0	i_n_z	i_HDR	Rem. (%)	ΔRem. (%)
Baseline	0.5	0.4	6	1	48.2	0.0
i_HRT (+50%)	1	0.4	6	1	79.3	31.2
i_HRT (-50%)	0.25	0.4	6	1	20.5	-27.7
i_f_dC0 (+50%)	0.5	0.8	6	1	72.2	24.0
i_f_dC0 (-50%)	0.5	0.2	6	1	48.0	-0.2
i_n_z (+50%)	0.5	0.4	9	1	46.9	-1.3
i_n_z (-50%)	0.5	0.4	3	1	57.8	9.6
i_HDR (+50%)	0.5	0.4	6	2	34.7	-13.5
i_HDR (-50%)	0.5	0.4	6	0.5	61.2	13.0

The changes in removal rates for each parameter tested for were then shown graphically for better visualization, as presented in Figure 3.8.

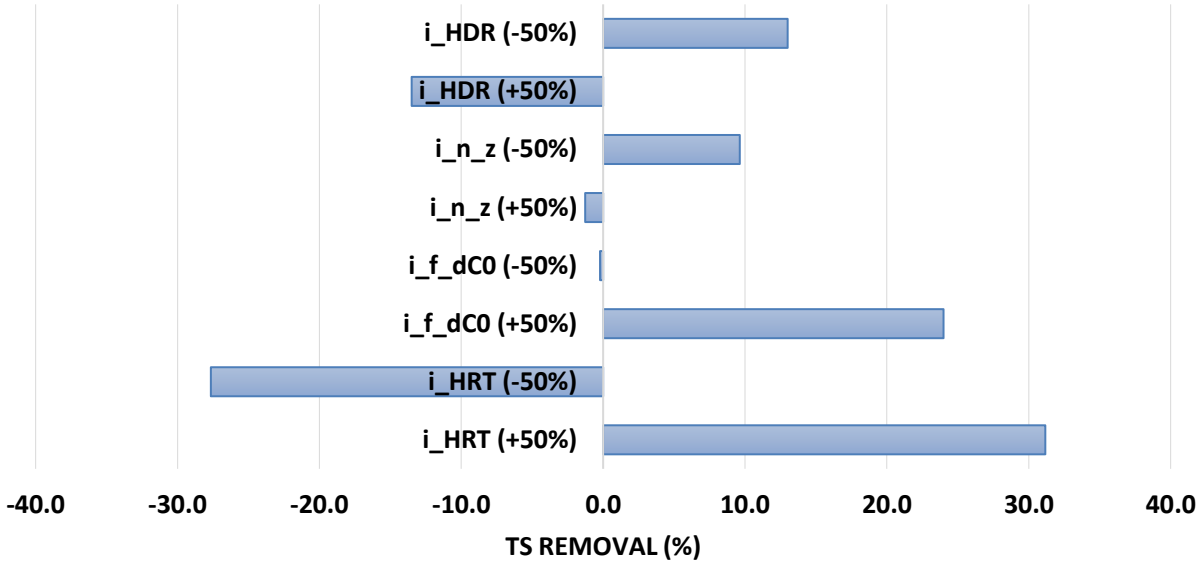

Figure 3.8. Results of the sensitivity analysis

Within the specified operational range, it was found that *i_HRT* was the variable to which solids removal was most sensitive in both directions, followed by *i_f_dC0* in the positive direction. *i_HDR* and *i_n_z* both had a modest effect in both directions. The results suggest that the most important variable was HRT, which was not a design parameter, but an operational one. This suggests that even if the design of the reactor is suboptimal, optimizing the HRT would yield considerable benefit in terms of treatment performance. There is a distinct preference towards low height-to-diameter ratios (*i_HDR*), which means it would be wise to design the reactor to be wide, rather than tall. The results also suggest a relatively larger central zone with a smaller number of zones will yield better overall treatment performance. This is because settling performance is increased when there is a single zone with a large surface area. However, having fewer zones can mean decreased conversion efficiency, so the decision with regards to reactor zoning depends on whether high solids destruction (disintegration and decay) is desired within

the system. If not, designing and running the CBR as a single zone clarifier will theoretically yield the highest settling efficiency at the expense of decay rates.

3.3.4. Surface Area Analysis of CBR vs. ABR

One of the premises of the CBR technology is that it can potentially lead to less heat lost to the environment compared to a traditional ABR when both reactors are run in Temperature-Phased Anaerobic Digestion (TPAD) mode (Han & Dague, 1997). For this analysis, two equal-volume, equal-height, equal-number-of-zones CBR and ABR units were compared side by side to determine how much of their total surface area is exposed directly to the environment, versus to subsequent reactor zones. The CBR was designed to be short and wide owing to the results of the analyses shown in previously, and the ABR long and narrow, following traditional designs. Visual representations of the systems that were compared are shown in Figure 3.9.

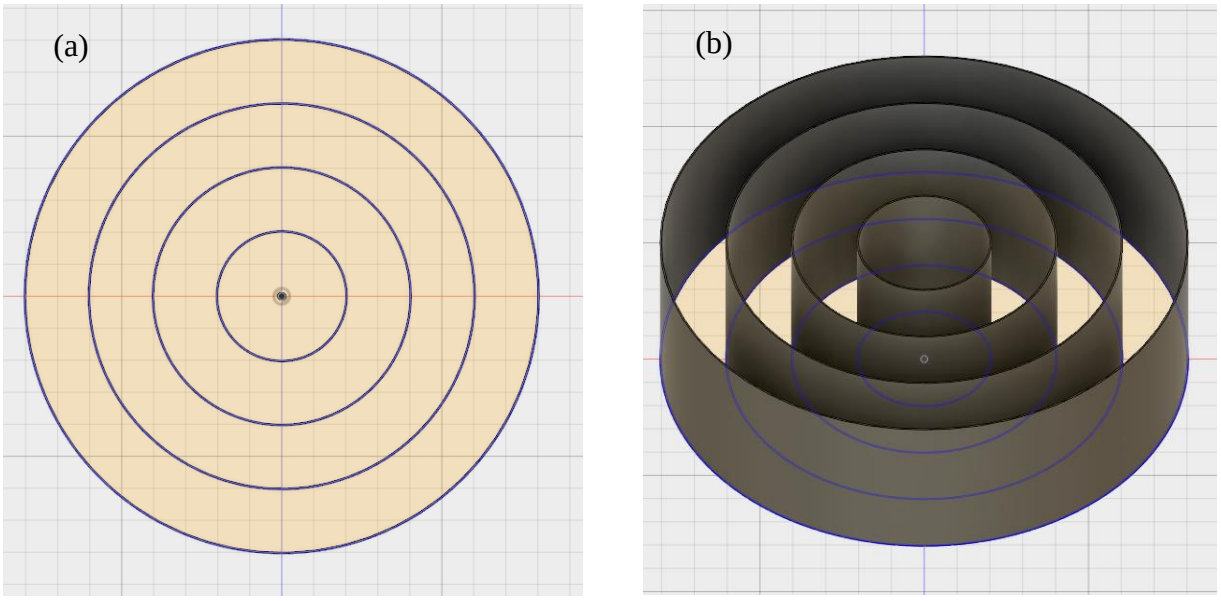

Figure 3.9. Visual representations of the (a) CBR (2D), (b) CBR (3D) and (c) ABR (2D), and (d) ABR (3D) systems used for the analysis

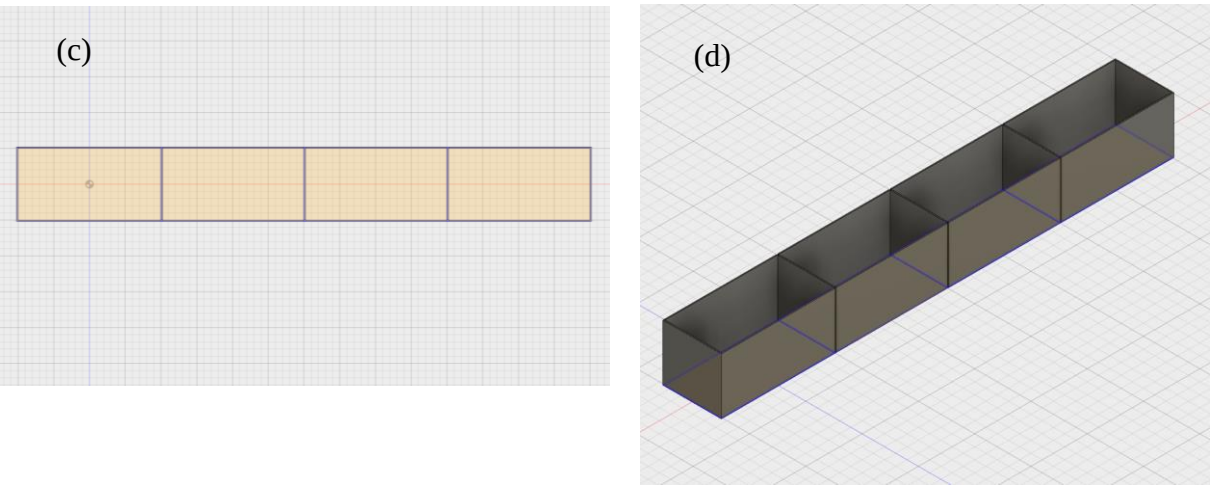

Figure 3.9. (Continued)

The reasoning for this analysis is that lower direct exposure to the environment of the entire reactor surface area (including surface area of each individual reactor zone) would lead to decreased heat losses to the environment before it can be utilized in the process – i.e. the heat would be better utilized if it is largely transferred to each subsequent reactor zone than lost outright to the environment. This is a preliminary analysis that should be followed with proper heat transfer modeling in order to definitively show any potential advantages of the CBR technology over traditional ABRs in terms of minimizing heat losses in TPAD mode. Geometric parameters used for the analysis is given in Table 3.11.

Table 3.11. Geometric parameters used for the analysis

Parameter	Value	Unit
Reactor Volume	1	m^3
Reactor Height	0.5	m
CBR Diameter	1.6	m
ABR Width	0.5	m
ABR Length	4	m

Table 3.11. (Continued)

Parameter	Value	Unit
Number of Zones	4	-
ABR Zone Spacing	1	m
CBR Zone Spacing	0.4	m

The analysis involves the calculation of the volumes (V), total surface areas (A), surface areas exposed to the environment (A_e), and surface areas exposed to a subsequent reactor zone (A_z) for each reactor zone. The first zone for the CBR is the innermost zone, whereas for the ABR it is the leftmost zone shown in Figure 3.9, since this is where the inlets are. At the end, the ratio of surface areas exposed to the environment is divided by the total reactor surface area to determine A_e/A ratio which can be used as a potential indicator for a reactor's predisposition for heat loss to the environment. The results of the analysis are given in Table 3.12.

Table 3.12. Results of the surface area analysis

	CBR					ABR				
	V	A	A_e	A_z	A_e/A	V	A	A_e	A_z	A_e/A
	m^3	m^2	m^2	m^2	-	m^3	m^2	m^2	m^2	-
Zone 1	0.06	0.88	0.25	0.63	0.29	0.25	2.5	2.25	0.25	0.90
Zone 2	0.19	2.00	0.75	1.25	0.37	0.25	2.25	2	0.25	0.89
Zone 3	0.31	3.13	1.25	1.88	0.40	0.25	2.25	2	0.25	0.89
Zone 4	0.44	4.26	4.26	0.00	1.00	0.25	2.25	2.25	0	1.00
Total	1	10.27	6.51	3.76	0.63	1	9.25	8.50	0.75	0.92

V: Volume, A: Total Surface Area, A_e: Surface Area Exposed to the Environment, A_z: Surface Area Exposed to a Zone

The analysis shows that under the current assumptions, the CBR yields a lower A_e/A ratio than the ABR, which may potentially point towards lower predisposition for heat loss to the environment. However, this is a preliminary analysis the results of which need further

exploration in the form of heat transfer modeling and/or empirical testing in order to be definitive.

3.4. Design and Manufacturing of the Experimental Prototype

The design of the experimental reactor prototype was based on the information gathered from the geometric and sensitivity analyses conducted using the Python model, in addition to the practical operational and manufacturing constraints considered for the design. According to the aforementioned analyses, the reactor would have a relatively large central zone, smaller number of zones, and a low height-to-diameter ratio to achieve high total solids removal rates. These considerations would, however, have to be evaluated along with engineering and manufacturing constraints specific to the design of the first protoypes.

One constraint was the spacing between the baffles: the spacings should be wide enough to prevent clogging. To this end, a minimum spacing criterion was selected for baffles, which would affect the number of zones that would be incorporated within the design with respect to the total reactor volume, reactor height, and central zone spacing selected. Since the reactor would be tested for temperature gradient formation, it was important that there were an adequate number of distinct reactor zones to yield such a gradient. Upflow zones were also spaced to be double the size of the downflow zones, since settling in the form of separation of solids from the liquid phase would theoretically only occur in the upflow zones. The total reactor volume was another constraint, as too large a reactor volume would require high amounts of feed to be prepared and stored, which may or may not be possible in a lab environment, especially if low HRT scenarios were to be tested. In addition, increasing reactor volume would require an increasing amount of membrane materials if the reactor were to be run in full MBR mode.

One major constraint was the way the baffles would be handled: the initial design was to have the baffles attached to the top and the bottom of the reactor interchangeably, but that raised some questions of stability of the reactor structure, and the functionality of the reactor lid – if half of the baffles were attached to the reactor lid, it would be difficult to remove the lid or run any maintenance on the reactor when needed. Therefore, instead of attaching half of the baffles to the lid, all of the baffles were attached to the bottom of the reactor, and the flow of the reactor contents was realized by punching holes through the baffles. The criteria that guided the manufacturing of the first CBR prototype are given in Table 3.13.

Table 3.13. Criteria for the design of the CBR protoype

Parameter	Value	Unit
Water Height	0.1	m
Number of Zones	7	-
Central Zone Diameter	0.15	m
Upflow Zone Baffle Spacing	0.1	m
Downflow Zone Baffle Spacing	0.05	m
Total Reactor Diameter	0.6	m
Reactor Design Water Volume	0.028	m3
	28	L
Reactor Actual Water Volume	32	L
Reactor Headspace Height	0.05	m
Height-to-Diameter Ratio (Total)	0.25	-
Height-to-Diameter Ratio (Water)	0.17	-
Inlet Pipe Diameter	0.5	in
	0.0127	m
Baffle Thickness	0.005	m
Outer Wall Thickness	0.01	m
Construction Material	Acrylic	-

The first prototype was manufactured using regular rectangular sheet acrylic. The round baffles and outermost wall were made by manually heating the sheets of acrylic using a heat gun and bending them into a perfectly cylindrical shape. The baffles were then glued to the bottom piece of the reactor. The round acrylic lid would need a large O-ring to increase gas-tightness, so a round bedding for the O-ring was etched onto the lid using a CNC mill. A total of 21 holes were punctured into the lid – 1 for the inlet, 1 for the gas line, 2 for the heat exchange lines, 2 for the level sensors, 1 for the headspace pressure sensor, 7 for sampling ports for each zone, and 7 for temperature sensors for each zone. The first prototype is shown in Figure 3.10.

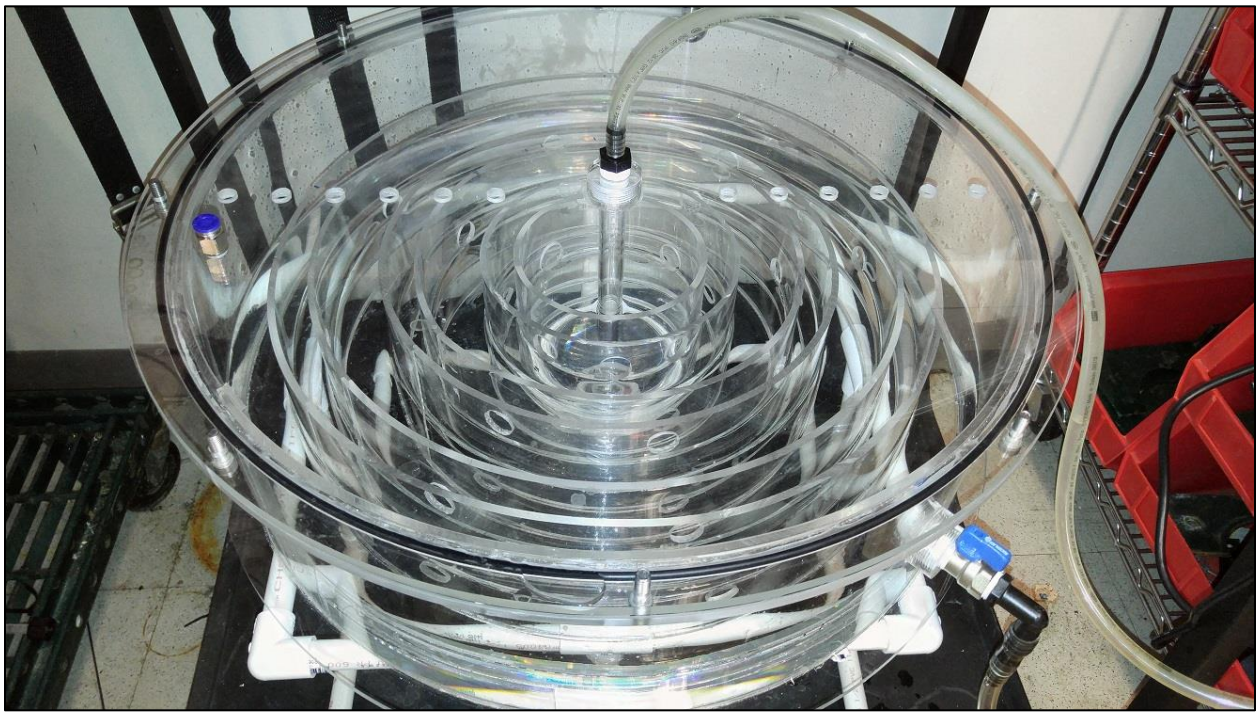

Figure 3.10. First CBR prototype

After the first prototype was made, a second prototype was manufactured, that was smaller than the first. The reactors were similar in every aspect, except the second one simply did

not have the last 2 zones of the first reactor, so it had 5 zones in total and was only 0.45 m in diameter. The reasoning for the second reactor was to use this reactor to test abiotic properties of the CBR, while using the larger prototype for biotic (anaerobic) testing simultaneously. Both reactors are shown in Figure 3.11.

Figure 3.11. The large (bottom) and small (top) CBR prototypes

Varying hydraulic retention times were used with the 5-zone experimental prototype in the subsequent trials. This necessitates the analysis of theoretical hydraulic retention times

expected to occur within each reactor zone of the 5-zone CBR prototype, the results of which are given in Table 3.14.

Table 3.14. Analysis of hydraulic retention times for the 5-zone CBR prototype

			Flow Rate (L/h)					
			31.8	4.0	2.7	1.3	0.7	0.5
Zones	**Spacing**	**Volume (L)**	**HRT (h)**					
1	0.15	1.8	0.06	0.4	0.7	1.3	2.7	3.7
2	0.05	1.4	0.04	0.3	0.5	1.0	2.1	2.9
3	0.10	3.9	0.12	1.0	1.5	3.0	5.9	8.1
4	0.05	2.6	0.08	0.6	1.0	1.9	3.9	5.3
5	0.10	6.3	0.20	1.6	2.4	4.7	9.5	13.0
Reactor	-	15.9	0.5	4	6	12	24	33

3.5. Abiotic Performance

The small CBR prototype was used to determine the abiotic temperature profile and solids removal performance of the system. To this end, a series of tests were conducted, where the HRT of the system was varied to see the effects of fluid flow on temperature and solids distributions within each reaction zone. The abiotic testing was important to distinguish the effects of biotic degradation on treatment performance versus simple settling and removal solids, and to see if a temperature gradient could be achieved using the current designs.

3.5.1. Methods

A 5-zone, 0.45 m diameter CBR system with an effective volume of 15 L was used for the analysis. The system is depicted in Figure 3.12.

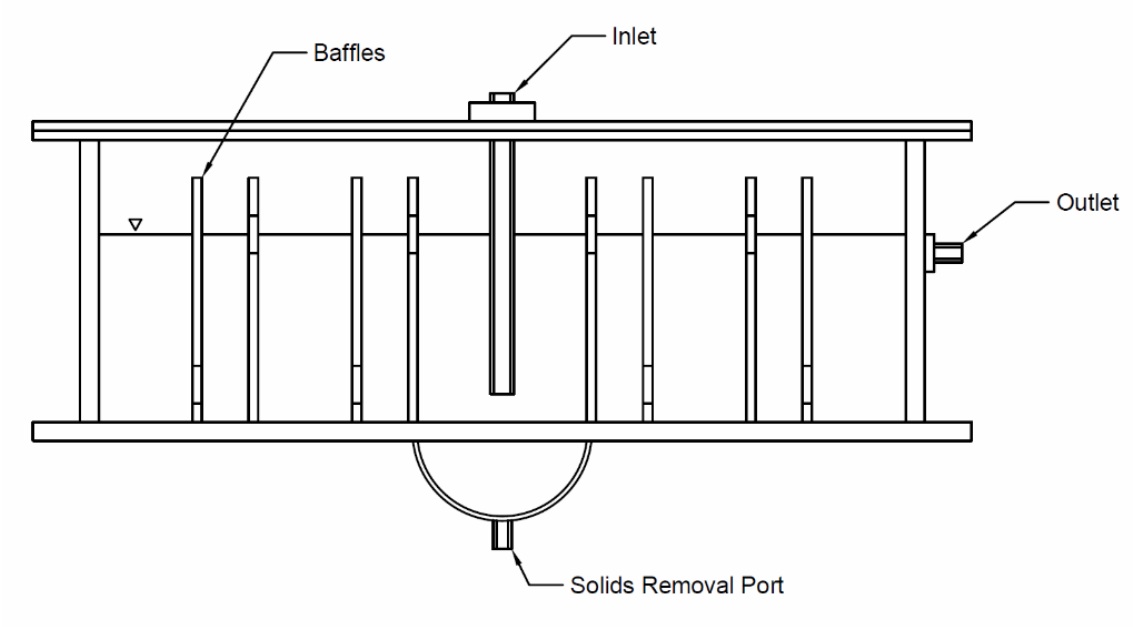

Figure 3.12. The 5-zone CBR system used for abiotic testing

The temperature for each zone was recorded using an Onset U30 data logging system, along with Onset temperature sensors submerged within each zone (Onset Computer Corporation, Bourne, MA, USA). Solids testing was done using Complex Organic Particulate Artificial Sewage (COPAS) as described by Prieto (2011). COPAS is basically finely ground and sieved (maximum particle diameter 1.7 mm) cat food which serves as a highly convenient synthetic feed alternative for wastewater treatment systems, especially where particulate solids within the feed are important to the process. Total Solids (TS) and Total Suspended Solids (TSS) measurements were done according to Standard Methods 21st Ed., Method 2540 (APHA *et al.*, 2005).

3.5.2. Results and Discussion

The results indicate successful temperature and suspended solids zoning within the CBR, with increasing differences in temperature between the zones observed with increasing HRT, which was expected (Figure 3.13).

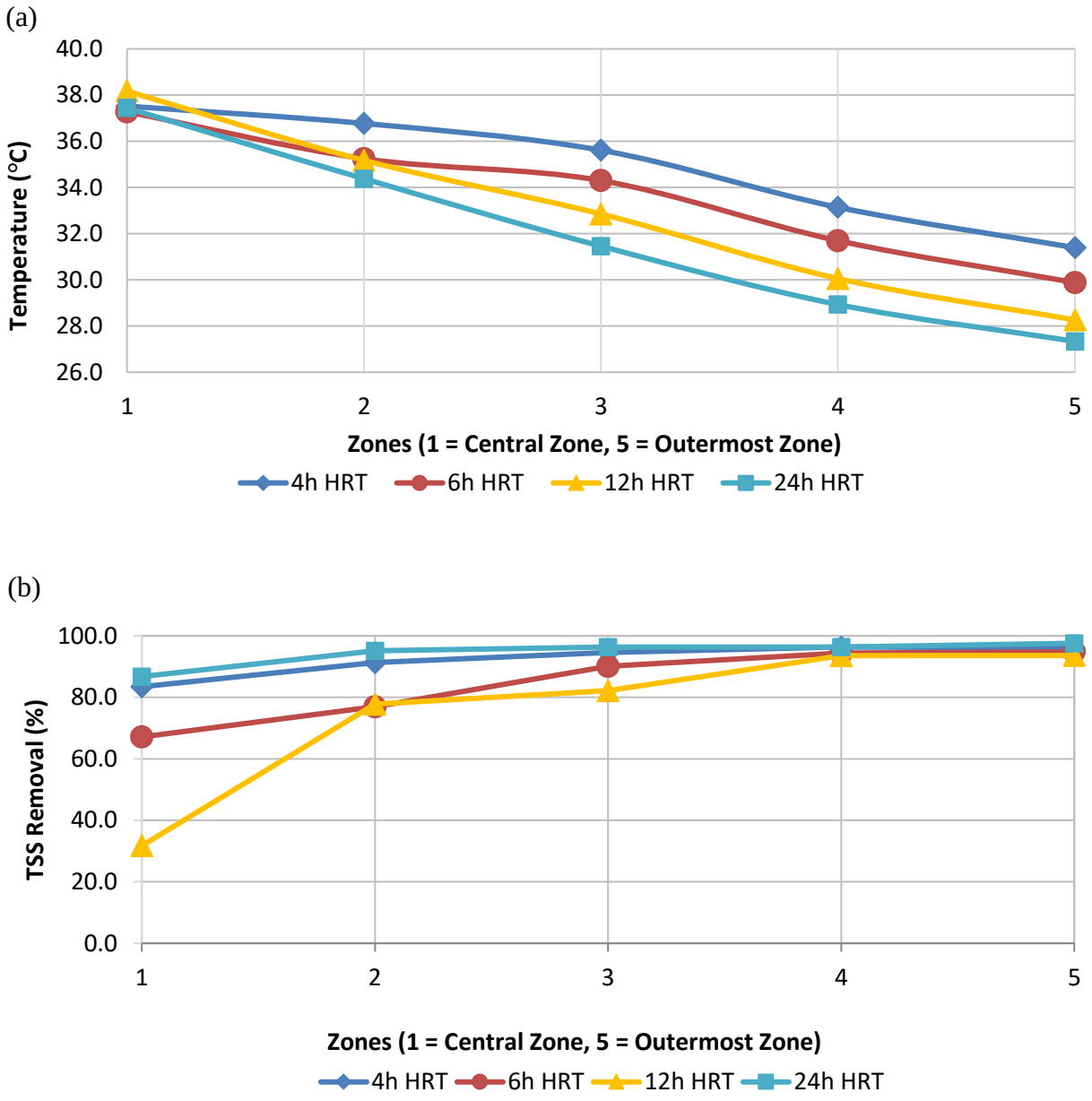

Figure 3.13. (a) Temperature and (b) TSS Removal profiles for the different HRTs tested

Due to the biodegradable nature of the feed, the TSS experiment results were not as clear cut, and there was no discernable pattern between HRT and removal rates observed in each zone. However, for all HRTs tested, the final removal rates for TSS were appreciably high, ranging from 93.6% to 97.6%.

The reactor showed a distinct temperature profile for all HRTs, with the greatest temperature differential between the innermost and the outermost zones taking place at the highest HRT tested. High TSS removal and a gradual decrease in TSS concentrations were observed for all HRTs, suggesting that removal did not only occur in the innermost zone, and subsequent zones were contributing to further removal of particulate solids.

3.6. Tracer Tests

Pulse injection tracer tests were conducted at varying HRT levels to determine the flow regime of the 5-zone experimental prototype. Vernier conductivity probes and a Lab Pro data logger were used to collect the conductivity data (Vernier Software & Technology, OR, USA). In the first test, reactor HRT was set to 33 h and distilled water was fed to the reactor over 45 h with a pulse NaCl solution injection at t=0 through the reactor inlet tubing. The conductivity profile of the first zone is given in Figure 3.14.

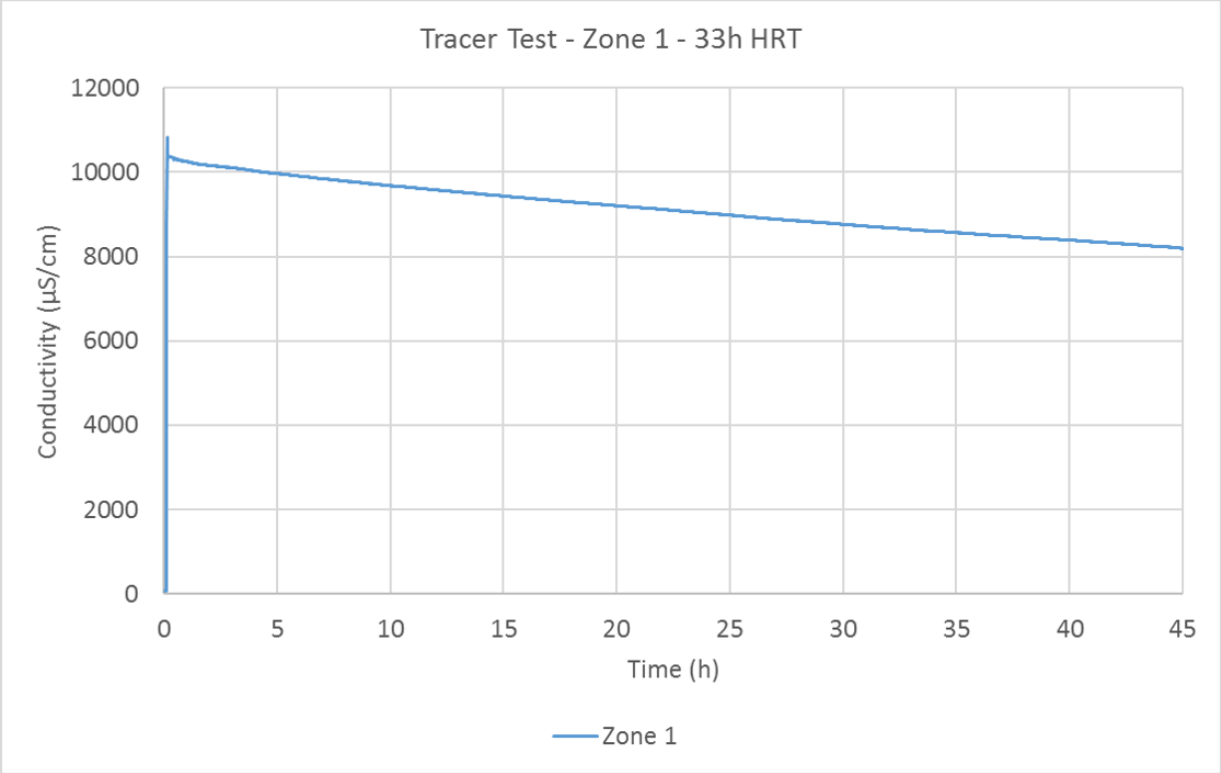

Figure 3.14. Zone 1 conductivity profile for the 33 h HRT trial

An initial spike of 10,839 µS/cm was observed within the first (i.e. the central) reactor zone at t=0.15 h, which gradually decreased to 8,221 µS/cm at t=45 h. A return to baseline conductivity levels of 63 µS/cm was not observed within the allotted experimental run time. The conductivity profiles of the remaining zones are given in Figure 3.15.

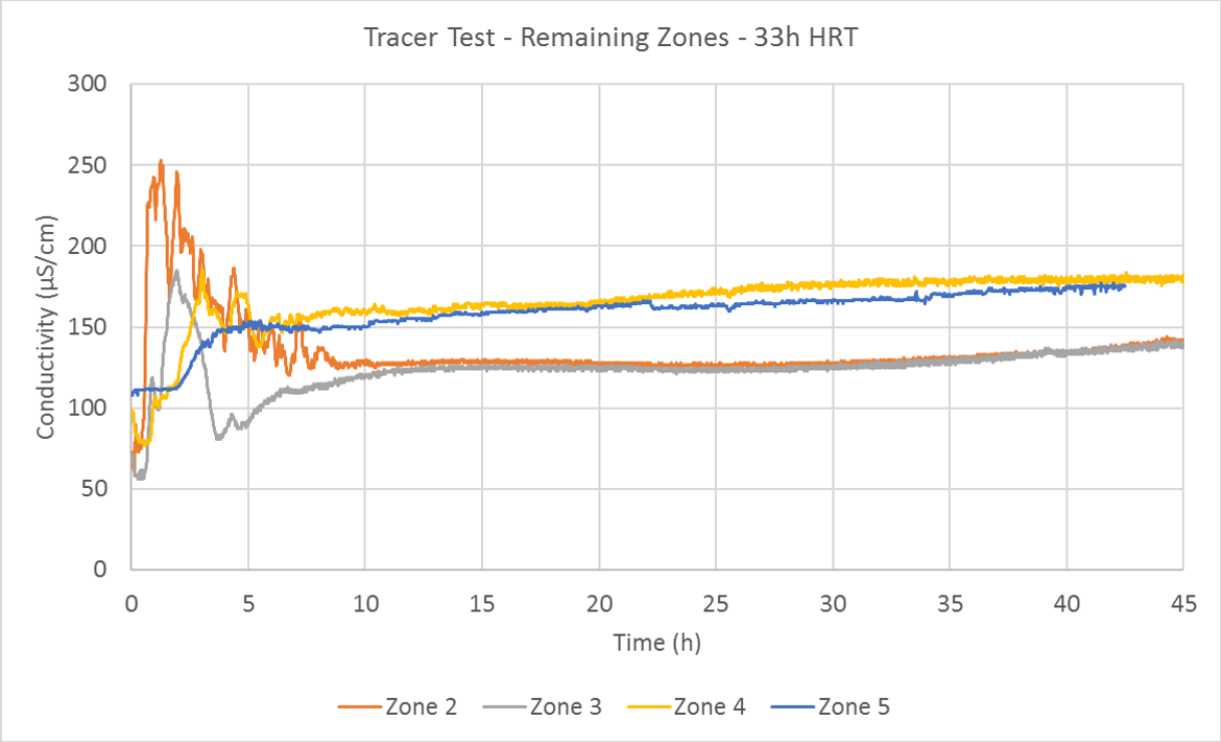

Figure 3.15. Conductivity profile of the remaining zones for the 33 h HRT trial

The initial peaks of 253 µS/cm, 185 µS/cm, 185 µS/cm, and 154 µS/cm for zones 2, 3, 4, and 5 occurred at t=1.27 h, t=1.96 h, t=3.03 h, and t=5.51 h, respectively. After the initial peaks, the conductivity levels in all zones other than Zone 1 decreased to a resting level that was greater than the initial baseline conductivity levels. Conductivity in all zones other than Zone 1 gradually increased as time progressed.

In the second tracer test, the HRT was set to 4 hours, and the test was repeated with another NaCl solution fed as a pulse into a continuous stream of distilled water. The experiment was run for 25 hours, but the initial baseline was not reached at the end of the experiment in this trial, either. The conductivity profile of the first zone is given in Figure 3.16.

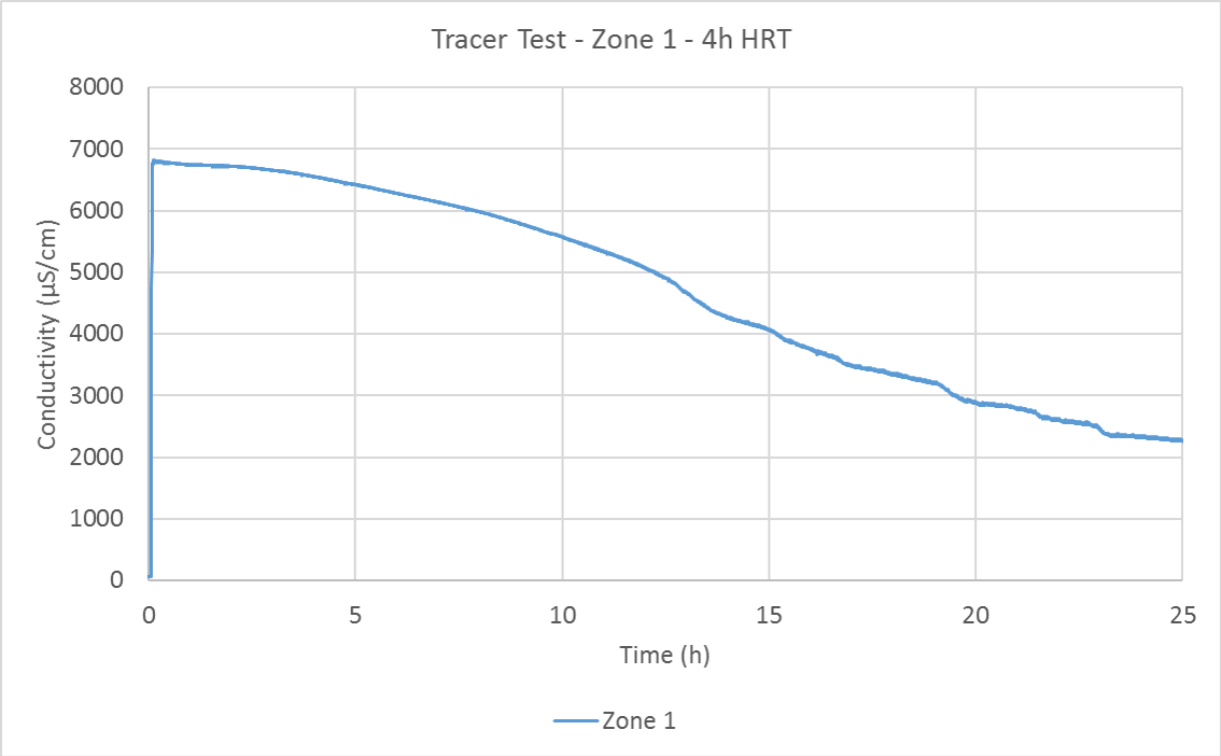

Figure 3.16. Zone 1 conductivity profile for the 4 h HRT trial

An initial spike of 6,819 µS/cm was observed within the first (i.e. the central) reactor zone at t=0.15 h, which gradually decreased to 2,298 µS/cm at t=25 h. A return to baseline conductivity levels of 59 µS/cm was not observed within the allotted experimental run time. The conductivity profiles of the remaining zones are given in Figure 3.17.

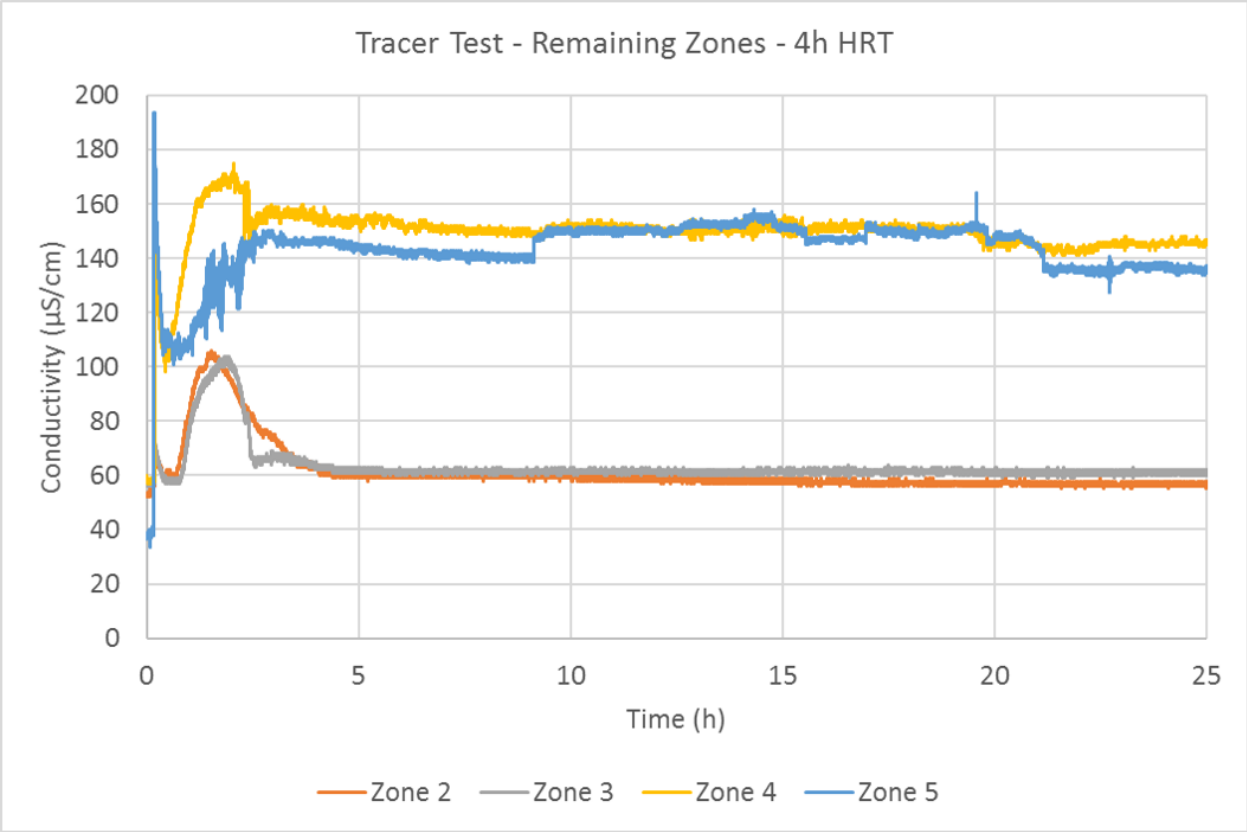

Figure 3.17. Conductivity profile of the remaining zones for the 4 h HRT trial

The initial peaks of 106 µS/cm, 104 µS/cm, 175 µS/cm, and 150 µS/cm for zones 2, 3, 4, and 5 occurred at t=1.52 h, t=1.84 h, t=2.05 h, and t=2.76 h, respectively. Before the mentioned peaks, however, conductivity spikes were recorded for all zones nearly coinciding (t=0.18 h) with the peak in the first zone – larger spikes for Zones 4 and 5, and smaller spikes for Zones 2 and 3. The reason for these spikes is unknown, but it is hypothesized that they may have been an electrical interference caused by the conductivity probe in the first zone that affected the other probes, or a spike caused by the initial jet of the pulse which traveled faster than the rest of the liquid. After the initial peaks, the conductivity levels in all zones other than Zone 1 decreased to a resting level that was greater than their respective initial baseline conductivity levels.

Since baseline levels were not reached in either of the initial two tracer tests, quantitative analysis of the results was not possible. Therefore, a third tracer test was conducted where the reactors were fed with tap water instead of distilled water due to the amount of water that would be needed to reach baseline levels. HRT was set to 0.5 hours for this test, and a pulse of 2.5 g NaCl dissolved in 10 mL tap water was added to the reactor at t=0. The conductivity profile of the first zone is given in Figure 3.18.

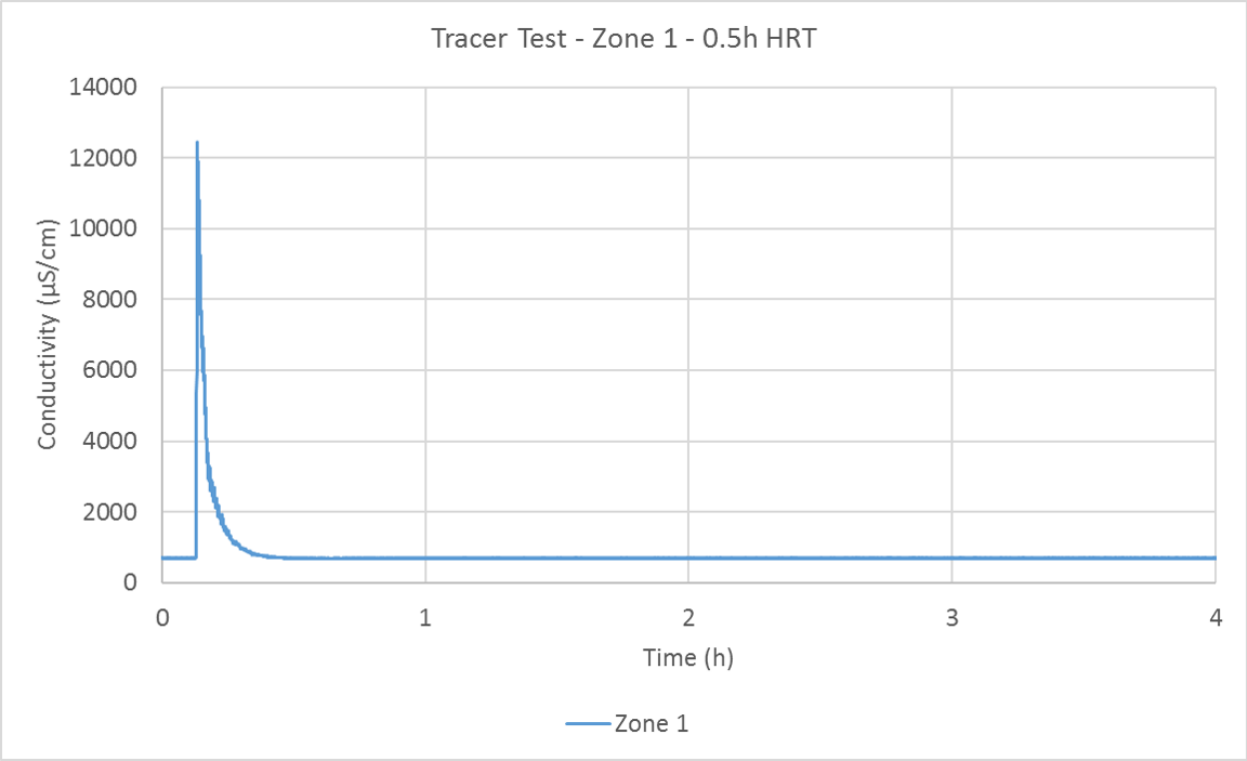

Figure 3.18. Zone 1 conductivity profile for the 0.5 h HRT trial

An initial spike of 12,451 µS/cm was observed within the first (i.e. the central) reactor zone at t=0.13 h, which decreased back to the baseline level of 699 µS/cm at t=0.45 h. The conductivity profiles of the remaining zones are given in Figure 3.19.

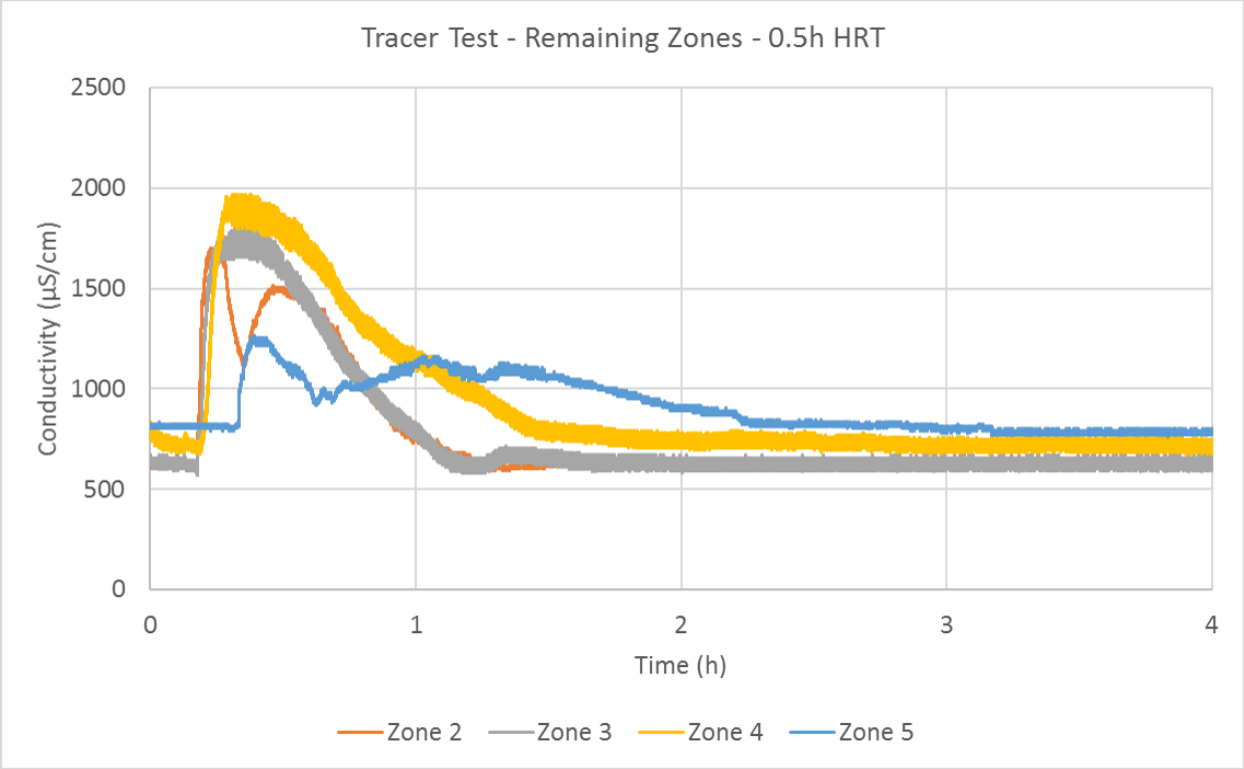

Figure 3.19. Conductivity profile of the remaining zones for the 0.5 h HRT trial

The initial peaks of 1703 µS/cm, 1813 µS/cm, 1967 µS/cm, and 1263 µS/cm for zones 2, 3, 4, and 5 occurred at t=0.23 h, t=0.33 h, t=0.31 h, and t=0.39 h, respectively. Conductivity readings for all zones had decreased back to their baseline levels by t=3.5 h. The baseline levels were 620 µS/cm, 634 µS/cm, 768 µS/cm, and 814 µS/cm for zones 2, 3, 4, and 5, respectively. The different readings for the baseline are due to the use of different probes in each zone. There is variance among the probes in terms of conductivity readings. A concentration-conductivity calibration curve was created using standard NaCl+tap water solutions, which is shown in Figure 3.20. This curve was generated using the same conductivity probe that was used in Zone 1 of the CBR for the tracer tests.

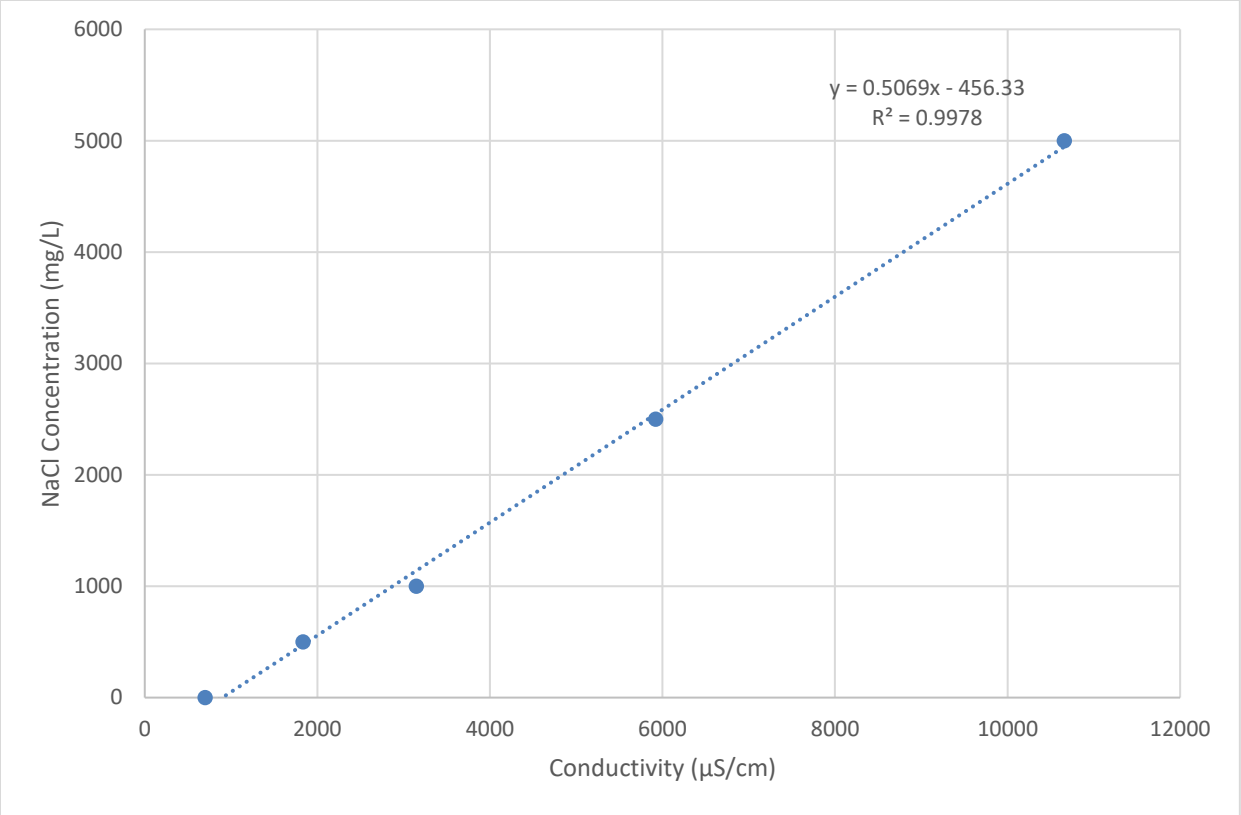

Figure 3.20. Calibration curve for the 0.5 h HRT trial

The first 200 readings starting from t=0 in the 0.5 h HRT test were averaged to determine an average conductivity level for all baselines, as indicated previously (699 µS/cm, 620 µS/cm, 634 µS/cm, 768 µS/cm, and 814 µS/cm for zones 1, 2, 3, 4, and 5, respectively). These values were normalized with respect to the baseline reading for Zone 1, for which the calibration curve was generated. Per this normalization, all recorded conductivity values were shifted by +79, +65, -69, and -115 for zones 2, 3, 4, and 5, respectively. Afterwards, NaCl concentration versus time graphs were plotted for all zones using the equation indicated on Figure 3.20 to convert conductivity values to NaCl concentration values. For these plots, the time of the NaCl pulse was taken as t=0, and the baseline data before this new t=0 was not plotted. The normalized NaCl concentration profile of the first zone is given in Figure 3.21.

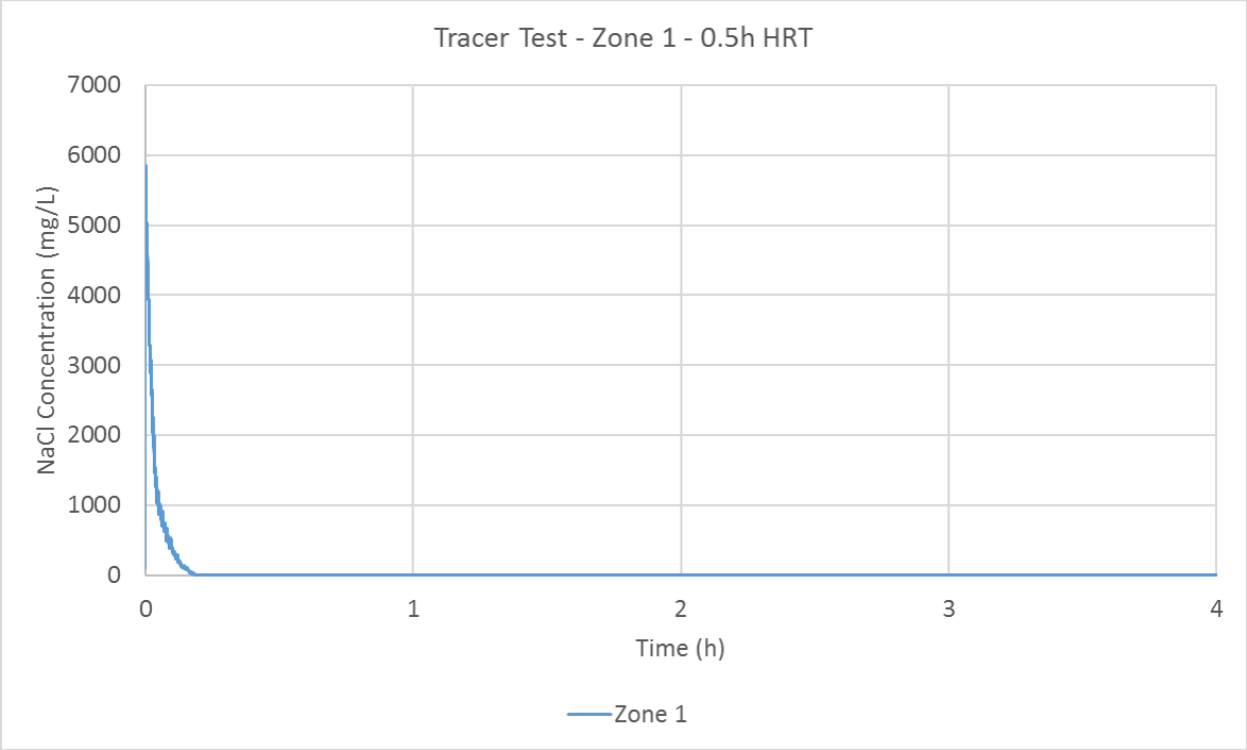

Figure 3.21. Zone 1 NaCl concentration profile for the 0.5 h HRT trial

The initial spike of the first zone corresponded to a NaCl concentration of 5,855 mg/L. The total volume of the first zone was 1.8 L. If the first reactor zone behaved like a CSTR, with the injected 2,500 mg NaCl, the concentration would have peaked at C_{peak} = 2,500 mg / 1.8 L = 1,415 mg/L at the time of the NaCl injection. Since the peak is much higher than this theoretical value, it can be suggested that the first zone is exhibiting behavior somewhere between an ideal PFR and an ideal CSTR. The NaCl concentration profiles of the remaining zones are given in Figure 3.22.

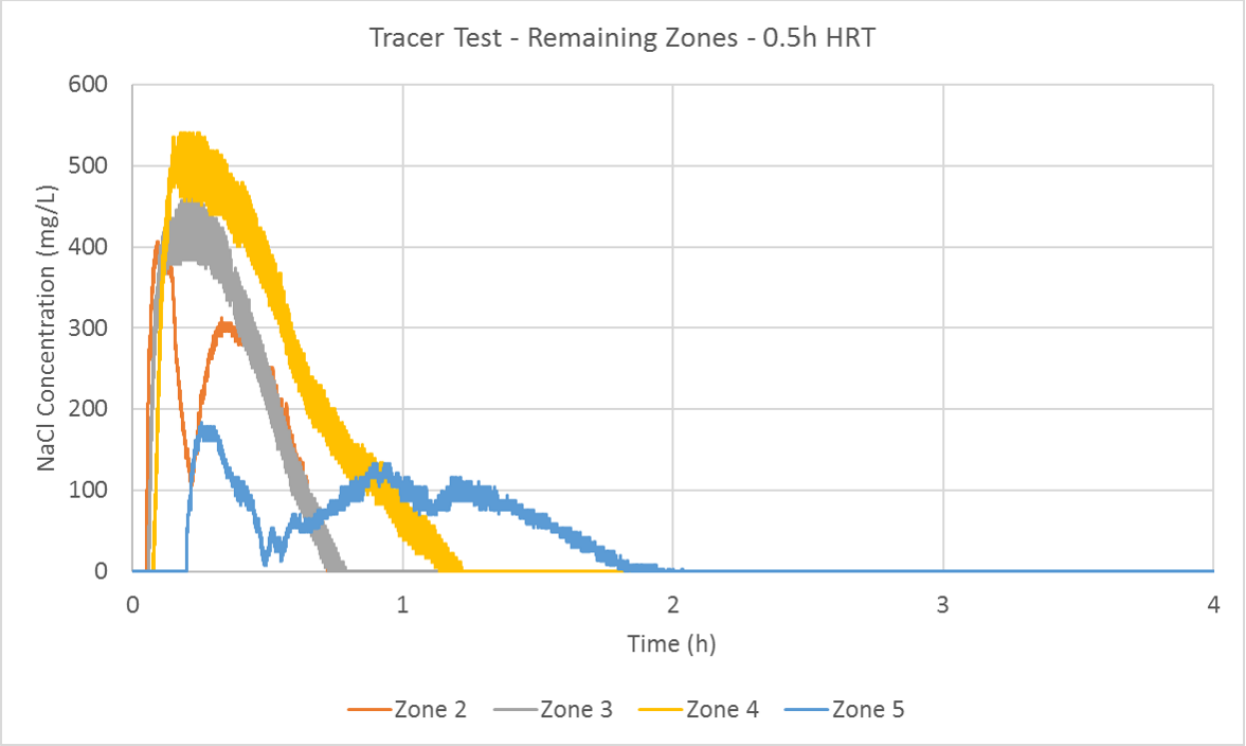

Figure 3.22. NaCl concentration profile of the remaining zones for the 0.5 h HRT trial

To be able to compare the experimental results to an ideal CSTRs-in-series configuration, a model was created using the below equation from Levenspiel (1999):

$$C_i = C_0 \frac{(\frac{t}{t_z})^{(i-1)}}{(i-1)!} e^{(\frac{-t}{t_z})} \quad (7)$$

In *Eq. 7*, C_i stands for concentration within zone *i* at time = *t*, C0 stands for initial concentration, and t_z stands for the hydraulic retention time within zone *i*. The CSTRs-in-series model had the hydraulic retention times as inputs for each zone shown in Table 3.14. The model results are given in Figure 3.23.

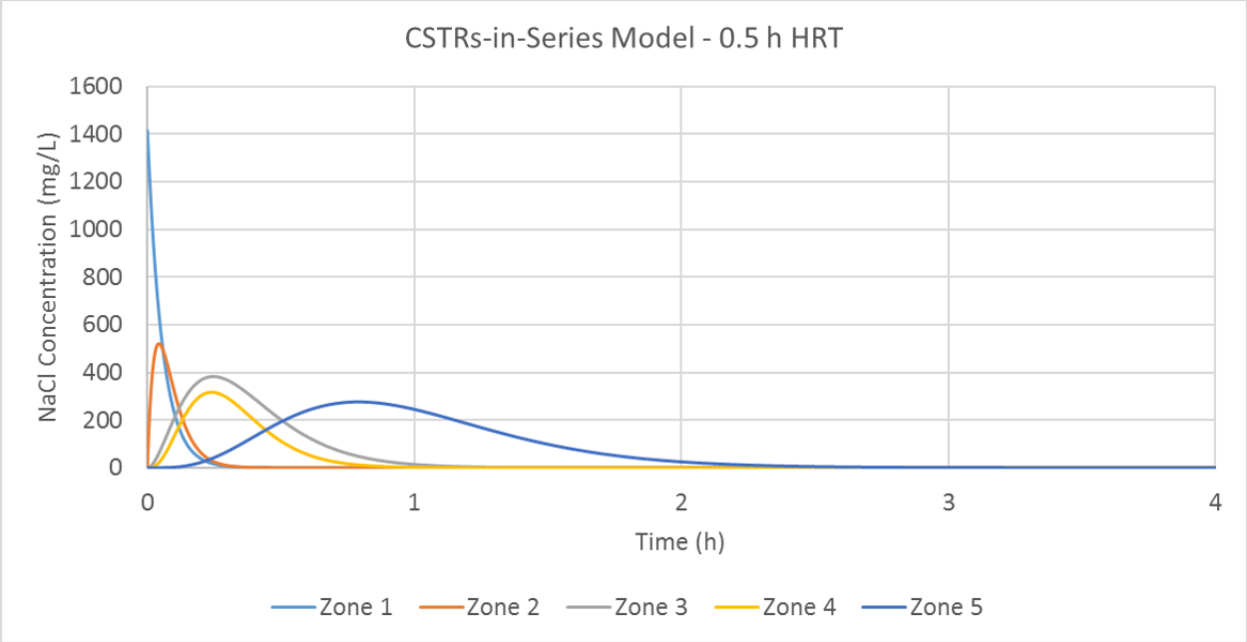

Figure 3.23. CSTRs-in-series model created for the 0.5 h HRT trial

A side-by-side comparison of the experimental and simulated NaCl concentration profiles for Zones 2, 3, 4, and 5 can be viewed in Figure 3.24.

Although the experimental and simulated profiles appear roughly similar, especially the profiles for zones 2 and 5 show irregular patterns suggesting nonideal conditions within these zones. The experimental peaks for zones 2 and 5 also appear markedly lower than the simulated ones, whereas the peaks for zones 3 and 4 seem to be markedly higher. The CBR seems to be behaving somewhat like a CSTRs-in-series as far as zones 2, 3, 4, and 5 are concerned, when the reactor is operated under an HRT of 0.5 h. However, the tracer profiles also show deviations in zones 2 and 5, which may point towards dead zones or short-circuiting within the reactor.

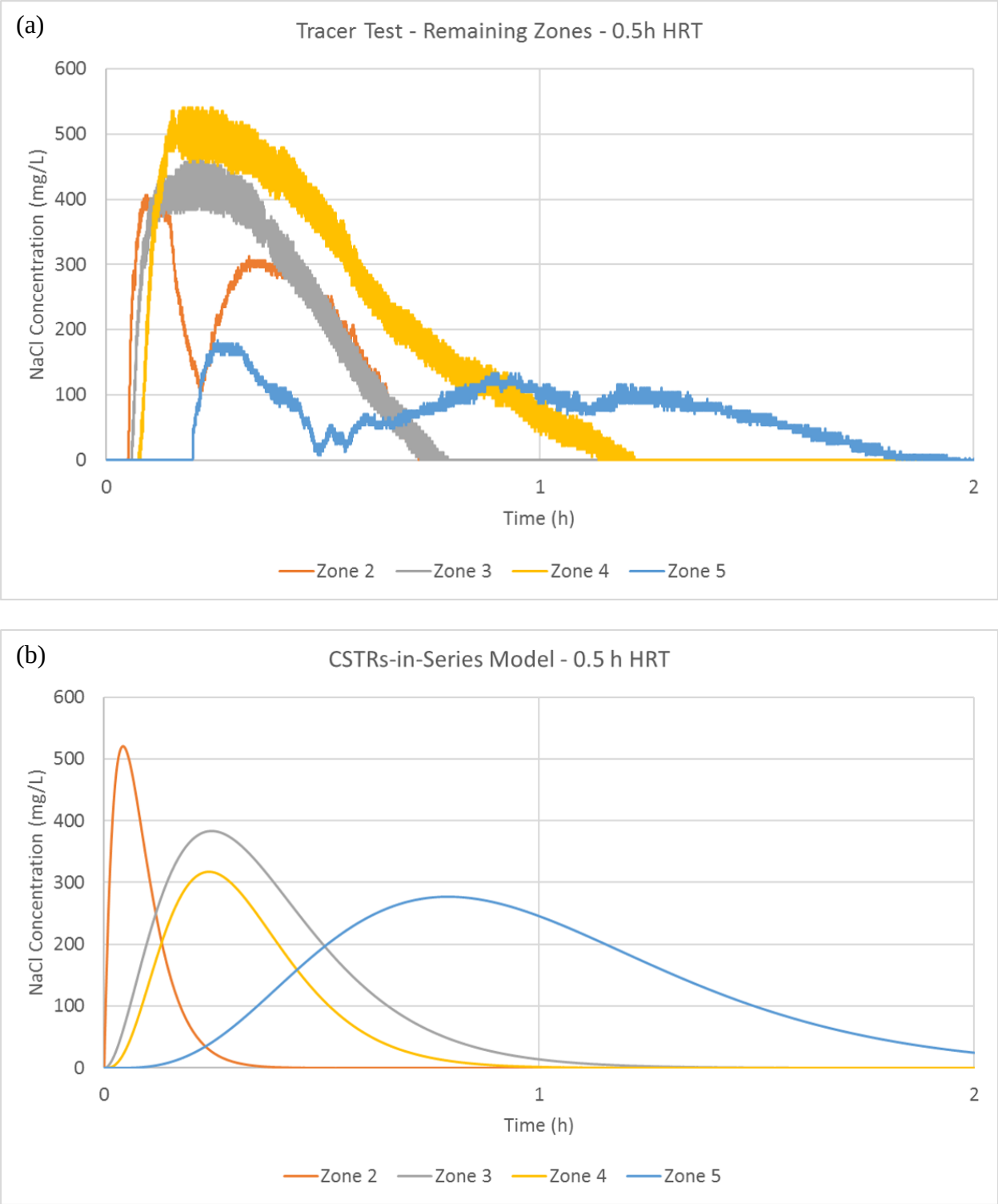

Figure 3.24. Comparison of the (a) experimental and (b) simulated NaCl concentration profiles for Zones 2, 3, 4, and 5

3.7. Conclusions

- Two CBR prototypes were designed and manufactured based on modeling and analysis work that let the author form rough guidelines to create a design with potential for satisfactory solids removal.
- A surface area analysis was conducted comparing a CBR with an ABR, where the CBR was shown to be potentially less exposed to the environment than an ABR under the assumptions used for the analysis. Decreased surface area exposure to the environment can point towards better heat retention, but the results need to be comfirmed with empirical data or heat transfer modeling.
- Abiotic testing resulted in over 90% suspended solids removal for the 4h to 24h HRT range tested. Distinct temperature and solids profiles were recorded for the 5-zone CBR.
- A CBR tracer test conducted at 0.5 h HRT revealed somewhat similar behavior to an ideal CSTR, but there were deviations pointing towards possible short-circuiting and dead zones.

Chapter 4: Low-Aeration PMBR Operation and Preliminary pH Trials

While the Concentrically Baffled Reactor was developed for degrading wastewater constituents anaerobically, an additional step was required to address the management of the nutrients in the waste stream, since a relatively small portion of nutrients are taken up during anaerobic treatment. To this end, a Phototrophic Membrane Bioreactor was used, being a relatively new and largely unexplored concept with a lot of potential for resource recovery from wastewater as well as production of commodities such as biofuels.

Nutrient management using phototrophic processes has been subject of research in the recent years, due to the synergy between wastewater treatment and the establishment of algal biorefineries. If simultaneous nutrient removal from wastewater as well as production of high-quality algal products can be achieved at the same time, this will bring down costs of both nutrient management and the production of commodities from algal biomass. In such a scenario algae require high quantities of nutrients and water to grow, which would be provided by wastewater streams. This seems to be one of the most promising strategies to make biofuel production from algal biomass, provided high-lipid-containing algae can be grown under environmental conditions and selection pressures that can be exerted upon algal communities, or these conditions can be feasibly controlled by external means.

This chapter aims to bridge the gap between current constraints in technology for the management of nutrients in wastewater with cultivation of phototrophic cultures for the production of new materials. For this purpose, the chapter was divided into two phases. The first phase of the study aims to demonstrate treatment of nutrient rich wastewater stream under low

aeration conditions to be competitive in energy consumption while meeting current surface water discharge standards. The second phase was designed to demonstrate the conditions under which phototrophic cultures can raise the pH of the system to facilitate the recovery of excess nitrogen and phosphorus from the system through post-processing.

4.1. Methods

Experiments were conducted using two identical 2 L borosilicate glass photobioreactor columns fitted with external 8-mm diameter tubular polyvinylidene fluoride (PVDF) ultrafiltration (UF) membranes (Pentair, X-Flow) with a nominal pore size of 0.03 µm and a membrane area of 0.025 m^2 per module (Figure 4.1).

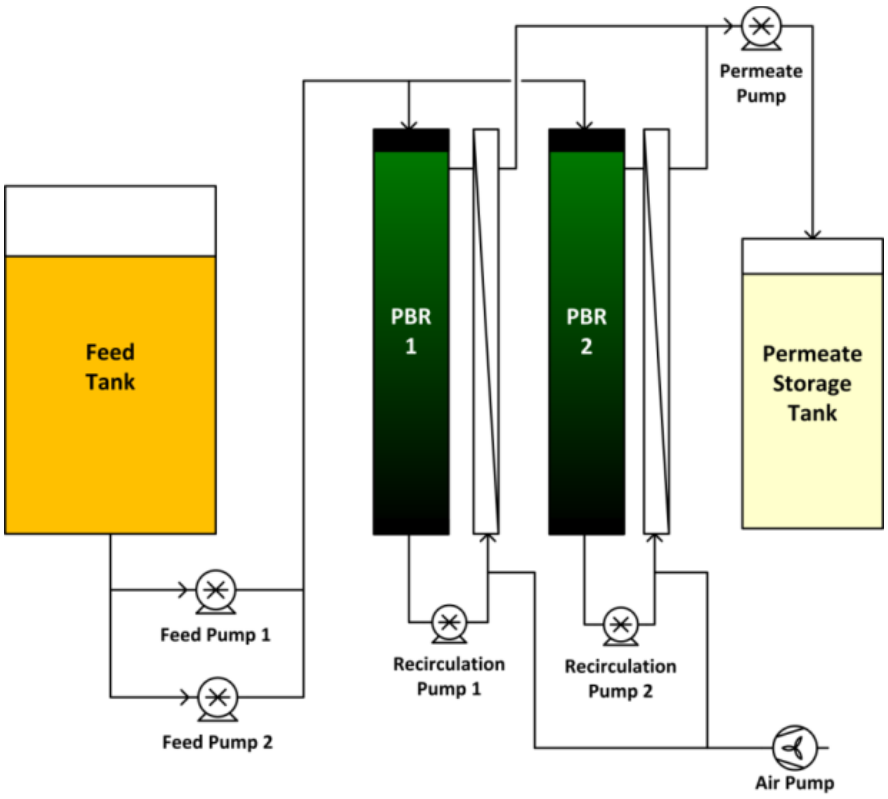

Figure 4.1. Phototrophic Membrane Bioreactor system

The reactors were seeded with a mixed phototrophic culture bioprospected from Howard Curren Advanced Wastewater Treatment Plant in Tampa, FL, USA. The feed for the systems for both phases was wash-water diluted human waste from a public toilet which was pre-filtered through a UF membrane before being fed to the system. For the first phase of the study, the system was operated with a hydraulic retention time (HRT) of 24 h and a solids retention time (SRT) of 40 d. The solids were wasted directly from each reactor via the removal of the mixed liquor twice a week. Reactors were aerated intermittently while the membranes were being backwashed with an interval of 30 s every 10 min. However, the external membranes were also being constantly sparged with air at 0.9 L/min, so the reactor contents were in constant contact with air at this flow rate. Other operational conditions are listed in Table 4.1.

Table 4.1. Operational conditions for Phase 1

HRT	24 h
SRT	40 d
Light Intensity	50 μmol/s/m^2
Dark/Light Cycle	14 h dark, 10 h light
Reactor Aeration Mode	Intermittent
Aeration Flow Rate	1.4 LPM
Aeration Duration	30s every 10 min
Membrane Air Sparging Mode	Continuous
Air Sparging Flow Rate	0.9 LPM
Backwash Regime	30s every 10 min @ 80 LMH
Crossflow Velocity	0.3 m/s
Total Energy Req.	18.1 W
Membrane Feed Pumps	8.5 W
Air Pump	2.6 W
Permeate Pump	5.8 W
Reactor Feed Pumps	0.8 W
Backwash Pump	0.4 W

Table 4.1. (Continued)

Lighting (14h D/10h L Cycle)	**20 W**
Volumetric Energy Req.	4.53 kW/m^3/d
	0.189 kWh/m^3 (not including lighting)
	0.397 kWh/m^3 (including lighting)

The total energy requirement of the system was 0.397 kWh/m^3 including energy draw for lighting, which is lower than the 0.5-1.0 kWh/m^3 typical of an aerobic MBR. If the system is set up outdoors and is able to utilize daylight, energy requirement can potentially be decreased to 0.189 kWh/m^3, provided a similar treatment performance is attainable.

For the second phase of the study, the system was converted into an airlift system, where the membrane recirculation pumps were removed, and the reactor contents moved through the external membranes via the uplifting force of the membrane air sparging pumps. This further reduced the energy consumption of the system to 0.100 kWh/m^3. One of the reactors was converted into a high-rate aeration system where the phototrophic culture was supplied with an additional 0.5 L/min fine bubble air supply, with 1 L/min being supplied to its external membrane for sparging and airlift, whereas the air sparging rate for the second reactor was halved to 0.5 L/min and no aeration was provided for the reactor itself. The reactors were run at a lower SRT of 10 d for 10 days of steady-state operation after acclimation for this phase of the study, for which the main parameter that was monitored was permeate pH. It was hypothesized that the lower SRT (and high aeration) would prevent the prevalence of nitrifying species in the system, preventing pH decline. pH probes were recalibrated every 3 days to keep them from drifting for this trial.

Optical Density (OD) of the cultures was monitored using a Hach DR 4000 UV/VIS Spectrophotometer at a wavelength of 680 nm. Chemical Oxygen Demand (COD), Total

Nitrogen (TN), Nitrate-Nitrogen (NO_3-N) and Ammonium-Nitrogen (NH_4-N) were analyzed using respective Hach Test'N'Tube Reagent Sets.

Membranes were chemically cleaned in between Phase 1 and Phase 2 using 500 ppm NaOCl solution at pH=10 for 20 min, followed by mineral acid cleaning using HCl at pH=2.5 for 30 min.

4.2. Results

Phase 1 saw an increase in COD removal throughout the 20 d experimental period from negative removal at t=0 to an average removal efficiency of 63.6% between t=14 d to 20 d (Figure 4.2).

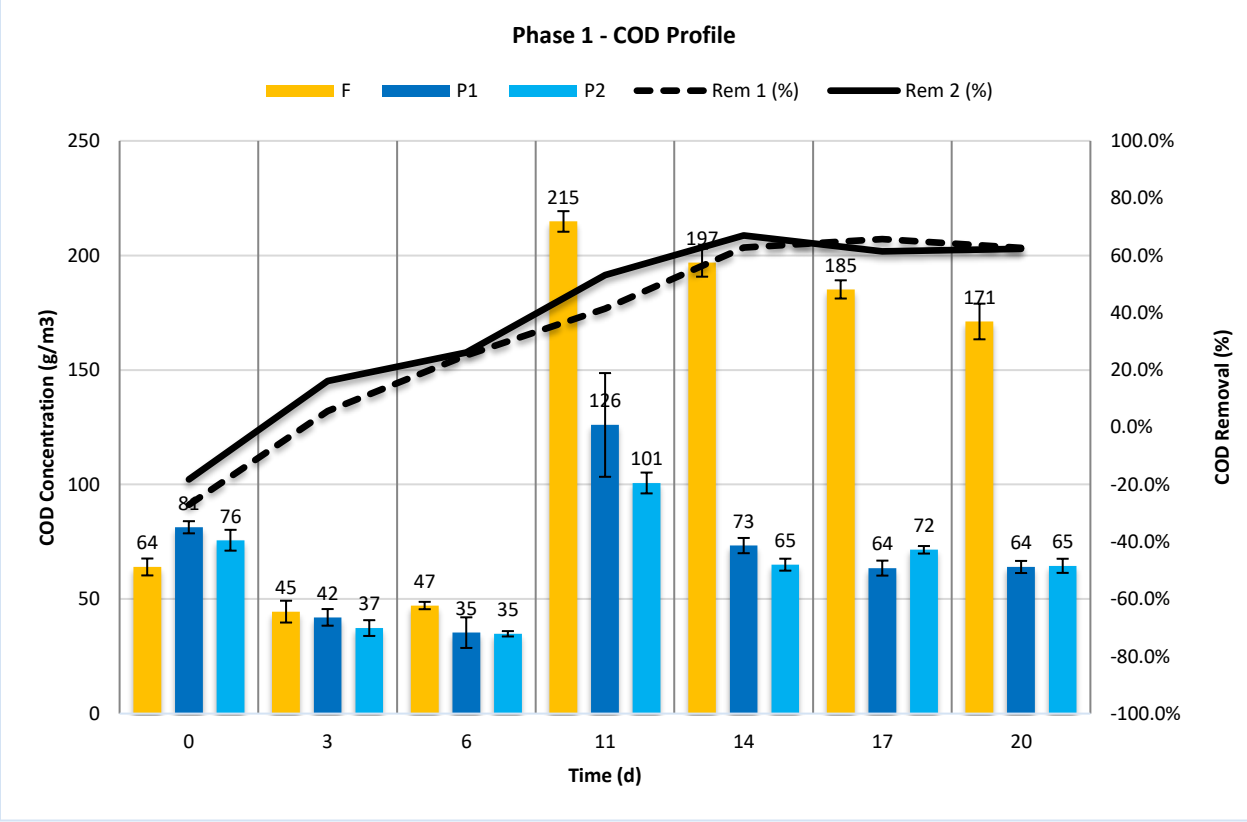

Figure 4.2. COD Profile for Phase 1 (F: Feed, P: Permeate)

Net ammonium nitrogen removal, while being as high as 86.8% for the first 6 d of operation, went down considerably and equilibrated at 12.3% from t=11 d onwards (Figure 4.3).

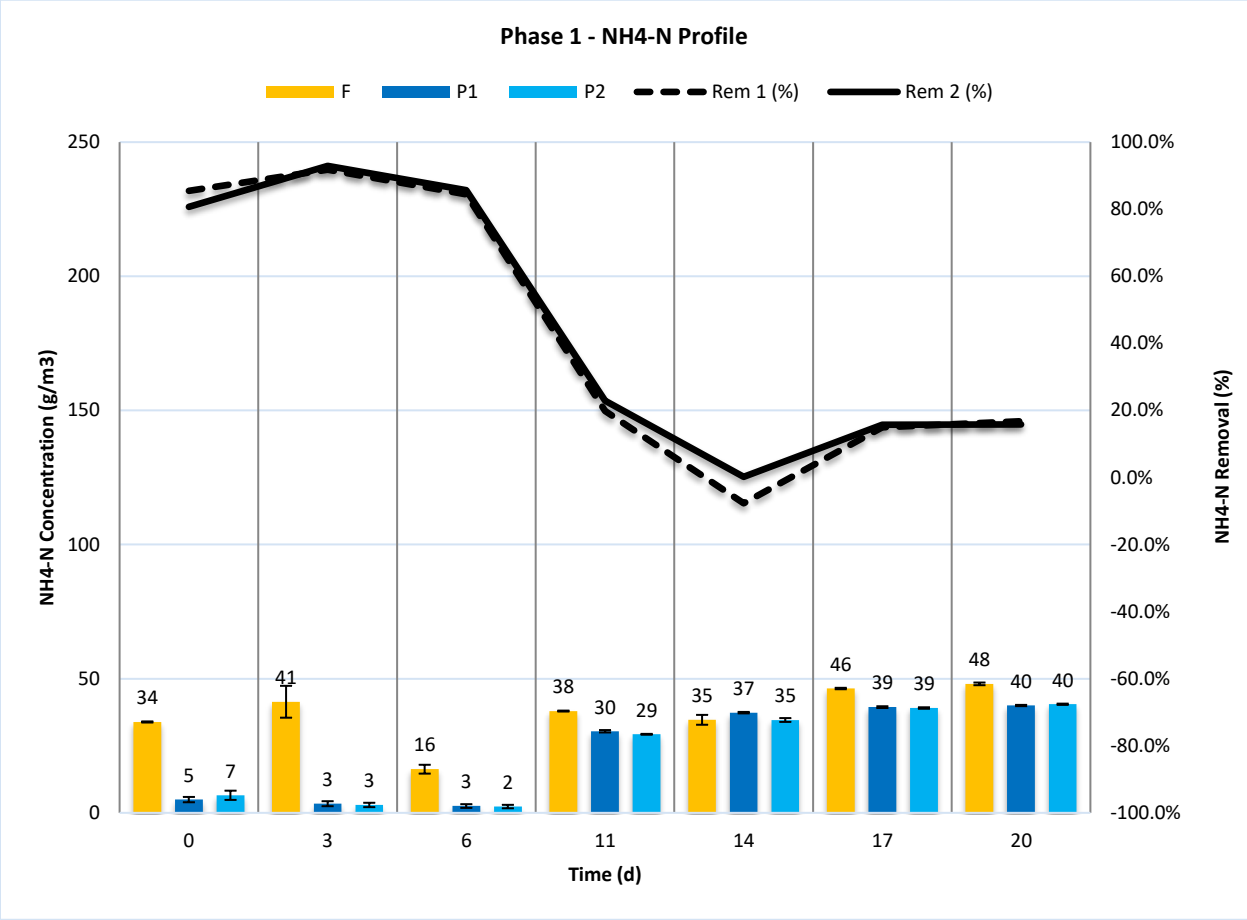

Figure 4.3. Ammonium-Nitrogen (NH_4-N) Profile for Phase 1 (F: Feed, P: Permeate)

The decrease in ammonium nitrogen removal efficiency correlated strongly with increase in nitrate concentrations within the two reactors. Nitrate concentrations increased 9.8 fold within the reactors from t=11 d on (Figure 4.4).

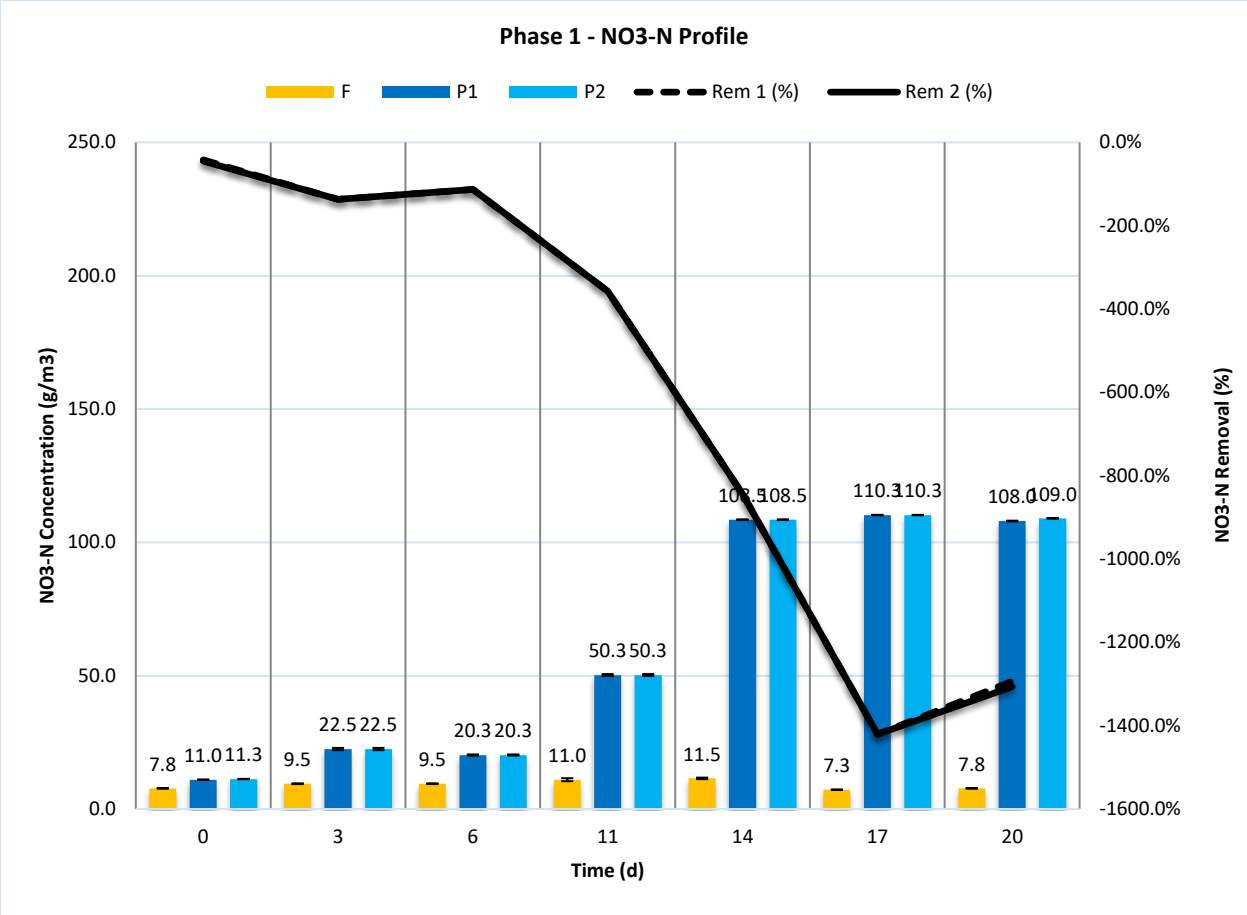

Figure 4.4. Nitrate-Nitrogen (NO_3-N) Profile for Phase 1 (F: Feed, P: Permeate)

The changes in ammonium and nitrate nitrogen levels and removal efficiencies can be explained by organic nitrogen being converted to ammonium and subsequently to nitrate, as evidenced by the relatively stable total nitrogen levels (Figure 4.5). Total nitrogen removal for the system after t=11 d was 9%, with influent TN levels being considerably higher than influent ammonium and nitrate nitrogen levels combined, indicating that most of the nitrogen in the feed was in organic nitrogen form when it entered the reactors.

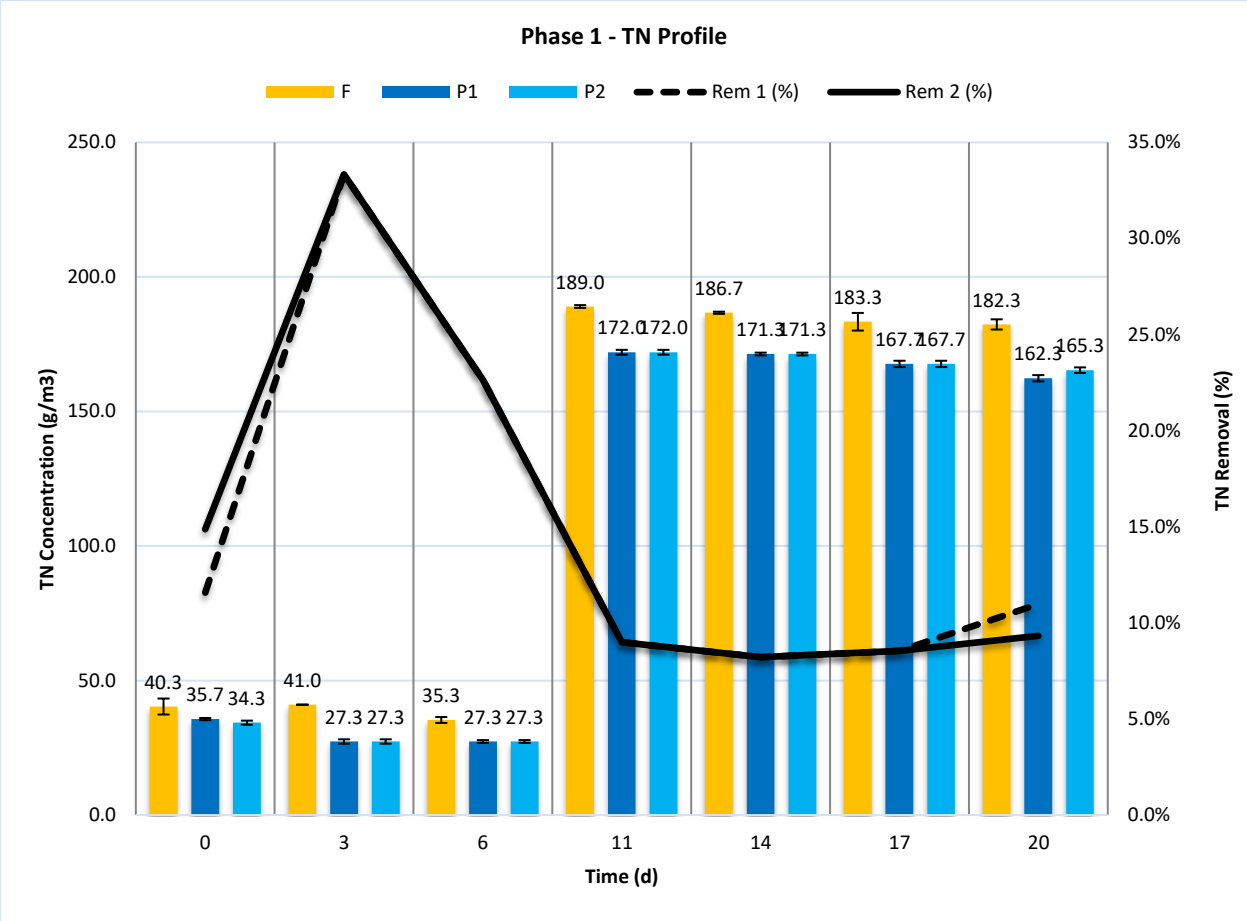

Figure 4.5. Total Nitrogen (TN) Profile for Phase 1 (F: Feed, P: Permeate)

A shift in microbial morphology was also qualitatively observed at the end of the experiment. While the starting culture was composed of mostly uniform homogenous cocci, the resulting culture had greater diversity in morphologies and more complex forms of life present (Figure 4.6).

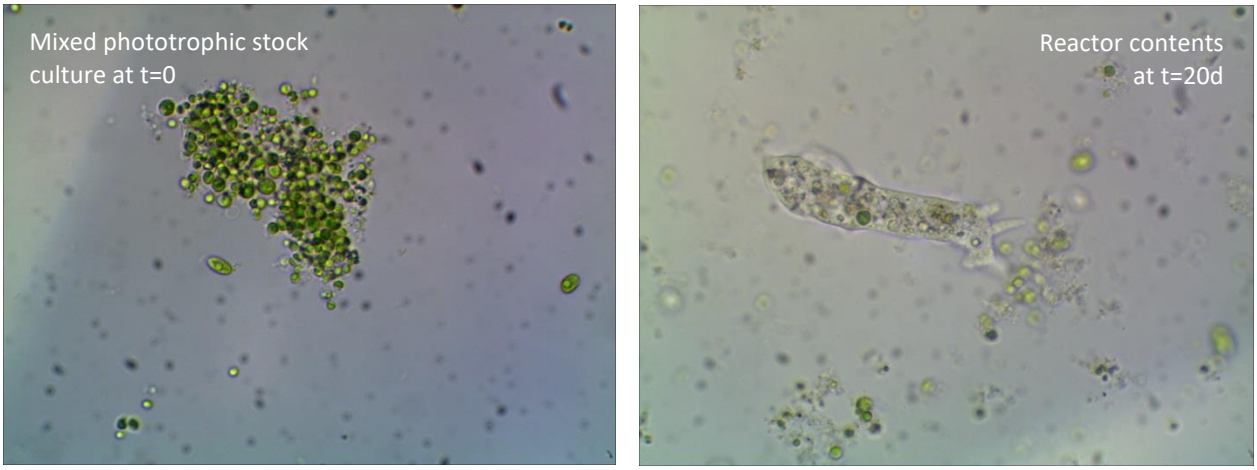

Figure 4.6. Microscopy results (40x) showing algal stock at time=0 (left), and the reactor contents at time=20d (right) for Phase 1

From the results of the first phase of experimentation, it was hypothesized that the pH decrease in reactors was caused by nitrification, which is known to consume alkalinity. In order to prevent nitrification, a high aeration rate-low SRT scenario was tested using a semi-batch fed 1 L clear glass reactor with continuous pH monitoring. After steady-state was reached, an increase in pH over 9.25 was observed within the light periods of the 14h/10h dark/light cycle (Figure 4.7).

In order to replicate the observed pH behavior in the PMBR system, Phase 2 was commenced with one of the reactors being operated under a high aeration rate delivered as fine bubbles and the other reactor under a lower aeration rate of 0.5 L/min for air sparging of the membranes, operated with an SRT of 8 d. However, this initial Phase 2 trial did not yield the same results as the semi batch experiment, and the pH remained below 9.25 over a period of 10 d (Figure 4.8). The pH differences between the day and night cycles were not as pronounced as seen in the semi batch experiment, although this may have been due to pH being measured on the permeate line of the PMBRs, rather than directly within the reactors. One important finding was

that the pH of the second reactor (R2) was consistently lower than that of the first reactor (R1). When the pH of the reactor contents was measured rather than the permeate lines, a difference of approximately 0.2-0.3 pH points in the positive direction was consistently measured for both reactors. The source of this difference is currently unknown.

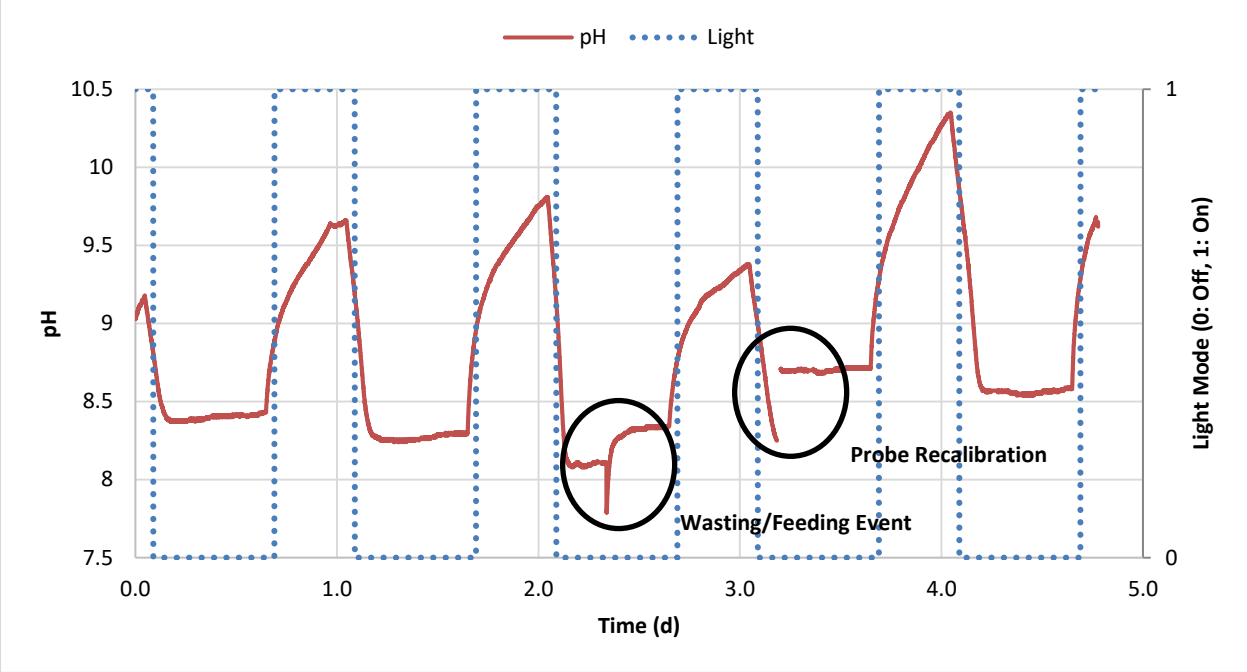

Figure 4.7. Parallel batch experiment pH profile - high aeration rate, fine bubbles, low SRT

Transmembrane pressure (TMP) was recorded as 5.9±0.2 kPa for the first phase of the study and 6.0±0.1 kPa for the second phase with an average membrane flux of 8.6 LMH. Membrane backwash was performed for 5 s every 10 min at a backwash flux of 150 LMH, creating a TMP spike of 20.9±1.7 kPa from the permeate side of the membrane to the feed side. Energy demand of system components was measured using a watt meter.

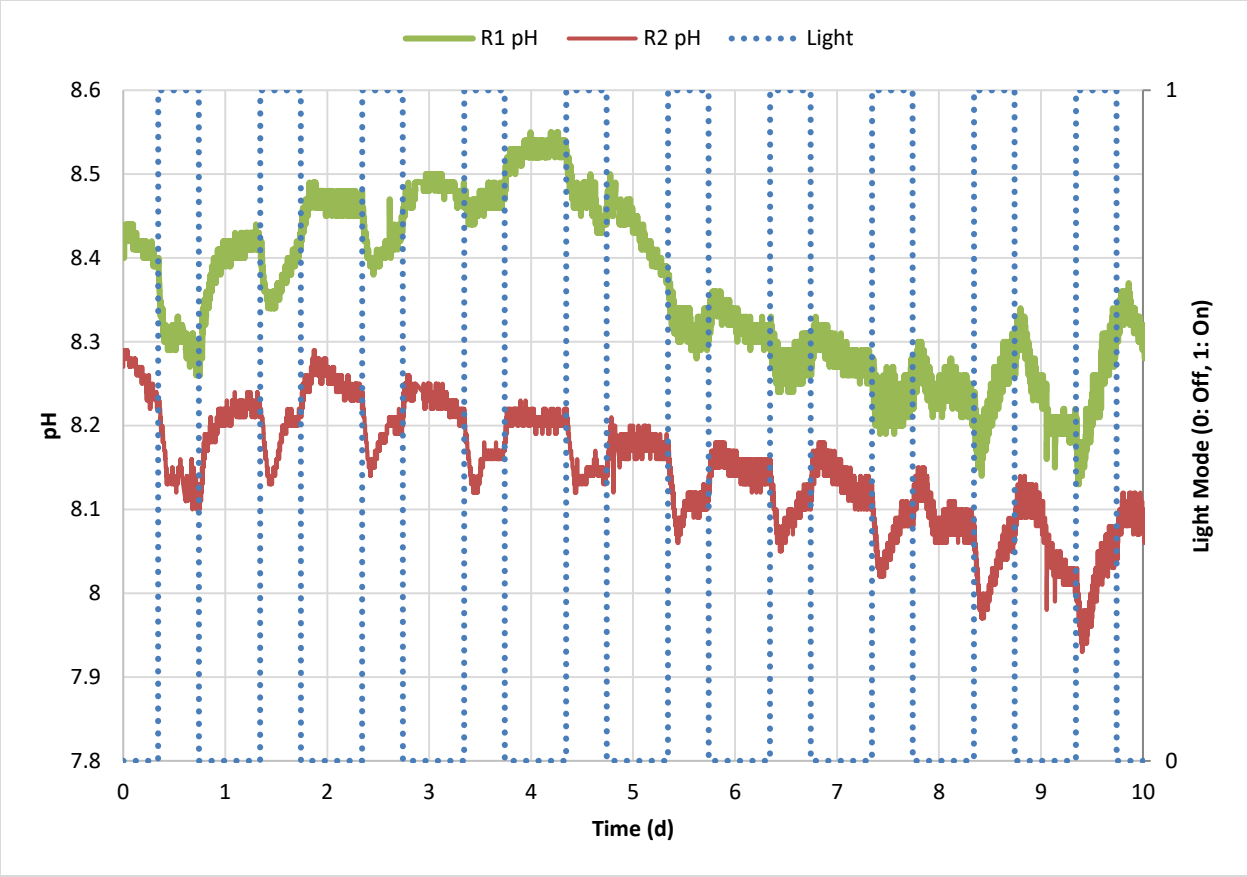

Figure 4.8. Phase 2 Trial 1 results showing Reactor 1 (R1) and Reactor 2 (R2) permeate pH profiles

4.3. Conclusions

- Under high SRT-low aeration conditions, reactors became nitrification dominated systems. Both reactors exhibited signs of acidification, with pH equilibrating slightly above 6.
- Transmembrane pressure remained low at 5.9±0.2 kPa and 6.0±0.1 kPa throughout both phases of the study.

- Energy requirement of the system for the first phase was 0.189 kWh/m^3 compared to 0.50 - 1.00 kWh/m^3 for (aerobic) MBR systems. For the second phase, it was further decreased to 0.100 kWh/m^3 by operating the system under airlift mode.
- TN removal efficiency of the system was inadequate for both phases under the tested operational conditions. However, relatively high COD removal (63.6%) was observed.
- The next chapter explores new hypotheses relating to algae-pH interactions.

Chapter 5: Demonstration of Phototrophic pH Increase

Phototrophic pH increase is a phenomenon that occurs naturally when rate of CO_2 uptake from the environment exceeds rate of CO_2 transfer into it. The net removal of CO_2 from the environment pushes the pH upwards. This phenomenon can potentially be further exacerbated when some algal species are subjected to an environment that contains little to no dissolved CO_2 to be used in photosynthesis, but has dissolved aqueous forms of inorganic carbon species, such as CO_3^{2-} and HCO_3^-. Under these conditions, algal species can take up the inorganic carbon from the environment, along with any protons attached to them, and convert these carbon species to CO_2, to be used in photosynthesis, and H_2O. This is called the carbon dioxide concentration mechanism (CCM), which seems to have evolved to help algal cells to continue to grow within environments that have no or little access to dissolved CO_2 (Kaplan & Reinhold, 1999). The additional pH increase in this case will be due to the net uptake of protons from the environment, along with the inorganic carbon species.

Phototrophic pH increase can potentially be used to induce pH-sensitive removal/recovery processes in water and wastewater treatment in future applications. An example of such a process is struvite (also called ammonium magnesium phosphate or MAP) recovery from wastewater streams: the rate of struvite precipitation and the nature of the precipitate changes with increased pH levels (Abbona *et al*., 1982; Wang *et al*., 2005; Wilsenach *et al*., 2007). Phototrophic pH increase can also potentially be used for stripping off ammoniacal nitrogen and precipitating PO_4^{3-} at pH levels above 9 (pK_a of NH_4^+ to NH_3 conversion is 9.25). However, increasing the pH to these levels will likely result in nutrient removal as opposed to

recovery, and should not be utilized unless the NH_3 and the PO_4^{3-} species can later be recovered by other means, or the pH should be kept below 9.25 in order to prevent the stripping of ammonia from the system.

5.1. Batch pH Increase Trials

In this study, batch reactors were used to induce and observe pH increase in phototrophic cultures for the first time in the field of wastewater treatment. Increasing pH of wastewater streams can help to facilitate the recovery or removal of nitrogen and phosphorus species. In addition, biologically induced pH increase by phototrophic cultures requires no mixing or supplying of air or CO_2 to the reactors, which can reduce the costs of algae cultivation.

5.1.1. Methods

This study was conducted using three identical 240 mL cylindrical batch reactors seeded with a mixed phototrophic culture originally bioprospected from primary and secondary clarifiers of Howard Curren Advanced Biological Wastewater Treatment Plant (Tampa, Florida, United States). Two distinct experimental phases were defined. The first phase of the study was conducted using the same experimental parameters for all reactors to statistically confirm the reproducibility of the pH increase phenomenon. In the second phase, differences in pH increase profiles were observed for different dilutions of feed fed to each reactor. In both phases, reactors were illuminated using an LED light panel consisting of 80% red (650 nm) and 20% blue (470 nm) LEDs, creating an illuminance of 1613±28 lux at the outer surface of the borosilicate glass reactors. Tap water was chosen instead of deionized water for dilutions while feeding for the availability of inorganic carbon as CO_3^{2-}. The reactors were not mixed or aerated throughout the

experiment, except when taking samples, for wasting and feeding events, and for manual pH and Optical Density (OD) measurements.

In the first phase, the cultures were fed with 24 mL of urine to achieve an initial dilution of 1:10 within the reactors (for 240 mL total volume). The pH profiles within the reactors were then observed for 12 days. There was no additional feeding or wasting during this time period.

In the second phase, the reactors were emptied and reseeded with fresh cultures. The cultures were fed with 1:5, 1:20, and 1:100 dilutions of urine in 40 mL urine + tap water solutions every 3 days, corresponding to 18 days of average Hydraulic Retention Time (HRT) and Solids Retention Time (SRT) for each reactor.

Total Nitrogen (TN), Ammonium Nitrogen (NH_4-N), Total Phosphorus (TP), and COD parameters were measured using commercially available Hach Test'n'Tube sets (Hach Methods 10072, 10031, 10127, and 8000 respectively) from Hach Company (Loveland, CO, USA). For the testing of soluble fractions, samples were centrifuged at 5000 Relative Centrifugal Force (RCF) for 10 min, and the resulting supernatant was filtered through 0.45 μm filters before being analyzed. Samples for these measurements were taken at the start of the experiment for the seed and the feed, and at the end of the experiment for the reactors. Reactor pH was measured continuously for each reactor using pH electrodes connected to a data logging system. Optical density of the samples was measured every 3 days using a Hach DR/4000 U, UV-Vis Spectrophotometer.

5.1.2. Results and Discussion

The first phase of the experiment saw the pH of the reactors increase from 6.42±0.13 to 8.87±0.06 within the first 6 days, at which point the pH values remained nearly constant until the

end of the experimental period. There was agreement among the three identical reactors, with slight variations in pH levels. A one-way ANOVA conducted using the entire dataset for the 3 samples resulted in a p value less than 0.001. In the second phase, Reactor 1 (R1) behaved similarly to the reactors in the first phase of the experiment. Reactor 2 (R2), however, had a more variable pH profile and a lower final pH value than R1, and Reactor 3 (R3) had a higher final pH value, 9.23, than R1 with a distinct diurnal pH pattern that correlated with the light/dark cycles: the pH of R3 would increase when there was light, and decrease in the absence of light, while following an increasing overall pH trend. Reactor feeding and wasting events also correlated with drops and subsequent recoveries in pH for all reactors. The pH profiles of the reactors for both experimental phases are presented in Figure 5.1.

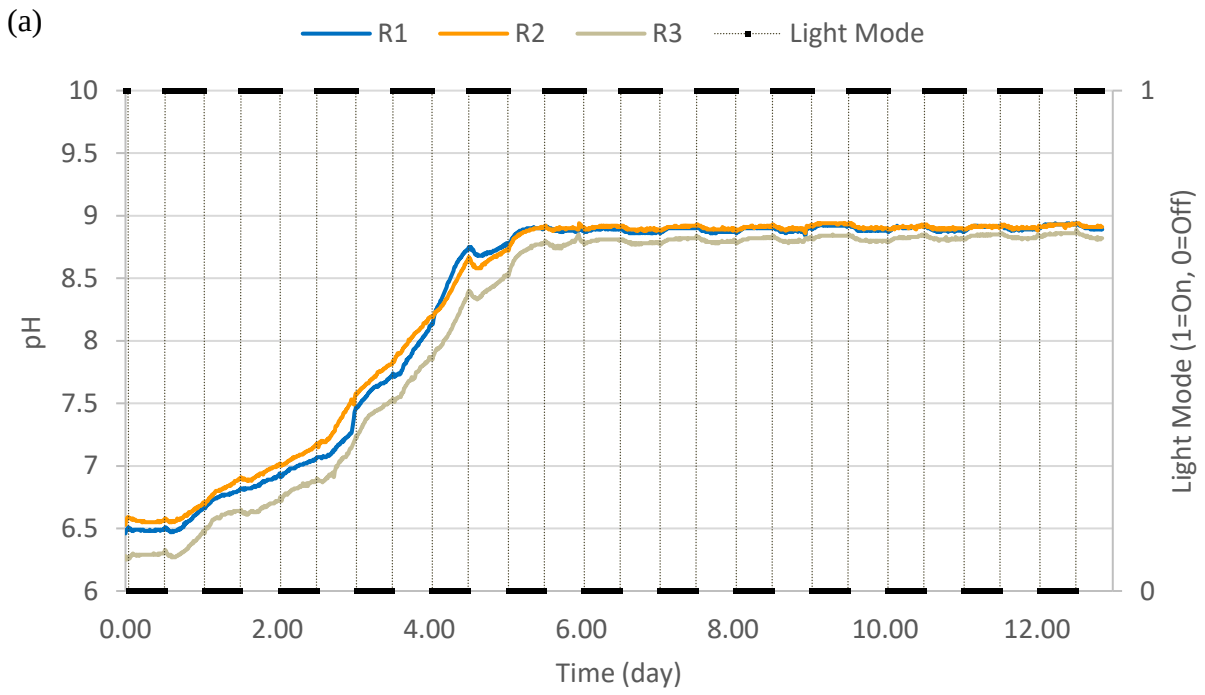

Figure 5.1. pH profiles for (a) experimental phase 1, and (b) experimental phase 2

(b)

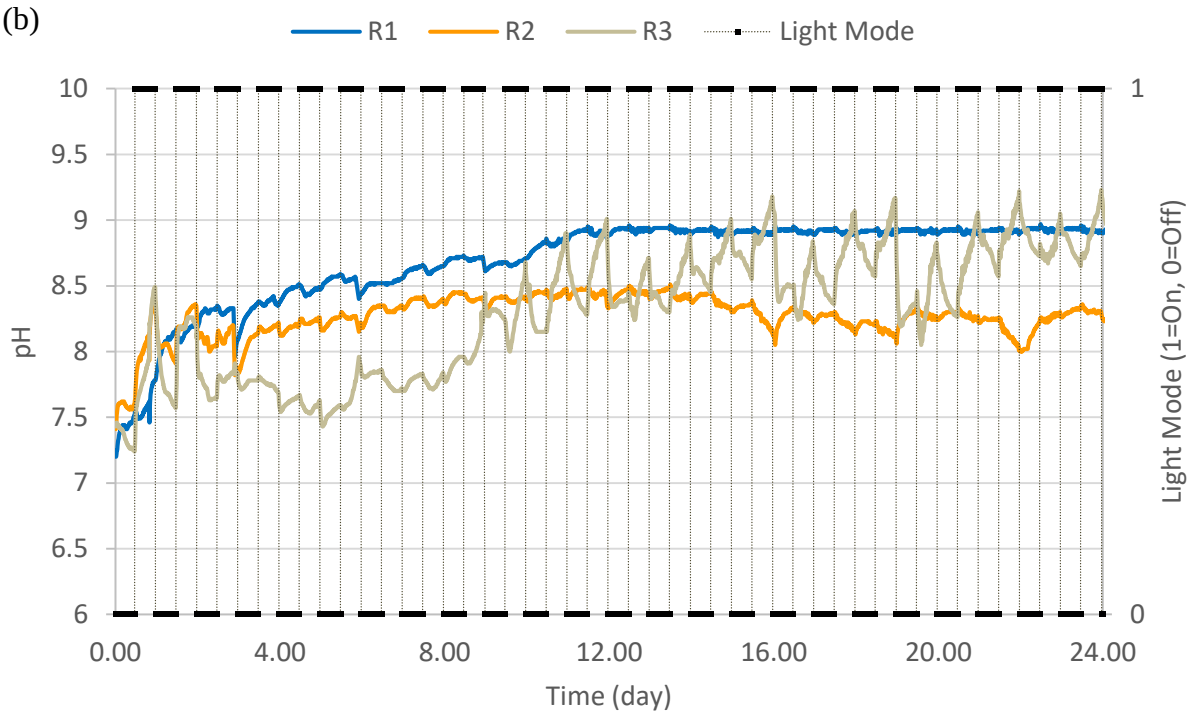

Figure 5.1. (Continued)

In order to determine whether the pH increase effect was a chemical one or the algae are indeed involved in the process, a 7-day control run was performed where the same 3 identical reactors were employed as the previous runs. In this case, the first reactor contained 10% urine and 90% tap water, the second reactor contained 10% urine and 90% algae, and the third reactor contained algae only. As shown in Figure 5.2, the 10% urine + 90% tap water-containing reactor did not exhibit any signs of pH increase, whereas the remaining two reactors containing algal cultures did. This proves that the pH increase phenomenon is not due to non-algae related conversion of reactor contents.

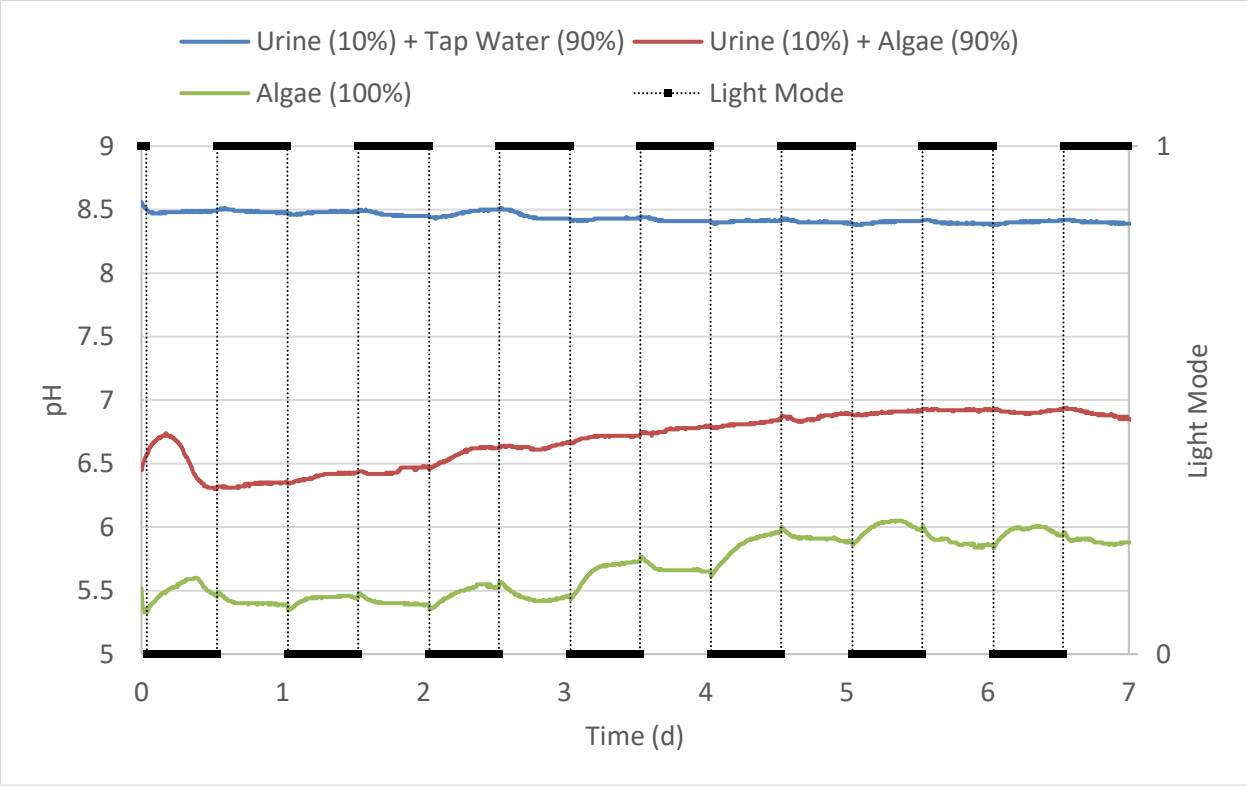

Figure 5.2. pH profiles the control run

The optical density profiles for all reactors in the first experimental phase were relatively stable after a slight initial drop. The second experimental phase saw a greater, more gradual drop in optical density levels, and a more gradual recovery for all reactors. Optical density profiles are presented in Figure 5.3.

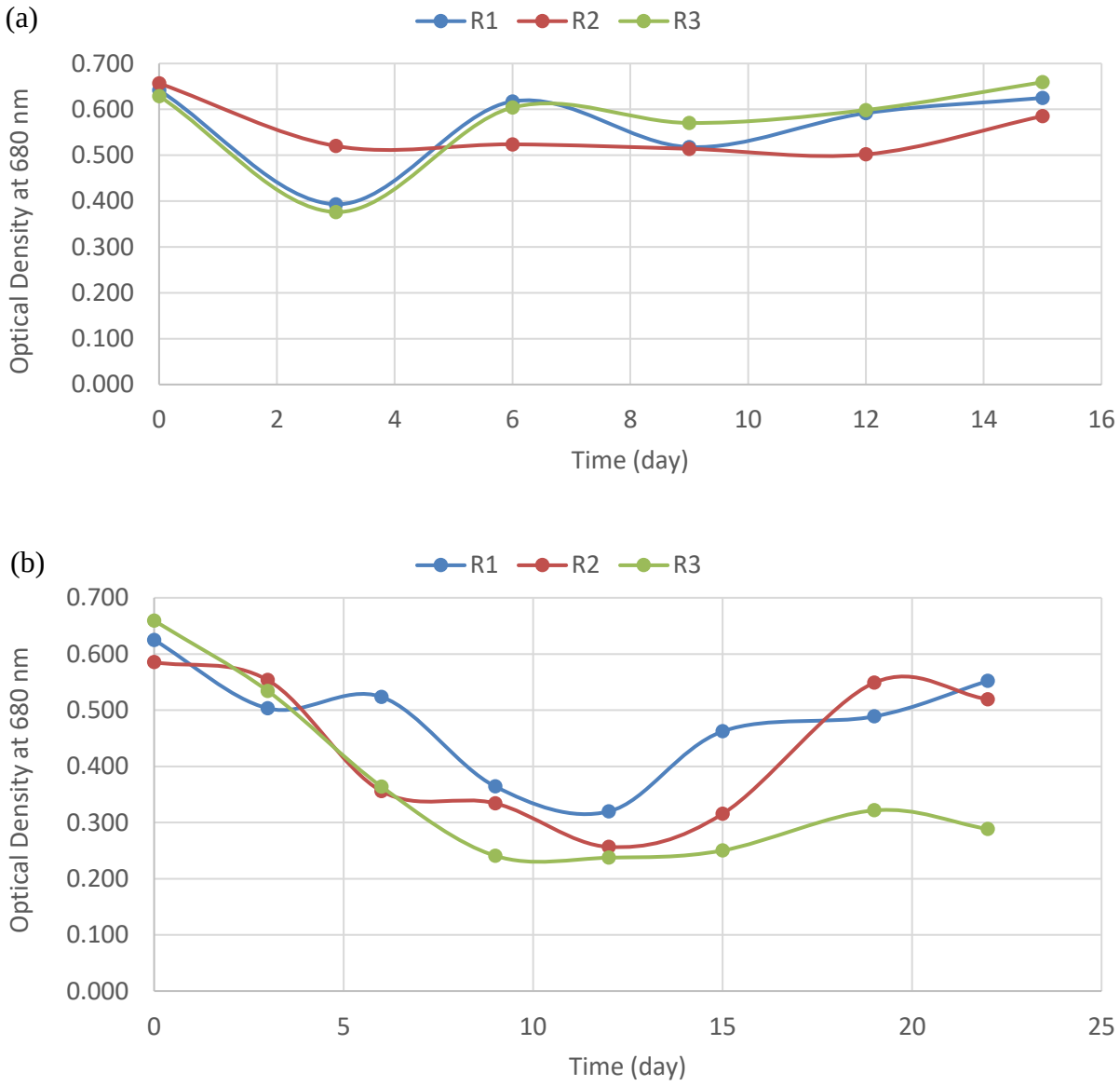

Figure 5.3. Optical density profiles for (a) experimental phase 1, and (b) experimental phase 2

Significant amounts of total and soluble fractions of COD, TN, and TP remained in the final liquor within the reactors in the first experimental phase as well as R1 and R2 in the second experimental phase, whereas no soluble TP or ammonium were detected within the contents of R3 at the end of the second experimental phase – which may potentially be attributed to the removal of nutrients due to direct pH effects, since R3 was the reactor that had the highest final

pH level. Characterization of the feed, seed, and final contents of reactors for each experimental phase are shown in Table 5.1.

Table 5.1. Characterization of urine, phototrophic seed culture and final reactor contents for (a) experimental phase 1, and (b) experimental phase 2

(a)	**Urine**	**Seed**	**R1(final)**	**R2(final)**	**R3(final)**
COD	10500±142	505±7	997±60	1000±276	1110±207
sCOD	10390±50	73±1	381±10	391±7	469±13
TN	7133±125	115±1	992±14	983±29	1092±14
sTN	6880±80	87±1	880±1	910±14	930±14
NH4-N	611±6	6±1	800±34	754±3	844±11
TP	619±3	23±1	65±1	64±5	69±2
sTP	472±1	7±1	11±1	8±1	12±1

(b)	**Urine**	**Seed**	**R1(final)**	**R2(final)**	**R3(final)**
COD	9920±255	513±11	550±28	559±21	288±23
sCOD	9570±184	71±11	283±11	106±6	51±6
TN	8400±141	126±1	760±28	138±4	84±3
sTN	8050±212	73±3	483±11	95±4	29±2
NH4-N	1090±42	9±1	408±1	74±3	0±1
TP	1093±32	27±1	149±2	59±1	28±1
sTP	890±21	7±1	17±1	3±1	0±1

Under the right environmental conditions, phototrophic cultures can increase the pH of the medium in which they are cultivated. This phenomenon can potentially be utilized in wastewater engineering to create new processes where nutrients can be recovered using pH-dependent reactions – i.e. combining phototrophic pH increase with struvite precipitation, for instance, can, in the future, potentially lead to more efficient ways of recovering struvite from wastewater streams. In addition, the light-dependency of pH increase and decrease can

potentially lead to applications where the end product is tailored to the specific needs of the treatment operation, and optimal pH levels could be maintained for cultivation of phototrophic cultures to create useful end products. In this instance, complete soluble phosphorus and ammoniacal nitrogen removal during a phototrophic pH increase process was demonstrated, as shown by the data collected from experimental phase 2, reactor 3, pointing towards at least a correlation between pH increase and nutrient removal.

5.2. Continuous pH Increase Trial

Even though the batch tests proved that it was possible to raise pH levels using phototrophic cultures, the same phenomenon would need to be demonstrated using continuously operated reactors in order to be compatible with how reactors are generally operated in the wastewater treatment field. To this end, a non-aerated, 2 L borosilicate glass column membrane photobioreactor fitted with an external, tubular, 0.03 μm polyvinylidene fluoride (PVDF) ultrafiltration membrane was operated continuously for a month to demonstrate phototrophic pH increase. The reactor was fed with a 0.05% w/w (500 mg/L) MaxiGro fertilizer solution (General Hydroponics Inc., Santa Rosa, CA, USA) containing nutrients essential for primary production for about a month. The nutrient composition of the fertilizer is given in Table 5.2.

Table 5.2. Nutrient composition of the fertilizer used for the experiment (w/w)

Total Nitrogen (as N)	10.0%
Ammoniacal Nitrogen (as N)	1.5%
Nitrate Nitrogen (as N)	8.5%
Available Phosphate (as P_2O_5)	5.0%
Soluble Potash (as K_2O)	14.0%
Calcium (as Ca)	6.0%

Table 5.2. (Continued)

Magnesium (as Mg)	**2.0%**
Sulfur (as S)	3.0%
Iron (as Fe)	0.12%
Manganese (as Mn)	0.05%

During the operational period, changes in pH were observed by logging in real time the pH measurements of the permeate from the membrane every minute. Note that there may be a difference between the actual pH within the reactor and the pH of the permeate. The volume of the permeate storage unit within which the pH probe was located was 25 mL. Since the reactor was operated at 1 d HRT during the operational period, with the storage unit measuring 25:2000 = 1.25% the total volume of the reactor and the amount of permeate passed through it every day, a dampening effect would be expected concerning the resolution of the pH readings, which may be important in the light of light/dark cycle-sensitive pH changes recorded in the batch experimentation phase. Reactor illumination for the continuous trial was done using an LED light panel consisting of 80% red (650 nm) and 20% blue (470 nm) LEDs, creating an illuminance of 3878±308 lux at the outer surface of the borosilicate glass reactor. The light/dark cycle was 10 h light/14 h dark. The pH profile observed for the experimental period is given in Figure 5.4.

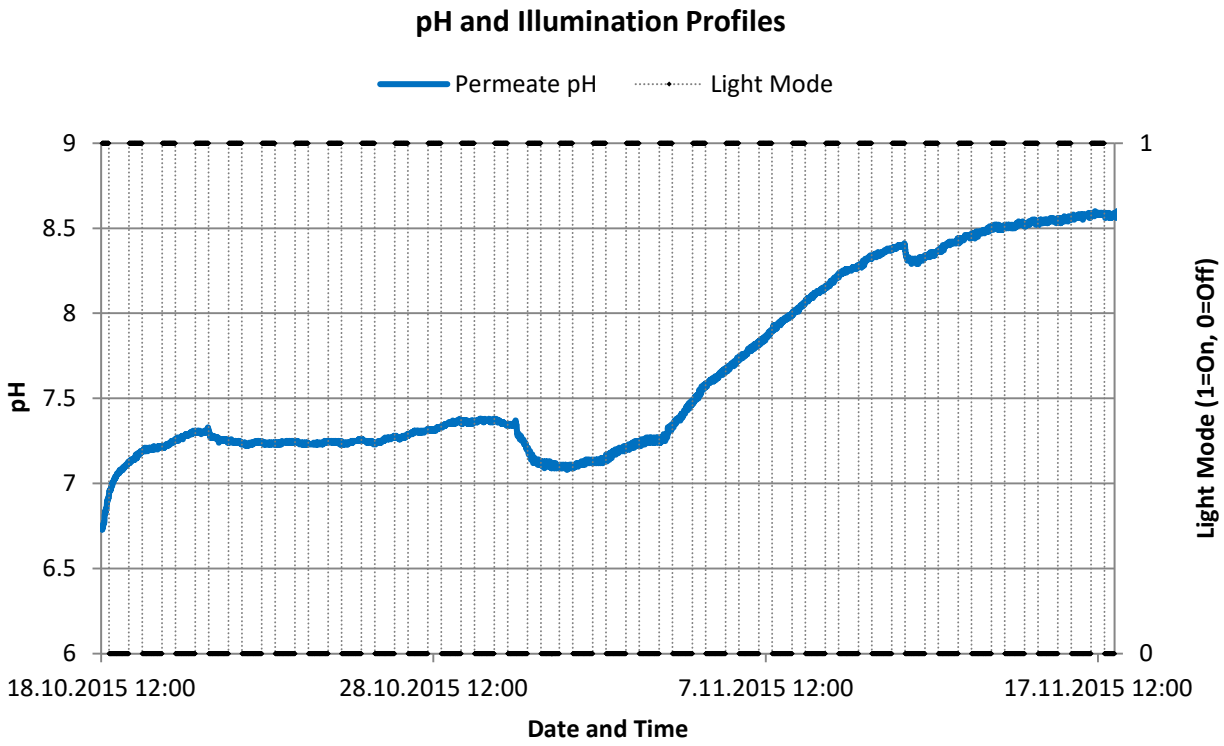

Figure 5.4. Permeate pH profile for the duration of the experiment

During the experimental phase, the pH of the permeate rose from a value of 6.73 to a value of 8.61. No light/dark-sensitive pH changes were observed for this continuous run, which may be attributed to the chosen operational conditions as well as the dampening effect on pH profile resolution as discussed in the previous paragraph. The results do indicate that it is indeed possible to raise permeate pH using a continuously operated phototrophic reactor system.

5.3. Conclusions

Phototrophic pH increase was demonstrated both with batch and continuous reactor systems. This phototrophic technology has, in future applications, the potential to be used for nutrient management due to the pH dependency of the solubility of the most common dissolved

forms of inorganic nitrogen and phosphorus. In addition, because the reactors do not need to be aerated or otherwise supplied with CO_2, the technology will potentially lead to systems with a lower energy requirements than more conventional phototrophic technologies.

Chapter 6: Integrated CBR-PMBR Operation

6.1. Introduction

The abiotic treatment performance of the Concentrically Baffled Reactor (CBR) was established in previous chapters. This chapter focuses on testing the Chemical Oxygen Demand (COD) removal performance of the CBR itself and the COD, Total Nitrogen (TN), and Total Phosphorus (TP) removal of a combined CBR-Phototrophic Membrane Bioreactor (PMBR) system. The CBR was operated as an Anaerobic Baffled Reactor (ABR) with and without post-membrane-filtration for this study, and tested with both high strength and low strength feeds in order to gauge its performance both as an alternative mainstream and sidestream domestic wastewater treatment process. Testing with and without the membrane filtration would give the author an idea of the performance of the CBR when it is operated as a standalone ABR or an Anaerobic Membrane Bioreactor (AnMBR) with baffles. Background literature on ABR and AnMBR systems can be found in Chapter 2.

The nutrients (TN & TP) would not be significantly removed by a well-functioning anaerobic treatment unit, and TN and TP in particulate form would be converted to their soluble forms through anaerobic digestion. Therefore, a post-anaerobic process is required to remove the nutrients coming out of the anaerobic system. In this study, Phototrophic Membrane Bioreactor (PMBR) units were integrated with the CBR to remove TN and TP. Phototrophic processes were chosen due to the mutual relationship between wastewater treatment and growing algae for biofuels and other useful end products (Pittman *et al*., 2011). However, the phototrophic cultures were not tested for their suitability for biofuel production – the focus of the study was their

viability as a way to remove or recover nutrients from CBR effluents, and how a pre-PMBR membrane filtration unit would affect the nutrient removal performance of the PMBRs. This was important because even though a membrane filtration unit between the CBR and the PMBR can increase both capital and operational costs, it may result in better PMBR performance by preventing particulate and microbial loading into the PMBR. This would also result in a more controlled environment for growing algal cultures to produce other end products.

6.2. Methods

The experimental setup used for this study featured a CBR unit consisting of 7 zones, a total diameter of 0.60 m, and a liquid volume of 32 L. 280 g of Kaldnes Filter Media (K1 Micro) was added in order to allow for attached growth within the reactor. Total liquid volume displaced by the added media was 340 mL. The exact dimensions and specifications of the CBR can be found in Table 3.3.1. The CBR was fitted with an external, vertically mounted membrane filtration unit featuring Polyvinylidene fluoride (PVDF) tubular ultrafiltration membranes with a nominal pore size of 0.03 μm (Pentair X-Flow, Enschede, The Netherlands). The central zone of the CBR was heated to mesophilic temperatures for the duration of the experiment using a heat exchange coil made of flexible vynil tubing. In addition to the CBR unit, two vertical column phototrophic membrane bioreactors (PMBRs) were used for the study. The photobioreactors, made of borosilicate glass, each had 2 L effective liquid volume. The PMBRs were also fitted with the same type of external membrane modules as the CBR, albeit with different effective filtration areas. The experimental setup is shown in Figure 6.1.

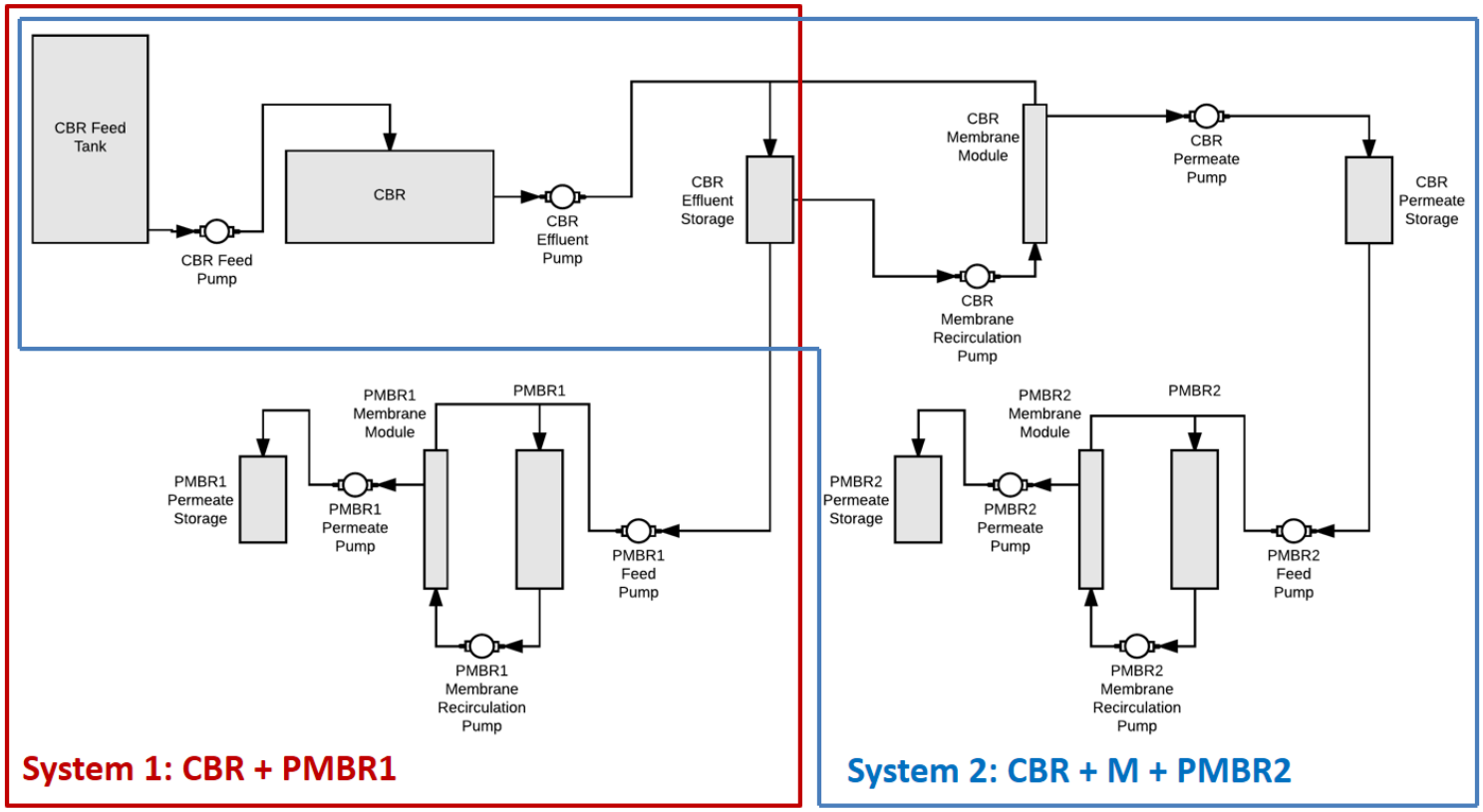

Figure 6.1. Flow diagram of the experimental setup used for the study

The CBR was fed with a synthetic feed composed of 20% sucrose and 80% Complex Organic Particulate Artificial Sewage (COPAS) as described by Prieto (2011), which is finely ground and sieved (maximum particle diameter 1.7 mm) cat food serving as a synthetic feed alternative for wastewater treatment systems, especially where particulate solids within the feed are important to the process. PMBR1 was fed with the unfiltered effluent from the CBR, and PMBR2 was fed with the filtered effluent (permeate) from the membrane module connected to the CBR. Photographs of the CBR and one of the PMBRs are presented in Figure 6.2.

Figure 6.2. Photos of (a) the CBR and (b) one of the PMBRs

The experiment was divided into two phases. The first phase tested the performance of the integrated CBR-PMBR systems treating high strength feed at a high HRT value. This was to demonstrate the viability of the system for any high strength applications ranging from sidestream waste treatment at a domestic wastewater treatment plant to treating high strength industrial wastewaters. In the second experimental phase, the feed strength and the HRT were lowered considerably to test for on-site domestic wastewater treatment applications. The operational differences between the two phases can be seen in Table 6.1.

Table 6.1. Operational conditions for the two experimental phases

Parameter	**Phase I**	**Phase II**
Experiment Duration	30 d	30 d
CBR Feed COD	17635±1674 mg/L	544±42 mg/L
CBR HRT	10 d	2 d
CBR SRT	∞	∞
CBR Membrane Area	0.0251 m^2	0.0882 m^2
CBR Backwash Frequency	Every 30 min	Every 5 min
CBR Backwash Duration	20 s	10 s
PMBR HRT	5 d	1 d
PMBR SRT	40 d	40 d
PMBR Membrane Area	0.0251 m^2	0.0251 m^2
PMBR Backwash Frequency	Every 60 min	Every 30 min
PMBR Backwash Duration	10 s	10 s
PMBR Aeration	None	None
PMBR Illumination	3750 lux	3750 lux
PMBR Light/Dark Cycle	12/12 h	12/12 h
PMBR Light Panel Composition	80% red (650 nm) and 20% blue (470 nm) LEDs	80% red (650 nm) and 20% blue (470 nm) LEDs

The temperature of the CBR zones was monitored by manual sampling using digital thermometers. The transmembrane pressure of the membrane modules was monitored using –

14.7 to 15 psig ±0.25%-Accuracy Compound Transmitters (Cole-Parmer Instrument Company, IL, USA) connected to a U30 Data Logger (Onset Computer Corporation, MA, USA).

Total Nitrogen (TN), Total Phosphorus (TP), and COD parameters were measured using commercially available Hach Test'n'Tube sets (Hach Methods 10072, 10127, and 8000 respectively) from Hach Company (Loveland, CO, USA).

6.3. Results

In the first phase, where HRT was at the higher value of 10 days, the temperature within the CBR had a gradient starting from 37.4±1.7°C within the first (central) zone going down to 25.9±0.5°C within the last (7^{th}) zone of the reactor. In the second (low HRT) phase, the temperature in the last zone was slightly higher at 26.6±0.3°C. The temperature distributions recorded are given in Table 6.2.

Table 6.2. Temperature distributions throughout (a) Phase I (high HRT), and (b) Phase II (low HRT) of the study, where Z: Zone, C: Central, Avg: Average, Stdev: Standard Deviation.

(a)	**Z1(C)**	**Z3**	**Z5**	**Z7**
Avg	37.4	30.5	27.1	25.9
Stdev	1.7	1.2	0.7	0.5

(b)	**Z1(C)**	**Z3**	**Z5**	**Z7**
Avg	37.2	32.5	28.1	26.6
Stdev	0.8	0.5	0.4	0.3

Average COD removal efficiency for the first (high HRT) phase of the study was 94.7±1.8%, which can be attributed to the high average feed COD concentration of 17635±1674 mg/L. Anaerobic systems are known to perform well with higher feed COD concentrations at

high HRTs, and not very well with low feed COD concentrations and HRTs. The average COD removal efficiency for the second (low HRT) phase of the study reflects this, resulting in 50.9±10.2% removal efficiency. However, when the membrane was used to filter the effluent from the CBR, the COD removal efficiency for the second phase increased to 90.9±2.4%. COD profiles are given in Figure 6.3.

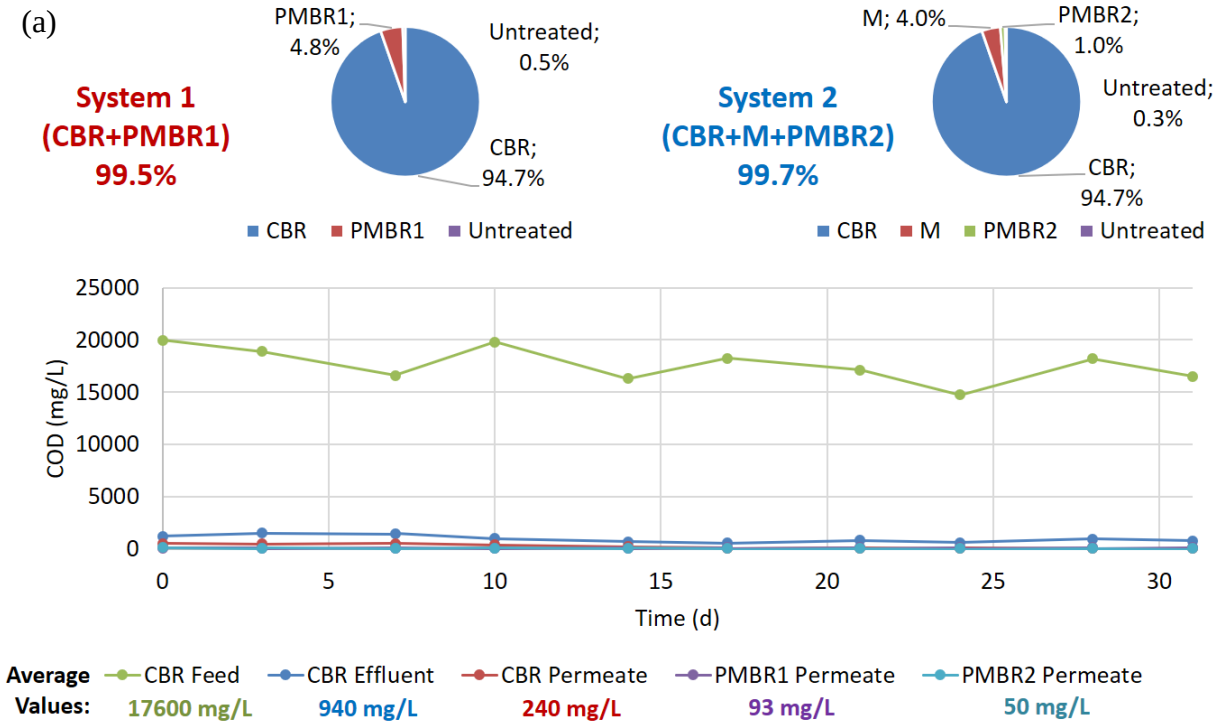

Figure 6.3. COD profiles of the CBR influent, CBR effluent, CBR permeate, PMBR1 permeate, and PMBR2 permeate throughout (a) Phase I (high HRT), and (b) Phase II (low HRT)

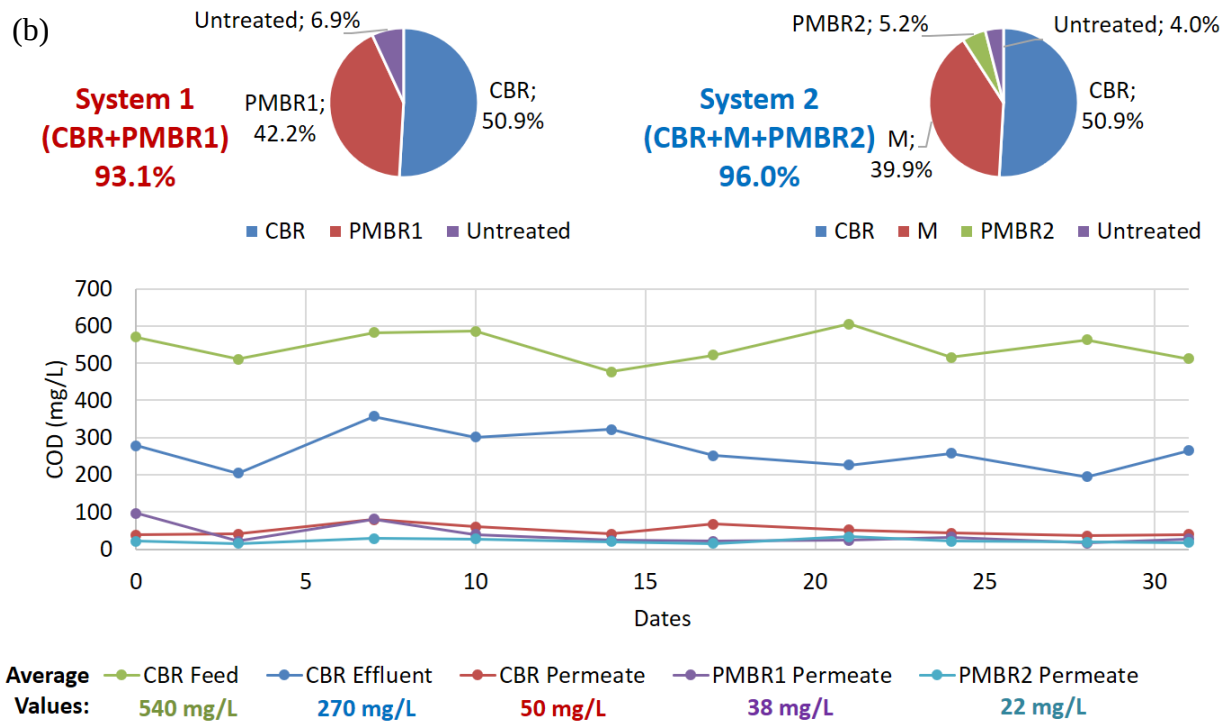

Figure 6.3. (Continued)

PMBR1, which treated the effluent from the CBR, performed better in both phases of the experiment than PMBR2, which treated the permeate from the membrane through which CBR effluent was filtered. However simply looking at removal efficiencies and concluding that PMBR1 is the better choice can be misleading, because the COD loading to PMBR2 was much lower to begin with compared to PMBR1, thanks to the removal of particulate COD by the membrane between the CBR and PMBR2 systems. A better way to compare the two systems would be to look at the combined COD removal efficiencies of the CBR+PMBR1 and CBR+M+PMBR2 systems. COD removal efficiency profiles of all systems are given in Table 6.3.

Table 6.3. COD Removal efficiencies of the systems* and their combinations* throughout (a) Phase I (high HRT), and (b) Phase II (low HRT)

(a)	COD Removal (%) – Phase I					
	CBR	**CBR+M**	**PMBR1**	**PMBR2**	**CBR+PMBR1**	**CBR+M+PMBR2**
6/8/2016	94.0	97.5	94.5	76.6	99.7	99.4
6/11/2016	92.0	97.5	95.6	82.8	99.7	99.6
6/15/2016	91.2	97.0	94.8	87.4	99.5	99.6
6/18/2016	95.1	98.1	92.4	81.8	99.6	99.7
6/22/2016	95.8	98.7	88.1	76.1	99.5	99.7
6/25/2016	97.0	99.6	83.0	56.9	99.5	99.8
6/29/2016	95.3	99.5	86.4	60.7	99.4	99.8
7/2/2016	96.0	99.5	79.8	65.3	99.2	99.8
7/6/2016	94.9	99.8	87.0	38.9	99.3	99.8
7/9/2016	95.5	99.8	83.7	50.0	99.3	99.9
Average	94.7	98.7	88.5	67.6	99.5	99.7
Stdev	1.8	1.1	5.6	15.9	0.2	0.2
(b)	**COD Removal (%) – Phase II**					
	CBR	**CBR+M**	**PMBR1**	**PMBR2**	**CBR+PMBR1**	**CBR+M+PMBR2**
7/27/2016	51.3	93.3	65.0	44.7	83.0	96.3
7/30/2016	60.1	92.0	89.7	63.4	95.9	97.1
8/3/2016	38.7	86.3	77.3	63.8	86.1	95.0
8/6/2016	48.6	89.8	87.0	55.0	93.3	95.4
8/10/2016	32.5	91.4	92.5	51.2	95.0	95.8
8/13/2016	51.7	87.2	91.7	77.6	96.0	97.1
8/17/2016	62.6	91.4	89.4	36.5	96.0	94.5
8/20/2016	50.1	91.7	87.5	51.2	93.8	95.9
8/24/2016	65.4	93.6	91.3	47.2	97.0	96.6
8/27/2016	48.2	92.2	89.8	55.0	94.7	96.5
Average	50.9	90.9	86.1	54.6	93.1	96.0
Stdev	10.2	2.4	8.6	11.5	4.7	0.9

* CBR+M denotes Concentrically Baffled Reactor treatment followed by membrane filtration. PMBRs 1 and 2 are the phototrophic MBRs used in the study, and the last two columns represent the removal efficiencies of the combined systems, where PMBR 1 is fed the effluent from CBR, and PMBR is fed the permeate from CBR+M.

TN removal efficiency of the CBR for the first phase of the project was 70.4±14.4%, which is rather high for an anaerobic system. This kind of TN removal can be attributed to the settling of particulate organics and the incomplete conversion of particulate organic nitrogen to its soluble forms. The membrane filtration process increased TN removal to 88.8±3.7% in the first experimental phase. The results of the second phase were more reasonable, with 25.6±11.3% removal without the membrane, and 49.6±10.0% with it. CBR TN profiles are shown in Figure 6.4.

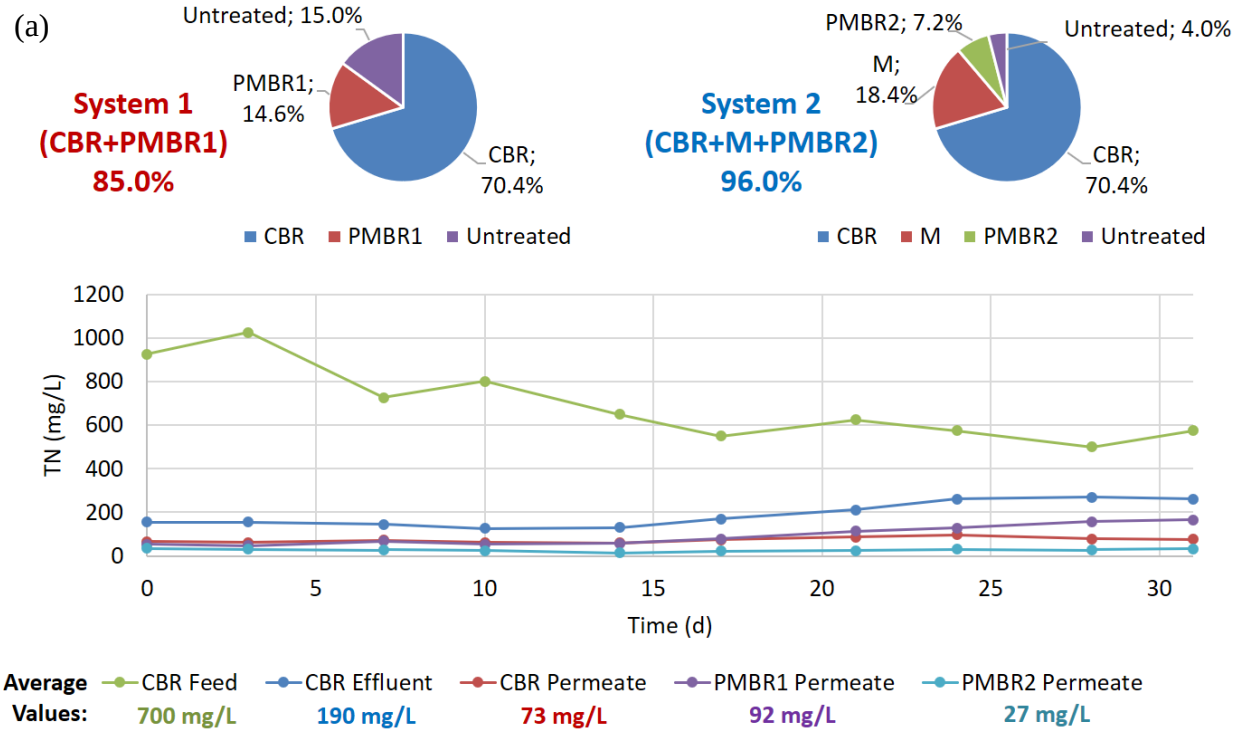

Figure 6.4. TN profiles of the CBR influent, CBR effluent, CBR permeate, PMBR1 permeate, and PMBR2 permeate throughout (a) Phase I (high HRT), and (b) Phase II (low HRT)

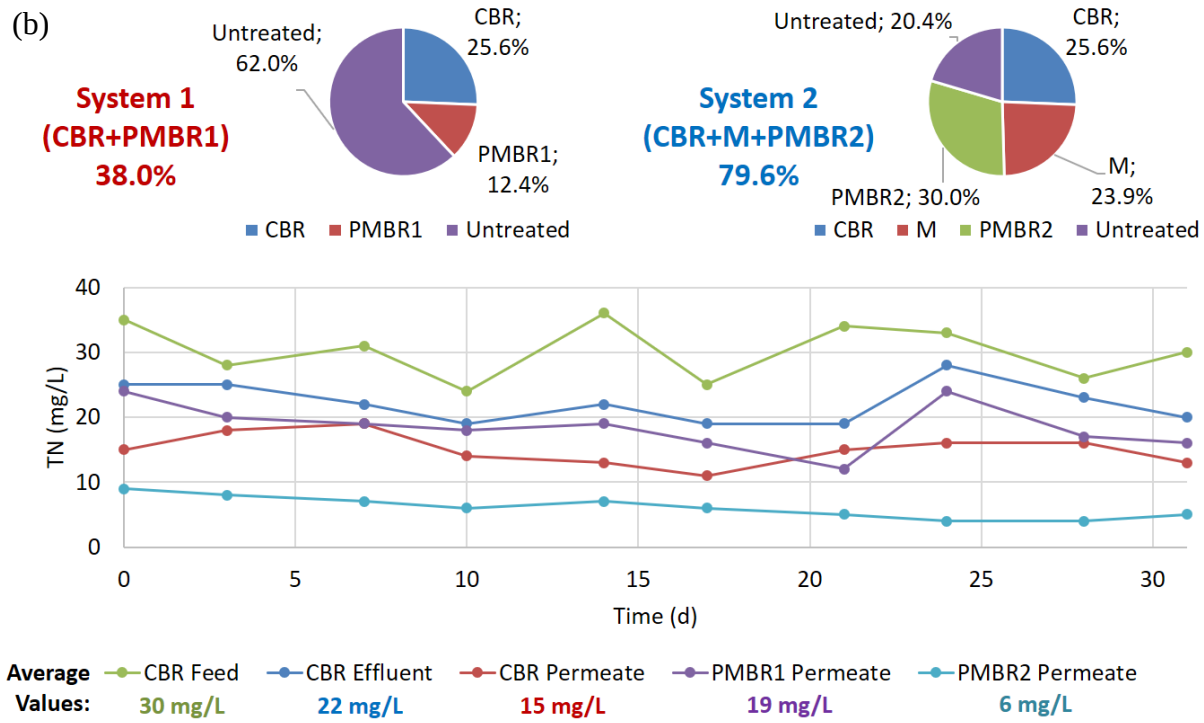

Figure 6.4. (Continued)

In terms of TN removal, PMBR1, which treated the unfiltered effluent from the CBR had a lower performance than PMBR2, which treated the filtered effluent for both experimental phases, with the gap in performance increasing in the second phase. In the first phase of the experiment, PMBR1 achieved a TN removal efficiency of 53.1±10.2% versus 62.9±9.2% for PMBR2. In the second phase, PMBR1 had a much lower TN removal efficiency of 17.0±9.6%, whereas PMBR2 saw only a slight decrease to 58.6±12.1%. The sharp decrease in performance of PMBR1 in the second (low HRT) phase can be attributed to greater anaerobic biomass washout from the CBR, which may have created unfavorable conditions for the phototrophic biomass. The combined TN removal efficiencies of CBR and PMBR systems were fairly high for the first phase of the experiment. However, in the second phase, only the CBR+M+PMBR2

system had high TN removal. TN removal efficiency profiles of all systems are given in Table 6.4.

Table 6.4. TN Removal efficiencies of the systems and their combinations throughout (a) Phase I (high HRT), and (b) Phase II (low HRT)

(a)	TN Removal (%) – Phase I					
	CBR	**CBR+M**	**PMBR1**	**PMBR2**	**CBR+PMBR1**	**CBR+M+PMBR2**
6/8/2016	83.2	92.9	66.1	49.2	94.3	96.4
6/11/2016	84.9	94.0	70.0	50.0	95.5	97.0
6/15/2016	80.0	90.1	53.1	59.7	90.6	96.0
6/18/2016	84.4	92.3	56.8	61.3	93.3	97.0
6/22/2016	80.0	90.9	56.2	76.3	91.2	97.8
6/25/2016	69.1	86.7	53.5	71.2	85.6	96.2
6/29/2016	66.4	86.2	46.2	70.9	81.9	96.0
7/2/2016	54.8	83.3	50.8	68.8	77.7	94.8
7/6/2016	46.0	84.5	41.7	64.5	68.5	94.5
7/9/2016	54.8	87.0	36.5	56.7	71.3	94.3
Average	70.4	88.8	53.1	62.9	85.0	96.0
Stdev	14.4	3.7	10.2	9.2	9.8	1.2
(b)	**TN Removal (%) – Phase II**					
	CBR	**CBR+M**	**PMBR1**	**PMBR2**	**CBR+PMBR1**	**CBR+M+PMBR2**
7/27/2016	28.6	57.1	4.0	40.0	31.4	74.3
7/30/2016	10.7	35.7	20.0	55.6	28.6	71.4
8/3/2016	29.0	38.7	13.6	63.2	38.7	77.4
8/6/2016	20.8	41.7	5.3	57.1	25.0	75.0
8/10/2016	38.9	63.9	13.6	46.2	47.2	80.6
8/13/2016	24.0	56.0	15.8	45.5	36.0	76.0
8/17/2016	44.1	55.9	36.8	66.7	64.7	85.3
8/20/2016	15.2	51.5	14.3	75.0	27.3	87.9
8/24/2016	11.5	38.5	26.1	75.0	34.6	84.6
8/27/2016	33.3	56.7	20.0	61.5	46.7	83.3
Average	25.6	49.6	17.0	58.6	38.0	79.6
Stdev	11.3	10.0	9.6	12.1	12.0	5.5

CBR TP removal profiles followed a similar pattern to TN, with 67.0±13.2% removal for the first phase and 26.1±10.1% for the second phase, pre-filtration. Post-filtration (i.e. CBR+M), the removal efficiencies rose to 91.9±3.5% and 50.6±6.6%, respectively. CBR TP profiles are shown in Figure 6.5.

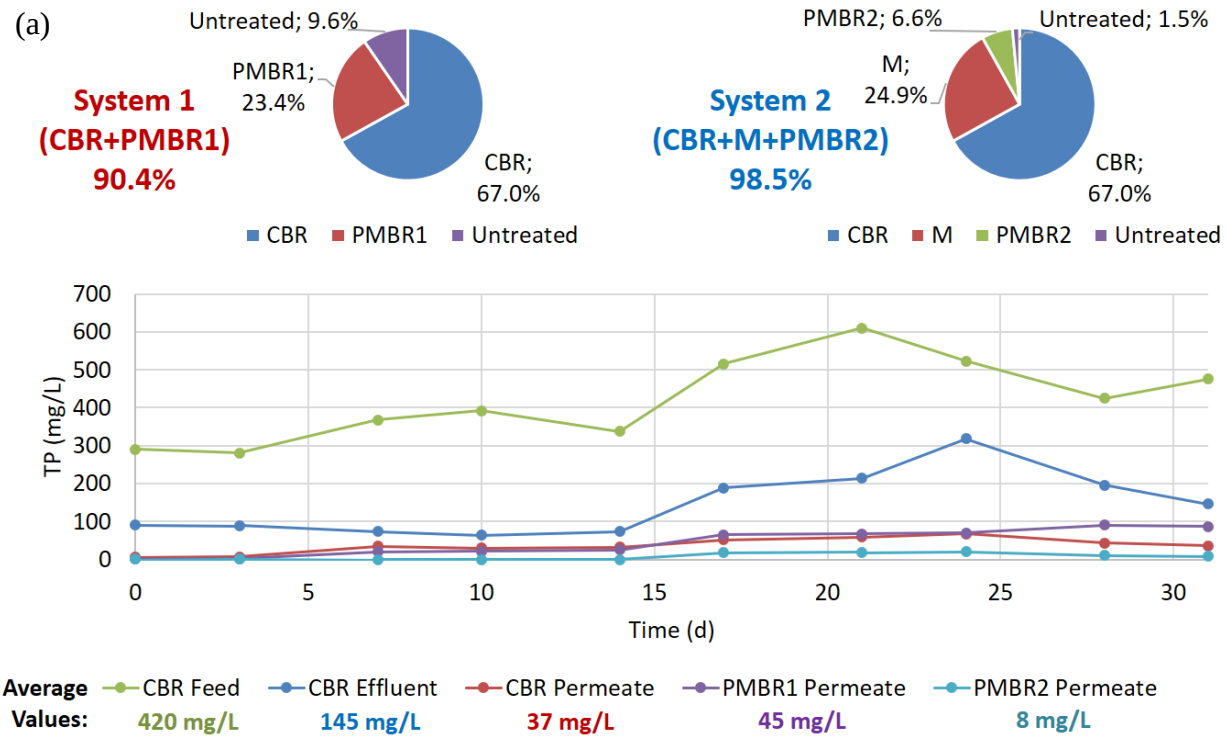

Figure 6.5. TP profiles of the CBR influent, CBR effluent, CBR permeate, PMBR1 permeate, and PMBR2 permeate throughout (a) Phase I (high HRT), and (b) Phase II (low HRT)

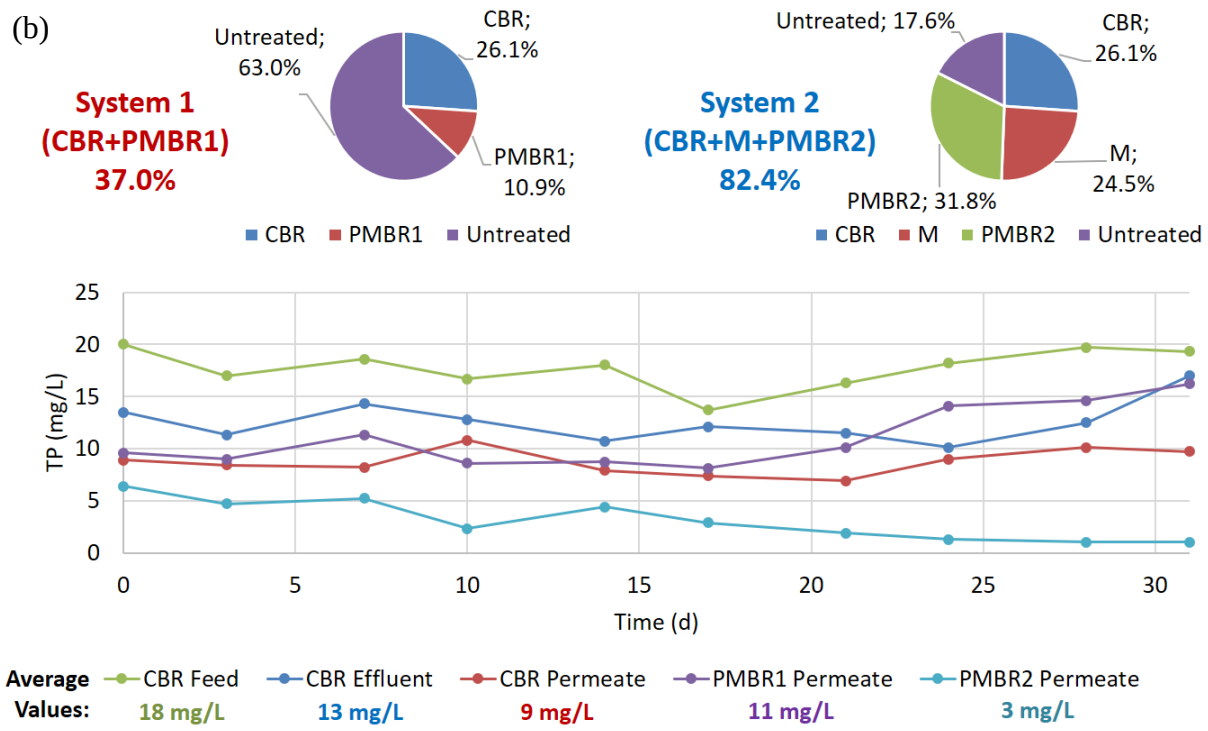

Figure 6.5. (Continued)

TP removal profiles for the PMBRs also followed a similar pattern to TN, where removal rates for PMBR1 were lower than PMBR2 throughout the experiment. TP removal efficiencies for the combined CBR+PMBR1 and CBR+M+PMBR2 systems were 90.4±7.0% and 98.5±1.6% respectively for the first phase, and 37.0±13.4% and 82.4±10.2% for the second phase. TP removal efficiency profiles of all systems are given in Table 6.5.

Table 6.5. TP Removal efficiencies of the systems and their combinations throughout (a) Phase I (high HRT), and (b) Phase II (low HRT)

(a)	TP Removal (%) – Phase I					
	CBR	**CBR+M**	**PMBR1**	**PMBR2**	**CBR+PMBR1**	**CBR+M+PMBR2**
6/8/2016	69.0	98.0	97.6	82.5	99.3	99.7
6/11/2016	68.0	97.8	97.5	82.4	99.2	99.6
6/15/2016	80.0	90.5	73.5	100.0	94.7	100.0
6/18/2016	83.8	92.4	67.1	100.0	94.7	100.0
6/22/2016	78.4	90.4	65.8	100.0	92.6	100.0
6/25/2016	63.5	90.0	65.5	65.6	87.4	96.6
6/29/2016	64.9	90.4	68.5	68.2	88.9	97.0
7/2/2016	39.0	87.1	77.9	70.0	86.5	96.1
7/6/2016	53.9	89.8	53.7	75.3	78.6	97.5
7/9/2016	69.3	92.4	40.2	77.2	81.6	98.3
Average	67.0	91.9	70.7	82.1	90.4	98.5
Stdev	13.2	3.5	17.6	13.5	7.0	1.6
(b)	**TP Removal (%) – Phase II**					
	CBR	**CBR+M**	**PMBR1**	**PMBR2**	**CBR+PMBR1**	**CBR+M+PMBR2**
7/27/2016	32.5	55.5	28.9	28.1	52.0	68.0
7/30/2016	33.5	50.6	20.4	44.0	47.1	72.4
8/3/2016	23.1	55.9	21.0	36.6	39.2	72.0
8/6/2016	23.4	35.3	19.5	78.7	38.3	86.2
8/10/2016	40.6	56.1	18.7	44.3	51.7	75.6
8/13/2016	11.7	46.0	8.3	60.8	19.0	78.8
8/17/2016	29.4	57.7	12.2	72.5	38.0	88.3
8/20/2016	18.1	50.5	5.4	85.6	22.5	92.9
8/24/2016	36.5	48.7	15.2	90.1	46.2	94.9
8/27/2016	11.9	49.7	4.7	89.7	16.1	94.8
Average	26.1	50.6	15.4	63.0	37.0	82.4
Stdev	10.1	6.6	7.8	23.4	13.4	10.2

The performance of the systems tested would need to be evaluated based on the effluent water qualities. To this end, refence COD, TN, and TP discharge limits of 125 mg COD/L (75%

min. removal), 10-15 mg TN/L (70%-80% min. removal), and 1-2 mg TP/L (80% min. removal) as required by Directive 91/271/EEC on Urban Waste Water Treatment, and Directive 98/15/EEC amending Directive 91/271/EEC of the European Commission should be kept in mind. Additionally, ISO standards are currently in development for non-sewered sanitation systems (IWA 24:2016), which require effluent limits of 150 mg COD/L, 15 mg TN/L, and 2 mg TP/L for Class 3 backend systems.

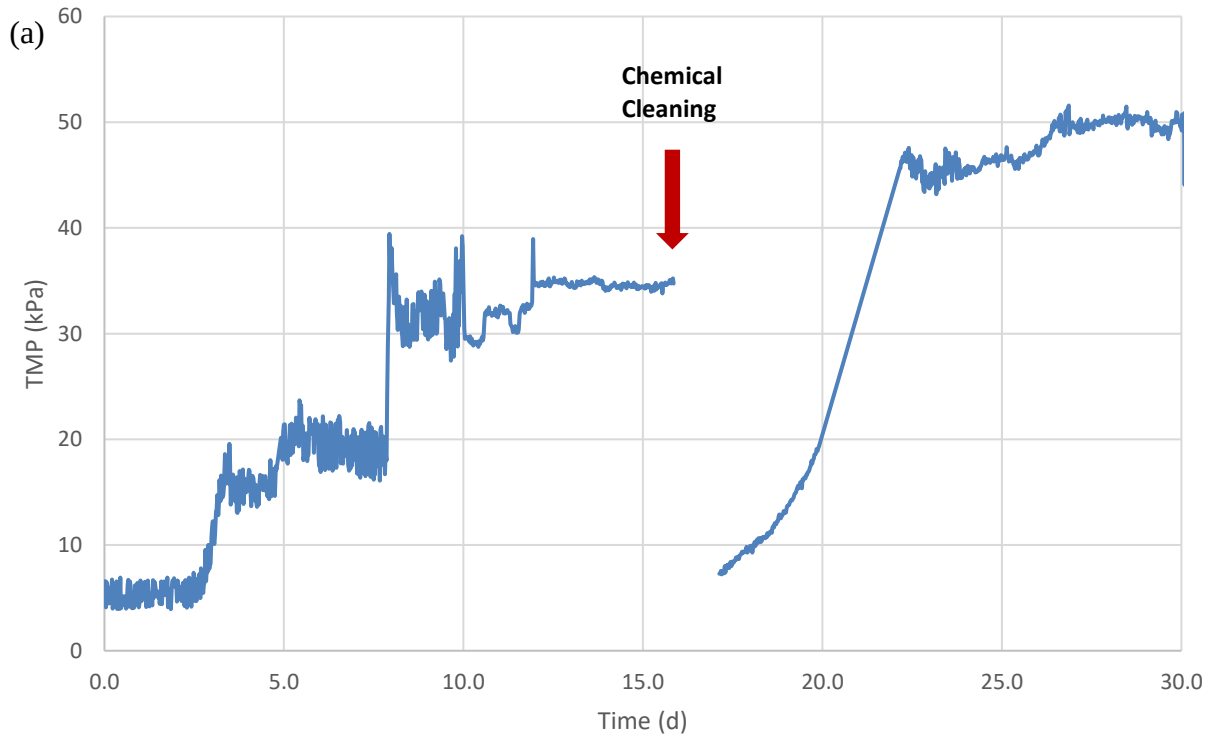

Figure 6.6. TMP profiles of the CBR throughout (a) Phase I (high HRT), and (b) Phase II (low HRT)

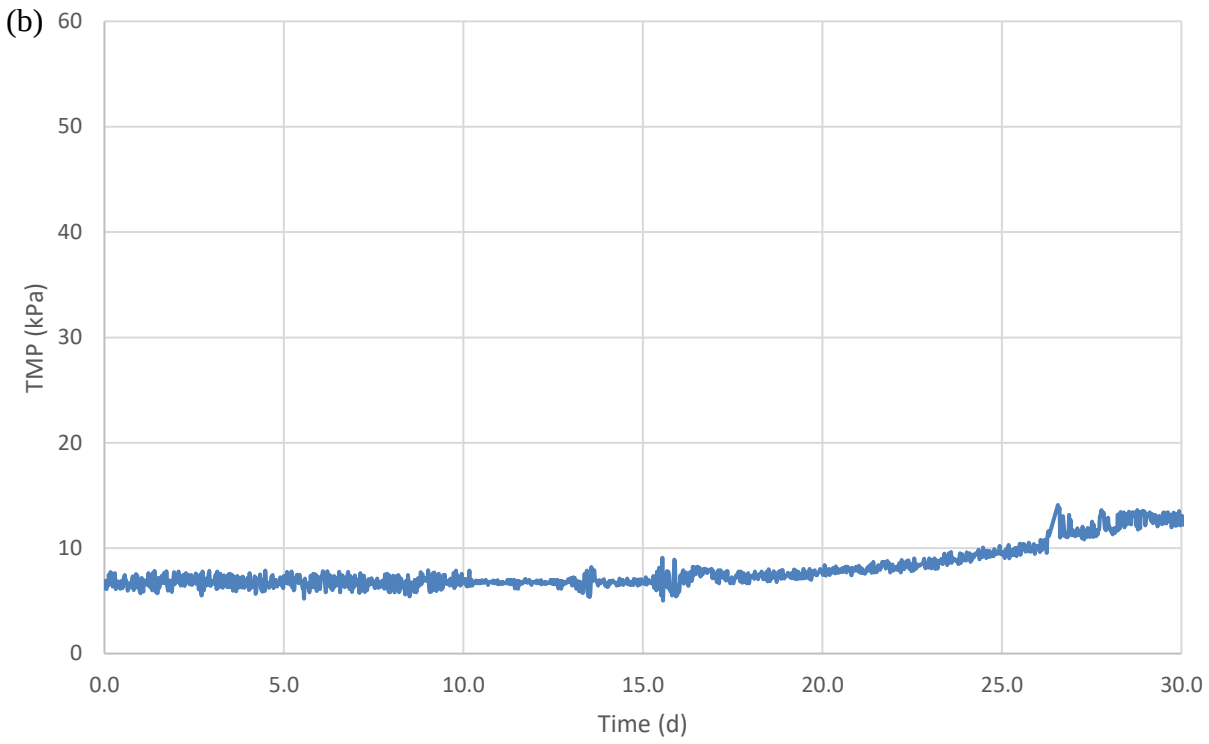

*Note that a new membrane module with larger filtration area was manufactured for Phase II

Figure 6.6. (Continued)

The average transmembrane pressure (TMP) for the first phase of the experiment was 29.6±15.2 kPa, with the high standard deviation caused by an increase in TMP, followed by chemical cleaning mid-phase, and a subsequent decrease and re-increase. The membrane module for the first experimental phase showed a high rate of fouling with the operational conditions imposed. The forward flux for this phase was 7.0 LMH, and backwash flux was measured at 148.1 LMH, with a backwash duration of 20 s every 30 min. For the second phase, a new membrane module was built with a higher filtration area to accommodate the decrease in HRT for this phase. The average TMP for the second phase was much lower at 8.3±2.2 kPa with an average flux of 8.5 LMH and backwash flux of 28.6 LMH. Backwash duration was 10 s every 5 min. TMP profiles for both phases are given in Figure 6.6.

6.4. Conclusions

The CBR can considerably reduce COD, TN, and TP loading for high strength feed streams on its own. Coupling the system with a membrane filter further increases the reduction, especially when dealing with low strength feed. However, the system needs to be further optimized for increased organic matter destruction, rather than just removal. PMBRs can further enhance the COD and nutrient removal in a combined CBR+PMBR system. Having a membrane between the CBR and the PMBR seems to stabilize the phototrophic process and result in higher nutrient removal efficiencies. For the combined system with post-CBR membrane filtration, the final COD and TN values for the low strength wastewater scenario were within the range of both European Commission and ISO discharge limits. For the high-strength scenario, only the COD limit was achieved.

Chapter 7: Conclusions and Future Work

It was the author's aim throughout this work to develop and test alternative ways of treating wastewaters using novel anaerobic-phototrophic biological systems. In the end, a way of raising pH of waste streams using phototrophic cultures was demonstrated, and a new type of baffled reactor was modeled, designed, and tested with synthetic feed, in an integrated anaerobic-phototrophic system. The results seem to be largely satisfactory within the conditions tested, however more optimization work is required especially in terms of ensuring organic matter destruction within the CBR, and increasing the nutrient removal rates of PMBRs for achieving acceptable final effluent TN and TP values. The combined CBR-PMBR system with post-CBR membrane filtration seems very close to achieving European Commission and ISO discharge limits. The phototrophic pH increase process could potentially be utilized to this end, combined with a nutrient recovery process that increases in efficiency with increasing pH, such as the struvite process. This is important in terms of the broader impacts of the technology, if it can be further optimized to achieve international discharge limits. The combined CBR-PMBR systems would then have the potential to be used for sidestream and non-sewered sanitation applications worldwide.

To summarize, the work conducted for the completion of this dissertation resulted in the below findings:

- While it was possible to reduce the energy demand of PMBRs by lowering aeration rates, the reduced aeration resulted in primarily nitrification dominated systems, where most of

the influent organic nitrogen was converted to nitrate, and little TN removal was observed.

- It is possible to raise the pH of diluted urine from 6.42±0.13 to 8.87±0.06 using batch phototrophic processes. When the dilution was at 1:100, the batch process showed sensitivity of pH levels to dark/light cycles and a final pH level of 9.23 was achieved. Using a continuously-fed reactor, where fertilizer solution was used as feed, the permeate pH value of 6.73 increased to a value of 8.61 during the experimental run. No light/dark-sensitive pH changes were observed.
- Distinct temperature profiles from mesophilic to psychrophilic temperature ranges were recorded for the CBR during abiotic experimentation, with temperature profiles changing with HRT. Same was true for suspended solids, which resulted in over 90% removal rates for all HRTs tested.
- Using the CBR alone, it was possible to achieve over 90% COD removal at 10 d HRT using high strength feed. At 2 d HRT with low strength feed, it was possible to achieve over 90% removal using post-CBR membrane filtration.
- Using the CBR alone, over 95% COD removal was only possible at 10 d HRT using high strength feed and post-CBR membrane filtration.
- Using the combined CBR-PMBR system, over 90% TN and TP removal were only possible for 10 d HRT operation at high strength feed conditions, with post-CBR membrane filtration.

Future work should focus on increasing organics destruction within the CBR by adding a mixing mechanism or effluent recycle/internal recirculation from the last zone to the central zone, or adding feed pretreatment. Different operational conditions for the PMBRs can be

explored, such as higher light intensities, lower shear within the reactors, better mixing, different SRTs, *etc*. The CBR and phototrophic pH increase process should be demonstrated using real wastewater as feed, preferably using a pilot scale reactor in order to account for the increased logistical demand associated with feed procurement. A stacked CBR configuration can be evaluated where the top CBR would have a much lower HRT and be used to quickly treat main stream wastewater, whereas the bottom CBR would receive the settled solids from the top CBR and treat these solids under a higher HRT to allow for solids destruction. The CBR model can further be expanded to describe biological processes and made dynamic. The new model can then be calibrated and validated using the experimental prototypes. Furthermore, the hydro- and thermo-dynamic behavior of the system can be evaluated using a multiphase computational fluid dynamics (CFD) model for the ability to design more optimized CBRs in the future. The outermost zone of the CBR could be turned into a photobioreactor, which could potentially lead to passive integration of the CBR and PMBR processes. Additional attached-growth carrier materials wither higher surface areas could be evaluated for their performance. Finally, thermophilic TPAD and pathogen destruction within the CBR can be evaluated, which would be especially valuable for high-temperature wastewater streams and developing world applications of the technology.

References

Abbona, F., Madsen, H. L., & Boistelle, R. (1982). Crystallization of two magnesium phosphates, struvite and newberyite: effect of pH and concentration. *Journal of Crystal Growth*, *57*(1), 6-14.

Adarme-Vega, T. C., Lim, D. K., Timmins, M., Vernen, F., Li, Y., & Schenk, P. M. (2012). Microalgal biofactories: a promising approach towards sustainable omega-3 fatty acid production. *Microbial Cell Factories*, *11*(1), 96.

American Public Health Association, American Water Works Association, & Water Environment Federation. (2005). *Standard methods for the examination of water & wastewater*. Washington, D.C.: American Public Health Association.

Bachmann, A., Beard, V. L., McCarty, P. L. (1985). Performance characteristics of the anaerobic baffled reactor. *Water Research*, *19*(1), 99–106. doi:10.1016/0043-1354(85)90330-6

Barber, W. P., & Stuckey, D. C. (1999). The use of the anaerobic baffled reactor (ABR) for wastewater treatment: a review. *Water Research*, *33*(7), 1559–1578. doi:10.1016/S0043-1354(98)00371-6

Butler, D., Friedler, E., & Gatt, K. (1995). Characterising the quantity and quality of domestic wastewater inflows. *Water Science and Technology*, *31*(7), 13–24. doi:10.1016/0273-1223(95)00318-H

Butler, R., & MacCormick, T. (1996). Opportunities for decentralized treatment, sewer mining and effluent re-use. *Desalination*, *106*(1-3), 273–283. doi:10.1016/S0011-9164(96)00119-1

Carvalho, A. P., Meireles, L. A., & Malcata, F. X. (2006). Microalgal reactors: a review of enclosed system designs and performances. *Biotechnology Progress*, *22*(6), 1490-1506.

Chen, C. Y., Yeh, K. L., Aisyah, R., Lee, D. J., & Chang, J. S. (2011). Cultivation, photobioreactor design and harvesting of microalgae for biodiesel production: a critical review. *Bioresource Technology*, *102*(1), 71-81.

Cheryan, M., & Rajagopalan, N. (1998). Membrane processing of oily streams. Wastewater treatment and waste reduction. *Journal of Membrane Science*, *151*(1), 13-28.

Christenson, L. B., & Sims, R. C. (2012). Rotating algal biofilm reactor and spool harvester for wastewater treatment with biofuels by-products. *Biotechnology and Bioengineering*, *109*(7), 1674-1684.

Comeau, Y., Hall, K. J., Hancock, R. E. W., & Oldham, W. K. (1986). Biochemical model for enhanced biological phosphorus removal. *Water Research*, *20*(12), 1511-1521.

Doughty, M. R., & Hammond, G. P. (2004). Sustainability and the built environment at and beyond the city scale. *Building and Environment*, *39*(10), 1223–1233. doi:10.1016/j.buildenv.2004.03.008

Galbraith, H., & Miller, T. B. (1973). Physicochemical Effects of Long Chain Fatty Acids on Bacterial Cells and their Protoplasts. *Journal of Applied Bacteriology*, *36*(4), 647–658. doi:10.1111/j.1365-2672.1973.tb04150.x

Gao, W. J., Leung, K. T., Qin, W. S., & Liao, B. Q. (2011). Effects of temperature and temperature shock on the performance and microbial community structure of a submerged anaerobic membrane bioreactor. *Bioresource Technology*, *102*(19), 8733–8740. doi:10.1016/j.biortech.2011.07.095

Garcia Alba, L., Torri, C., Samorì, C., van der Spek, J., Fabbri, D., Kersten, S. R., & Brilman, D. W. (2011). Hydrothermal treatment (HTT) of microalgae: evaluation of the process as conversion method in an algae biorefinery concept. *Energy & Fuels*, *26*(1), 642-657.

Ge, H., Jensen, P. D., & Batstone, D. J. (2011). Temperature phased anaerobic digestion increases apparent hydrolysis rate for waste activated sludge. *Water Research*, *45*(4), 1597–1606. doi:10.1016/j.watres.2010.11.042

Gikas, P., & Tchobanoglous, G. (2009). The role of satellite and decentralized strategies in water resources management. *Journal of Environmental Management*, *90*(1), 144–152. doi:10.1016/j.jenvman.2007.08.016

Girardet, H. (1996). *The Gaia Atlas of Cities: new directions for sustainable urban living*. UN-HABITAT.

Gupta, B. B., Howell, J. A., Wu, D., & Field, R. W. (1995). A helical baffle for cross-flow microfiltration. *Journal of Membrane Science*, *102*, 31-42.

Hagin, J., & Lowengart, A. (1995). Fertigation for minimizing environmental pollution by fertilizers. *Fertilizer research*, *43*(1-3), 5-7.

Han, Y., & Dague, R. R. (1997). Laboratory studies on the temperature-phased anaerobic digestion of domestic primary sludge. *Water Environment Research*, 1139-1143.

Hu, A. Y., & Stuckey, D. C. (2006). Treatment of Dilute Wastewaters Using a Novel Submerged Anaerobic Membrane Bioreactor. *Journal of Environmental Engineering*, *132*(2), 190–198. doi:10.1061/(ASCE)0733-9372(2006)132:2(190)

Hu, A. Y., & Stuckey, D. C. (2007). Activated Carbon Addition to a Submerged Anaerobic Membrane Bioreactor: Effect on Performance, Transmembrane Pressure, and Flux. *Journal of Environmental Engineering*, *133*(1), 73–80. doi:10.1061/(ASCE)0733-9372(2007)133:1(73)

International Association on Water Pollution Research and Control. (1998). *Activated sludge process design and control: theory and practice* (2nd ed.). Lancaster, Pa: Technomic Pub.

Jeganathan, J., Nakhla, G., & Bassi, A. (2006). Long-term performance of high-rate anaerobic reactors for the treatment of oily wastewater. *Environmental science & technology*, *40*(20), 6466-6472.

Judd, S. (2008). The status of membrane bioreactor technology. *Trends in Biotechnology*, *26*(2), 109–116. doi:10.1016/j.tibtech.2007.11.005

Kaplan, A., & Reinhold, L. (1999). CO_2 concentrating mechanisms in photosynthetic microorganisms. *Annual Review of Plant Biology*, *50*(1), 539-570.

Kim, J., Kim, K., Ye, H., Lee, E., Shin, C., McCarty, P. L., & Bae, J. (2011). Anaerobic Fluidized Bed Membrane Bioreactor for Wastewater Treatment. *Environmental Science & Technology*, *45*(2), 576–581. doi:10.1021/es1027103

Kumar, A., Yuan, X., Sahu, A. K., Dewulf, J., Ergas, S. J., & Van Langenhove, H. (2010). A hollow fiber membrane photo-bioreactor for CO2 sequestration from combustion gas coupled with wastewater treatment: a process engineering approach. *Journal of Chemical Technology and Biotechnology*, *85*(3), 387-394.

Le-Clech, P. (2010). Membrane bioreactors and their uses in wastewater treatments. *Applied Microbiology and Biotechnology*, *88*(6), 1253–1260. doi:10.1007/s00253-010-2885-8

Lettinga, G. (2001). Challenge of psychrophilic anaerobic wastewater treatment. *Trends in Biotechnology*, *19*(9), 363–370. doi:10.1016/S0167-7799(01)01701-2

Levenspiel, O. (1999). Chemical reaction engineering. *Industrial & Engineering Chemistry Research*, *38*(11), 4140-4143.

Levine, A. D., Tchobanoglous, G., & Asano, T. (1991). Size distributions of particulate contaminants in wastewater and their impact on treatability. *Water Research, 25*(8), 911-922.

Lopez-Archilla, A. I., Moreira, D., López-García, P., & Guerrero, C. (2004). Phytoplankton diversity and cyanobacterial dominance in a hypereutrophic shallow lake with biologically produced alkaline pH. *Extremophiles, 8*(2), 109-115.

Mallick, N. (2002). Biotechnological potential of immobilized algae for wastewater N, P and metal removal: a review. *Biometals*, *15*(4), 377-390.

McCarty, P. L., Bae, J., & Kim, J. (2011). Domestic Wastewater Treatment as a Net Energy Producer–Can This be Achieved? *Environmental Science & Technology*, *45*(17), 7100–7106. doi:10.1021/es2014264

Melin, T., Jefferson, B., Bixio, D., Thoeye, C., De Wilde, W., De Koning, J., … Wintgens, T. (2006). Membrane bioreactor technology for wastewater treatment and reuse. *Desalination, 187*(1-3), 271–282. doi:10.1016/j.desal.2005.04.086

Middelboe, A. L., & Hansen, P. J. (2007). High pH in shallow-water macroalgal habitats. *Marine Ecology Progress Series*, *338*, 107.

Moss, B. (1973). The influence of environmental factors on the distribution of freshwater algae: an experimental study: II. The role of pH and the carbon dioxide-bicarbonate system. *The Journal of Ecology*, 157-177.

Nachaiyasit, S., & Stuckey, D. C. (1997). Effect of low temperatures on the performance of an anaerobic baffled reactor (ABR). *Journal of Chemical Technology & Biotechnology*, *69*(2), 276–284. doi:10.1002/(SICI)1097-4660(199706)69:2<276::AID-JCTB711>3.0.CO;2-T

Ni, X., Mackley, M. R., Harvey, A. P., Stonestreet, P., Baird, M. H. I., & Rao, N. R. (2003). Mixing through oscillations and pulsations—a guide to achieving process enhancements in the chemical and process industries. *Chemical Engineering Research and Design*, *81*(3), 373-383.

O'Brien, W. J., & DeNoyelles, F. (1972). Photosynthetically elevated pH as a factor in zooplankton mortality in nutrient enriched ponds. *Ecology*, 605-614.

Olguín, E. J. (2012). Dual purpose microalgae–bacteria-based systems that treat wastewater and produce biodiesel and chemical products within a biorefinery. *Biotechnology Advances*, *30*(5), 1031–1046. doi:10.1016/j.biotechadv.2012.05.001

Orhon, D., Ateş, E., Sözen, S., & Çokgör, E. U. (1997). Characterization and COD fractionation of domestic wastewaters. *Environmental Pollution*, *95*(2), 191-204.

Ozgun, H., Dereli, R. K., Ersahin, M. E., Kinaci, C., Spanjers, H., & van Lier, J. B. (2013). A review of anaerobic membrane bioreactors for municipal wastewater treatment: integration options, limitations and expectations. *Separation and Purification Technology*, *118*, 89-104.

Park, J. B. K., Craggs, R. J., & Shilton, A. N. (2011). Wastewater treatment high rate algal ponds for biofuel production. *Bioresource Technology*, *102*(1), 35-42.

Park, J., Jin, H.-F., Lim, B.-R., Park, K.-Y., & Lee, K. (2010). Ammonia removal from anaerobic digestion effluent of livestock waste using green alga Scenedesmus sp. *Bioresource Technology*, *101*(22), 8649–8657. doi:10.1016/j.biortech.2010.06.142

Pereira, M. A., Pires, O. C., Mota, M., & Alves, M. M. (2005). Anaerobic biodegradation of oleic and palmitic acids: Evidence of mass transfer limitations caused by long chain fatty acid accumulation onto the anaerobic sludge. *Biotechnology and Bioengineering*, *92*(1), 15–23. doi:10.1002/bit.20548

Pillay, S., Foxon, K. M., & Buckley, C. A. (2008). An anaerobic baffled reactor/membrane bioreactor (ABR/MBR) for on-site sanitation in low income areas. *Desalination*, *231*(1-3), 91–98. doi:10.1016/j.desal.2007.10.023

Pittman, J. K., Dean, A. P., & Osundeko, O. (2011). The potential of sustainable algal biofuel production using wastewater resources. *Bioresource technology*, *102*(1), 17-25.

Porwal, S., Kumar, T., Lal, S., Rani, A., Kumar, S., Cheema, S., … Kalia, V. C. (2008). Hydrogen and polyhydroxybutyrate producing abilities of microbes from diverse habitats by dark fermentative process. *Bioresource Technology*, *99*(13), 5444–5451. doi:10.1016/j.biortech.2007.11.011

Prieto, A. L. (2011). *Sequential Anaerobic and Algal Membrane Bioreactor (A2MBR) System for Sustainable Sanitation and Resource Recovery from Domestic Wastewater* (Doctoral dissertation, University of South Florida).

Prieto, A. L., Futselaar, H., Lens, P. N., Bair, R., & Yeh, D. H. (2013). Development and start up of a gas-lift anaerobic membrane bioreactor (Gl-AnMBR) for conversion of sewage to energy, water and nutrients. *Journal of Membrane Science*, *441*, 158-167.

Redclift, M. (2005). Sustainable development (1987–2005): an oxymoron comes of age. *Sustainable development*, *13*(4), 212-227.

Rees, W. E. (1992). Ecological footprints and appropriated carrying capacity: what urban economics leaves out. *Environment and urbanization*, *4*(2), 121-130.

Rittmann, B. E., & McCarty, P. L. (2001). *Environmental biotechnology: principles and applications*. Boston: McGraw-Hill.

Russell, N. J. (2000). Toward a molecular understanding of cold activity of enzymes from psychrophiles. *Extremophiles*, *4*(2), 83–90. doi:10.1007/s007920050141

Seghezzo, L., Zeeman, G., van Lier, J. B., Hamelers, H. V. M., & Lettinga, G. (1998). A review: The anaerobic treatment of sewage in UASB and EGSB reactors. *Bioresource Technology*, *65*(3), 175–190. doi:10.1016/S0960-8524(98)00046-7

Sigma-Aldrich. (1998). *Bulletin 855B: Analyzing fatty acids by capillary gas chromatography*. Retrieved, January 7, 2014, from http://www.sigmaaldrich.com/content/dam/sigma-aldrich/docs/Supelco/Application_Notes/4509.pdf

Singh, J., & Gu, S. (2010). Commercialization potential of microalgae for biofuels production. *Renewable and Sustainable Energy Reviews*, *14*(9), 2596-2610.

Smith, A. L., Stadler, L. B., Love, N. G., Skerlos, S. J., & Raskin, L. (2012). Perspectives on anaerobic membrane bioreactor treatment of domestic wastewater: A critical review. *Bioresource Technology*, *122*, 149–159. doi:10.1016/j.biortech.2012.04.055

Strathmann, H. (2011). *Introduction to membrane science and technology*. Weinheim, Germany: Wiley-VCH Verlag & Co.

Subhadra, B. G. (2010). Sustainability of algal biofuel production using integrated renewable energy park (IREP) and algal biorefinery approach.*Energy Policy*, *38*(10), 5892-5901.

Subhadra, B., & Grinson-George. (2011). Algal biorefinery-based industry: An approach to address fuel and food insecurity for a carbon-smart world. *Journal of the Science of Food and Agriculture*, *91*(1), 2-13. doi:10.1002/jsfa.4207

Talling, J. F. (1976). The depletion of carbon dioxide from lake water by phytoplankton. *Journal of Ecology*, *64*(1), 79-121.

Tasnim, S. H., & Collins, M. R. (2004). Numerical analysis of heat transfer in a square cavity with a baffle on the hot wall. *International Communications in Heat and Mass Transfer*, *31*(5), 639-650.

Tyagi, V., & Lo, S.-L. (2011). Application of physico-chemical pretreatment methods to enhance the sludge disintegration and subsequent anaerobic digestion: an up to date review. *Reviews in Environmental Science and Bio/Technology*, *10*(3), 215–242. doi:10.1007/s11157-011-9244-9

U.S. Environmental Protection Agency. (2002). *Clean water and drinking water infrastructure gap analysis*. EPA-816-R-02-020

Van Lier, J. B., Tilche, A., Ahring, B. K., Macarie, H., Moletta, R., Dohanyos, M., Hulshoff Pol, L.W., Lens, P., & Verstraete W. Management Committee of the IWA Anaerobic Digestion Specialised Group. (2001). New perspectives in anaerobic digestion. *Water Science and Technology*, *43*(1), 1–18.

Vunjak-Novakovic, G., Kim, Y., Wu, X., Berzin, I., & Merchuk, J. C. (2005). Air-lift bioreactors for algal growth on flue gas: mathematical modeling and pilot-plant studies. *Industrial & Engineering Chemistry Research*, *44*(16), 6154-6163.

Wang, J., Burken, J. G., Zhang, X., & Surampalli, R. (2005). Engineered struvite precipitation: Impacts of component-ion molar ratios and pH. *Journal of Environmental Engineering*, *131*(10), 1433-1440.

Wijffels, R. H., Barbosa, M. J., & Eppink, M. H. M. (2010). Microalgae for the production of bulk chemicals and biofuels. *Biofuels, Bioproducts and Biorefining*, *4*(3), 287–295. doi:10.1002/bbb.215

Wilsenach, J. A., Schuurbiers, C. A. H., & Van Loosdrecht, M. C. M. (2007). Phosphate and potassium recovery from source separated urine through struvite precipitation. *Water Research*, *41*(2), 458-466.

Wisniewski, C. (2007). Membrane bioreactor for water reuse. *Desalination*, *203*(1-3), 15–19. doi:10.1016/j.desal.2006.05.002

Wu, B. (2010). CFD simulation of mixing in egg-shaped anaerobic digesters. *Water Research*, *44*(5), 1507-1519.

Yamamoto, K., Hiasa, M., Mahmood, T., & Matsuo, T. (1989). Direct solid-liquid separation using hollow fiber membrane in an activated sludge aeration tank. *Water Science & Technology*, *21*(4-5), 43-54.

Yoo, R., Kim, J., McCarty, P. L., & Bae, J. (2012). Anaerobic treatment of municipal wastewater with a staged anaerobic fluidized membrane bioreactor (SAF-MBR) system. *Bioresource Technology*, *120*, 133-139.

Yoo, R. H., Kim, J. H., McCarty, P. L., & Bae, J. H. (2013). Effect of temperature on the treatment of domestic wastewater with a staged anaerobic fluidized membrane bioreactor. *Water Science & Technology, 69*(6), 1145-1150. doi:10.2166/wst.2013.793

Zhou, S., McCorquodale, J. A., & Vitasovic, Z. (1992). Influences of density on circular clarifiers with baffles. *ASCE Journal of Environmental Engineering*, *118*(6), 829-847.

Appendix A: Python Code for the CBR Model

```
import sys
import functions
import csv
from collections import defaultdict
import os
import math
from math import exp as exp
from scipy.stats import norm as norm
root = os.path.dirname(os.path.realpath("__file__")) # fetch directory path for where this Python
script is located

# Baffle Spacing: Evenly Spaced
# Influent Flow Direction: Top Down
# Processes: Settling, Disintegration, Decay
# Flow Type: Plug Flow

# f: fraction, v: volume, t: time, T: temperature, n: number, d: distance (length), dn: density,
dv: dynamic viscosity
# g: acceleration, k: rate constant, q: flow rate, cd: downflow compartment, cu: upflow
compartment

# Reactor
v_reactor_volume = 10 #[m3] Reactor volume
f_reactor_height_diameter_ratio = 0.1 #[-] Reactor height/diameter ratio
t_hydraulic_retention_time = 10 #[d] Hydraulic Retention Time (HRT)
t_solids_retention_time = 20 #[d] Solids Retention Time (SRT)
n_number_of_zones = 5 #[-] Number of zones (1 zone = 2 compartments (downflow+upflow))
n_number_of_compartments = n_number_of_zones*2 #[-] Number of compartments including central zone
(C0)
f_central_compartment_diameter_fraction = 0.9 #[-] Central compartment diameter fraction with
respect to reactor diameter
f_downflow_compartment_baffle_spacing_fraction = 0.2 #[-] Downflow compartment baffle spacing
fraction with respect to spacing of one zone (example: if this is set to 0.5, downflow
compartments will have the same baffle spacing distance value as upflow compartments)
f_inlet_pipe_diameter_fraction = 0.05 #[-] Inlet pipe diameter fraction with respect to diameter
of central compartment
f_inlet_pipe_wall_thickness_fraction = 0.1 #[-] Inlet pipe wall thickness fraction with respect
to inlet pipe diameter
#f_baffle_thickness_fraction = 0.005 #[-]Baffle thickness fraction with respect to reactor
diameter
d_baffle_thickness = 0.02 #[m], Baffle thickness

# Influent
c_influent_solids_concentration = 1000 #[g/m3] Influent solids concentration
f_influent_settlable_inert_solids_fraction = 0.25 #[-] Influent settlable inert solids fraction
(w/w)
f_influent_settlable_reactive_solids_fraction = 0.25 #[-] Influent settlable reactive solids
fraction (w/w)
f_influent_dissolved_inert_solids_fraction = 0.25 #[-] Influent dissolved inert solids fraction
(w/w)
f_influent_dissolved_reactive_solids_fraction = 0.25 #[-] Influent dissolved reactive solids
fraction (w/w)
d_mean_particle_size_settlable_solids = 200 #[µm] Mean particle size for settlable solids
d_standard_deviation_sspsd_curve = 100 #[µm] Standard deviation for settlable solids particle
size distribution (SSPSD) curve
d_max_particle_size_settlable_solids = d_mean_particle_size_settlable_solids*2 #[µm] Max particle
size for settlable solids
T_influent_temperature = 20 #[°C] Influent temperature

# Settling
```

```
dn_median_density_of_settlable_solids = 1925 #[kg/m3] Median density of settlable solids
dn_density_of_water = 998.21 #[kg/m3] Density of water at 20°C
dv_dynamic_viscosity_of_water = 1.002*(10**(-3)) #[kg/m/s] Dynamic viscosity of water at 20°C
kv_kinematic_viscosity_of_water = 1.004*(10**(-6)) #[m2/s] Kinematic viscosity of water at 20°C
g_gravitational_acceleration = 9.80665 #[m/s2] Gravitational acceleration

# Disintegration and Decay
k_disintegration = 1 #[1/d] 1st order constant for disintegration of particulate (settlable)
solids into dissolved solids
k_decay = 10 #[1/d] 1st order constant for reactions involving the degradation (decay) of
dissolved solids

# Geometric Model
# Indices -> 0: C0, 1: C1, 2: C2, 3: C3, etc.
# Order of Compartments -> C0d > C0u > C1d > C1u > ... > Cnd > Cnu
d_reactor_diameter = (v_reactor_volume*4/f_reactor_height_diameter_ratio/math.pi)**(1/3.0) #[m],
Reactor diameter
d_reactor_liquid_height = f_reactor_height_diameter_ratio*d_reactor_diameter #[m], Reactor liquid
height
q_flow_rate = v_reactor_volume/t_hydraulic_retention_time #[m3/d], Influent flow rate
d_diameter_C0 = f_central_compartment_diameter_fraction*d_reactor_diameter #[m], Diameter of
central compartment (C0)
n_number_of_baffles = n_number_of_compartments-2 #[-], Number of baffles (excluding C0d and outer
wall of the reactor)
n_number_of_baffles_2D_cross_section = n_number_of_baffles*2 #[-], Number of baffles looking at a
2D cross section of the CBR from the side view (i.e. each baffle is counted twice - this is the
number relevant to the calculations)
n_number_of_zones_2D_cross_section = n_number_of_baffles_2D_cross_section/2 #[-], Number of zones
looking at a 2D cross section of the CBR from the side view
d_spacing_zone_total = d_reactor_diameter-d_diameter_C0-
n_number_of_baffles_2D_cross_section*d_baffle_thickness #[m], Total (U+D) baffle spacing of all
zones
d_spacing_zone = d_spacing_zone_total/n_number_of_zones_2D_cross_section #[m], Spacing for one
zone
d_spacing_Cd = d_spacing_zone*f_downflow_compartment_baffle_spacing_fraction #[m], Downflow
compartment baffle spacing
d_spacing_Cu = d_spacing_zone*(1-f_downflow_compartment_baffle_spacing_fraction) #[m], Upflow
compartment baffle spacing

# Central Compartment Definitions - Diameters
d_C0di = 0 #[m], C0 downflow compartment inner diameter - if this were a doughnut like the rest
of the compartments. It is not, so zero.
d_C0do =  d_diameter_C0*f_inlet_pipe_diameter_fraction #[m], Inlet pipe diameter
d_C0dw = d_C0do*(1+f_inlet_pipe_wall_thickness_fraction*2) #[m], Inlet pipe diameter with pipe
wall

# Central Compartment Definitions - Downflow
cd_ID = [d_C0di] #[m], C0d Downflow Compartment Inner Diameter
cd_OD = [d_C0do] #[m], C0d Downflow Compartment Outer Diameter
cd_ODb = [d_C0dw] #[m], C0d Downflow Compartment Outer Diameter with Inlet Pipe Wall
cd_CA = [math.pi/4*(cd_OD[0]**2-cd_ID[0]**2)] #[m2], C0d Downflow Compartment Crossectional Area
cd_V = [cd_CA[0]*d_reactor_liquid_height] #[m3], C0d Downflow Compartment Volume
cd_HRT = [cd_V[0]/q_flow_rate] #[d], C0d Downflow Compartment HRT
cd_u = [q_flow_rate/cd_CA[0]/24] #[m/h], C0d Downflow Compartment Fluid Velocity

# Central Compartment Definitions - Upflow
cu_ID = [cd_ODb[0]] #[m], C0u Upflow Compartment Inner Diameter
cu_OD = [d_diameter_C0] #[m], C0u Upflow Compartment Outer Diameter
cu_ODb = [cu_OD[0]+2*d_baffle_thickness] #[m], C0u Upflow Compartment Outer Diameter with Baffle
cu_CA = [math.pi/4*(cu_OD[0]**2-cu_ID[0]**2)] #[m2], C0u Upflow Compartment Crossectional Area
cu_V = [cu_CA[0]*d_reactor_liquid_height] #[m3], C0u Upflow Compartment Volume
cu_HRT = [cu_V[0]/q_flow_rate] #[d], C0u Upflow Compartment HRT
cu_u = [q_flow_rate/cu_CA[0]/24] #[m/h], C0u Upflow Compartment Fluid Velocity

for i in range(1,int(n_number_of_zones)): # Starts at 1 (not 0), because 0 is the central
compartment indice, and it has been defined separately above
    # Compartment Definitions - Downflow
    cd_ID.append(cu_ODb[i-1]) #[m], Downflow Compartment Inner Diameter
    cd_OD.append(cd_ID[i]+2*d_spacing_Cd) #[m], Downflow Compartment Outer Diameter
    cd_ODb.append(cd_OD[i]+2*d_baffle_thickness) #[m], C0d Downflow Compartment Outer Diameter
with Baffle
```

```
    cd_CA.append(math.pi/4*(cd_OD[i]**2-cd_ID[i]**2)) #[m2], Downflow Compartment Crossectional
Area
    cd_V.append(cd_CA[i]*d_reactor_liquid_height) #[m3], Downflow Compartment Volume
    cd_HRT.append(cd_V[i]/q_flow_rate) #[d], Downflow Compartment HRT
    cd_u.append(q_flow_rate/cd_CA[i]/24) #[m/h], Downflow Compartment Fluid Velocity
    # Compartment Definitions - Upflow
    cu_ID.append(cd_ODb[i]) #[m], Upflow Compartment Inner Diameter
    cu_OD.append(cu_ID[i]+2*d_spacing_Cu) #[m], Upflow Compartment Outer Diameter
    cu_ODb.append(cu_OD[i]+2*d_baffle_thickness) #[m], C0u Upflow Compartment Outer Diameter with
Baffle
    cu_CA.append(math.pi/4*(cu_OD[i]**2-cu_ID[i]**2)) #[m2], Upflow Compartment Crossectional
Area
    cu_V.append(cu_CA[i]*d_reactor_liquid_height) #[m3], Upflow Compartment Volume
    cu_HRT.append(cu_V[i]/q_flow_rate) #[d], Upflow Compartment HRT
    cu_u.append(q_flow_rate/cu_CA[i]/24) #[m/h], Upflow Compartment Fluid Velocity

# Error checking
for i in range(0,int(n_number_of_zones)):
    if (cu_u[i]<0):
        sys.exit('Error: Upflow velocity cannot be negative.')

# Settling, Disintegration, Decay
# Initialize variables and arrays
Xi_in = c_influent_solids_concentration*f_influent_settlable_inert_solids_fraction #[g/m3]
Influent settlable inert solids concentration
Xr_in = c_influent_solids_concentration*f_influent_settlable_reactive_solids_fraction #[g/m3]
Influent settlable reactive solids concentration
Si_in = c_influent_solids_concentration*f_influent_dissolved_inert_solids_fraction #[g/m3]
Influent dissolved inert solids concentration
Sr_in = c_influent_solids_concentration*f_influent_dissolved_reactive_solids_fraction #[g/m3]
Influent dissolved reactive solids concentration
dn_p = dn_median_density_of_settlable_solids #[kg/m3] Median density of settlable solids
dn_w = dn_density_of_water #[kg/m3] Density of water
dia = d_mean_particle_size_settlable_solids*(10**(-6)) #[m] Mean particle diameter
g = g_gravitational_acceleration #[m/s2] Gravitational acceleration
dv_w = dv_dynamic_viscosity_of_water #[kg/m/s] Dynamic viscosity of water at 20°C
kv_w = kv_kinematic_viscosity_of_water #[m2/s] Kinematic viscosity of water at 20°C
d_max = [d_max_particle_size_settlable_solids*(10**(-6))] # Array for storing max particle
diameter entering each upflow compartment
settling = 1 # Boolean variable to determine if settling is happening in current compartment or
not
upflow_velocity = [cu_u[0]] # Initialize array to store upflow velocities for each upflow
compartment
Xid_in = [Xi_in] # Initialize array to hold downflow compartment inputs for Xi
Xrd_in = [Xr_in] # Initialize array to hold downflow compartment inputs for Xr
Sid_in = [Si_in] # Initialize array to hold downflow compartment inputs for Si
Srd_in = [Sr_in] # Initialize array to hold downflow compartment inputs for Sr

# The big loop
for i in range(0,int(n_number_of_zones)):

    # Downflow compartment calculations
    # ---------------------------------
    print('Downflow Compartment: '+str(i))
    print('-----------------------------------')

    # Downflow compartment inputs
    if (i>0): # Outputs from previous upflow compartment are inputs for this downflow
compartment, except when i=0 - i.e. when this is the first downflow compartment
        Xid_in.append(Xiu_out[i-1])
        Xrd_in.append(Xru_out[i-1])
        Sid_in.append(Siu_out[i-1])
        Srd_in.append(Sru_out[i-1])

    # Downflow compartment state variables
    t_hrt = cd_HRT[i]
    Xid = Xid_in[i]
    Xrd = Xrd_in[i]
    Sid = Sid_in[i]
    Srd = Srd_in[i]
```

```
    # Downflow compartment disintegration based on HRT
    Xrd = Xrd*exp(-t_hrt*k_disintegration)
    delta_Sr = Xrd_in[i]-Xrd # Disintegration of Xr creates Sr
    Srd = Srd+delta_Sr

    # Downflow compartment decay based on HRT
    Srd = Srd*exp(-t_hrt*k_decay)

    # Downflow compartment outputs
    if (i==0):
        Xid_out = [Xid]
        Xrd_out = [Xrd]
        Sid_out = [Sid]
        Srd_out = [Srd]
    else:
        Xid_out.append(Xid)
        Xrd_out.append(Xrd)
        Sid_out.append(Sid)
        Srd_out.append(Srd)

    # Print results
    print('Xi_in: '+str(round(Xid_in[i],1))+' / Xi_out: '+str(round(Xid_out[i],1)))
    print('Xr_in: '+str(round(Xrd_in[i],1))+' / Xr_out: '+str(round(Xrd_out[i],1)))
    print('Si_in: '+str(round(Sid_in[i],1))+' / Si_out: '+str(round(Sid_out[i],1)))
    print('Sr_in: '+str(round(Srd_in[i],1))+' / Sr_out: '+str(round(Srd_out[i],1)))
    print()

    # Upflow compartment calculations
    # -------------------------------
    print('Upflow Compartment: '+str(i))
    print('-----------------------------------')
    #print('Upflow Velocity (m/h): '+str(round(cu_u[i],4)))

    # Upflow compartment inputs
    if (i==0): # If it is the first upflow compartment, initialize arrays
        Xiu_in = [Xid_out[i]]
        Xru_in = [Xrd_out[i]]
        Siu_in = [Sid_out[i]]
        Sru_in = [Srd_out[i]]
    else: # Otherwise append to previously initialized arrays
        Xiu_in.append(Xid_out[i])
        Xru_in.append(Xrd_out[i])
        Siu_in.append(Sid_out[i])
        Sru_in.append(Srd_out[i])

    # Upflow compartment state variables
    t_hrt = cu_HRT[i]
    t_srt = t_solids_retention_time
    Xiu = Xiu_in[i]
    Xru = Xru_in[i]
    Siu = Siu_in[i]
    Sru = Sru_in[i]

    # Upflow compartment settling
    # Check if settling can happen in current compartment based on upflow velocity
    if (i>0): # Settling can always happen in central compartment, so it is skipped
        upflow_velocity.append(cu_u[i]) # Store current upflow velocity in the upflow_velocity
array
        if (cu_u[i]>min(upflow_velocity)): # If current upflow velocity is higher than the
minimum upflow velocity observed in previous compartments, no settling will occur in this
compartment (since everything that could settle already did in earlier compartments)
            settling = 0
        else: # Otherwise settling will occur
            settling = 1
    print('Settling: '+str(settling))

    if (settling == 1):
        # Reynolds number checks
        # Calculate Reynolds number for pipe flow
        Q = q_flow_rate/86400 #[m3/s] Flow rate
        Dh = cu_OD[i]-cu_ID[i] #[m] Hydraulic diameter
```

```
        Ac = cu_CA[i] #[m2] Cross-sectional area
        vis = kv_kinematic_viscosity_of_water #[m2/s] Kinematic viscosity of water
        Re = Q*Dh/Ac/vis #Reynolds number for pipe flow (Re < 2000: Laminar pipe flow, Re > 4000:
Turbulent pipe flow, 2000 < Re < 4000: Transitional regime)
        #print('Fluid Reynolds Number: '+str(round(Re,1)))

        # Calculate particle Reynolds number for max. particle diameter in influent
        u = cu_u[i]/3600 #[m/s] Upflow velocity in upflow compartment i
        Re_p = d_max[i]*u/kv_w
        #print('Max. Particle Reynolds Number: '+str(round(Re_p,6)))

        # Calculate particle diameter cut-off from simple Stokes settling velocity for laminar
flow range
        dia = (18*u*dv_w/(dn_p-dn_w)/g)**(0.5)
        #print('Particle Diameter Settlability Cut-off: '+str(round(dia*(10**6),2))+' µm')

        # Estimate particle size cut-off (% of particles that will settle)
        x = dia*(10**6)
        d = d_mean_particle_size_settlable_solids
        sigma = d_standard_deviation_sspsd_curve
        probability = norm.cdf(x,d,sigma) # Particle size probability is determined using a
cumulative normal distribution function (scipy.stats.norm)

        # Store the probability in an array (it is 1-probability because probability itself
actually gives the probability of staying afloat)
        if (i==0): # If i==0, initialize
            p = [1-probability]
            dp = p[i]
        else: # Otherwise, append
            p.append(1-probability)
            dp = p[i]-p[i-1]

        #print('Percentage of Settled Solids: '+str(round(dp*100,2))+'%')

        # Assign new maximum particle size for the next upflow compartment Reynolds number check
(dia cut-off is the new max, because everything above this diameter settled in this compartment)
        d_max.append(dia)

        # Calculate settled (_s) particulate solids concentrations
        Xiu_s = Xiu*dp # Inert fraction
        Xru_s = Xru*dp # Reactive fraction
    else:
        # Assign new maximum particle size for the next upflow compartment Reynolds number check
(we just add the current diameter to the array to advance the array index)
        d_max.append(d_max[i])
        p.append(p[i-1])

        # Calculate settled (_s) particulate solids concentrations - this is the case for no
settling, so zero
        Xiu_s = 0 # Inert fraction
        Xru_s = 0 # Reactive fraction

    # Calculate the non-settled (_ns) particulate solids concentrations
    Xiu_ns = Xiu-Xiu_s
    Xru_ns = Xru-Xru_s

    # Upflow compartment disintegration based on HRT (acting on Xru_ns)
    Xru_ns_dis = Xru_ns*exp(-t_hrt*k_disintegration)
    delta_Sr = Xru_ns-Xru_ns_dis # Disintegration of Xr creates Sr
    Sru = Sru+delta_Sr

    # Upflow compartment disintegration based on SRT (acting on Xru_s)
    Xru_s_dis = Xru_s*exp(-t_srt*k_disintegration)
    delta_Sr = Xru_s-Xru_s_dis # Disintegration of Xr creates Sr
    Sru = Sru+delta_Sr

    # Upflow compartment decay based on HRT (acting on Sru)
    Sru = Sru*exp(-t_hrt*k_decay)

    # Convert state variables to output variables
```

```
    Xiu = Xiu_ns # This is the fraction of Xi that is remaining (i.e. not settled) and able to
travel to the next compartment
    Xru = Xru_ns_dis # This is the fraction of Xr that is remaining (i.e. not settled or
disintegrated) and able to travel to the next compartment

    # Upflow compartment outputs
    if (i==0):
        Xiu_out = [Xiu]
        Xru_out = [Xru]
        Siu_out = [Siu]
        Sru_out = [Sru]
    else:
        Xiu_out.append(Xiu)
        Xru_out.append(Xru)
        Siu_out.append(Siu)
        Sru_out.append(Sru)

    # Print results
    print('Xi_in: '+str(round(Xiu_in[i],1))+' / Xi_out: '+str(round(Xiu_out[i],1)))
    print('Xr_in: '+str(round(Xru_in[i],1))+' / Xr_out: '+str(round(Xru_out[i],1)))
    print('Si_in: '+str(round(Siu_in[i],1))+' / Si_out: '+str(round(Siu_out[i],1)))
    print('Sr_in: '+str(round(Sru_in[i],1))+' / Sr_out: '+str(round(Sru_out[i],1)))
    print()
```

Appendix B: Python Code for Geometric Analysis

```
import sys
import time
import functions
import csv
from collections import defaultdict
import os
import math
from math import exp as exp
from scipy.stats import norm as norm
root = os.path.dirname(os.path.realpath("__file__")) # fetch directory path for where this Python
script is located
clear = lambda: os.system('cls')

# Baffle Spacing: Evenly Spaced
# Influent Flow Direction: Top Down
# Processes: Settling, Disintegration, Decay
# Flow Type: Plug Flow

# f: fraction, v: volume, t: time, T: temperature, n: number, d: distance (length), dn: density,
dv: dynamic viscosity
# g: acceleration, k: rate constant, q: flow rate, cd: downflow compartment, cu: upflow
compartment

# Geometric Analysis Inputs
#-----------------------------------------------------------------------------------------------
----------#
#-----------------------------------------------------------------------------------------------
----------#

# Generate output file header
path_out = root+'\\outputs\\cbrout, '+time.strftime("%m-%d-%Y, %H%M%S")+'.csv'
f = open(path_out, "wt") # Write the column names
f.write('i_f_Xi'+','+
'i_f_Xr'+','+
'i_f_Si'+','+
'i_f_Sr'+','+
'i_V_r'+','+
'i_C_t'+','+
'i_HRT'+','+
'i_SRT'+','+
'i_k_dis'+','+
'i_k_dec'+','+
'i_f_dC0'+','+
'i_n_z'+','+
'i_HDR'+','+
'i_MPD'+','+
'i_f_std_PSD'+','+
'i_rho'+','+
'o_Xi'+','+
'o_Xr'+','+
'o_Si'+','+
'o_Sr'+','+
'o_rem_Xi'+','+
'o_rem_Xr'+','+
'o_rem_Si'+','+
'o_rem_Sr'+','+
'o_rem_X'+','+
'o_rem_S'+','+
'o_rem_i'+','+
'o_rem_r'+','+
```

```
'o_rem_tot'+'\n')
f.close()

# Input constants
i_f_Xi = 0.25 # [-] Influent fraction, particulate inert
i_f_Xr = 0.25 # [-] Influent fraction, particulate reactive
i_f_Si = 0.25 # [-] Influent fraction, soluble inert
i_f_Sr = 0.25 # [-] Influent fraction, soluble reactive
i_V_r = 1000 # [m3] Total reactor volume
i_C_t = 1000 # [g/m3] Influent solids concentration

# Input arrays
max_index = 2
a_HRT = [0.2,1] # [d] Hydraulic retention time (i_1)
a_SRT = [5,25] # [d] Solids retention time (i_2)
a_k_dis = [0.01,0.05] # [1/d] Disintegration rate constant for particulate solids (i_3)
a_k_dec = [0.2,1] # [1/d] Decay rate constant for soluble solids (i_4)
a_f_dC0 = [0.2,0.8] # [-] Fraction of central compartment diameter with respect to reactor
diameter (i_5)
a_n_z = [3,9] # [-] Number of zones (i_6)
a_HDR = [0.2,5] # [-] Reactor height:diameter ratio (i_7)
a_MPD = [50,200] # [µm] Mean particle diameter for particulate solids (i_8)
a_f_std_PSD = [0.2,0.8] # [-] Standard deviation fraction of the particle size distribution curve
(i_9)
a_rho = [1250,2500] # [kg/m3] Mean particle density of particulate solids (i_10)

'''max_index = 3
a_HRT = [0.2,1,5] # [d] Hydraulic retention time (i_1)
a_SRT = [5,20,50] # [d] Solids retention time (i_2)
a_k_dis = [0.01,0.05,0.2] # [1/d] Disintegration rate constant for particulate solids (i_3)
a_k_dec = [0.2,1,5] # [1/d] Decay rate constant for soluble solids (i_4)
a_f_dC0 = [0.2,0.5,0.8] # [-] Fraction of central compartment diameter with respect to reactor
diameter (i_5)
a_n_z = [3,6,9] # [-] Number of zones (i_6)
a_HDR = [0.2,1,5] # [-] Reactor height:diameter ratio (i_7)
a_MPD = [50,100,200] # [µm] Mean particle diameter for particulate solids (i_8)
a_f_std_PSD = [0.2,0.5,0.8] # [-] Standard deviation fraction of the particle size distribution
curve (i_9)
a_rho = [1250,1750,2500] # [kg/m3] Mean particle density of particulate solids (i_10)'''

# Loop to run through all parameter combinations
iteration_counter = 0
for i_1 in range (0,max_index):
    for i_2 in range (0,max_index):
        for i_3 in range (0,max_index):
            for i_4 in range (0,max_index):
                for i_5 in range (0,max_index):
                    for i_6 in range (0,max_index):
                        for i_7 in range (0,max_index):
                            for i_8 in range (0,max_index):
                                for i_9 in range (0,max_index):
                                    for i_10 in range (0,max_index):
                                        # Progressively assign values to variables
                                        i_HRT = a_HRT[i_1]
                                        i_SRT = a_SRT[i_2]
                                        i_k_dis = a_k_dis[i_3]
                                        i_k_dec = a_k_dec[i_4]
                                        i_f_dC0 = a_f_dC0[i_5]
                                        i_n_z = a_n_z[i_6]
                                        i_HDR = a_HDR[i_7]
                                        i_MPD = a_MPD[i_8]
                                        i_f_std_PSD = a_f_std_PSD[i_9]
                                        i_rho = a_rho[i_10]

                                        # Inputs for Current Run
                                        #-----------------------------------------------------------
-----------------------------------------------#
                                        #-----------------------------------------------------------
-----------------------------------------------#

                                        # Reactor
```

```
                                        v_reactor_volume = i_V_r #[m3] Reactor volume
                                        f_reactor_height_diameter_ratio = i_HDR #[-] Reactor
height/diameter ratio
                                        t_hydraulic_retention_time = i_HRT #[d] Hydraulic
Retention Time (HRT)
                                        t_solids_retention_time = i_SRT #[d] Solids Retention
Time (SRT)
                                        n_number_of_zones = i_n_z #[-] Number of zones (1 zone =
2 compartments (downflow+upflow))
                                        n_number_of_compartments = n_number_of_zones*2 #[-]
Number of compartments including central zone (C0)
                                        f_central_compartment_diameter_fraction = i_f_dC0 #[-]
Central compartment diameter fraction with respect to reactor diameter
                                        f_downflow_compartment_baffle_spacing_fraction = 0.2 #[-]
Downflow compartment baffle spacing fraction with respect to spacing of one zone (example: if
this is set to 0.5, downflow compartments will have the same baffle spacing distance value as
upflow compartments)
                                        f_inlet_pipe_diameter_fraction = 0.05 #[-] Inlet pipe
diameter fraction with respect to diameter of central compartment
                                        f_inlet_pipe_wall_thickness_fraction = 0.1 #[-] Inlet
pipe wall thickness fraction with respect to inlet pipe diameter
                                        #f_baffle_thickness_fraction = 0.005 #[-]Baffle thickness
fraction with respect to reactor diameter
                                        d_baffle_thickness = 0.01 #[m], Baffle thickness

                                        # Influent
                                        c_influent_solids_concentration = i_C_t #[g/m3] Influent
solids concentration
                                        f_influent_settlable_inert_solids_fraction = i_f_Xi #[-]
Influent settlable inert solids fraction (w/w)
                                        f_influent_settlable_reactive_solids_fraction = i_f_Xr
#[-] Influent settlable reactive solids fraction (w/w)
                                        f_influent_dissolved_inert_solids_fraction = i_f_Si #[-]
Influent dissolved inert solids fraction (w/w)
                                        f_influent_dissolved_reactive_solids_fraction = i_f_Sr
#[-] Influent dissolved reactive solids fraction (w/w)
                                        d_mean_particle_size_settlable_solids = i_MPD #[µm] Mean
particle size for settlable solids
                                        f_standard_deviation_sspsd_curve = i_f_std_PSD #[-] % of
stdev with respect to mean particle size
                                        d_standard_deviation_sspsd_curve =
d_mean_particle_size_settlable_solids*f_standard_deviation_sspsd_curve #[µm] Standard deviation
for settlable solids particle size distribution (SSPSD) curve
                                        d_max_particle_size_settlable_solids =
d_mean_particle_size_settlable_solids*2 #[µm] Max particle size for settlable solids
                                        T_influent_temperature = 20 #[°C] Influent temperature

                                        # Settling
                                        dn_median_density_of_settlable_solids = i_rho #[kg/m3]
Median density of settlable solids
                                        dn_density_of_water = 998.21 #[kg/m3] Density of water at
20°C
                                        dv_dynamic_viscosity_of_water = 1.002*(10**(-3))
#[kg/m/s] Dynamic viscosity of water at 20°C
                                        kv_kinematic_viscosity_of_water = 1.004*(10**(-6))
#[m2/s] Kinematic viscosity of water at 20°C
                                        g_gravitational_acceleration = 9.80665 #[m/s2]
Gravitational acceleration

                                        # Disintegration and Decay
                                        k_disintegration = i_k_dis #[1/d] 1st order constant for
disintegration of particulate (settlable) solids into dissolved solids
                                        k_decay = i_k_dec #[1/d] 1st order constant for reactions
involving the degradation (decay) of dissolved solids

                                        # Reactor Model
                                        #-------------------------------------------------------
-------------------------------------------------#
                                        #-------------------------------------------------------
-------------------------------------------------#
                                        # Indices -> 0: C0, 1: C1, 2: C2, 3: C3, etc.
```

```
                                        # Order of Compartments -> C0d > C0u > C1d > C1u > ... >
Cnd > Cnu
                                        d_reactor_diameter =
(v_reactor_volume*4/f_reactor_height_diameter_ratio/math.pi)**(1/3.0) #[m], Reactor diameter
                                        d_reactor_liquid_height =
f_reactor_height_diameter_ratio*d_reactor_diameter #[m], Reactor liquid height
                                        q_flow_rate = v_reactor_volume/t_hydraulic_retention_time
#[m3/d], Influent flow rate
                                        d_diameter_C0 =
f_central_compartment_diameter_fraction*d_reactor_diameter #[m], Diameter of central compartment
(C0)
                                        n_number_of_baffles = n_number_of_compartments-2 #[-],
Number of baffles (excluding C0d and outer wall of the reactor)
                                        n_number_of_baffles_2D_cross_section =
n_number_of_baffles*2 #[-], Number of baffles looking at a 2D cross section of the CBR from the
side view (i.e. each baffle is counted twice - this is the number relevant to the calculations)
                                        n_number_of_zones_2D_cross_section =
n_number_of_baffles_2D_cross_section/2 #[-], Number of zones looking at a 2D cross section of the
CBR from the side view
                                        d_spacing_zone_total = d_reactor_diameter-d_diameter_C0-
n_number_of_baffles_2D_cross_section*d_baffle_thickness #[m], Total (U+D) baffle spacing of all
zones
                                        d_spacing_zone =
d_spacing_zone_total/n_number_of_zones_2D_cross_section #[m], Spacing for one zone
                                        '''print(d_spacing_zone)'''
                                        d_spacing_Cd =
d_spacing_zone*f_downflow_compartment_baffle_spacing_fraction #[m], Downflow compartment baffle
spacing
                                        d_spacing_Cu = d_spacing_zone*(1-
f_downflow_compartment_baffle_spacing_fraction) #[m], Upflow compartment baffle spacing

                                        # Central Compartment Definitions - Diameters
                                        d_C0di = 0 #[m], C0 downflow compartment inner diameter -
if this were a doughnut like the rest of the compartments. It is not, so zero.
                                        d_C0do =  d_diameter_C0*f_inlet_pipe_diameter_fraction
#[m], Inlet pipe diameter
                                        d_C0dw =
d_C0do*(1+f_inlet_pipe_wall_thickness_fraction*2) #[m], Inlet pipe diameter with pipe wall

                                        # Central Compartment Definitions - Downflow
                                        cd_ID = [d_C0di] #[m], C0d Downflow Compartment Inner
Diameter
                                        cd_OD = [d_C0do] #[m], C0d Downflow Compartment Outer
Diameter
                                        cd_ODb = [d_C0dw] #[m], C0d Downflow Compartment Outer
Diameter with Inlet Pipe Wall
                                        cd_CA = [math.pi/4*(cd_OD[0]**2-cd_ID[0]**2)] #[m2], C0d
Downflow Compartment Crossectional Area
                                        cd_V = [cd_CA[0]*d_reactor_liquid_height] #[m3], C0d
Downflow Compartment Volume
                                        cd_HRT = [cd_V[0]/q_flow_rate] #[d], C0d Downflow
Compartment HRT
                                        cd_u = [q_flow_rate/cd_CA[0]/24] #[m/h], C0d Downflow
Compartment Fluid Velocity

                                        # Central Compartment Definitions - Upflow
                                        cu_ID = [cd_ODb[0]] #[m], C0u Upflow Compartment Inner
Diameter
                                        cu_OD = [d_diameter_C0] #[m], C0u Upflow Compartment
Outer Diameter
                                        cu_ODb = [cu_OD[0]+2*d_baffle_thickness] #[m], C0u Upflow
Compartment Outer Diameter with Baffle
                                        cu_CA = [math.pi/4*(cu_OD[0]**2-cu_ID[0]**2)] #[m2], C0u
Upflow Compartment Crossectional Area
                                        cu_V = [cu_CA[0]*d_reactor_liquid_height] #[m3], C0u
Upflow Compartment Volume
                                        cu_HRT = [cu_V[0]/q_flow_rate] #[d], C0u Upflow
Compartment HRT
                                        cu_u = [q_flow_rate/cu_CA[0]/24] #[m/h], C0u Upflow
Compartment Fluid Velocity
```

```
                                    for i in range(1,int(n_number_of_zones)): # Starts at 1
(not 0), because 0 is the central compartment indice, and it has been defined separately above
                                        # Compartment Definitions - Downflow
                                        cd_ID.append(cu_ODb[i-1]) #[m], Downflow Compartment
Inner Diameter
                                        cd_OD.append(cd_ID[i]+2*d_spacing_Cd) #[m], Downflow
Compartment Outer Diameter
                                        cd_ODb.append(cd_OD[i]+2*d_baffle_thickness) #[m],
C0d Downflow Compartment Outer Diameter with Baffle
                                        cd_CA.append(math.pi/4*(cd_OD[i]**2-cd_ID[i]**2))
#[m2], Downflow Compartment Crossectional Area
                                        cd_V.append(cd_CA[i]*d_reactor_liquid_height) #[m3],
Downflow Compartment Volume
                                        cd_HRT.append(cd_V[i]/q_flow_rate) #[d], Downflow
Compartment HRT
                                        cd_u.append(q_flow_rate/cd_CA[i]/24) #[m/h], Downflow
Compartment Fluid Velocity
                                        # Compartment Definitions - Upflow
                                        cu_ID.append(cd_ODb[i]) #[m], Upflow Compartment
Inner Diameter
                                        cu_OD.append(cu_ID[i]+2*d_spacing_Cu) #[m], Upflow
Compartment Outer Diameter
                                        cu_ODb.append(cu_OD[i]+2*d_baffle_thickness) #[m],
C0u Upflow Compartment Outer Diameter with Baffle
                                        cu_CA.append(math.pi/4*(cu_OD[i]**2-cu_ID[i]**2))
#[m2], Upflow Compartment Crossectional Area
                                        cu_V.append(cu_CA[i]*d_reactor_liquid_height) #[m3],
Upflow Compartment Volume
                                        cu_HRT.append(cu_V[i]/q_flow_rate) #[d], Upflow
Compartment HRT
                                        cu_u.append(q_flow_rate/cu_CA[i]/24) #[m/h], Upflow
Compartment Fluid Velocity

                                    # Error checking
                                    for i in range(0,int(n_number_of_zones)):
                                        if (cu_u[i]<0):
                                            sys.exit('Error: Upflow velocity cannot be
negative.')

                                    # Settling, Disintegration, Decay
                                    #-----------------------------------------------------------
-------------------------------------------------#
                                    #-----------------------------------------------------------
-------------------------------------------------#

                                    # Initialize variables and arrays
                                    Xi_in =
c_influent_solids_concentration*f_influent_settlable_inert_solids_fraction #[g/m3] Influent
settlable inert solids concentration
                                    Xr_in =
c_influent_solids_concentration*f_influent_settlable_reactive_solids_fraction #[g/m3] Influent
settlable reactive solids concentration
                                    Si_in =
c_influent_solids_concentration*f_influent_dissolved_inert_solids_fraction #[g/m3] Influent
dissolved inert solids concentration
                                    Sr_in =
c_influent_solids_concentration*f_influent_dissolved_reactive_solids_fraction #[g/m3] Influent
dissolved reactive solids concentration
                                    dn_p = dn_median_density_of_settlable_solids #[kg/m3]
Median density of settlable solids
                                    dn_w = dn_density_of_water #[kg/m3] Density of water
                                    dia = d_mean_particle_size_settlable_solids*(10**(-6))
#[m] Mean particle diameter
                                    g = g_gravitational_acceleration #[m/s2] Gravitational
acceleration
                                    dv_w = dv_dynamic_viscosity_of_water #[kg/m/s] Dynamic
viscosity of water at 20°C
                                    kv_w = kv_kinematic_viscosity_of_water #[m2/s] Kinematic
viscosity of water at 20°C
                                    d_max = [d_max_particle_size_settlable_solids*(10**(-6))]
# Array for storing max particle diameter entering each upflow compartment
```

```
                                    settling = 1 # Boolean variable to determine if settling
is happening in current compartment or not
                                    upflow_velocity = [cu_u[0]] # Initialize array to store
upflow velocities for each upflow compartment
                                    Xid_in = [Xi_in] # Initialize array to hold downflow
compartment inputs for Xi
                                    Xrd_in = [Xr_in] # Initialize array to hold downflow
compartment inputs for Xr
                                    Sid_in = [Si_in] # Initialize array to hold downflow
compartment inputs for Si
                                    Srd_in = [Sr_in] # Initialize array to hold downflow
compartment inputs for Sr

                                    # The big loop
                                    for i in range(0,int(n_number_of_zones)):

                                        # Downflow compartment calculations
                                        # ---------------------------------
                                        '''print('Downflow Compartment: '+str(i))
                                        print('---------------------------------')'''

                                        # Downflow compartment inputs
                                        if (i>0): # Outputs from previous upflow compartment
are inputs for this downflow compartment, except when i=0 - i.e. when this is the first downflow
compartment
                                            Xid_in.append(Xiu_out[i-1])
                                            Xrd_in.append(Xru_out[i-1])
                                            Sid_in.append(Siu_out[i-1])
                                            Srd_in.append(Sru_out[i-1])

                                        # Downflow compartment state variables
                                        t_hrt = cd_HRT[i]
                                        Xid = Xid_in[i]
                                        Xrd = Xrd_in[i]
                                        Sid = Sid_in[i]
                                        Srd = Srd_in[i]

                                        # Downflow compartment disintegration based on HRT
                                        Xrd = Xrd*exp(-t_hrt*k_disintegration)
                                        delta_Sr = Xrd_in[i]-Xrd # Disintegration of Xr
creates Sr
                                        Srd = Srd+delta_Sr

                                        # Downflow compartment decay based on HRT
                                        Srd = Srd*exp(-t_hrt*k_decay)

                                        # Downflow compartment outputs
                                        if (i==0):
                                            Xid_out = [Xid]
                                            Xrd_out = [Xrd]
                                            Sid_out = [Sid]
                                            Srd_out = [Srd]
                                        else:
                                            Xid_out.append(Xid)
                                            Xrd_out.append(Xrd)
                                            Sid_out.append(Sid)
                                            Srd_out.append(Srd)

                                        '''# Downflow compartment printing press
                                        print('Xi_in: '+str(round(Xid_in[i],1))+' / Xi_out:
'+str(round(Xid_out[i],1)))
                                        print('Xr_in: '+str(round(Xrd_in[i],1))+' / Xr_out:
'+str(round(Xrd_out[i],1)))
                                        print('Si_in: '+str(round(Sid_in[i],1))+' / Si_out:
'+str(round(Sid_out[i],1)))
                                        print('Sr_in: '+str(round(Srd_in[i],1))+' / Sr_out:
'+str(round(Srd_out[i],1)))
                                        print()'''

                                        # Upflow compartment calculations
                                        # -------------------------------
```

```
                                        '''print('Upflow Compartment: '+str(i))
                                        print('----------------------------------')'''
                                        #print('Upflow Velocity (m/h):
'+str(round(cu_u[i],4)))

                                        # Upflow compartment inputs
                                        if (i==0): # If it is the first upflow compartment,
initialize arrays
                                            Xiu_in = [Xid_out[i]]
                                            Xru_in = [Xrd_out[i]]
                                            Siu_in = [Sid_out[i]]
                                            Sru_in = [Srd_out[i]]
                                        else: # Otherwise append to previously initialized
arrays
                                            Xiu_in.append(Xid_out[i])
                                            Xru_in.append(Xrd_out[i])
                                            Siu_in.append(Sid_out[i])
                                            Sru_in.append(Srd_out[i])

                                        # Upflow compartment state variables
                                        t_hrt = cu_HRT[i]
                                        t_srt = t_solids_retention_time
                                        Xiu = Xiu_in[i]
                                        Xru = Xru_in[i]
                                        Siu = Siu_in[i]
                                        Sru = Sru_in[i]

                                        # Upflow compartment settling
                                        # Check if settling can happen in current compartment
based on upflow velocity
                                        if (i>0): # Settling can always happen in central
compartment, so it is skipped
                                            upflow_velocity.append(cu_u[i]) # Store current
upflow velocity in the upflow_velocity array
                                            if (cu_u[i]>min(upflow_velocity)): # If current
upflow velocity is higher than the minimum upflow velocity observed in previous compartments, no
settling will occur in this compartment (since everything that could settle already did in
earlier compartments)
                                                settling = 0
                                            else: # Otherwise settling will occur
                                                settling = 1
                                        '''print('Settling: '+str(settling))'''

                                        if (settling == 1):
                                            # Reynolds number checks
                                            # Calculate Reynolds number for pipe flow
                                            Q = q_flow_rate/86400 #[m3/s] Flow rate
                                            Dh = cu_OD[i]-cu_ID[i] #[m] Hydraulic diameter
                                            Ac = cu_CA[i] #[m2] Cross-sectional area
                                            vis = kv_kinematic_viscosity_of_water #[m2/s]
Kinematic viscosity of water
                                            Re = Q*Dh/Ac/vis #Reynolds number for pipe flow
(Re < 2000: Laminar pipe flow, Re > 4000: Turbulent pipe flow, 2000 < Re < 4000: Transitional
regime)
                                            #print('Fluid Reynolds Number:
'+str(round(Re,1)))

                                            # Calculate particle Reynolds number for max.
particle diameter in influent
                                            u = cu_u[i]/3600 #[m/s] Upflow velocity in upflow
compartment i
                                            Re_p = d_max[i]*u/kv_w
                                            #print('Max. Particle Reynolds Number:
'+str(round(Re_p,6)))

                                            # Calculate particle diameter cut-off from simple
Stokes settling velocity for laminar flow range
                                            dia = (18*u*dv_w/(dn_p-dn_w)/g)**(0.5)
                                            #print('Particle Diameter Settlability Cut-off:
'+str(round(dia*(10**6),2))+' µm')
```

```
                                                # Estimate particle size cut-off (% of particles
that will settle)
                                                x = dia*(10**6)
                                                d = d_mean_particle_size_settlable_solids
                                                sigma = d_standard_deviation_sspsd_curve
                                                probability = norm.cdf(x,d,sigma) # Particle size
probability is determined using a cumulative normal distribution function (scipy.stats.norm)

                                                # Store the probability in an array (it is 1-
probability because probability itself actually gives the probability of staying afloat)
                                                if (i==0): # If i==0, initialize
                                                    p = [1-probability]
                                                    dp = p[i]
                                                else: # Otherwise, append
                                                    p.append(1-probability)
                                                    dp = p[i]-p[i-1]

                                                #print('Percentage of Settled Solids:
'+str(round(dp*100,2))+'%')

                                                # Assign new maximum particle size for the next
upflow compartment Reynolds number check (dia cut-off is the new max, because everything above
this diameter settled in this compartment)
                                                d_max.append(dia)

                                                # Calculate settled (_s) particulate solids
concentrations
                                                Xiu_s = Xiu*dp # Inert fraction
                                                Xru_s = Xru*dp # Reactive fraction
                                            else:
                                                # Assign new maximum particle size for the next
upflow compartment Reynolds number check (we just add the current diameter to the array to
advance the array index)
                                                d_max.append(d_max[i])
                                                p.append(p[i-1])

                                                # Calculate settled (_s) particulate solids
concentrations - this is the case for no settling, so zero
                                                Xiu_s = 0 # Inert fraction
                                                Xru_s = 0 # Reactive fraction

                                            # Calculate the non-settled (_ns) particulate solids
concentrations
                                            Xiu_ns = Xiu-Xiu_s
                                            Xru_ns = Xru-Xru_s

                                            # Upflow compartment disintegration based on HRT
(acting on Xru_ns)
                                            Xru_ns_dis = Xru_ns*exp(-t_hrt*k_disintegration)
                                            delta_Sr = Xru_ns-Xru_ns_dis # Disintegration of Xr
creates Sr
                                            Sru = Sru+delta_Sr

                                            # Upflow compartment disintegration based on SRT
(acting on Xru_s)
                                            Xru_s_dis = Xru_s*exp(-t_srt*k_disintegration)
                                            delta_Sr = Xru_s-Xru_s_dis # Disintegration of Xr
creates Sr
                                            Sru = Sru+delta_Sr

                                            # Upflow compartment decay based on HRT (acting on
Sru)
                                            Sru = Sru*exp(-t_hrt*k_decay)

                                            # Convert state variables to output variables
                                            Xiu = Xiu_ns # This is the fraction of Xi that is
remaining (i.e. not settled) and able to travel to the next compartment
                                            Xru = Xru_ns_dis # This is the fraction of Xr that is
remaining (i.e. not settled or disintegrated) and able to travel to the next compartment

                                            # Upflow compartment outputs
```

```
            if (i==0):
                Xiu_out = [Xiu]
                Xru_out = [Xru]
                Siu_out = [Siu]
                Sru_out = [Sru]
            else:
                Xiu_out.append(Xiu)
                Xru_out.append(Xru)
                Siu_out.append(Siu)
                Sru_out.append(Sru)

            '''# Upflow compartment printing press
            print('Xi_in: '+str(round(Xiu_in[i],1))+' / Xi_out:
'+str(round(Xiu_out[i],1)))

            print('Xr_in: '+str(round(Xru_in[i],1))+' / Xr_out:
'+str(round(Xru_out[i],1)))

            print('Si_in: '+str(round(Siu_in[i],1))+' / Si_out:
'+str(round(Siu_out[i],1)))

            print('Sr_in: '+str(round(Sru_in[i],1))+' / Sr_out:
'+str(round(Sru_out[i],1)))

            print()'''

            o_Xi = round(Xiu_out[i],3)
            o_Xr = round(Xru_out[i],3)
            o_Si = round(Siu_out[i],3)
            o_Sr = round(Sru_out[i],3)

        # Prepare output variables for writing to output file
        o_rem_Xi = 100*(1-(o_Xi/(i_C_t*i_f_Xi)))
        o_rem_Xr = 100*(1-(o_Xr/(i_C_t*i_f_Xr)))
        o_rem_Si = 100*(1-(o_Si/(i_C_t*i_f_Si)))
        o_rem_Sr = 100*(1-(o_Sr/(i_C_t*i_f_Sr)))
        o_rem_X = 100*(1-((o_Xi+o_Xr)/(i_C_t*(i_f_Xi+i_f_Xr))))
        o_rem_S = 100*(1-((o_Si+o_Sr)/(i_C_t*(i_f_Si+i_f_Sr))))
        o_rem_i = 100*(1-((o_Xi+o_Si)/(i_C_t*(i_f_Xi+i_f_Si))))
        o_rem_r = 100*(1-((o_Xr+o_Sr)/(i_C_t*(i_f_Xr+i_f_Sr))))
        o_rem_tot = 100*(1-(o_Xi+o_Xr+o_Si+o_Sr)/i_C_t)

        # Write to csv file
        f = open(path_out, "a") # Append the data

        f.write(str(i_f_Xi)+','+
        str(i_f_Xr)+','+
        str(i_f_Si)+','+
        str(i_f_Sr)+','+
        str(i_V_r)+','+
        str(i_C_t)+','+
        str(i_HRT)+','+
        str(i_SRT)+','+
        str(i_k_dis)+','+
        str(i_k_dec)+','+
        str(i_f_dC0)+','+
        str(i_n_z)+','+
        str(i_HDR)+','+
        str(i_MPD)+','+
        str(i_f_std_PSD)+','+
        str(i_rho)+','+
        str(o_Xi)+','+
        str(o_Xr)+','+
        str(o_Si)+','+
        str(o_Sr)+','+
        str(o_rem_Xi)+','+
        str(o_rem_Xr)+','+
        str(o_rem_Si)+','+
        str(o_rem_Sr)+','+
        str(o_rem_X)+','+
        str(o_rem_S)+','+
        str(o_rem_i)+','+
        str(o_rem_r)+','+
        str(o_rem_tot)+'\n')
        f.close()
```

```
                                    iteration_counter = iteration_counter+1
                                    print(iteration_counter)
                                    if iteration_counter%100 == 0:
                                        clear()

print('Done!')
```

Appendix C: Python Code for Sensitivity Analysis

```
import sys
import time
import functions
import csv
from collections import defaultdict
import os
import math
from math import exp as exp
from scipy.stats import norm as norm
root = os.path.dirname(os.path.realpath("__file__")) # fetch directory path for where this Python
script is located
clear = lambda: os.system('cls')

# Baffle Spacing: Evenly Spaced
# Influent Flow Direction: Top Down
# Processes: Settling, Disintegration, Decay
# Flow Type: Plug Flow

# f: fraction, v: volume, t: time, T: temperature, n: number, d: distance (length), dn: density,
dv: dynamic viscosity
# g: acceleration, k: rate constant, q: flow rate, cd: downflow compartment, cu: upflow
compartment

# Geometric Analysis Inputs
#-------------------------------------------------------------------------------------------------
----------#
#-------------------------------------------------------------------------------------------------
----------#

# Generate output file header
path_out = root+'\\outputs\\act-mbr-sensitivity, '+time.strftime("%m-%d-%Y, %H%M%S")+'.csv'
f = open(path_out, "wt") # Write the column names
f.write('i_f_Xi'+','+
'i_f_Xr'+','+
'i_f_Si'+','+
'i_f_Sr'+','+
'i_V_r'+','+
'i_C_t'+','+
'i_HRT'+','+
'i_SRT'+','+
'i_k_dis'+','+
'i_k_dec'+','+
'i_f_dC0'+','+
'i_n_z'+','+
'i_HDR'+','+
'i_MPD'+','+
'i_f_std_PSD'+','+
'i_rho'+','+
'o_Xi'+','+
'o_Xr'+','+
'o_Si'+','+
'o_Sr'+','+
'o_rem_Xi'+','+
'o_rem_Xr'+','+
'o_rem_Si'+','+
'o_rem_Sr'+','+
'o_rem_X'+','+
'o_rem_S'+','+
'o_rem_i'+','+
'o_rem_r'+','+
```

```
'o_rem_tot'+'\n')
f.close()

# Input constants
i_f_Xi = 0.10 # [-] Influent fraction, particulate inert
i_f_Xr = 0.50 # [-] Influent fraction, particulate reactive
i_f_Si = 0.05 # [-] Influent fraction, soluble inert
i_f_Sr = 0.35 # [-] Influent fraction, soluble reactive
i_V_r = 1000 # [m3] Total reactor volume
i_C_t = 1000 # [g/m3] Influent solids concentration

i_SRT = 100 # [d] Solids retention time
i_k_dis = 0.1 # [1/d] Disintegration rate constant for particulate solids
i_k_dec = 3 # [1/d] Decay rate constant for soluble solids
i_MPD = 100 # [µm] Mean particle diameter for particulate solids
i_f_std_PSD = 0.3 # [-] Standard deviation fraction of the particle size distribution curve
i_rho = 1250 # [kg/m3] Mean particle density of particulate solids

# Input arrays
'''max_index = 2
a_HRT = [0.2,1] # [d] Hydraulic retention time (i_1)
a_SRT = [5,20] # [d] Solids retention time (i_2)
a_k_dis = [0.01,0.05] # [1/d] Disintegration rate constant for particulate solids (i_3)
a_k_dec = [0.2,1] # [1/d] Decay rate constant for soluble solids (i_4)
a_f_dC0 = [0.2,0.8] # [-] Fraction of central compartment diameter with respect to reactor
diameter (i_5)
a_n_z = [3,9] # [-] Number of zones (i_6)
a_HDR = [0.2,5] # [-] Reactor height:diameter ratio (i_7)
a_MPD = [100,300] # [µm] Mean particle diameter for particulate solids (i_8)
a_f_std_PSD = [0.2,0.8] # [-] Standard deviation fraction of the particle size distribution curve
(i_9)
a_rho = [1250,2500] # [kg/m3] Mean particle density of particulate solids (i_10)'''

max_index = 3
a_HRT = [0.25,0.5,1] # [d] Hydraulic retention time (i_1)
# a_SRT = [5,20,100] # [d] Solids retention time (i_2)
# a_k_dis = [0.01,0.05,0.2] # [1/d] Disintegration rate constant for particulate solids (i_3)
# a_k_dec = [0.2,1,5] # [1/d] Decay rate constant for soluble solids (i_4)
a_f_dC0 = [0.2,0.4,0.8] # [-] Fraction of central compartment diameter with respect to reactor
diameter (i_5)
a_n_z = [3,6,9] # [-] Number of zones (i_6)
a_HDR = [0.5,1,2] # [-] Reactor height:diameter ratio (i_7)
# a_MPD = [50,100,200] # [µm] Mean particle diameter for particulate solids (i_8)
# a_f_std_PSD = [0.2,0.5,0.8] # [-] Standard deviation fraction of the particle size distribution
curve (i_9)
# a_rho = [1250,1750,2500] # [kg/m3] Mean particle density of particulate solids (i_10)

# Loop to run through all parameter combinations
iteration_counter = 0
for i_1 in range (0,max_index):
    # for i_2 in range (0,max_index):
    # for i_3 in range (0,max_index):
    # for i_4 in range (0,max_index):
    for i_5 in range (0,max_index):
        for i_6 in range (0,max_index):
            for i_7 in range (0,max_index):
                # for i_8 in range (0,max_index):
                # for i_9 in range (0,max_index):
                # for i_10 in range (0,max_index):

                # Progressively assign values to variables
                i_HRT = a_HRT[i_1]
                #i_SRT = a_SRT[i_2]
                #i_k_dis = a_k_dis[i_3]
                #i_k_dec = a_k_dec[i_4]
                i_f_dC0 = a_f_dC0[i_5]
                i_n_z = a_n_z[i_6]
                i_HDR = a_HDR[i_7]
                #i_MPD = a_MPD[i_8]
                #i_f_std_PSD = a_f_std_PSD[i_9]
                #i_rho = a_rho[i_10]
```

```
                # Inputs for Current Run
                #-------------------------------------------------------------------------------
-------------------------#
                #-------------------------------------------------------------------------------
-------------------------#

                # Reactor
                v_reactor_volume = i_V_r #[m3] Reactor volume
                f_reactor_height_diameter_ratio = i_HDR #[-] Reactor height/diameter ratio
                t_hydraulic_retention_time = i_HRT #[d] Hydraulic Retention Time (HRT)
                t_solids_retention_time = i_SRT #[d] Solids Retention Time (SRT)
                n_number_of_zones = i_n_z #[-] Number of zones (1 zone = 2 compartments
(downflow+upflow))
                n_number_of_compartments = n_number_of_zones*2 #[-] Number of compartments
including central zone (C0)
                f_central_compartment_diameter_fraction = i_f_dC0 #[-] Central compartment
diameter fraction with respect to reactor diameter
                f_downflow_compartment_baffle_spacing_fraction = 0.2 #[-] Downflow compartment
baffle spacing fraction with respect to spacing of one zone (example: if this is set to 0.5,
downflow compartments will have the same baffle spacing distance value as upflow compartments)
                f_inlet_pipe_diameter_fraction = 0.05 #[-] Inlet pipe diameter fraction with
respect to diameter of central compartment
                f_inlet_pipe_wall_thickness_fraction = 0.1 #[-] Inlet pipe wall thickness
fraction with respect to inlet pipe diameter
                #f_baffle_thickness_fraction = 0.005 #[-]Baffle thickness fraction with respect
to reactor diameter
                d_baffle_thickness = 0.01 #[m], Baffle thickness

                # Influent
                c_influent_solids_concentration = i_C_t #[g/m3] Influent solids concentration
                f_influent_settlable_inert_solids_fraction = i_f_Xi #[-] Influent settlable inert
solids fraction (w/w)
                f_influent_settlable_reactive_solids_fraction = i_f_Xr #[-] Influent settlable
reactive solids fraction (w/w)
                f_influent_dissolved_inert_solids_fraction = i_f_Si #[-] Influent dissolved inert
solids fraction (w/w)
                f_influent_dissolved_reactive_solids_fraction = i_f_Sr #[-] Influent dissolved
reactive solids fraction (w/w)
                d_mean_particle_size_settlable_solids = i_MPD #[µm] Mean particle size for
settlable solids
                f_standard_deviation_sspsd_curve = i_f_std_PSD #[-] % of stdev with respect to
mean particle size
                d_standard_deviation_sspsd_curve =
d_mean_particle_size_settlable_solids*f_standard_deviation_sspsd_curve #[µm] Standard deviation
for settlable solids particle size distribution (SSPSD) curve
                d_max_particle_size_settlable_solids = d_mean_particle_size_settlable_solids*2
#[µm] Max particle size for settlable solids
                T_influent_temperature = 20 #[°C] Influent temperature

                # Settling
                dn_median_density_of_settlable_solids = i_rho #[kg/m3] Median density of
settlable solids
                dn_density_of_water = 998.21 #[kg/m3] Density of water at 20°C
                dv_dynamic_viscosity_of_water = 1.002*(10**(-3)) #[kg/m/s] Dynamic viscosity of
water at 20°C
                kv_kinematic_viscosity_of_water = 1.004*(10**(-6)) #[m2/s] Kinematic viscosity of
water at 20°C
                g_gravitational_acceleration = 9.80665 #[m/s2] Gravitational acceleration

                # Disintegration and Decay
                k_disintegration = i_k_dis #[1/d] 1st order constant for disintegration of
particulate (settlable) solids into dissolved solids
                k_decay = i_k_dec #[1/d] 1st order constant for reactions involving the
degradation (decay) of dissolved solids

                # Reactor Model
                #-------------------------------------------------------------------------------
-------------------------#
                #-------------------------------------------------------------------------------
-------------------------#
```

```
                # Indices -> 0: C0, 1: C1, 2: C2, 3: C3, etc.
                # Order of Compartments -> C0d > C0u > C1d > C1u > ... > Cnd > Cnu
                d_reactor_diameter =
(v_reactor_volume*4/f_reactor_height_diameter_ratio/math.pi)**(1/3.0) #[m], Reactor diameter
                d_reactor_liquid_height = f_reactor_height_diameter_ratio*d_reactor_diameter
#[m], Reactor liquid height
                q_flow_rate = v_reactor_volume/t_hydraulic_retention_time #[m3/d], Influent flow
rate
                d_diameter_C0 = f_central_compartment_diameter_fraction*d_reactor_diameter #[m],
Diameter of central compartment (C0)
                n_number_of_baffles = n_number_of_compartments-2 #[-], Number of baffles
(excluding C0d and outer wall of the reactor)
                n_number_of_baffles_2D_cross_section = n_number_of_baffles*2 #[-], Number of
baffles looking at a 2D cross section of the CBR from the side view (i.e. each baffle is counted
twice - this is the number relevant to the calculations)
                n_number_of_zones_2D_cross_section = n_number_of_baffles_2D_cross_section/2 #[-],
Number of zones looking at a 2D cross section of the CBR from the side view
                d_spacing_zone_total = d_reactor_diameter-d_diameter_C0-
n_number_of_baffles_2D_cross_section*d_baffle_thickness #[m], Total (U+D) baffle spacing of all
zones
                d_spacing_zone = d_spacing_zone_total/n_number_of_zones_2D_cross_section #[m],
Spacing for one zone
                '''print(d_spacing_zone)'''
                d_spacing_Cd = d_spacing_zone*f_downflow_compartment_baffle_spacing_fraction
#[m], Downflow compartment baffle spacing
                d_spacing_Cu = d_spacing_zone*(1-f_downflow_compartment_baffle_spacing_fraction)
#[m], Upflow compartment baffle spacing

                # Central Compartment Definitions - Diameters
                d_C0di = 0 #[m], C0 downflow compartment inner diameter - if this were a doughnut
like the rest of the compartments. It is not, so zero.
                d_C0do =  d_diameter_C0*f_inlet_pipe_diameter_fraction #[m], Inlet pipe diameter
                d_C0dw = d_C0do*(1+f_inlet_pipe_wall_thickness_fraction*2) #[m], Inlet pipe
diameter with pipe wall

                # Central Compartment Definitions - Downflow
                cd_ID = [d_C0di] #[m], C0d Downflow Compartment Inner Diameter
                cd_OD = [d_C0do] #[m], C0d Downflow Compartment Outer Diameter
                cd_ODb = [d_C0dw] #[m], C0d Downflow Compartment Outer Diameter with Inlet Pipe
Wall
                cd_CA = [math.pi/4*(cd_OD[0]**2-cd_ID[0]**2)] #[m2], C0d Downflow Compartment
Crossectional Area
                cd_V = [cd_CA[0]*d_reactor_liquid_height] #[m3], C0d Downflow Compartment Volume
                cd_HRT = [cd_V[0]/q_flow_rate] #[d], C0d Downflow Compartment HRT
                cd_u = [q_flow_rate/cd_CA[0]/24] #[m/h], C0d Downflow Compartment Fluid Velocity

                # Central Compartment Definitions - Upflow
                cu_ID = [cd_ODb[0]] #[m], C0u Upflow Compartment Inner Diameter
                cu_OD = [d_diameter_C0] #[m], C0u Upflow Compartment Outer Diameter
                cu_ODb = [cu_OD[0]+2*d_baffle_thickness] #[m], C0u Upflow Compartment Outer
Diameter with Baffle
                cu_CA = [math.pi/4*(cu_OD[0]**2-cu_ID[0]**2)] #[m2], C0u Upflow Compartment
Crossectional Area
                cu_V = [cu_CA[0]*d_reactor_liquid_height] #[m3], C0u Upflow Compartment Volume
                cu_HRT = [cu_V[0]/q_flow_rate] #[d], C0u Upflow Compartment HRT
                cu_u = [q_flow_rate/cu_CA[0]/24] #[m/h], C0u Upflow Compartment Fluid Velocity

                for i in range(1,int(n_number_of_zones)): # Starts at 1 (not 0), because 0 is the
central compartment indice, and it has been defined separately above
                    # Compartment Definitions - Downflow
                    cd_ID.append(cu_ODb[i-1]) #[m], Downflow Compartment Inner Diameter
                    cd_OD.append(cd_ID[i]+2*d_spacing_Cd) #[m], Downflow Compartment Outer
Diameter
                    cd_ODb.append(cd_OD[i]+2*d_baffle_thickness) #[m], C0d Downflow Compartment
Outer Diameter with Baffle
                    cd_CA.append(math.pi/4*(cd_OD[i]**2-cd_ID[i]**2)) #[m2], Downflow Compartment
Crossectional Area
                    cd_V.append(cd_CA[i]*d_reactor_liquid_height) #[m3], Downflow Compartment
Volume
                    cd_HRT.append(cd_V[i]/q_flow_rate) #[d], Downflow Compartment HRT
```

```
                    cd_u.append(q_flow_rate/cd_CA[i]/24) #[m/h], Downflow Compartment Fluid
Velocity
                    # Compartment Definitions - Upflow
                    cu_ID.append(cd_ODb[i]) #[m], Upflow Compartment Inner Diameter
                    cu_OD.append(cu_ID[i]+2*d_spacing_Cu) #[m], Upflow Compartment Outer Diameter
                    cu_ODb.append(cu_OD[i]+2*d_baffle_thickness) #[m], C0u Upflow Compartment
Outer Diameter with Baffle
                    cu_CA.append(math.pi/4*(cu_OD[i]**2-cu_ID[i]**2)) #[m2], Upflow Compartment
Crossectional Area
                    cu_V.append(cu_CA[i]*d_reactor_liquid_height) #[m3], Upflow Compartment
Volume
                    cu_HRT.append(cu_V[i]/q_flow_rate) #[d], Upflow Compartment HRT
                    cu_u.append(q_flow_rate/cu_CA[i]/24) #[m/h], Upflow Compartment Fluid
Velocity

                # Error checking
                for i in range(0,int(n_number_of_zones)):
                    if (cu_u[i]<0):
                        sys.exit('Error: Upflow velocity cannot be negative.')

                # Settling, Disintegration, Decay
                #-------------------------------------------------------------------------------
-------------------------#
                #-------------------------------------------------------------------------------
-------------------------#

                # Initialize variables and arrays
                Xi_in =
c_influent_solids_concentration*f_influent_settlable_inert_solids_fraction #[g/m3] Influent
settlable inert solids concentration
                Xr_in =
c_influent_solids_concentration*f_influent_settlable_reactive_solids_fraction #[g/m3] Influent
settlable reactive solids concentration
                Si_in =
c_influent_solids_concentration*f_influent_dissolved_inert_solids_fraction #[g/m3] Influent
dissolved inert solids concentration
                Sr_in =
c_influent_solids_concentration*f_influent_dissolved_reactive_solids_fraction #[g/m3] Influent
dissolved reactive solids concentration
                dn_p = dn_median_density_of_settlable_solids #[kg/m3] Median density of settlable
solids
                dn_w = dn_density_of_water #[kg/m3] Density of water
                dia = d_mean_particle_size_settlable_solids*(10**(-6)) #[m] Mean particle
diameter
                g = g_gravitational_acceleration #[m/s2] Gravitational acceleration
                dv_w = dv_dynamic_viscosity_of_water #[kg/m/s] Dynamic viscosity of water at 20°C
                kv_w = kv_kinematic_viscosity_of_water #[m2/s] Kinematic viscosity of water at
20°C
                d_max = [d_max_particle_size_settlable_solids*(10**(-6))] # Array for storing max
particle diameter entering each upflow compartment
                settling = 1 # Boolean variable to determine if settling is happening in current
compartment or not
                upflow_velocity = [cu_u[0]] # Initialize array to store upflow velocities for
each upflow compartment
                Xid_in = [Xi_in] # Initialize array to hold downflow compartment inputs for Xi
                Xrd_in = [Xr_in] # Initialize array to hold downflow compartment inputs for Xr
                Sid_in = [Si_in] # Initialize array to hold downflow compartment inputs for Si
                Srd_in = [Sr_in] # Initialize array to hold downflow compartment inputs for Sr

                # The big loop
                for i in range(0,int(n_number_of_zones)):

                    # Downflow compartment calculations
                    # ---------------------------------
                    '''print('Downflow Compartment: '+str(i))
                    print('-----------------------------------')'''

                    # Downflow compartment inputs
                    if (i>0): # Outputs from previous upflow compartment are inputs for this
downflow compartment, except when i=0 - i.e. when this is the first downflow compartment
                        Xid_in.append(Xiu_out[i-1])
```

```
                    Xrd_in.append(Xru_out[i-1])
                    Sid_in.append(Siu_out[i-1])
                    Srd_in.append(Sru_out[i-1])

                # Downflow compartment state variables
                t_hrt = cd_HRT[i]
                Xid = Xid_in[i]
                Xrd = Xrd_in[i]
                Sid = Sid_in[i]
                Srd = Srd_in[i]

                # Downflow compartment disintegration based on HRT
                Xrd = Xrd*exp(-t_hrt*k_disintegration)
                delta_Sr = Xrd_in[i]-Xrd # Disintegration of Xr creates Sr
                Srd = Srd+delta_Sr

                # Downflow compartment decay based on HRT
                Srd = Srd*exp(-t_hrt*k_decay)

                # Downflow compartment outputs
                if (i==0):
                    Xid_out = [Xid]
                    Xrd_out = [Xrd]
                    Sid_out = [Sid]
                    Srd_out = [Srd]
                else:
                    Xid_out.append(Xid)
                    Xrd_out.append(Xrd)
                    Sid_out.append(Sid)
                    Srd_out.append(Srd)

                '''# Downflow compartment printing press
                print('Xi_in: '+str(round(Xid_in[i],1))+' / Xi_out:
'+str(round(Xid_out[i],1)))
                print('Xr_in: '+str(round(Xrd_in[i],1))+' / Xr_out:
'+str(round(Xrd_out[i],1)))
                print('Si_in: '+str(round(Sid_in[i],1))+' / Si_out:
'+str(round(Sid_out[i],1)))
                print('Sr_in: '+str(round(Srd_in[i],1))+' / Sr_out:
'+str(round(Srd_out[i],1)))
                print()'''

                # Upflow compartment calculations
                # ----------------------------------
                '''print('Upflow Compartment: '+str(i))
                print('----------------------------------')'''
                #print('Upflow Velocity (m/h): '+str(round(cu_u[i],4)))

                # Upflow compartment inputs
                if (i==0): # If it is the first upflow compartment, initialize arrays
                    Xiu_in = [Xid_out[i]]
                    Xru_in = [Xrd_out[i]]
                    Siu_in = [Sid_out[i]]
                    Sru_in = [Srd_out[i]]
                else: # Otherwise append to previously initialized arrays
                    Xiu_in.append(Xid_out[i])
                    Xru_in.append(Xrd_out[i])
                    Siu_in.append(Sid_out[i])
                    Sru_in.append(Srd_out[i])

                # Upflow compartment state variables
                t_hrt = cu_HRT[i]
                t_srt = t_solids_retention_time
                Xiu = Xiu_in[i]
                Xru = Xru_in[i]
                Siu = Siu_in[i]
                Sru = Sru_in[i]

                # Upflow compartment settling
                # Check if settling can happen in current compartment based on upflow
velocity
```

```
                    if (i>0): # Settling can always happen in central compartment, so it is
skipped
                        upflow_velocity.append(cu_u[i]) # Store current upflow velocity in the
upflow_velocity array
                        if (cu_u[i]>min(upflow_velocity)): # If current upflow velocity is higher
than the minimum upflow velocity observed in previous compartments, no settling will occur in
this compartment (since everything that could settle already did in earlier compartments)
                            settling = 0
                        else: # Otherwise settling will occur
                            settling = 1
                    '''print('Settling: '+str(settling))'''

                    if (settling == 1):
                        # Reynolds number checks
                        # Calculate Reynolds number for pipe flow
                        Q = q_flow_rate/86400 #[m3/s] Flow rate
                        Dh = cu_OD[i]-cu_ID[i] #[m] Hydraulic diameter
                        Ac = cu_CA[i] #[m2] Cross-sectional area
                        vis = kv_kinematic_viscosity_of_water #[m2/s] Kinematic viscosity of
water
                        Re = Q*Dh/Ac/vis #Reynolds number for pipe flow (Re < 2000: Laminar pipe
flow, Re > 4000: Turbulent pipe flow, 2000 < Re < 4000: Transitional regime)
                        #print('Fluid Reynolds Number: '+str(round(Re,1)))

                        # Calculate particle Reynolds number for max. particle diameter in
influent
                        u = cu_u[i]/3600 #[m/s] Upflow velocity in upflow compartment i
                        Re_p = d_max[i]*u/kv_w
                        #print('Max. Particle Reynolds Number: '+str(round(Re_p,6)))

                        # Calculate particle diameter cut-off from simple Stokes settling
velocity for laminar flow range
                        dia = (18*u*dv_w/(dn_p-dn_w)/g)**(0.5)
                        #print('Particle Diameter Settlability Cut-off:
'+str(round(dia*(10**6),2))+' µm')

                        # Estimate particle size cut-off (% of particles that will settle)
                        x = dia*(10**6)
                        d = d_mean_particle_size_settlable_solids
                        sigma = d_standard_deviation_sspsd_curve
                        probability = norm.cdf(x,d,sigma) # Particle size probability is
determined using a cumulative normal distribution function (scipy.stats.norm)

                        # Store the probability in an array (it is 1-probability because
probability itself actually gives the probability of staying afloat)
                        if (i==0): # If i==0, initialize
                            p = [1-probability]
                            dp = p[i]
                        else: # Otherwise, append
                            p.append(1-probability)
                            dp = p[i]-p[i-1]

                        #print('Percentage of Settled Solids: '+str(round(dp*100,2))+'%')

                        # Assign new maximum particle size for the next upflow compartment
Reynolds number check (dia cut-off is the new max, because everything above this diameter settled
in this compartment)
                        d_max.append(dia)

                        # Calculate settled (_s) particulate solids concentrations
                        Xiu_s = Xiu*dp # Inert fraction
                        Xru_s = Xru*dp # Reactive fraction
                    else:
                        # Assign new maximum particle size for the next upflow compartment
Reynolds number check (we just add the current diameter to the array to advance the array index)
                        d_max.append(d_max[i])
                        p.append(p[i-1])

                        # Calculate settled (_s) particulate solids concentrations - this is the
case for no settling, so zero
                        Xiu_s = 0 # Inert fraction
```

```
                    Xru_s = 0 # Reactive fraction

                # Calculate the non-settled (_ns) particulate solids concentrations
                Xiu_ns = Xiu-Xiu_s
                Xru_ns = Xru-Xru_s

                # Upflow compartment disintegration based on HRT (acting on Xru_ns)
                Xru_ns_dis = Xru_ns*exp(-t_hrt*k_disintegration)
                delta_Sr = Xru_ns-Xru_ns_dis # Disintegration of Xr creates Sr
                Sru = Sru+delta_Sr

                # Upflow compartment disintegration based on SRT (acting on Xru_s)
                Xru_s_dis = Xru_s*exp(-t_srt*k_disintegration)
                delta_Sr = Xru_s-Xru_s_dis # Disintegration of Xr creates Sr
                Sru = Sru+delta_Sr

                # Upflow compartment decay based on HRT (acting on Sru)
                Sru = Sru*exp(-t_hrt*k_decay)

                # Convert state variables to output variables
                Xiu = Xiu_ns # This is the fraction of Xi that is remaining (i.e. not
settled) and able to travel to the next compartment
                Xru = Xru_ns_dis # This is the fraction of Xr that is remaining (i.e. not
settled or disintegrated) and able to travel to the next compartment

                # Upflow compartment outputs
                if (i==0):
                    Xiu_out = [Xiu]
                    Xru_out = [Xru]
                    Siu_out = [Siu]
                    Sru_out = [Sru]
                else:
                    Xiu_out.append(Xiu)
                    Xru_out.append(Xru)
                    Siu_out.append(Siu)
                    Sru_out.append(Sru)

                '''# Upflow compartment printing press
                print('Xi_in: '+str(round(Xiu_in[i],1))+' / Xi_out:
'+str(round(Xiu_out[i],1)))
                print('Xr_in: '+str(round(Xru_in[i],1))+' / Xr_out:
'+str(round(Xru_out[i],1)))
                print('Si_in: '+str(round(Siu_in[i],1))+' / Si_out:
'+str(round(Siu_out[i],1)))
                print('Sr_in: '+str(round(Sru_in[i],1))+' / Sr_out:
'+str(round(Sru_out[i],1)))
                print()'''

                o_Xi = round(Xiu_out[i],3)
                o_Xr = round(Xru_out[i],3)
                o_Si = round(Siu_out[i],3)
                o_Sr = round(Sru_out[i],3)

            # Prepare output variables for writing to output file
            o_rem_Xi = 100*(1-(o_Xi/(i_C_t*i_f_Xi)))
            o_rem_Xr = 100*(1-(o_Xr/(i_C_t*i_f_Xr)))
            o_rem_Si = 100*(1-(o_Si/(i_C_t*i_f_Si)))
            o_rem_Sr = 100*(1-(o_Sr/(i_C_t*i_f_Sr)))
            o_rem_X = 100*(1-((o_Xi+o_Xr)/(i_C_t*(i_f_Xi+i_f_Xr))))
            o_rem_S = 100*(1-((o_Si+o_Sr)/(i_C_t*(i_f_Si+i_f_Sr))))
            o_rem_i = 100*(1-((o_Xi+o_Si)/(i_C_t*(i_f_Xi+i_f_Si))))
            o_rem_r = 100*(1-((o_Xr+o_Sr)/(i_C_t*(i_f_Xr+i_f_Sr))))
            o_rem_tot = 100*(1-(o_Xi+o_Xr+o_Si+o_Sr)/i_C_t)

            # Write to csv file
            f = open(path_out, "a") # Append the data

            f.write(str(i_f_Xi)+','+
            str(i_f_Xr)+','+
            str(i_f_Si)+','+
            str(i_f_Sr)+','+
```

```
                    str(i_V_r)+','+
                    str(i_C_t)+','+
                    str(i_HRT)+','+
                    str(i_SRT)+','+
                    str(i_k_dis)+','+
                    str(i_k_dec)+','+
                    str(i_f_dC0)+','+
                    str(i_n_z)+','+
                    str(i_HDR)+','+
                    str(i_MPD)+','+
                    str(i_f_std_PSD)+','+
                    str(i_rho)+','+
                    str(o_Xi)+','+
                    str(o_Xr)+','+
                    str(o_Si)+','+
                    str(o_Sr)+','+
                    str(o_rem_Xi)+','+
                    str(o_rem_Xr)+','+
                    str(o_rem_Si)+','+
                    str(o_rem_Sr)+','+
                    str(o_rem_X)+','+
                    str(o_rem_S)+','+
                    str(o_rem_i)+','+
                    str(o_rem_r)+','+
                    str(o_rem_tot)+'\n')
                    f.close()

                    iteration_counter = iteration_counter+1
                    print(iteration_counter)
                    if iteration_counter%100 == 0:
                        clear()

print('Done!')
```

Appendix D: Geometric Model Responses (Top 10%)

Table D1. All equal scenario

i_HRT	i_SRT	i_k_dis	i_k_dec	i_f_dC0	i_n_z	i_HDR	i_MPD	i_f_std_PSD	i_rho	o_rem_tot
5	10	0.01	0.5	0.2	3	0.2	200	0.2	1825	72.7306
5	10	0.01	0.5	0.8	3	0.2	200	0.2	1825	72.7055
5	10	0.01	0.5	0.8	3	0.2	50	0.2	1825	72.7053
5	10	0.01	0.5	0.8	3	0.2	200	0.2	1050	72.7053
5	10	0.01	0.5	0.2	3	5	200	0.2	1825	72.6722
5	10	0.01	0.5	0.2	9	0.2	200	0.2	1825	72.6406
5	10	0.01	0.5	0.8	3	5	200	0.2	1825	72.6215
5	10	0.01	0.5	0.2	3	0.2	200	0.2	1050	72.6117
5	10	0.01	0.5	0.2	3	0.2	50	0.2	1825	72.6107
5	10	0.01	0.5	0.8	3	5	50	0.2	1825	72.6053
5	10	0.01	0.5	0.8	3	5	200	0.2	1050	72.6053
5	10	0.01	0.5	0.8	3	0.2	50	0.2	1050	72.5859
5	10	0.01	0.5	0.8	9	0.2	200	0.2	1825	72.5676
5	10	0.01	0.5	0.8	9	0.2	50	0.2	1825	72.5674
5	10	0.01	0.5	0.8	9	0.2	200	0.2	1050	72.5674
5	10	0.01	0.5	0.2	9	0.2	200	0.2	1050	72.5212
5	10	0.01	0.5	0.2	9	0.2	50	0.2	1825	72.5203
5	10	0.01	0.5	0.8	9	0.2	50	0.2	1050	72.448
5	10	0.01	0.5	0.2	9	5	200	0.2	1825	72.3929
5	10	0.01	0.5	0.8	9	5	200	0.2	1825	72.1783
5	10	0.01	0.5	0.8	9	5	50	0.2	1825	72.1621
5	10	0.01	0.5	0.8	9	5	200	0.2	1050	72.1621
5	50	0.01	0.5	0.2	3	0.2	200	0.2	1825	72.1124
5	10	0.05	0.5	0.2	3	0.2	200	0.2	1825	72.1123
5	50	0.01	0.5	0.8	3	0.2	200	0.2	1825	72.0783
5	50	0.01	0.5	0.8	3	0.2	50	0.2	1825	72.0781
5	50	0.01	0.5	0.8	3	0.2	200	0.2	1050	72.0781
5	10	0.05	0.5	0.8	3	0.2	200	0.2	1825	72.0779
5	10	0.05	0.5	0.8	3	0.2	50	0.2	1825	72.0777
5	10	0.05	0.5	0.8	3	0.2	200	0.2	1050	72.0777
5	10	0.05	0.5	0.2	3	5	200	0.2	1825	72.0438
5	50	0.01	0.5	0.2	3	5	200	0.2	1825	72.0427
5	10	0.05	0.5	0.2	3	0.2	200	0.2	1050	72.0034
5	10	0.05	0.5	0.2	3	0.2	50	0.2	1825	72.0025
5	10	0.05	0.5	0.2	9	0.2	200	0.2	1825	71.9978

Table D1. (Continued)

5	50	0.01	0.5	0.2	9	0.2	200	0.2	1825	71.9978
5	50	0.01	0.5	0.2	3	0.2	200	0.2	1050	71.995
5	50	0.01	0.5	0.2	3	0.2	50	0.2	1825	71.994
5	50	0.01	0.5	0.8	3	5	200	0.2	1825	71.9714
5	10	0.05	0.5	0.8	3	5	200	0.2	1825	71.9711
5	10	0.05	0.5	0.8	3	0.2	50	0.2	1050	71.9679
5	50	0.01	0.5	0.8	3	0.2	50	0.2	1050	71.9602
5	10	0.05	0.5	0.8	3	5	200	0.2	1050	71.9561
5	10	0.05	0.5	0.8	3	5	50	0.2	1825	71.956
5	50	0.01	0.5	0.8	3	5	50	0.2	1825	71.9554
5	50	0.01	0.5	0.8	3	5	200	0.2	1050	71.9554
5	50	0.01	0.5	0.8	9	0.2	200	0.2	1825	71.9028
5	50	0.01	0.5	0.8	9	0.2	50	0.2	1825	71.9026
5	50	0.01	0.5	0.8	9	0.2	200	0.2	1050	71.9026
5	10	0.05	0.5	0.8	9	0.2	200	0.2	1825	71.9023
5	10	0.05	0.5	0.8	9	0.2	50	0.2	1825	71.9021
5	10	0.05	0.5	0.8	9	0.2	200	0.2	1050	71.9021
5	10	0.05	0.5	0.2	9	0.2	200	0.2	1050	71.8872
5	10	0.05	0.5	0.2	9	0.2	50	0.2	1825	71.8863
5	50	0.01	0.5	0.2	9	0.2	200	0.2	1050	71.88
5	50	0.01	0.5	0.2	9	0.2	50	0.2	1825	71.8792
5	10	0.05	0.5	0.8	9	0.2	50	0.2	1050	71.7919
5	50	0.01	0.5	0.8	9	0.2	50	0.2	1050	71.7847
5	10	0.05	0.5	0.2	9	5	200	0.2	1825	71.6882
5	50	0.01	0.5	0.2	9	5	200	0.2	1825	71.6873
5	50	0.01	0.5	0.8	9	5	200	0.2	1825	71.4071
5	10	0.05	0.5	0.8	9	5	200	0.2	1825	71.4067
5	10	0.05	0.5	0.8	9	5	50	0.2	1825	71.3916
5	10	0.05	0.5	0.8	9	5	200	0.2	1050	71.3916
5	50	0.01	0.5	0.8	9	5	50	0.2	1825	71.3912
5	50	0.01	0.5	0.8	9	5	200	0.2	1050	71.3912
5	50	0.05	0.5	0.2	3	0.2	200	0.2	1825	71.0255
5	50	0.05	0.5	0.8	3	0.2	200	0.2	1825	70.9756
5	50	0.05	0.5	0.8	3	0.2	50	0.2	1825	70.9754
5	50	0.05	0.5	0.8	3	0.2	200	0.2	1050	70.9754
5	50	0.05	0.5	0.2	3	5	200	0.2	1825	70.9371
5	50	0.05	0.5	0.2	3	0.2	200	0.2	1050	70.9192
5	50	0.05	0.5	0.2	3	0.2	50	0.2	1825	70.9183
5	50	0.05	0.5	0.8	3	0.2	50	0.2	1050	70.8682
5	50	0.05	0.5	0.2	9	0.2	200	0.2	1825	70.8678
5	50	0.05	0.5	0.8	3	5	200	0.2	1825	70.8286
5	50	0.05	0.5	0.8	3	5	200	0.2	1050	70.814

Table D1. (Continued)

5	50	0.05	0.5	0.8	3	5	50	0.2	1825	70.8139
5	50	0.05	0.5	0.2	9	0.2	200	0.2	1050	70.76
5	50	0.05	0.5	0.2	9	0.2	50	0.2	1825	70.7591
5	50	0.05	0.5	0.8	9	0.2	200	0.2	1825	70.7338
5	50	0.05	0.5	0.8	9	0.2	50	0.2	1825	70.7336
5	50	0.05	0.5	0.8	9	0.2	200	0.2	1050	70.7336
5	50	0.05	0.5	0.8	9	0.2	50	0.2	1050	70.6262
5	10	0.01	0.5	0.2	3	0.2	50	0.2	1050	70.6096
5	50	0.05	0.5	0.2	9	5	200	0.2	1825	70.4478
5	50	0.05	0.5	0.8	9	5	200	0.2	1825	70.0513
5	50	0.05	0.5	0.8	9	5	50	0.2	1825	70.0366
5	50	0.05	0.5	0.8	9	5	200	0.2	1050	70.0366
5	10	0.05	0.5	0.2	3	0.2	50	0.2	1050	70.0205
5	50	0.01	0.5	0.2	3	0.2	50	0.2	1050	69.8906
5	10	0.01	0.5	0.2	3	5	50	0.2	1825	68.8085
5	50	0.05	0.5	0.2	3	0.2	50	0.2	1050	68.7765
5	10	0.01	0.5	0.2	3	5	200	0.2	1050	68.7667
5	10	0.05	0.5	0.2	3	5	50	0.2	1825	68.3713
5	10	0.05	0.5	0.2	3	5	200	0.2	1050	68.3332
5	50	0.01	0.5	0.2	3	5	50	0.2	1825	68.1163
5	50	0.01	0.5	0.2	3	5	200	0.2	1050	68.0753
5	10	0.01	0.5	0.8	3	0.2	200	0.8	1825	67.2278
5	50	0.05	0.5	0.2	3	5	50	0.2	1825	67.1719
5	50	0.05	0.5	0.2	3	5	200	0.2	1050	67.1352
5	10	0.01	0.5	0.8	9	0.2	200	0.8	1825	67.0855

Table D2. All particulate inert scenario

i_HRT	i_SRT	i_k_dis	i_k_dec	i_f_dC0	i_n_z	i_HDR	i_MPD	i_f_std_PSD	i_rho	o_rem_tot
1	10	0.01	0.1	0.8	3	0.2	200	0.2	1825	99.9999
1	10	0.01	0.1	0.8	9	0.2	200	0.2	1825	99.9999
1	10	0.01	0.5	0.8	3	0.2	200	0.2	1825	99.9999
1	10	0.01	0.5	0.8	9	0.2	200	0.2	1825	99.9999
1	10	0.05	0.1	0.8	3	0.2	200	0.2	1825	99.9999
1	10	0.05	0.1	0.8	9	0.2	200	0.2	1825	99.9999
1	10	0.05	0.5	0.8	3	0.2	200	0.2	1825	99.9999
1	10	0.05	0.5	0.8	9	0.2	200	0.2	1825	99.9999
1	50	0.01	0.1	0.8	3	0.2	200	0.2	1825	99.9999
1	50	0.01	0.1	0.8	9	0.2	200	0.2	1825	99.9999
1	50	0.01	0.5	0.8	3	0.2	200	0.2	1825	99.9999
1	50	0.01	0.5	0.8	9	0.2	200	0.2	1825	99.9999
1	50	0.05	0.1	0.8	3	0.2	200	0.2	1825	99.9999

Table D2. (Continued)

1	50	0.05	0.1	0.8	9	0.2	200	0.2	1825	99.9999
1	50	0.05	0.5	0.8	3	0.2	200	0.2	1825	99.9999
1	50	0.05	0.5	0.8	9	0.2	200	0.2	1825	99.9999
5	10	0.01	0.1	0.8	3	0.2	200	0.2	1825	99.9999
5	10	0.01	0.1	0.8	9	0.2	200	0.2	1825	99.9999
5	10	0.01	0.5	0.8	3	0.2	200	0.2	1825	99.9999
5	10	0.01	0.5	0.8	9	0.2	200	0.2	1825	99.9999
5	10	0.05	0.1	0.8	3	0.2	200	0.2	1825	99.9999
5	10	0.05	0.1	0.8	9	0.2	200	0.2	1825	99.9999
5	10	0.05	0.5	0.8	3	0.2	200	0.2	1825	99.9999
5	10	0.05	0.5	0.8	9	0.2	200	0.2	1825	99.9999
5	50	0.01	0.1	0.8	3	0.2	200	0.2	1825	99.9999
5	50	0.01	0.1	0.8	9	0.2	200	0.2	1825	99.9999
5	50	0.01	0.5	0.8	3	0.2	200	0.2	1825	99.9999
5	50	0.01	0.5	0.8	9	0.2	200	0.2	1825	99.9999
5	50	0.05	0.1	0.8	3	0.2	200	0.2	1825	99.9999
5	50	0.05	0.1	0.8	9	0.2	200	0.2	1825	99.9999
5	50	0.05	0.5	0.8	3	0.2	200	0.2	1825	99.9999
5	50	0.05	0.5	0.8	9	0.2	200	0.2	1825	99.9999
5	10	0.01	0.1	0.8	3	5	200	0.2	1825	99.9998
5	10	0.01	0.1	0.8	9	5	200	0.2	1825	99.9998
5	10	0.01	0.5	0.8	3	5	200	0.2	1825	99.9998
5	10	0.01	0.5	0.8	9	5	200	0.2	1825	99.9998
5	10	0.05	0.1	0.8	3	5	200	0.2	1825	99.9998
5	10	0.05	0.1	0.8	9	5	200	0.2	1825	99.9998
5	10	0.05	0.5	0.8	3	5	200	0.2	1825	99.9998
5	10	0.05	0.5	0.8	9	5	200	0.2	1825	99.9998
5	50	0.01	0.1	0.8	3	5	200	0.2	1825	99.9998
5	50	0.01	0.1	0.8	9	5	200	0.2	1825	99.9998
5	50	0.01	0.5	0.8	3	5	200	0.2	1825	99.9998
5	50	0.01	0.5	0.8	9	5	200	0.2	1825	99.9998
5	50	0.05	0.1	0.8	3	5	200	0.2	1825	99.9998
5	50	0.05	0.1	0.8	9	5	200	0.2	1825	99.9998
5	50	0.05	0.5	0.8	3	5	200	0.2	1825	99.9998
5	50	0.05	0.5	0.8	9	5	200	0.2	1825	99.9998
5	10	0.01	0.1	0.2	3	0.2	200	0.2	1825	99.9996
5	10	0.01	0.1	0.2	9	0.2	200	0.2	1825	99.9996
5	10	0.01	0.1	0.8	3	0.2	50	0.2	1825	99.9996
5	10	0.01	0.1	0.8	3	0.2	200	0.2	1050	99.9996
5	10	0.01	0.1	0.8	9	0.2	50	0.2	1825	99.9996
5	10	0.01	0.1	0.8	9	0.2	200	0.2	1050	99.9996

Table D2. (Continued)

5	10	0.01	0.5	0.2	3	0.2	200	0.2	1825	99.9996
5	10	0.01	0.5	0.2	9	0.2	200	0.2	1825	99.9996
5	10	0.01	0.5	0.8	3	0.2	50	0.2	1825	99.9996
5	10	0.01	0.5	0.8	3	0.2	200	0.2	1050	99.9996
5	10	0.01	0.5	0.8	9	0.2	50	0.2	1825	99.9996
5	10	0.01	0.5	0.8	9	0.2	200	0.2	1050	99.9996
5	10	0.05	0.1	0.2	3	0.2	200	0.2	1825	99.9996
5	10	0.05	0.1	0.2	9	0.2	200	0.2	1825	99.9996
5	10	0.05	0.1	0.8	3	0.2	50	0.2	1825	99.9996
5	10	0.05	0.1	0.8	3	0.2	200	0.2	1050	99.9996
5	10	0.05	0.1	0.8	9	0.2	50	0.2	1825	99.9996
5	10	0.05	0.1	0.8	9	0.2	200	0.2	1050	99.9996
5	10	0.05	0.5	0.2	3	0.2	200	0.2	1825	99.9996
5	10	0.05	0.5	0.2	9	0.2	200	0.2	1825	99.9996
5	10	0.05	0.5	0.8	3	0.2	50	0.2	1825	99.9996
5	10	0.05	0.5	0.8	3	0.2	200	0.2	1050	99.9996
5	10	0.05	0.5	0.8	9	0.2	50	0.2	1825	99.9996
5	10	0.05	0.5	0.8	9	0.2	200	0.2	1050	99.9996
5	50	0.01	0.1	0.2	3	0.2	200	0.2	1825	99.9996
5	50	0.01	0.1	0.2	9	0.2	200	0.2	1825	99.9996
5	50	0.01	0.1	0.8	3	0.2	50	0.2	1825	99.9996
5	50	0.01	0.1	0.8	3	0.2	200	0.2	1050	99.9996
5	50	0.01	0.1	0.8	9	0.2	50	0.2	1825	99.9996
5	50	0.01	0.1	0.8	9	0.2	200	0.2	1050	99.9996
5	50	0.01	0.5	0.2	3	0.2	200	0.2	1825	99.9996
5	50	0.01	0.5	0.2	9	0.2	200	0.2	1825	99.9996
5	50	0.01	0.5	0.8	3	0.2	50	0.2	1825	99.9996
5	50	0.01	0.5	0.8	3	0.2	200	0.2	1050	99.9996
5	50	0.01	0.5	0.8	9	0.2	50	0.2	1825	99.9996
5	50	0.01	0.5	0.8	9	0.2	200	0.2	1050	99.9996
5	50	0.05	0.1	0.2	3	0.2	200	0.2	1825	99.9996
5	50	0.05	0.1	0.2	9	0.2	200	0.2	1825	99.9996
5	50	0.05	0.1	0.8	3	0.2	50	0.2	1825	99.9996
5	50	0.05	0.1	0.8	3	0.2	200	0.2	1050	99.9996
5	50	0.05	0.1	0.8	9	0.2	50	0.2	1825	99.9996
5	50	0.05	0.1	0.8	9	0.2	200	0.2	1050	99.9996
5	50	0.05	0.5	0.2	3	0.2	200	0.2	1825	99.9996
5	50	0.05	0.5	0.2	9	0.2	200	0.2	1825	99.9996
5	50	0.05	0.5	0.8	3	0.2	50	0.2	1825	99.9996
5	50	0.05	0.5	0.8	3	0.2	200	0.2	1050	99.9996
5	50	0.05	0.5	0.8	9	0.2	50	0.2	1825	99.9996
5	50	0.05	0.5	0.8	9	0.2	200	0.2	1050	99.9996

Table D2. (Continued)

1	10	0.01	0.1	0.8	3	5	200	0.2	1825	99.998
1	10	0.01	0.1	0.8	9	5	200	0.2	1825	99.998
1	10	0.01	0.5	0.8	3	5	200	0.2	1825	99.998
1	10	0.01	0.5	0.8	9	5	200	0.2	1825	99.998
1	10	0.05	0.1	0.8	3	5	200	0.2	1825	99.998
1	10	0.05	0.1	0.8	9	5	200	0.2	1825	99.998

Table D3. All particulate reactive scenario

i_HRT	i_SRT	i_k_dis	i_k_dec	i_f_dC0	i_n_z	i_HDR	i_MPD	i_f_std_PSD	i_rho	o_rem_tot
5	10	0.01	0.5	0.2	3	0.2	200	0.2	1825	99.2107
5	10	0.01	0.5	0.8	3	0.2	200	0.2	1825	99.1989
5	10	0.01	0.5	0.8	3	0.2	50	0.2	1825	99.1986
5	10	0.01	0.5	0.8	3	0.2	200	0.2	1050	99.1986
5	10	0.01	0.5	0.2	9	0.2	200	0.2	1825	99.1794
5	10	0.01	0.5	0.8	3	5	200	0.2	1825	99.1696
5	10	0.01	0.5	0.2	3	5	200	0.2	1825	99.1644
5	10	0.01	0.5	0.8	9	0.2	200	0.2	1825	99.1508
5	10	0.01	0.5	0.8	9	0.2	50	0.2	1825	99.1505
5	10	0.01	0.5	0.8	9	0.2	200	0.2	1050	99.1505
5	10	0.01	0.5	0.8	3	5	200	0.2	1050	99.1378
5	10	0.01	0.5	0.8	3	5	50	0.2	1825	99.1375
5	10	0.01	0.5	0.2	9	5	200	0.2	1825	99.067
5	10	0.01	0.5	0.8	9	5	200	0.2	1825	99.0149
5	10	0.01	0.5	0.8	9	5	200	0.2	1050	98.983
5	10	0.01	0.5	0.8	9	5	50	0.2	1825	98.9828
5	10	0.01	0.5	0.2	3	0.2	200	0.2	1050	98.9786
5	10	0.01	0.5	0.2	3	0.2	50	0.2	1825	98.9768
5	10	0.01	0.5	0.8	3	0.2	50	0.2	1050	98.9653
5	10	0.01	0.5	0.2	9	0.2	200	0.2	1050	98.9457
5	10	0.01	0.5	0.2	9	0.2	50	0.2	1825	98.9439
5	10	0.01	0.5	0.8	9	0.2	50	0.2	1050	98.9167
5	10	0.05	0.5	0.2	3	0.2	200	0.2	1825	96.7377
5	50	0.01	0.5	0.2	3	0.2	200	0.2	1825	96.7377
5	50	0.01	0.5	0.8	3	0.2	200	0.2	1825	96.6901
5	50	0.01	0.5	0.8	3	0.2	50	0.2	1825	96.6898
5	50	0.01	0.5	0.8	3	0.2	200	0.2	1050	96.6898
5	10	0.05	0.5	0.8	3	0.2	200	0.2	1825	96.6886
5	10	0.05	0.5	0.8	3	0.2	50	0.2	1825	96.6883
5	10	0.05	0.5	0.8	3	0.2	200	0.2	1050	96.6883

Table D3. (Continued)

5	10	0.05	0.5	0.2	3	5	200	0.2	1825	96.6508
5	50	0.01	0.5	0.2	3	5	200	0.2	1825	96.6463
5	10	0.05	0.5	0.2	9	0.2	200	0.2	1825	96.6083
5	50	0.01	0.5	0.2	9	0.2	200	0.2	1825	96.6083
5	50	0.01	0.5	0.8	3	5	200	0.2	1825	96.5692
5	10	0.05	0.5	0.8	3	5	200	0.2	1825	96.5675
5	10	0.05	0.5	0.2	3	0.2	200	0.2	1050	96.5455
5	10	0.05	0.5	0.2	3	0.2	50	0.2	1825	96.544
5	10	0.05	0.5	0.8	3	5	200	0.2	1050	96.5409
5	10	0.05	0.5	0.8	3	5	50	0.2	1825	96.5407
5	50	0.01	0.5	0.8	3	5	200	0.2	1050	96.5384
5	50	0.01	0.5	0.8	3	5	50	0.2	1825	96.5381
5	50	0.01	0.5	0.2	3	0.2	200	0.2	1050	96.5117
5	50	0.01	0.5	0.2	3	0.2	50	0.2	1825	96.5099
5	10	0.05	0.5	0.8	3	0.2	50	0.2	1050	96.4929
5	50	0.01	0.5	0.8	9	0.2	200	0.2	1825	96.4913
5	50	0.01	0.5	0.8	9	0.2	50	0.2	1825	96.491
5	50	0.01	0.5	0.8	9	0.2	200	0.2	1050	96.491
5	10	0.05	0.5	0.8	9	0.2	200	0.2	1825	96.4897
5	10	0.05	0.5	0.8	9	0.2	50	0.2	1825	96.4894
5	10	0.05	0.5	0.8	9	0.2	200	0.2	1050	96.4894
5	50	0.01	0.5	0.8	3	0.2	50	0.2	1050	96.4626
5	10	0.05	0.5	0.2	9	0.2	200	0.2	1050	96.4096
5	10	0.05	0.5	0.2	9	0.2	50	0.2	1825	96.408
5	50	0.01	0.5	0.2	9	0.2	200	0.2	1050	96.3809
5	50	0.01	0.5	0.2	9	0.2	50	0.2	1825	96.3792
5	10	0.05	0.5	0.8	9	0.2	50	0.2	1050	96.2923
5	50	0.01	0.5	0.8	9	0.2	50	0.2	1050	96.2638
5	10	0.05	0.5	0.2	9	5	200	0.2	1825	96.2483
5	50	0.01	0.5	0.2	9	5	200	0.2	1825	96.2447
5	50	0.01	0.5	0.8	9	5	200	0.2	1825	95.93
5	10	0.05	0.5	0.8	9	5	200	0.2	1825	95.928
5	10	0.05	0.5	0.8	9	5	200	0.2	1050	95.9011
5	10	0.05	0.5	0.8	9	5	50	0.2	1825	95.9009
5	50	0.01	0.5	0.8	9	5	200	0.2	1050	95.8991
5	50	0.01	0.5	0.8	9	5	50	0.2	1825	95.8989
5	10	0.01	0.5	0.2	3	0.2	50	0.2	1050	94.9709
5	10	0.01	0.1	0.2	3	0.2	200	0.2	1825	94.216
1	10	0.01	0.5	0.2	3	0.2	200	0.2	1825	94.2091
1	10	0.01	0.5	0.8	3	0.2	200	0.2	1825	94.199
5	10	0.01	0.1	0.8	3	0.2	200	0.2	1825	94.1954
5	10	0.01	0.1	0.8	3	0.2	50	0.2	1825	94.1951

Table D3. (Continued)

5	10	0.01	0.1	0.8	3	0.2	200	0.2	1050	94.1951
1	10	0.01	0.5	0.8	3	0.2	200	0.2	1050	94.1917
1	10	0.01	0.5	0.8	3	0.2	50	0.2	1825	94.1916
5	10	0.01	0.1	0.2	9	0.2	200	0.2	1825	94.1708
1	10	0.01	0.5	0.2	9	0.2	200	0.2	1825	94.164
5	10	0.01	0.1	0.2	3	5	200	0.2	1825	94.1639
1	10	0.01	0.5	0.8	3	5	200	0.2	1825	94.1554
5	10	0.01	0.1	0.8	3	5	200	0.2	1825	94.1536
1	10	0.01	0.5	0.8	9	0.2	200	0.2	1825	94.1309
5	10	0.01	0.1	0.8	9	0.2	200	0.2	1825	94.1273
5	10	0.01	0.1	0.8	9	0.2	50	0.2	1825	94.127
5	10	0.01	0.1	0.8	9	0.2	200	0.2	1050	94.127
1	10	0.01	0.5	0.8	9	0.2	200	0.2	1050	94.1236
1	10	0.01	0.5	0.8	9	0.2	50	0.2	1825	94.1235
5	10	0.01	0.1	0.8	3	5	200	0.2	1050	94.1228
5	10	0.01	0.1	0.8	3	5	50	0.2	1825	94.1225
5	10	0.01	0.1	0.2	9	5	200	0.2	1825	94.0298
5	10	0.01	0.1	0.2	3	0.2	200	0.2	1050	93.99
5	10	0.01	0.1	0.2	3	0.2	50	0.2	1825	93.9882
5	10	0.01	0.1	0.8	3	0.2	50	0.2	1050	93.9687
1	10	0.01	0.5	0.8	9	5	200	0.2	1825	93.9523
5	10	0.01	0.1	0.8	9	5	200	0.2	1825	93.9503
5	10	0.01	0.1	0.2	9	0.2	200	0.2	1050	93.9442
5	10	0.01	0.1	0.2	9	0.2	50	0.2	1825	93.9424
5	10	0.01	0.1	0.8	9	5	200	0.2	1050	93.9195
5	10	0.01	0.1	0.8	9	5	50	0.2	1825	93.9193
5	10	0.01	0.1	0.8	9	0.2	50	0.2	1050	93.9005
5	10	0.05	0.5	0.2	3	0.2	50	0.2	1050	92.6145
5	50	0.05	0.5	0.2	3	0.2	200	0.2	1825	92.3902
5	50	0.05	0.5	0.8	3	0.2	200	0.2	1825	92.2794

Table D4. All soluble inert scenario

i_HRT	i_SRT	i_k_dis	i_k_dec	i_f_dC0	i_n_z	i_HDR	i_MPD	i_f_std_PSD	i_rho	o_rem_tot
1	10	0.01	0.1	0.2	3	0.2	50	0.2	1050	0
1	10	0.01	0.1	0.2	3	0.2	50	0.2	1825	0
1	10	0.01	0.1	0.2	3	0.2	50	0.8	1050	0
1	10	0.01	0.1	0.2	3	0.2	50	0.8	1825	0
1	10	0.01	0.1	0.2	3	0.2	200	0.2	1050	0
1	10	0.01	0.1	0.2	3	0.2	200	0.2	1825	0
1	10	0.01	0.1	0.2	3	0.2	200	0.8	1050	0
1	10	0.01	0.1	0.2	3	0.2	200	0.8	1825	0

Table D4. (Continued)

1	10	0.01	0.1	0.2	3	5	50	0.2	1050	0
1	10	0.01	0.1	0.2	3	5	50	0.2	1825	0
1	10	0.01	0.1	0.2	3	5	50	0.8	1050	0
1	10	0.01	0.1	0.2	3	5	50	0.8	1825	0
1	10	0.01	0.1	0.2	3	5	200	0.2	1050	0
1	10	0.01	0.1	0.2	3	5	200	0.2	1825	0
1	10	0.01	0.1	0.2	3	5	200	0.8	1050	0
1	10	0.01	0.1	0.2	3	5	200	0.8	1825	0
1	10	0.01	0.1	0.2	9	0.2	50	0.2	1050	0
1	10	0.01	0.1	0.2	9	0.2	50	0.2	1825	0
1	10	0.01	0.1	0.2	9	0.2	50	0.8	1050	0
1	10	0.01	0.1	0.2	9	0.2	50	0.8	1825	0
1	10	0.01	0.1	0.2	9	0.2	200	0.2	1050	0
1	10	0.01	0.1	0.2	9	0.2	200	0.2	1825	0
1	10	0.01	0.1	0.2	9	0.2	200	0.8	1050	0
1	10	0.01	0.1	0.2	9	0.2	200	0.8	1825	0
1	10	0.01	0.1	0.2	9	5	50	0.2	1050	0
1	10	0.01	0.1	0.2	9	5	50	0.2	1825	0
1	10	0.01	0.1	0.2	9	5	50	0.8	1050	0
1	10	0.01	0.1	0.2	9	5	50	0.8	1825	0
1	10	0.01	0.1	0.2	9	5	200	0.2	1050	0
1	10	0.01	0.1	0.2	9	5	200	0.2	1825	0
1	10	0.01	0.1	0.2	9	5	200	0.8	1050	0
1	10	0.01	0.1	0.2	9	5	200	0.8	1825	0
1	10	0.01	0.1	0.8	3	0.2	50	0.2	1050	0
1	10	0.01	0.1	0.8	3	0.2	50	0.2	1825	0
1	10	0.01	0.1	0.8	3	0.2	50	0.8	1050	0
1	10	0.01	0.1	0.8	3	0.2	50	0.8	1825	0
1	10	0.01	0.1	0.8	3	0.2	200	0.2	1050	0
1	10	0.01	0.1	0.8	3	0.2	200	0.2	1825	0
1	10	0.01	0.1	0.8	3	0.2	200	0.8	1050	0
1	10	0.01	0.1	0.8	3	0.2	200	0.8	1825	0
1	10	0.01	0.1	0.8	3	5	50	0.2	1050	0
1	10	0.01	0.1	0.8	3	5	50	0.2	1825	0
1	10	0.01	0.1	0.8	3	5	50	0.8	1050	0
1	10	0.01	0.1	0.8	3	5	50	0.8	1825	0
1	10	0.01	0.1	0.8	3	5	200	0.2	1050	0
1	10	0.01	0.1	0.8	3	5	200	0.2	1825	0
1	10	0.01	0.1	0.8	3	5	200	0.8	1050	0
1	10	0.01	0.1	0.8	3	5	200	0.8	1825	0
1	10	0.01	0.1	0.8	9	0.2	50	0.2	1050	0
1	10	0.01	0.1	0.8	9	0.2	50	0.2	1825	0

Table D4. (Continued)

1	10	0.01	0.1	0.8	9	0.2	50	0.8	1050	0
1	10	0.01	0.1	0.8	9	0.2	50	0.8	1825	0
1	10	0.01	0.1	0.8	9	0.2	200	0.2	1050	0
1	10	0.01	0.1	0.8	9	0.2	200	0.2	1825	0
1	10	0.01	0.1	0.8	9	0.2	200	0.8	1050	0
1	10	0.01	0.1	0.8	9	0.2	200	0.8	1825	0
1	10	0.01	0.1	0.8	9	5	50	0.2	1050	0
1	10	0.01	0.1	0.8	9	5	50	0.2	1825	0
1	10	0.01	0.1	0.8	9	5	50	0.8	1050	0
1	10	0.01	0.1	0.8	9	5	50	0.8	1825	0
1	10	0.01	0.1	0.8	9	5	200	0.2	1050	0
1	10	0.01	0.1	0.8	9	5	200	0.2	1825	0
1	10	0.01	0.1	0.8	9	5	200	0.8	1050	0
1	10	0.01	0.1	0.8	9	5	200	0.8	1825	0
1	10	0.01	0.5	0.2	3	0.2	50	0.2	1050	0
1	10	0.01	0.5	0.2	3	0.2	50	0.2	1825	0
1	10	0.01	0.5	0.2	3	0.2	50	0.8	1050	0
1	10	0.01	0.5	0.2	3	0.2	50	0.8	1825	0
1	10	0.01	0.5	0.2	3	0.2	200	0.2	1050	0
1	10	0.01	0.5	0.2	3	0.2	200	0.2	1825	0
1	10	0.01	0.5	0.2	3	0.2	200	0.8	1050	0
1	10	0.01	0.5	0.2	3	0.2	200	0.8	1825	0
1	10	0.01	0.5	0.2	3	5	50	0.2	1050	0
1	10	0.01	0.5	0.2	3	5	50	0.2	1825	0
1	10	0.01	0.5	0.2	3	5	50	0.8	1050	0
1	10	0.01	0.5	0.2	3	5	50	0.8	1825	0
1	10	0.01	0.5	0.2	3	5	200	0.2	1050	0
1	10	0.01	0.5	0.2	3	5	200	0.2	1825	0
1	10	0.01	0.5	0.2	3	5	200	0.8	1050	0
1	10	0.01	0.5	0.2	3	5	200	0.8	1825	0
1	10	0.01	0.5	0.2	9	0.2	50	0.2	1050	0
1	10	0.01	0.5	0.2	9	0.2	50	0.2	1825	0
1	10	0.01	0.5	0.2	9	0.2	50	0.8	1050	0
1	10	0.01	0.5	0.2	9	0.2	50	0.8	1825	0
1	10	0.01	0.5	0.2	9	0.2	200	0.2	1050	0
1	10	0.01	0.5	0.2	9	0.2	200	0.2	1825	0
1	10	0.01	0.5	0.2	9	0.2	200	0.8	1050	0
1	10	0.01	0.5	0.2	9	0.2	200	0.8	1825	0
1	10	0.01	0.5	0.2	9	5	50	0.2	1050	0
1	10	0.01	0.5	0.2	9	5	50	0.2	1825	0
1	10	0.01	0.5	0.2	9	5	50	0.8	1050	0
1	10	0.01	0.5	0.2	9	5	50	0.8	1825	0

Table D4. (Continued)

1	10	0.01	0.5	0.2	9	5	200	0.2	1050	0
1	10	0.01	0.5	0.2	9	5	200	0.2	1825	0
1	10	0.01	0.5	0.2	9	5	200	0.8	1050	0
1	10	0.01	0.5	0.2	9	5	200	0.8	1825	0
1	10	0.01	0.5	0.8	3	0.2	50	0.2	1050	0
1	10	0.01	0.5	0.8	3	0.2	50	0.2	1825	0
1	10	0.01	0.5	0.8	3	0.2	50	0.8	1050	0
1	10	0.01	0.5	0.8	3	0.2	50	0.8	1825	0
1	10	0.01	0.5	0.8	3	0.2	200	0.2	1050	0
1	10	0.01	0.5	0.8	3	0.2	200	0.2	1825	0

Table D5. All soluble reactive scenario

i_HRT	i_SRT	i_k_dis	i_k_dec	i_f_dC0	i_n_z	i_HDR	i_MPD	i_f_std_PSD	i_rho	o_rem_tot
5	10	0.01	0.5	0.2	3	0.2	50	0.2	1050	91.7121
5	10	0.01	0.5	0.2	3	0.2	50	0.2	1825	91.7121
5	10	0.01	0.5	0.2	3	0.2	50	0.8	1050	91.7121
5	10	0.01	0.5	0.2	3	0.2	50	0.8	1825	91.7121
5	10	0.01	0.5	0.2	3	0.2	200	0.2	1050	91.7121
5	10	0.01	0.5	0.2	3	0.2	200	0.2	1825	91.7121
5	10	0.01	0.5	0.2	3	0.2	200	0.8	1050	91.7121
5	10	0.01	0.5	0.2	3	0.2	200	0.8	1825	91.7121
5	10	0.05	0.5	0.2	3	0.2	50	0.2	1050	91.7121
5	10	0.05	0.5	0.2	3	0.2	50	0.2	1825	91.7121
5	10	0.05	0.5	0.2	3	0.2	50	0.8	1050	91.7121
5	10	0.05	0.5	0.2	3	0.2	50	0.8	1825	91.7121
5	10	0.05	0.5	0.2	3	0.2	200	0.2	1050	91.7121
5	10	0.05	0.5	0.2	3	0.2	200	0.2	1825	91.7121
5	10	0.05	0.5	0.2	3	0.2	200	0.8	1050	91.7121
5	10	0.05	0.5	0.2	3	0.2	200	0.8	1825	91.7121
5	50	0.01	0.5	0.2	3	0.2	50	0.2	1050	91.7121
5	50	0.01	0.5	0.2	3	0.2	50	0.2	1825	91.7121
5	50	0.01	0.5	0.2	3	0.2	50	0.8	1050	91.7121
5	50	0.01	0.5	0.2	3	0.2	50	0.8	1825	91.7121
5	50	0.01	0.5	0.2	3	0.2	200	0.2	1050	91.7121
5	50	0.01	0.5	0.2	3	0.2	200	0.2	1825	91.7121
5	50	0.01	0.5	0.2	3	0.2	200	0.8	1050	91.7121
5	50	0.01	0.5	0.2	3	0.2	200	0.8	1825	91.7121
5	50	0.05	0.5	0.2	3	0.2	50	0.2	1050	91.7121
5	50	0.05	0.5	0.2	3	0.2	50	0.2	1825	91.7121
5	50	0.05	0.5	0.2	3	0.2	50	0.8	1050	91.7121
5	50	0.05	0.5	0.2	3	0.2	50	0.8	1825	91.7121

Table D5. (Continued)

5	50	0.05	0.5	0.2	3	0.2	200	0.2	1050	91.7121
5	50	0.05	0.5	0.2	3	0.2	200	0.2	1825	91.7121
5	50	0.05	0.5	0.2	3	0.2	200	0.8	1050	91.7121
5	50	0.05	0.5	0.2	3	0.2	200	0.8	1825	91.7121
5	10	0.01	0.5	0.8	3	0.2	50	0.2	1050	91.6228
5	10	0.01	0.5	0.8	3	0.2	50	0.2	1825	91.6228
5	10	0.01	0.5	0.8	3	0.2	50	0.8	1050	91.6228
5	10	0.01	0.5	0.8	3	0.2	50	0.8	1825	91.6228
5	10	0.01	0.5	0.8	3	0.2	200	0.2	1050	91.6228
5	10	0.01	0.5	0.8	3	0.2	200	0.2	1825	91.6228
5	10	0.01	0.5	0.8	3	0.2	200	0.8	1050	91.6228
5	10	0.01	0.5	0.8	3	0.2	200	0.8	1825	91.6228
5	10	0.05	0.5	0.8	3	0.2	50	0.2	1050	91.6228
5	10	0.05	0.5	0.8	3	0.2	50	0.2	1825	91.6228
5	10	0.05	0.5	0.8	3	0.2	50	0.8	1050	91.6228
5	10	0.05	0.5	0.8	3	0.2	50	0.8	1825	91.6228
5	10	0.05	0.5	0.8	3	0.2	200	0.2	1050	91.6228
5	10	0.05	0.5	0.8	3	0.2	200	0.2	1825	91.6228
5	10	0.05	0.5	0.8	3	0.2	200	0.8	1050	91.6228
5	10	0.05	0.5	0.8	3	0.2	200	0.8	1825	91.6228
5	50	0.01	0.5	0.8	3	0.2	50	0.2	1050	91.6228
5	50	0.01	0.5	0.8	3	0.2	50	0.2	1825	91.6228
5	50	0.01	0.5	0.8	3	0.2	50	0.8	1050	91.6228
5	50	0.01	0.5	0.8	3	0.2	50	0.8	1825	91.6228
5	50	0.01	0.5	0.8	3	0.2	200	0.2	1050	91.6228
5	50	0.01	0.5	0.8	3	0.2	200	0.2	1825	91.6228
5	50	0.01	0.5	0.8	3	0.2	200	0.8	1050	91.6228
5	50	0.01	0.5	0.8	3	0.2	200	0.8	1825	91.6228
5	50	0.05	0.5	0.8	3	0.2	50	0.2	1050	91.6228
5	50	0.05	0.5	0.8	3	0.2	50	0.2	1825	91.6228
5	50	0.05	0.5	0.8	3	0.2	50	0.8	1050	91.6228
5	50	0.05	0.5	0.8	3	0.2	50	0.8	1825	91.6228
5	50	0.05	0.5	0.8	3	0.2	200	0.2	1050	91.6228
5	50	0.05	0.5	0.8	3	0.2	200	0.2	1825	91.6228
5	50	0.05	0.5	0.8	3	0.2	200	0.8	1050	91.6228
5	50	0.05	0.5	0.8	3	0.2	200	0.8	1825	91.6228
5	10	0.01	0.5	0.2	3	5	50	0.2	1050	91.5581
5	10	0.01	0.5	0.2	3	5	50	0.2	1825	91.5581
5	10	0.01	0.5	0.2	3	5	50	0.8	1050	91.5581
5	10	0.01	0.5	0.2	3	5	50	0.8	1825	91.5581
5	10	0.01	0.5	0.2	3	5	200	0.2	1050	91.5581
5	10	0.01	0.5	0.2	3	5	200	0.2	1825	91.5581

Table D5. (Continued)

5	10	0.01	0.5	0.2	3	5	200	0.8	1050	91.5581
5	10	0.01	0.5	0.2	3	5	200	0.8	1825	91.5581
5	10	0.05	0.5	0.2	3	5	50	0.2	1050	91.5581
5	10	0.05	0.5	0.2	3	5	50	0.2	1825	91.5581
5	10	0.05	0.5	0.2	3	5	50	0.8	1050	91.5581
5	10	0.05	0.5	0.2	3	5	50	0.8	1825	91.5581
5	10	0.05	0.5	0.2	3	5	200	0.2	1050	91.5581
5	10	0.05	0.5	0.2	3	5	200	0.2	1825	91.5581
5	10	0.05	0.5	0.2	3	5	200	0.8	1050	91.5581
5	10	0.05	0.5	0.2	3	5	200	0.8	1825	91.5581
5	50	0.01	0.5	0.2	3	5	50	0.2	1050	91.5581
5	50	0.01	0.5	0.2	3	5	50	0.2	1825	91.5581
5	50	0.01	0.5	0.2	3	5	50	0.8	1050	91.5581
5	50	0.01	0.5	0.2	3	5	50	0.8	1825	91.5581
5	50	0.01	0.5	0.2	3	5	200	0.2	1050	91.5581
5	50	0.01	0.5	0.2	3	5	200	0.2	1825	91.5581
5	50	0.01	0.5	0.2	3	5	200	0.8	1050	91.5581
5	50	0.01	0.5	0.2	3	5	200	0.8	1825	91.5581
5	50	0.05	0.5	0.2	3	5	50	0.2	1050	91.5581
5	50	0.05	0.5	0.2	3	5	50	0.2	1825	91.5581
5	50	0.05	0.5	0.2	3	5	50	0.8	1050	91.5581
5	50	0.05	0.5	0.2	3	5	50	0.8	1825	91.5581
5	50	0.05	0.5	0.2	3	5	200	0.2	1050	91.5581
5	50	0.05	0.5	0.2	3	5	200	0.2	1825	91.5581
5	50	0.05	0.5	0.2	3	5	200	0.8	1050	91.5581
5	50	0.05	0.5	0.2	3	5	200	0.8	1825	91.5581
5	10	0.01	0.5	0.2	9	0.2	50	0.2	1050	91.3833
5	10	0.01	0.5	0.2	9	0.2	50	0.2	1825	91.3833
5	10	0.01	0.5	0.2	9	0.2	50	0.8	1050	91.3833
5	10	0.01	0.5	0.2	9	0.2	50	0.8	1825	91.3833
5	10	0.01	0.5	0.2	9	0.2	200	0.2	1050	91.3833
5	10	0.01	0.5	0.2	9	0.2	200	0.2	1825	91.3833

Table D6. All particulate scenario

i_HRT	i_SRT	i_k_dis	i_k_dec	i_f_dC0	i_n_z	i_HDR	i_MPD	i_f_std_PSD	i_rho	o_rem_tot
5	10	0.01	0.5	0.2	3	0.2	200	0.2	1825	99.6051
5	10	0.01	0.5	0.8	3	0.2	200	0.2	1825	99.5995
5	10	0.01	0.5	0.8	3	0.2	50	0.2	1825	99.5991
5	10	0.01	0.5	0.8	3	0.2	200	0.2	1050	99.5991
5	10	0.01	0.5	0.2	9	0.2	200	0.2	1825	99.5895
5	10	0.01	0.5	0.8	3	5	200	0.2	1825	99.5847

Table D6. (Continued)

5	10	0.01	0.5	0.8	9	0.2	200	0.2	1825	99.5754
5	10	0.01	0.5	0.8	9	0.2	50	0.2	1825	99.575
5	10	0.01	0.5	0.8	9	0.2	200	0.2	1050	99.575
5	10	0.01	0.5	0.2	3	5	200	0.2	1825	99.5654
5	10	0.01	0.5	0.8	3	5	200	0.2	1050	99.5522
5	10	0.01	0.5	0.8	3	5	50	0.2	1825	99.552
5	10	0.01	0.5	0.2	9	5	200	0.2	1825	99.5167
5	10	0.01	0.5	0.8	9	5	200	0.2	1825	99.5073
5	10	0.01	0.5	0.8	9	5	200	0.2	1050	99.4748
5	10	0.01	0.5	0.8	9	5	50	0.2	1825	99.4746
5	10	0.01	0.5	0.2	3	0.2	200	0.2	1050	99.3672
5	10	0.01	0.5	0.2	3	0.2	50	0.2	1825	99.3655
5	10	0.01	0.5	0.8	3	0.2	50	0.2	1050	99.3603
5	10	0.01	0.5	0.2	9	0.2	200	0.2	1050	99.3508
5	10	0.01	0.5	0.2	9	0.2	50	0.2	1825	99.3491
5	10	0.01	0.5	0.8	9	0.2	50	0.2	1050	99.3361
5	50	0.01	0.5	0.2	3	0.2	200	0.2	1825	98.3687
5	10	0.05	0.5	0.2	3	0.2	200	0.2	1825	98.3686
5	50	0.01	0.5	0.8	3	0.2	200	0.2	1825	98.3451
5	50	0.01	0.5	0.8	3	0.2	50	0.2	1825	98.3447
5	50	0.01	0.5	0.8	3	0.2	200	0.2	1050	98.3447
5	10	0.05	0.5	0.8	3	0.2	200	0.2	1825	98.3443
5	10	0.05	0.5	0.8	3	0.2	50	0.2	1825	98.3439
5	10	0.05	0.5	0.8	3	0.2	200	0.2	1050	98.3439
5	10	0.05	0.5	0.2	3	5	200	0.2	1825	98.3086
5	50	0.01	0.5	0.2	3	5	200	0.2	1825	98.3064
5	50	0.01	0.5	0.2	9	0.2	200	0.2	1825	98.304
5	10	0.05	0.5	0.2	9	0.2	200	0.2	1825	98.3039
5	50	0.01	0.5	0.8	3	5	200	0.2	1825	98.2845
5	10	0.05	0.5	0.8	3	5	200	0.2	1825	98.2837
5	10	0.05	0.5	0.8	3	5	200	0.2	1050	98.2538
5	10	0.05	0.5	0.8	3	5	50	0.2	1825	98.2536
5	50	0.01	0.5	0.8	3	5	200	0.2	1050	98.2525
5	50	0.01	0.5	0.8	3	5	50	0.2	1825	98.2523
5	50	0.01	0.5	0.8	9	0.2	200	0.2	1825	98.2457
5	50	0.01	0.5	0.8	9	0.2	50	0.2	1825	98.2453
5	50	0.01	0.5	0.8	9	0.2	200	0.2	1050	98.2453
5	10	0.05	0.5	0.8	9	0.2	200	0.2	1825	98.2449
5	10	0.05	0.5	0.8	9	0.2	50	0.2	1825	98.2445
5	10	0.05	0.5	0.8	9	0.2	200	0.2	1050	98.2445
5	10	0.05	0.5	0.2	3	0.2	200	0.2	1050	98.1507
5	10	0.05	0.5	0.2	3	0.2	50	0.2	1825	98.1491

Table D6. (Continued)

5	50	0.01	0.5	0.2	3	0.2	200	0.2	1050	98.1338
5	50	0.01	0.5	0.2	3	0.2	50	0.2	1825	98.1321
5	10	0.05	0.5	0.8	3	0.2	50	0.2	1050	98.1242
5	50	0.01	0.5	0.8	3	0.2	50	0.2	1050	98.109
5	10	0.05	0.5	0.2	9	5	200	0.2	1825	98.1074
5	50	0.01	0.5	0.2	9	5	200	0.2	1825	98.1056
5	10	0.05	0.5	0.2	9	0.2	200	0.2	1050	98.0827
5	10	0.05	0.5	0.2	9	0.2	50	0.2	1825	98.0811
5	50	0.01	0.5	0.2	9	0.2	200	0.2	1050	98.0684
5	50	0.01	0.5	0.2	9	0.2	50	0.2	1825	98.0667
5	10	0.05	0.5	0.8	9	0.2	50	0.2	1050	98.0239
5	50	0.01	0.5	0.8	9	0.2	50	0.2	1050	98.0096
5	50	0.01	0.5	0.8	9	5	200	0.2	1825	97.9649
5	10	0.05	0.5	0.8	9	5	200	0.2	1825	97.9639
5	10	0.05	0.5	0.8	9	5	200	0.2	1050	97.9339
5	10	0.05	0.5	0.8	9	5	50	0.2	1825	97.9337
5	50	0.01	0.5	0.8	9	5	200	0.2	1050	97.9329
5	50	0.01	0.5	0.8	9	5	50	0.2	1825	97.9327
5	10	0.01	0.1	0.2	3	0.2	200	0.2	1825	97.1078
1	10	0.01	0.5	0.2	3	0.2	200	0.2	1825	97.1006
1	10	0.01	0.5	0.8	3	0.2	200	0.2	1825	97.0993
5	10	0.01	0.1	0.8	3	0.2	200	0.2	1825	97.0978
5	10	0.01	0.1	0.8	3	0.2	50	0.2	1825	97.0974
5	10	0.01	0.1	0.8	3	0.2	200	0.2	1050	97.0974
1	10	0.01	0.5	0.8	3	0.2	50	0.2	1825	97.0918
1	10	0.01	0.5	0.8	3	0.2	200	0.2	1050	97.0918
5	10	0.01	0.1	0.2	9	0.2	200	0.2	1825	97.0852
1	10	0.01	0.5	0.2	9	0.2	200	0.2	1825	97.078
1	10	0.01	0.5	0.8	3	5	200	0.2	1825	97.0767
5	10	0.01	0.1	0.8	3	5	200	0.2	1825	97.0767
1	10	0.01	0.5	0.8	9	0.2	200	0.2	1825	97.0653
5	10	0.01	0.1	0.2	3	5	200	0.2	1825	97.0651
5	10	0.01	0.1	0.8	9	0.2	200	0.2	1825	97.0637
5	10	0.01	0.1	0.8	9	0.2	50	0.2	1825	97.0633
5	10	0.01	0.1	0.8	9	0.2	200	0.2	1050	97.0633
1	10	0.01	0.5	0.8	9	0.2	50	0.2	1825	97.0578
1	10	0.01	0.5	0.8	9	0.2	200	0.2	1050	97.0578
5	10	0.01	0.1	0.8	3	5	200	0.2	1050	97.0447
5	10	0.01	0.1	0.8	3	5	50	0.2	1825	97.0445
5	10	0.01	0.1	0.2	9	5	200	0.2	1825	96.9982
1	10	0.01	0.5	0.8	9	5	200	0.2	1825	96.9751
5	10	0.01	0.1	0.8	9	5	200	0.2	1825	96.9751

Table D6. (Continued)

5	10	0.01	0.1	0.8	9	5	200	0.2	1050	96.943
5	10	0.01	0.1	0.8	9	5	50	0.2	1825	96.9428
5	10	0.01	0.1	0.2	3	0.2	200	0.2	1050	96.8729
5	10	0.01	0.1	0.2	3	0.2	50	0.2	1825	96.8713
5	10	0.01	0.1	0.8	3	0.2	50	0.2	1050	96.862
5	10	0.01	0.1	0.2	9	0.2	200	0.2	1050	96.85
5	10	0.01	0.1	0.2	9	0.2	50	0.2	1825	96.8483
5	10	0.01	0.1	0.8	9	0.2	50	0.2	1050	96.8279
5	50	0.05	0.5	0.2	3	0.2	200	0.2	1825	96.1949
5	50	0.05	0.5	0.8	3	0.2	200	0.2	1825	96.1397
5	50	0.05	0.5	0.8	3	0.2	50	0.2	1825	96.1393
5	50	0.05	0.5	0.8	3	0.2	200	0.2	1050	96.1393

Table D7. All soluble scenario

i_HRT	i_SRT	i_k_dis	i_k_dec	i_f_dC0	i_n_z	i_HDR	i_MPD	i_f_std_PSD	i_rho	o_rem_tot
5	10	0.01	0.5	0.2	3	0.2	50	0.2	1050	45.8561
5	10	0.01	0.5	0.2	3	0.2	50	0.2	1825	45.8561
5	10	0.01	0.5	0.2	3	0.2	50	0.8	1050	45.8561
5	10	0.01	0.5	0.2	3	0.2	50	0.8	1825	45.8561
5	10	0.01	0.5	0.2	3	0.2	200	0.2	1050	45.8561
5	10	0.01	0.5	0.2	3	0.2	200	0.2	1825	45.8561
5	10	0.01	0.5	0.2	3	0.2	200	0.8	1050	45.8561
5	10	0.01	0.5	0.2	3	0.2	200	0.8	1825	45.8561
5	10	0.05	0.5	0.2	3	0.2	50	0.2	1050	45.8561
5	10	0.05	0.5	0.2	3	0.2	50	0.2	1825	45.8561
5	10	0.05	0.5	0.2	3	0.2	50	0.8	1050	45.8561
5	10	0.05	0.5	0.2	3	0.2	50	0.8	1825	45.8561
5	10	0.05	0.5	0.2	3	0.2	200	0.2	1050	45.8561
5	10	0.05	0.5	0.2	3	0.2	200	0.2	1825	45.8561
5	10	0.05	0.5	0.2	3	0.2	200	0.8	1050	45.8561
5	10	0.05	0.5	0.2	3	0.2	200	0.8	1825	45.8561
5	50	0.01	0.5	0.2	3	0.2	50	0.2	1050	45.8561
5	50	0.01	0.5	0.2	3	0.2	50	0.2	1825	45.8561
5	50	0.01	0.5	0.2	3	0.2	50	0.8	1050	45.8561
5	50	0.01	0.5	0.2	3	0.2	50	0.8	1825	45.8561
5	50	0.01	0.5	0.2	3	0.2	200	0.2	1050	45.8561
5	50	0.01	0.5	0.2	3	0.2	200	0.2	1825	45.8561
5	50	0.01	0.5	0.2	3	0.2	200	0.8	1050	45.8561
5	50	0.01	0.5	0.2	3	0.2	200	0.8	1825	45.8561
5	50	0.05	0.5	0.2	3	0.2	50	0.2	1050	45.8561
5	50	0.05	0.5	0.2	3	0.2	50	0.2	1825	45.8561

Table D7. (Continued)

5	50	0.05	0.5	0.2	3	0.2	50	0.8	1050	45.8561
5	50	0.05	0.5	0.2	3	0.2	50	0.8	1825	45.8561
5	50	0.05	0.5	0.2	3	0.2	200	0.2	1050	45.8561
5	50	0.05	0.5	0.2	3	0.2	200	0.2	1825	45.8561
5	50	0.05	0.5	0.2	3	0.2	200	0.8	1050	45.8561
5	50	0.05	0.5	0.2	3	0.2	200	0.8	1825	45.8561
5	10	0.01	0.5	0.8	3	0.2	50	0.2	1050	45.8114
5	10	0.01	0.5	0.8	3	0.2	50	0.2	1825	45.8114
5	10	0.01	0.5	0.8	3	0.2	50	0.8	1050	45.8114
5	10	0.01	0.5	0.8	3	0.2	50	0.8	1825	45.8114
5	10	0.01	0.5	0.8	3	0.2	200	0.2	1050	45.8114
5	10	0.01	0.5	0.8	3	0.2	200	0.2	1825	45.8114
5	10	0.01	0.5	0.8	3	0.2	200	0.8	1050	45.8114
5	10	0.01	0.5	0.8	3	0.2	200	0.8	1825	45.8114
5	10	0.05	0.5	0.8	3	0.2	50	0.2	1050	45.8114
5	10	0.05	0.5	0.8	3	0.2	50	0.2	1825	45.8114
5	10	0.05	0.5	0.8	3	0.2	50	0.8	1050	45.8114
5	10	0.05	0.5	0.8	3	0.2	50	0.8	1825	45.8114
5	10	0.05	0.5	0.8	3	0.2	200	0.2	1050	45.8114
5	10	0.05	0.5	0.8	3	0.2	200	0.2	1825	45.8114
5	10	0.05	0.5	0.8	3	0.2	200	0.8	1050	45.8114
5	10	0.05	0.5	0.8	3	0.2	200	0.8	1825	45.8114
5	50	0.01	0.5	0.8	3	0.2	50	0.2	1050	45.8114
5	50	0.01	0.5	0.8	3	0.2	50	0.2	1825	45.8114
5	50	0.01	0.5	0.8	3	0.2	50	0.8	1050	45.8114
5	50	0.01	0.5	0.8	3	0.2	50	0.8	1825	45.8114
5	50	0.01	0.5	0.8	3	0.2	200	0.2	1050	45.8114
5	50	0.01	0.5	0.8	3	0.2	200	0.2	1825	45.8114
5	50	0.01	0.5	0.8	3	0.2	200	0.8	1050	45.8114
5	50	0.01	0.5	0.8	3	0.2	200	0.8	1825	45.8114
5	50	0.05	0.5	0.8	3	0.2	50	0.2	1050	45.8114
5	50	0.05	0.5	0.8	3	0.2	50	0.2	1825	45.8114
5	50	0.05	0.5	0.8	3	0.2	50	0.8	1050	45.8114
5	50	0.05	0.5	0.8	3	0.2	50	0.8	1825	45.8114
5	50	0.05	0.5	0.8	3	0.2	200	0.2	1050	45.8114
5	50	0.05	0.5	0.8	3	0.2	200	0.2	1825	45.8114
5	50	0.05	0.5	0.8	3	0.2	200	0.8	1050	45.8114
5	50	0.05	0.5	0.8	3	0.2	200	0.8	1825	45.8114
5	10	0.01	0.5	0.2	3	5	50	0.2	1050	45.7791
5	10	0.01	0.5	0.2	3	5	50	0.2	1825	45.7791
5	10	0.01	0.5	0.2	3	5	50	0.8	1050	45.7791
5	10	0.01	0.5	0.2	3	5	50	0.8	1825	45.7791

Table D7. (Continued)

5	10	0.01	0.5	0.2	3	5	200	0.2	1050	45.7791
5	10	0.01	0.5	0.2	3	5	200	0.2	1825	45.7791
5	10	0.01	0.5	0.2	3	5	200	0.8	1050	45.7791
5	10	0.01	0.5	0.2	3	5	200	0.8	1825	45.7791
5	10	0.05	0.5	0.2	3	5	50	0.2	1050	45.7791
5	10	0.05	0.5	0.2	3	5	50	0.2	1825	45.7791
5	10	0.05	0.5	0.2	3	5	50	0.8	1050	45.7791
5	10	0.05	0.5	0.2	3	5	50	0.8	1825	45.7791
5	10	0.05	0.5	0.2	3	5	200	0.2	1050	45.7791
5	10	0.05	0.5	0.2	3	5	200	0.2	1825	45.7791
5	10	0.05	0.5	0.2	3	5	200	0.8	1050	45.7791
5	10	0.05	0.5	0.2	3	5	200	0.8	1825	45.7791
5	50	0.01	0.5	0.2	3	5	50	0.2	1050	45.7791
5	50	0.01	0.5	0.2	3	5	50	0.2	1825	45.7791
5	50	0.01	0.5	0.2	3	5	50	0.8	1050	45.7791
5	50	0.01	0.5	0.2	3	5	50	0.8	1825	45.7791
5	50	0.01	0.5	0.2	3	5	200	0.2	1050	45.7791
5	50	0.01	0.5	0.2	3	5	200	0.2	1825	45.7791
5	50	0.01	0.5	0.2	3	5	200	0.8	1050	45.7791
5	50	0.01	0.5	0.2	3	5	200	0.8	1825	45.7791
5	50	0.05	0.5	0.2	3	5	50	0.2	1050	45.7791
5	50	0.05	0.5	0.2	3	5	50	0.2	1825	45.7791
5	50	0.05	0.5	0.2	3	5	50	0.8	1050	45.7791
5	50	0.05	0.5	0.2	3	5	50	0.8	1825	45.7791
5	50	0.05	0.5	0.2	3	5	200	0.2	1050	45.7791
5	50	0.05	0.5	0.2	3	5	200	0.2	1825	45.7791
5	50	0.05	0.5	0.2	3	5	200	0.8	1050	45.7791
5	50	0.05	0.5	0.2	3	5	200	0.8	1825	45.7791
5	10	0.01	0.5	0.2	9	0.2	50	0.2	1050	45.6917
5	10	0.01	0.5	0.2	9	0.2	50	0.2	1825	45.6917
5	10	0.01	0.5	0.2	9	0.2	50	0.8	1050	45.6917
5	10	0.01	0.5	0.2	9	0.2	50	0.8	1825	45.6917
5	10	0.01	0.5	0.2	9	0.2	200	0.2	1050	45.6917
5	10	0.01	0.5	0.2	9	0.2	200	0.2	1825	45.6917

Table D8. All inert scenario

i_HRT	i_SRT	i_k_dis	i_k_dec	i_f_dC0	i_n_z	i_HDR	i_MPD	i_f_std_PSD	i_rho	o_rem_tot
5	10	0.01	0.1	0.8	3	0.2	200	0.2	1825	50
5	10	0.01	0.1	0.8	9	0.2	200	0.2	1825	50
5	10	0.01	0.5	0.8	3	0.2	200	0.2	1825	50
5	10	0.01	0.5	0.8	9	0.2	200	0.2	1825	50

Table D8. (Continued)

5	10	0.05	0.1	0.8	3	0.2	200	0.2	1825	50
5	10	0.05	0.1	0.8	9	0.2	200	0.2	1825	50
5	10	0.05	0.5	0.8	3	0.2	200	0.2	1825	50
5	10	0.05	0.5	0.8	9	0.2	200	0.2	1825	50
5	50	0.01	0.1	0.8	3	0.2	200	0.2	1825	50
5	50	0.01	0.1	0.8	9	0.2	200	0.2	1825	50
5	50	0.01	0.5	0.8	3	0.2	200	0.2	1825	50
5	50	0.01	0.5	0.8	9	0.2	200	0.2	1825	50
5	50	0.05	0.1	0.8	3	0.2	200	0.2	1825	50
5	50	0.05	0.1	0.8	9	0.2	200	0.2	1825	50
5	50	0.05	0.5	0.8	3	0.2	200	0.2	1825	50
5	50	0.05	0.5	0.8	9	0.2	200	0.2	1825	50
1	10	0.01	0.1	0.8	3	0.2	200	0.2	1825	49.9999
1	10	0.01	0.1	0.8	9	0.2	200	0.2	1825	49.9999
1	10	0.01	0.5	0.8	3	0.2	200	0.2	1825	49.9999
1	10	0.01	0.5	0.8	9	0.2	200	0.2	1825	49.9999
1	10	0.05	0.1	0.8	3	0.2	200	0.2	1825	49.9999
1	10	0.05	0.1	0.8	9	0.2	200	0.2	1825	49.9999
1	10	0.05	0.5	0.8	3	0.2	200	0.2	1825	49.9999
1	10	0.05	0.5	0.8	9	0.2	200	0.2	1825	49.9999
1	50	0.01	0.1	0.8	3	0.2	200	0.2	1825	49.9999
1	50	0.01	0.1	0.8	9	0.2	200	0.2	1825	49.9999
1	50	0.01	0.5	0.8	3	0.2	200	0.2	1825	49.9999
1	50	0.01	0.5	0.8	9	0.2	200	0.2	1825	49.9999
1	50	0.05	0.1	0.8	3	0.2	200	0.2	1825	49.9999
1	50	0.05	0.1	0.8	9	0.2	200	0.2	1825	49.9999
1	50	0.05	0.5	0.8	3	0.2	200	0.2	1825	49.9999
1	50	0.05	0.5	0.8	9	0.2	200	0.2	1825	49.9999
5	10	0.01	0.1	0.8	3	5	200	0.2	1825	49.9999
5	10	0.01	0.1	0.8	9	5	200	0.2	1825	49.9999
5	10	0.01	0.5	0.8	3	5	200	0.2	1825	49.9999
5	10	0.01	0.5	0.8	9	5	200	0.2	1825	49.9999
5	10	0.05	0.1	0.8	3	5	200	0.2	1825	49.9999
5	10	0.05	0.1	0.8	9	5	200	0.2	1825	49.9999
5	10	0.05	0.5	0.8	3	5	200	0.2	1825	49.9999
5	10	0.05	0.5	0.8	9	5	200	0.2	1825	49.9999
5	50	0.01	0.1	0.8	3	5	200	0.2	1825	49.9999
5	50	0.01	0.1	0.8	9	5	200	0.2	1825	49.9999
5	50	0.01	0.5	0.8	3	5	200	0.2	1825	49.9999
5	50	0.01	0.5	0.8	9	5	200	0.2	1825	49.9999
5	50	0.05	0.1	0.8	3	5	200	0.2	1825	49.9999
5	50	0.05	0.1	0.8	9	5	200	0.2	1825	49.9999

Table D8. (Continued)

5	50	0.05	0.5	0.8	3	5	200	0.2	1825	49.9999
5	50	0.05	0.5	0.8	9	5	200	0.2	1825	49.9999
5	10	0.01	0.1	0.2	3	0.2	200	0.2	1825	49.9998
5	10	0.01	0.1	0.2	9	0.2	200	0.2	1825	49.9998
5	10	0.01	0.1	0.8	3	0.2	50	0.2	1825	49.9998
5	10	0.01	0.1	0.8	3	0.2	200	0.2	1050	49.9998
5	10	0.01	0.1	0.8	9	0.2	50	0.2	1825	49.9998
5	10	0.01	0.1	0.8	9	0.2	200	0.2	1050	49.9998
5	10	0.01	0.5	0.2	3	0.2	200	0.2	1825	49.9998
5	10	0.01	0.5	0.2	9	0.2	200	0.2	1825	49.9998
5	10	0.01	0.5	0.8	3	0.2	50	0.2	1825	49.9998
5	10	0.01	0.5	0.8	3	0.2	200	0.2	1050	49.9998
5	10	0.01	0.5	0.8	9	0.2	50	0.2	1825	49.9998
5	10	0.01	0.5	0.8	9	0.2	200	0.2	1050	49.9998
5	10	0.05	0.1	0.2	3	0.2	200	0.2	1825	49.9998
5	10	0.05	0.1	0.2	9	0.2	200	0.2	1825	49.9998
5	10	0.05	0.1	0.8	3	0.2	50	0.2	1825	49.9998
5	10	0.05	0.1	0.8	3	0.2	200	0.2	1050	49.9998
5	10	0.05	0.1	0.8	9	0.2	50	0.2	1825	49.9998
5	10	0.05	0.1	0.8	9	0.2	200	0.2	1050	49.9998
5	10	0.05	0.5	0.2	3	0.2	200	0.2	1825	49.9998
5	10	0.05	0.5	0.2	9	0.2	200	0.2	1825	49.9998
5	10	0.05	0.5	0.8	3	0.2	50	0.2	1825	49.9998
5	10	0.05	0.5	0.8	3	0.2	200	0.2	1050	49.9998
5	10	0.05	0.5	0.8	9	0.2	50	0.2	1825	49.9998
5	10	0.05	0.5	0.8	9	0.2	200	0.2	1050	49.9998
5	50	0.01	0.1	0.2	3	0.2	200	0.2	1825	49.9998
5	50	0.01	0.1	0.2	9	0.2	200	0.2	1825	49.9998
5	50	0.01	0.1	0.8	3	0.2	50	0.2	1825	49.9998
5	50	0.01	0.1	0.8	3	0.2	200	0.2	1050	49.9998
5	50	0.01	0.1	0.8	9	0.2	50	0.2	1825	49.9998
5	50	0.01	0.1	0.8	9	0.2	200	0.2	1050	49.9998
5	50	0.01	0.5	0.2	3	0.2	200	0.2	1825	49.9998
5	50	0.01	0.5	0.2	9	0.2	200	0.2	1825	49.9998
5	50	0.01	0.5	0.8	3	0.2	50	0.2	1825	49.9998
5	50	0.01	0.5	0.8	3	0.2	200	0.2	1050	49.9998
5	50	0.01	0.5	0.8	9	0.2	50	0.2	1825	49.9998
5	50	0.01	0.5	0.8	9	0.2	200	0.2	1050	49.9998
5	50	0.05	0.1	0.2	3	0.2	200	0.2	1825	49.9998
5	50	0.05	0.1	0.2	9	0.2	200	0.2	1825	49.9998
5	50	0.05	0.1	0.8	3	0.2	50	0.2	1825	49.9998
5	50	0.05	0.1	0.8	3	0.2	200	0.2	1050	49.9998

Table D8. (Continued)

5	50	0.05	0.1	0.8	9	0.2	50	0.2	1825	49.9998
5	50	0.05	0.1	0.8	9	0.2	200	0.2	1050	49.9998
5	50	0.05	0.5	0.2	3	0.2	200	0.2	1825	49.9998
5	50	0.05	0.5	0.2	9	0.2	200	0.2	1825	49.9998
5	50	0.05	0.5	0.8	3	0.2	50	0.2	1825	49.9998
5	50	0.05	0.5	0.8	3	0.2	200	0.2	1050	49.9998
5	50	0.05	0.5	0.8	9	0.2	50	0.2	1825	49.9998
5	50	0.05	0.5	0.8	9	0.2	200	0.2	1050	49.9998
1	10	0.01	0.1	0.8	3	5	200	0.2	1825	49.999
1	10	0.01	0.1	0.8	9	5	200	0.2	1825	49.999
1	10	0.01	0.5	0.8	3	5	200	0.2	1825	49.999
1	10	0.01	0.5	0.8	9	5	200	0.2	1825	49.999
1	10	0.05	0.1	0.8	3	5	200	0.2	1825	49.999
1	10	0.05	0.1	0.8	9	5	200	0.2	1825	49.999

Table D9. All reactive scenario

i_HRT	i_SRT	i_k_dis	i_k_dec	i_f_dC0	i_n_z	i_HDR	i_MPD	i_f_std_PSD	i_rho	o_rem_tot
5	10	0.01	0.5	0.2	3	0.2	200	0.2	1825	95.4614
5	10	0.01	0.5	0.8	3	0.2	200	0.2	1825	95.4109
5	10	0.01	0.5	0.8	3	0.2	50	0.2	1825	95.4107
5	10	0.01	0.5	0.8	3	0.2	200	0.2	1050	95.4107
5	10	0.01	0.5	0.2	3	5	200	0.2	1825	95.3612
5	10	0.01	0.5	0.2	3	0.2	200	0.2	1050	95.3453
5	10	0.01	0.5	0.2	3	0.2	50	0.2	1825	95.3445
5	10	0.01	0.5	0.8	3	0.2	50	0.2	1050	95.294
5	10	0.01	0.5	0.2	9	0.2	200	0.2	1825	95.2813
5	10	0.01	0.5	0.8	3	5	200	0.2	1825	95.2433
5	10	0.01	0.5	0.8	3	5	200	0.2	1050	95.2274
5	10	0.01	0.5	0.8	3	5	50	0.2	1825	95.2273
5	10	0.01	0.5	0.2	9	0.2	200	0.2	1050	95.1645
5	10	0.01	0.5	0.2	9	0.2	50	0.2	1825	95.1637
5	10	0.01	0.5	0.8	9	0.2	200	0.2	1825	95.1353
5	10	0.01	0.5	0.8	9	0.2	50	0.2	1825	95.1351
5	10	0.01	0.5	0.8	9	0.2	200	0.2	1050	95.1351
5	10	0.01	0.5	0.8	9	0.2	50	0.2	1050	95.0182
5	10	0.01	0.5	0.2	9	5	200	0.2	1825	94.8026
5	10	0.01	0.5	0.8	9	5	200	0.2	1825	94.357
5	10	0.01	0.5	0.8	9	5	200	0.2	1050	94.341
5	10	0.01	0.5	0.8	9	5	50	0.2	1825	94.3409
5	10	0.05	0.5	0.2	3	0.2	200	0.2	1825	94.2249
5	50	0.01	0.5	0.2	3	0.2	200	0.2	1825	94.2249

Table D9. (Continued)

5	50	0.01	0.5	0.8	3	0.2	200	0.2	1825	94.1565
5	50	0.01	0.5	0.8	3	0.2	50	0.2	1825	94.1563
5	50	0.01	0.5	0.8	3	0.2	200	0.2	1050	94.1563
5	10	0.05	0.5	0.8	3	0.2	200	0.2	1825	94.1557
5	10	0.05	0.5	0.8	3	0.2	50	0.2	1825	94.1555
5	10	0.05	0.5	0.8	3	0.2	200	0.2	1050	94.1555
5	10	0.05	0.5	0.2	3	0.2	200	0.2	1050	94.1288
5	10	0.05	0.5	0.2	3	0.2	50	0.2	1825	94.1281
5	50	0.01	0.5	0.2	3	0.2	200	0.2	1050	94.1118
5	50	0.01	0.5	0.2	3	0.2	50	0.2	1825	94.1111
5	10	0.05	0.5	0.2	3	5	200	0.2	1825	94.1045
5	50	0.01	0.5	0.2	3	5	200	0.2	1825	94.1022
5	10	0.05	0.5	0.8	3	0.2	50	0.2	1050	94.0579
5	50	0.01	0.5	0.8	3	0.2	50	0.2	1050	94.0427
5	10	0.05	0.5	0.2	9	0.2	200	0.2	1825	93.9958
5	50	0.01	0.5	0.2	9	0.2	200	0.2	1825	93.9958
5	50	0.01	0.5	0.8	3	5	200	0.2	1825	93.9431
5	10	0.05	0.5	0.8	3	5	200	0.2	1825	93.9423
5	10	0.05	0.5	0.8	3	5	200	0.2	1050	93.929
5	10	0.05	0.5	0.8	3	5	50	0.2	1825	93.9289
5	50	0.01	0.5	0.8	3	5	200	0.2	1050	93.9277
5	50	0.01	0.5	0.8	3	5	50	0.2	1825	93.9276
5	10	0.05	0.5	0.2	9	0.2	200	0.2	1050	93.8964
5	10	0.05	0.5	0.2	9	0.2	50	0.2	1825	93.8957
5	50	0.01	0.5	0.2	9	0.2	200	0.2	1050	93.8821
5	50	0.01	0.5	0.2	9	0.2	50	0.2	1825	93.8813
5	50	0.01	0.5	0.8	9	0.2	200	0.2	1825	93.8056
5	50	0.01	0.5	0.8	9	0.2	50	0.2	1825	93.8054
5	50	0.01	0.5	0.8	9	0.2	200	0.2	1050	93.8054
5	10	0.05	0.5	0.8	9	0.2	200	0.2	1825	93.8047
5	10	0.05	0.5	0.8	9	0.2	50	0.2	1825	93.8045
5	10	0.05	0.5	0.8	9	0.2	200	0.2	1050	93.8045
5	10	0.05	0.5	0.8	9	0.2	50	0.2	1050	93.706
5	50	0.01	0.5	0.8	9	0.2	50	0.2	1050	93.6917
5	10	0.05	0.5	0.2	9	5	200	0.2	1825	93.3932
5	50	0.01	0.5	0.2	9	5	200	0.2	1825	93.3914
5	10	0.01	0.5	0.2	3	0.2	50	0.2	1050	93.3415
5	50	0.01	0.5	0.8	9	5	200	0.2	1825	92.8145
5	10	0.05	0.5	0.8	9	5	200	0.2	1825	92.8135
5	10	0.05	0.5	0.8	9	5	200	0.2	1050	92.8001
5	10	0.05	0.5	0.8	9	5	50	0.2	1825	92.8
5	50	0.01	0.5	0.8	9	5	200	0.2	1050	92.7991

Table D9. (Continued)

5	50	0.01	0.5	0.8	9	5	50	0.2	1825	92.799
5	10	0.05	0.5	0.2	3	0.2	50	0.2	1050	92.1633
5	50	0.05	0.5	0.2	3	0.2	200	0.2	1825	92.0511
5	50	0.05	0.5	0.2	3	0.2	200	0.2	1050	91.9603
5	50	0.05	0.5	0.2	3	0.2	50	0.2	1825	91.9597
5	50	0.05	0.5	0.8	3	0.2	200	0.2	1825	91.9511
5	50	0.05	0.5	0.8	3	0.2	50	0.2	1825	91.9509
5	50	0.05	0.5	0.8	3	0.2	200	0.2	1050	91.9509
5	50	0.01	0.5	0.2	3	0.2	50	0.2	1050	91.9035
5	50	0.05	0.5	0.2	3	5	200	0.2	1825	91.8911
5	50	0.05	0.5	0.8	3	0.2	50	0.2	1050	91.8587
5	50	0.05	0.5	0.2	9	0.2	200	0.2	1825	91.7358
5	50	0.05	0.5	0.8	3	5	200	0.2	1825	91.6572
5	50	0.05	0.5	0.8	3	5	200	0.2	1050	91.6447
5	50	0.05	0.5	0.8	3	5	50	0.2	1825	91.6446
5	50	0.05	0.5	0.2	9	0.2	200	0.2	1050	91.6419
5	50	0.05	0.5	0.2	9	0.2	50	0.2	1825	91.6412
5	10	0.01	0.5	0.2	3	5	50	0.2	1825	91.5459
5	10	0.01	0.5	0.2	3	5	200	0.2	1050	91.5051
5	50	0.05	0.5	0.8	9	0.2	200	0.2	1825	91.4677
5	50	0.05	0.5	0.8	9	0.2	50	0.2	1825	91.4675
5	50	0.05	0.5	0.8	9	0.2	200	0.2	1050	91.4675
5	50	0.05	0.5	0.8	9	0.2	50	0.2	1050	91.3747
5	50	0.05	0.5	0.2	9	5	200	0.2	1825	90.9123
5	10	0.05	0.5	0.2	3	5	50	0.2	1825	90.6713
5	10	0.05	0.5	0.2	3	5	200	0.2	1050	90.6381
5	50	0.01	0.5	0.2	3	5	50	0.2	1825	90.1616
5	50	0.01	0.5	0.2	3	5	200	0.2	1050	90.1223
5	50	0.05	0.5	0.8	9	5	200	0.2	1825	90.1027
5	50	0.05	0.5	0.8	9	5	200	0.2	1050	90.0902
5	50	0.05	0.5	0.8	9	5	50	0.2	1825	90.0901
5	10	0.01	0.5	0.8	3	0.2	200	0.8	1825	90.057
5	10	0.01	0.5	0.8	9	0.2	200	0.8	1825	89.7723
5	50	0.05	0.5	0.2	3	0.2	50	0.2	1050	89.6753
5	10	0.05	0.5	0.8	3	0.2	200	0.8	1825	89.6738
5	10	0.05	0.5	0.8	9	0.2	200	0.8	1825	89.2841

Appendix E: Analysis of Geometric Model Responses

Table E1. All equal scenario

		top 10%		top 5%		top 1%	
i_HRT	Low	0	0%	0	0%	0	0%
	High	102	100%	51	100%	10	100%
i_SRT	Low	52	51%	36	71%	10	100%
	High	50	49%	15	29%	0	0%
i_k_dis	Low	52	51%	37	73%	10	100%
	High	50	49%	14	27%	0	0%
i_k_dec	Low	0	0%	0	0%	0	0%
	High	102	100%	51	100%	10	100%
i_f_dC0	Low	44	43%	18	35%	5	50%
	High	58	57%	33	65%	5	50%
i_n_z	Low	57	56%	33	65%	9	90%
	High	45	44%	18	35%	1	10%
i_HDR	Low	62	61%	35	69%	7	70%
	High	40	39%	16	31%	3	30%
i_MPD	Low	40	39%	18	35%	3	30%
	High	62	61%	33	65%	7	70%
i_f_std_PSD	Low	100	98%	51	100%	10	100%
	High	2	2%	0	0%	0	0%
i_rho	Low	40	39%	17	33%	2	20%
	High	62	61%	34	67%	8	80%

Table E2. All particulate inert scenario

		top 10%		top 5%		top 1%	
i_HRT	Low	22	22%	16	31%	10	100%
	High	80	78%	35	69%	0	0%
i_SRT	Low	54	53%	27	53%	8	80%
	High	48	47%	24	47%	2	20%
i_k_dis	Low	52	51%	27	53%	6	60%
	High	50	49%	24	47%	4	40%
i_k_dec	Low	52	51%	27	53%	6	60%
	High	50	49%	24	47%	4	40%

Table E2. (Continued)

i_f_dC0	Low	16	16%	2	4%	0	0%
	High	86	84%	49	96%	10	100%
i_n_z	Low	51	50%	26	51%	5	50%
	High	51	50%	25	49%	5	50%
i_HDR	Low	80	78%	35	69%	10	100%
	High	22	22%	16	31%	0	0%
i_MPD	Low	16	16%	1	2%	0	0%
	High	86	84%	50	98%	10	100%
i_f_std_PSD	Low	102	100%	51	100%	10	100%
	High	0	0%	0	0%	0	0%
i_rho	Low	16	16%	0	0%	0	0%
	High	86	84%	51	100%	10	100%

Table E3. All particulate reactive scenario

		top 10%		**top 5%**		**top 1%**	
i_HRT	Low	10	10%	0	0%	0	0%
	High	92	90%	51	100%	10	100%
i_SRT	Low	78	76%	37	73%	10	100%
	High	24	24%	14	27%	0	0%
i_k_dis	Low	77	75%	36	71%	10	100%
	High	25	25%	15	29%	0	0%
i_k_dec	Low	22	22%	0	0%	0	0%
	High	80	78%	51	100%	10	100%
i_f_dC0	Low	37	36%	18	35%	3	30%
	High	65	64%	33	65%	7	70%
i_n_z	Low	53	52%	32	63%	6	60%
	High	49	48%	19	37%	4	40%
i_HDR	Low	68	67%	35	69%	8	80%
	High	34	33%	16	31%	2	20%
i_MPD	Low	36	35%	17	33%	2	20%
	High	66	65%	34	67%	8	80%
i_f_std_PSD	Low	102	100%	51	100%	10	100%
	High	0	0%	0	0%	0	0%
i_rho	Low	36	35%	17	33%	2	20%
	High	66	65%	34	67%	8	80%

Table E4. All soluble reactive scenario

		top 10%		top 5%		top 1%	
i_HRT	Low	0	0%	0	0%	0	0%
	High	102	100%	51	100%	10	100%
i_SRT	Low	54	53%	32	63%	10	100%
	High	48	47%	19	37%	0	0%
i_k_dis	Low	54	53%	27	53%	8	80%
	High	48	47%	24	47%	2	20%
i_k_dec	Low	0	0%	0	0%	0	0%
	High	102	100%	51	100%	10	100%
i_f_dC0	Low	70	69%	32	63%	10	100%
	High	32	31%	19	37%	0	0%
i_n_z	Low	96	94%	51	100%	10	100%
	High	6	6%	0	0%	0	0%
i_HDR	Low	70	69%	51	100%	10	100%
	High	32	31%	0	0%	0	0%
i_MPD	Low	52	51%	27	53%	6	60%
	High	50	49%	24	47%	4	40%
i_f_std_PSD	Low	52	51%	26	51%	6	60%
	High	50	49%	25	49%	4	40%
i_rho	Low	51	50%	26	51%	5	50%
	High	51	50%	25	49%	5	50%

Table E5. All particulate scenario

		top 10%		top 5%		top 1%	
i_HRT	Low	10	10%	0	0%	0	0%
	High	92	90%	51	100%	10	100%
i_SRT	Low	76	75%	37	73%	10	100%
	High	26	25%	14	27%	0	0%
i_k_dis	Low	76	75%	36	71%	10	100%
	High	26	25%	15	29%	0	0%
i_k_dec	Low	22	22%	0	0%	0	0%
	High	80	78%	51	100%	10	100%
i_f_dC0	Low	35	34%	18	35%	3	30%
	High	67	66%	33	65%	7	70%
i_n_z	Low	53	52%	32	63%	6	60%
	High	49	48%	19	37%	4	40%
i_HDR	Low	68	67%	35	69%	8	80%
	High	34	33%	16	31%	2	20%

Table E5. (Continued)

i_MPD	**Low**	**35**	**34%**	**17**	**33%**	**2**	**20%**
	High	67	66%	34	67%	8	80%
i_f_std_PSD	Low	102	100%	51	100%	10	100%
	High	0	0%	0	0%	0	0%
i_rho	Low	35	34%	17	33%	2	20%
	High	67	66%	34	67%	8	80%

Table E6. All soluble scenario

		top 10%		**top 5%**		**top 1%**	
i_HRT	Low	0	0%	0	0%	0	0%
	High	102	100%	51	100%	10	100%
i_SRT	Low	54	53%	32	63%	10	100%
	High	48	47%	19	37%	0	0%
i_k_dis	Low	54	53%	27	53%	8	80%
	High	48	47%	24	47%	2	20%
i_k_dec	Low	0	0%	0	0%	0	0%
	High	102	100%	51	100%	10	100%
i_f_dC0	Low	70	69%	32	63%	10	100%
	High	32	31%	19	37%	0	0%
i_n_z	Low	96	94%	51	100%	10	100%
	High	6	6%	0	0%	0	0%
i_HDR	Low	70	69%	51	100%	10	100%
	High	32	31%	0	0%	0	0%
i_MPD	Low	52	51%	27	53%	6	60%
	High	50	49%	24	47%	4	40%
i_f_std_PSD	Low	52	51%	26	51%	6	60%
	High	50	49%	25	49%	4	40%
i_rho	Low	51	50%	26	51%	5	50%
	High	51	50%	25	49%	5	50%

Table E7. All inert scenario

		top 10%		**top 5%**		**top 1%**	
i_HRT	Low	22	22%	16	31%	0	0%
	High	80	78%	35	69%	10	100%
i_SRT	Low	54	53%	27	53%	8	80%
	High	48	47%	24	47%	2	20%
i_k_dis	Low	52	51%	27	53%	6	60%
	High	50	49%	24	47%	4	40%

Table E7. (Continued)

i_k_dec	**Low**	**52**	**51%**	**27**	**53%**	**6**	**60%**
	High	50	49%	24	47%	4	40%
i_f_dC0	Low	16	16%	2	4%	0	0%
	High	86	84%	49	96%	10	100%
i_n_z	Low	51	50%	26	51%	5	50%
	High	51	50%	25	49%	5	50%
i_HDR	Low	80	78%	35	69%	10	100%
	High	22	22%	16	31%	0	0%
i_MPD	Low	16	16%	1	2%	0	0%
	High	86	84%	50	98%	10	100%
i_f_std_PSD	Low	102	100%	51	100%	10	100%
	High	0	0%	0	0%	0	0%
i_rho	Low	16	16%	0	0%	0	0%
	High	86	84%	51	100%	10	100%

Table E8. All reactive scenario

		top 10%		**top 5%**		**top 1%**	
i_HRT	Low	0	0%	0	0%	0	0%
	High	102	100%	51	100%	10	100%
i_SRT	Low	54	53%	36	71%	10	100%
	High	48	47%	15	29%	0	0%
i_k_dis	Low	52	51%	37	73%	10	100%
	High	50	49%	14	27%	0	0%
i_k_dec	Low	0	0%	0	0%	0	0%
	High	102	100%	51	100%	10	100%
i_f_dC0	Low	42	41%	22	43%	5	50%
	High	60	59%	29	57%	5	50%
i_n_z	Low	56	55%	33	65%	9	90%
	High	46	45%	18	35%	1	10%
i_HDR	Low	64	63%	35	69%	8	80%
	High	38	37%	16	31%	2	20%
i_MPD	Low	39	38%	18	35%	3	30%
	High	63	62%	33	65%	7	70%
i_f_std_PSD	Low	98	96%	51	100%	10	100%
	High	4	4%	0	0%	0	0%
i_rho	Low	39	38%	18	35%	3	30%
	High	63	62%	33	65%	7	70%